Propellant grade hydrogen peroxide production and thermo pseudo hypergolicity investigation for dual mode green propulsion systems

Jaime Quesada Mañas

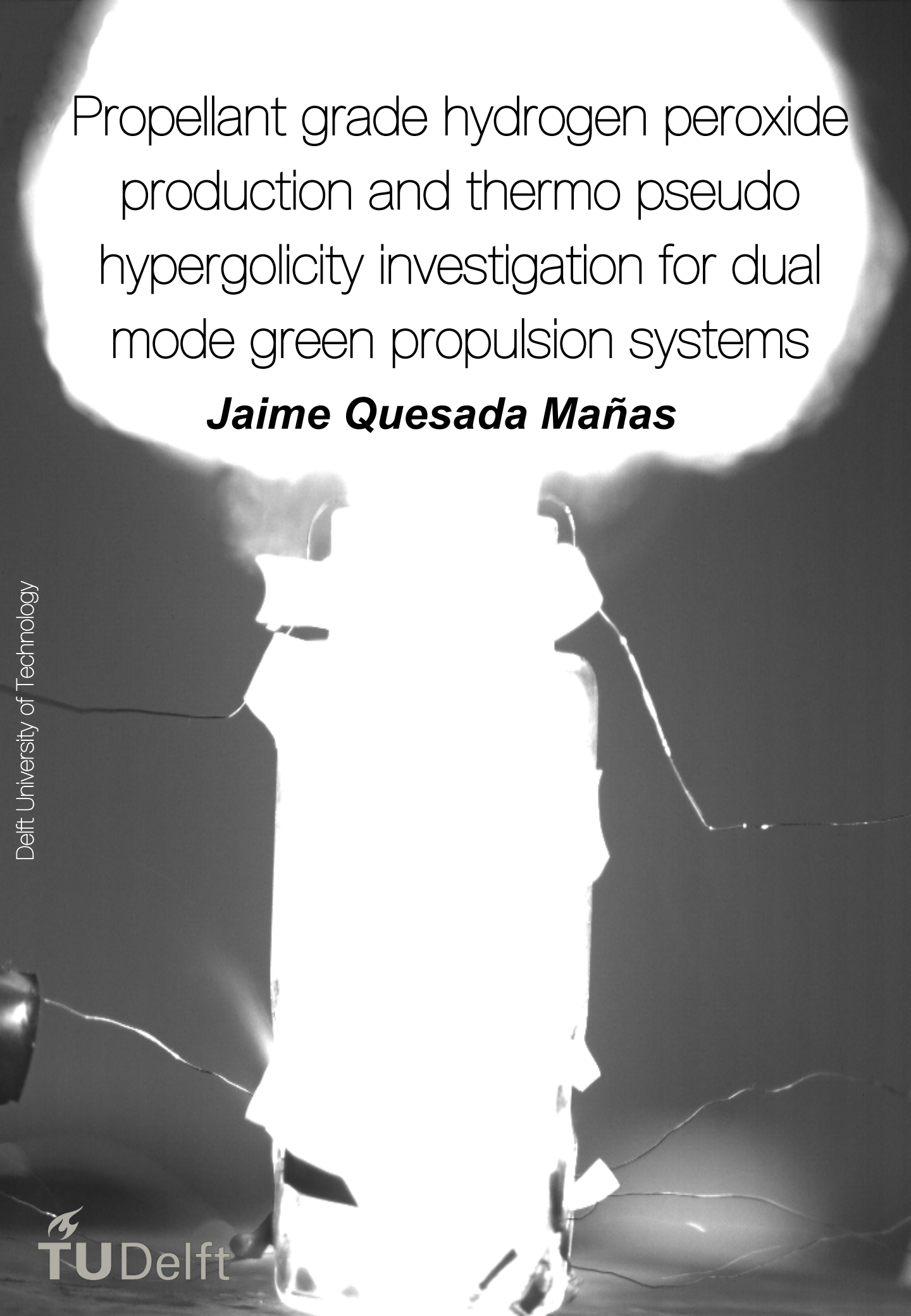

Delft University of Technology

TUDelft

Propellant grade hydrogen peroxide production and thermo pseudo hypergolicity investigation for dual mode green propulsion system

by

Jaime Quesada Mañas

to obtain the degree of Master of Science
at the Delft University of Technology,
to be defended publicly on Thursday January 23, 2020 at 09:30 AM.

Student number:	4353889	
Project duration:	May 16, 2019 – January 23, 2020	
Thesis committee:	Prof. dr. E.K.A. Gill,	TU Delft, chairman of committee
	Dr. B. V. S. Jyoti,	TU Delft, supervisor
	Ir. MBA. K. J. Cowan,	TU Delft

This thesis is confidential and cannot be made public until June 13th, 2020, due to patent regulations.

TU Delft

Preface

The work hereby typed in words marks the end of the project which is my Master's thesis to graduate as an Space Engineer from the faculty of Aerospace Engineering at the Delft University of Technology. The months I have spent working on this project have made me find a new passion which I though I had , but never dared to test. The laboratory work on propulsion systems has presented to me like a breeze of fresh air in the university where I now have spent 6 years. The hours spent in the laboratory looking for an answer which I never thought I could find have taught me hard that sometimes, you need to embrace the unknown and keep trying. For this work, I must say that the words hereby written do not make justice to the hours and head puzzles I have gone through in the laboratory. Nonetheless, it would have not been possible without some of the incredible people I have found along the way and to who I want to dedicate some special thanks.

First and foremost, I need to thank my supervisor B. V. S. Jyoti for being the true fuel to this entire work. Her enthusiasm and relentless energy she transmits is a major reason for the success of this research work. With the fear to sound cliché, this would have not been possible without your guidance. She gave me the freedom to investigate out in the open research arena, guided the steps we took in the lab and always welcomed a discussion over a point. I cannot stress enough how much positive impact she had as a supervisor, the level of involvement she gave us on our work and the perks that came with it have been true motivators for this work. Furthermore, I would want to thank my laboratory partner and friend Pranav Gurumallappa. His dedication and involvement in this project have been essential for the level of depth we have achieved. His presence and positive attitude have also being the reason why I managed to spent so many hours in the lab without quitting. All the achievements done on patents, collaborations, budget allocations and scientific publications are both yours as the are mine. Likewise, I want to extend my thanks to Johan Bijleveld and the guys in the laboratory, Durga Marineli, Mr. Grashof and everyone. Their openness and help at the beginning of my work are the reason why this could be done in the first place. Without their understanding and technical support, this research was possible. Equally, I want to extend my gratitude to Mr. Norder for being so helpful with the equipment even when we were in different faculties.

Siguiente, quiero agradecer a mi familia su ayuda y apoyo inamovible sin importar cúando, cómo o dónde. A mi madre, a quién tantas veces me he quejado de las complicaciones técnicas que no podía entender. Y que sin comprender enteramente mis quejas, siempre me ha apoyado y empujando a seguir, gracias. A mi padre y a Patricia, por haberme empujado a continuar por un camino que en momentos no me pareció el adecuado, gracias. A mis hermanos, por su interés en mi trabajo y por entender mis necesidades cuando he debido de trabajar y no de pasarlo bien. A mi novia Ida, mi confidente y la mayor sufridora de mis quejas y tiempo invertido en este trabajo. Estuviste conmigo desde el principio de este trabajo y ahora los vemos terminar. Gracias por haber estado ahí.

To my friends, housemates and travel companions through our long and rough times in Delft. To Anthony, Jaime, Steph and Tino, you guys have suffered with me all the outcomes of these years and without you I would probably be insane by now. Thank you. To my good friends Pablo, Roberto, Vlad and Angel, for being there also at awesome times and at more delicate ones. The times we have spent together will always linger in mind when I look back at the time I spent in Delft.

"El que quiere algo conseguirá un medio, el que no, una excusa."

Jaime Quesada Mañas
Delft, January 2020

Abstract

With the boom of space activities in recent years and the increasing concern for clean technologies, green space propulsion is becoming a topic of interest within the space sector. Unfortunately, most of the propellants used for space activities tend to be highly toxic, corrosives, and even carcinogenic. Toxicity is especially critical for the hypergolics, which in most cases are the preferred propellant due to their simple application as they ignite upon contact. Throughout the history of space propulsion, some chemicals have been left aside due to their low performance when benchmarked against these more powerful hypergolic propellants. However, the trend of "green" technologies is pushing research towards green lower performance propellants. This is the case of hydrogen peroxide, H_2O_2 , which was left aside due to its reduced effectiveness and the complexity to exploit its energy.

Nonetheless, the work with hydrogen peroxide has recently acquired a new focus. Its green perspective has instigated large projects by the European Commission, such as GRASP, and approaches to exploit its energetic content are a topic of research. Currently, the use of catalysts to decompose the chemical is the usual procedure. However, their complexity and effect on performance raise some problems. In this thesis, a new approach through thermal energy supply aims at avoiding the catalyst approach to decompose hydrogen peroxide and overcome their related problems. The feasibility of this approach is tested and characterized for different combinations of temperatures and concentrations of hydrogen peroxide.

In order to characterize this, a first look into the procurement of the chemical is done. The different approaches presented lead to a successful refining technique, which is now patented. This innovative approach allows acquiring hydrogen peroxide in concentrations in excess of 99% in the span of 1-2 days for a reduced price. The simplicity of this technique is unrivaled to the stringent regulations surrounding its commercial availability. The resulting solution is investigated in terms of stability over time and concentration. The final selected concentrations for this study are 75, 80, 85, 90, and 95% H_2O_2 .

The thermal activation of hydrogen peroxide is first investigated. Through an open-air drop-test study, the droplets of H_2O_2 are generated and precipitated over a heating plate at various temperatures. The combinations of temperature and concentration, which lead to decomposition, are recorded and analyzed through a set of thermocouples and a high-speed camera at 6400 fps. For the valid combinations, the analysis returns their maximum temperatures and decomposition delay times. Values of up to 800°C for 90 and 95% H_2O_2 are achieved, and low decomposition delay times below 100 ms were measured for heating plate temperatures of 250 and 270 °C. This information is put against the decomposition with catalyst MnO_2 for comparison, showing a more significant temperature released for the thermal approach, but a slower decomposition.

With the valid decomposition combinations, an ignition study is conducted with ethanol as the fuel and hydrogen peroxide as the oxidizer. Through a drop test on a heating plate, the mechanisms leading to the ignition are researched. The tests showed that ignition is pseudo-hypergolic and can achieve increases in temperature of up to 700°C for 95% H_2O_2 and ethanol, reaching maximum temperatures over 1000°C at points. The tests showed that combinations with 90 and 95% H_2O_2 result on average ignition delay times below 100 ms. The conducted test cases showed that the ignition temperature profiles can be correlated with the recorded filming and that the lessons learned can be applied for a future combustion chamber. In order to test performance-boosting techniques, the gelling of the fuel was done and tested. The results are promising, the ignition of ethanol with 1.8% wt. of hydroxypropyl cellulose reached such temperatures that melted a thermocouple, proving the ability to raise the performance.

Lastly, the gel sample was characterized in terms of a rheology study by performing a strain sweep to find its yield point. Moreover, a shear rate analysis was performed, and its thixotropic nature was tested through a hysteresis loop. The effect of temperature was also analyzed and fitted to an exponential Arrhenius-like form.

Contents

List of Figures

List of Tables

List of Abbreviations and Symbols

Abbreviations/Acronyms

ADR	European Agreements Concerning the International Carriage of Dangerous Goods by Road
DAQ	Data Acquisition Card
DASML	Delft Aerospace Structures and Materials Laboratory
ESA	European Space Agency
EtOH	Ethanol
FM	Fumehood
FTK	Fine gauge K-type Thermocouple
GRASP	GReen Advanced Space Propulsion
HPC	Hydroxy Propyl Cellulose
HSP	High-Speed Camera
HP	Heating Plate
HPC	HydroxyPropyl Cellulose
HTP	High Test Peroxide
ICAO	International Civil Aviation Organization
IMO	International Maritime Organization
IQR	Inter Quartile Range
LIS	Light Source
LOX	Liquid Oxygen
MMH	Mono MethylHydrazine
MON	Mixed Oxides of Nitrogen
MSDS	Material Safety Data Sheet
NTO	Nitrogen Tetraoxide
PC	Personal Computer
RFNA	Red Fumming Nitric Acid
RGHP	Rocket Grade Hydrogen Peroxide
SYP	Syringe Pump
TNO	Toegepast Natuurwetenschappelijk Onderzoek
UMDH	Unisymmetrical MonoMethylHydrazine
VES	Borosilicate Vessel
WFNA	White Fumming Nitric Acid

Symbols

Roman

a	Density of water at selected temperature	[kg m^{-3}]
A	Pre-exponential factor	[-]
AOL	Active Oxygen Loss	[%]
C_i	Concentration of H_2O_2 at moment i	[%]
DDT	Decomposition Time Delay	[ms]
DDT_{DAQ}	Decomposition Delay Time according to DAQ	[ms]
DDT_{HSP}	Decomposition Delay Time according to HSP	[ms]
E_a	Activation energy	[J mol^{-1}]
fps	Frames per Second	[fps]
G'	Storage modulus	[Pa]
G"	Loss modulus	[Pa]
Isp	Specific Impulse	[s]
IDT	Ignition Delay Time	[ms]
k	Reaction rate constant	[-]
M	Molecular weight	[g mol^{-1}]
N	Number of moles	[mol]
n_D	Refractive index	[-]
OF	Oxidizer to Fuel ratio	[-]
R	Universal gas constant	[8.3145 J K^{-1} mol^{-1}]
t	Time	[s] [h]
T	Temperature	[K] [°C]
T_{HP}	Heating plate temperature	[°C]
$T_{decomposition}$	Decomposition temperature	[°C]
$T_{ignition}$	Ignition temperature	[°C]
T_{max}	Maximum temperature	[°C]
W_i	Weight at moment i	[kg]
Y_i	Yield at moment i	[%]
z	Mass fraction	[-]

Greek

ρ	Density	[kg m^{-3}]
η	Viscosity	[Pa·s]
η^*	Complex viscosity	[Pa·s]
τ	Shear stress	[Pa]
ΔH	Standard enthalpy	[kJ mol^{-1}]
$\Delta_f H$	Standard enthalpy of formation	[kJ mol^{-1}]
$\Delta_r H$	Standard enthalpy of reaction	[kJ mol^{-1}]

1 Introduction

This chapter provides an introduction to the research topic overall, with the purpose of situating the reader within the framework of the current study. Section 1.1 introduces the field of hypergolic propellants as the field in which this research has been conducted. The direction this research focuses on comprises Section 1.2, where the green approach is presented as a sub field investigated in this study. In turn, formal research questions and goals are presented in Section 1.3. Finally, a road map of this research is presented together with this report's structure in Section 1.4.

1.1. Hypergolicity within the space sector

Ignition design has long been a major focus for combustion chambers in propulsion systems. Such considerations are common in the spatial, automobile, aeronautical and maritime sectors alike. This key design factor is what enables energy contained within the propellant system to be exploited to propel, heat or generate auxiliary power. A range of methods exist to ignite propellants. Among these, hypergolicity (hypergolic propellant combination) is one of the most sophisticated propellant ignition methods. Hypergolicity avoids the need for an igniter, and instead involves the combination of two propellants - a fuel type and an oxidizer - causing spontaneous ignition upon contact.

Hypergolic propellant terminology came to the fore as early as 1930, with German chemists experimenting with hypergolic fuels and propellants during and throughout the early 1940s. The term derives from the Greek "work" and the suffix -ol, denoting the presence of alcohol. The concept / propellant have varied since, avoiding the need of alcohol compounds in the hypergolic ignition process. Some examples of hypergolic propellant combinations can be found in Table 1.1, where chemical siblings may also behave hypergolically, as with cases in the fluor family components. [8]

Corrosivity, toxicity and carcinogenicity are common among the propellants employed, which have made their usage within the sector a safety risk and, in turn, expensive to handle. This is the case for the hydrazines (UDMH, MMH, etc.), and nitrogen oxides (NTO, MON, etc.), among others. The fluoride family warrants special mention due to their highly toxic nature and outstanding reactivity with almost anything; so much so, that no real application has ever been successfully found for them. Conversely, some of the listed hypergolics such as cryogenic liquid oxygen (LOX) and hydrogen peroxide are relatively innocuous and are considered ''green" propellants within the sector [2] [18].

Table 1.1: Hypergolic propellant combinations. Adapted from [58]

Oxidiser	**Hypergolic with**
Oxygen	Triethylaluminium, Analine
Hydrogen peroxide (>60%)	Hydrazine hydrate
Nitrogen tetroxide (NTO), Nitric Acid, Mixed oxides of nitrogen (MON)	Hydrazine, mono-methylhydrazine (MMH), unsymmetrical dimethylhydrazine (UDMH)
Fluorine, chlorine trifluoride, difluor-oxide	Almost all fuels

Bearing this in mind, the application of hypergolic propellants in the space sector is nonetheless extensive and common. Among others, examples of missions that made use of hypergolic propellants are the Titan launcher families, the lunar descent vehicles in the Apollo missions, the Ariane 5 upper stages (Aestus engine) and multiple Russian engines [58].

1.2. Research gap: the green approach

As technology progresses generally and within the space sector, so does the concern for more sustainable engineering practices. There is an increasing push for greener gateways into space which aim at palliating the pollutant effects of hypergolic propellant combination, while retaining the advantages they offer by way of simplicity and performance [53]. To achieve this objective, green(er) propellants should be innocuous for humans to use and handle, avoiding current concerns regarding toxicity and carcinogenicity present in them. This trend can be visualized by the steady increase in scientific literature on or including topics on ''green propellants", which has risen from 13 in the 1990s, to 109 in the 2000s, to 346 in the 2010s[1]. A number of international organizations have advocated for a shift towards greener propellants in the space sector. The European Space Agency (ESA) for instance, has promoted conferences with this focus since 2001. Likewise, the European Commission allocated some 3.5 million€ in funding to its GRASP (GReen Advanced Space Propulsion) initiative (2008 - 2011) which sought to spur innovation in green propulsion technology and infrastructure programmes.

Although cryogenic such as LOX and liquid hydrogen do solve some of these problems, in turn they require of igniters and cryogenic handling, arising new problems. Consequently, finding new propellants which are harmless to handlers, but still are as useful as hypergolics is the new most desired space goal. For this goal, a clear candidate presents itself, which is highly concentrated hydrogen peroxide, known as High Test Peroxide (HTP) in Europe and as Rocket Grade Hydrogen Peroxide (RGHP) within American markets. These chemical is hydrogen peroxide with concentrations in excess of 70%. As it became clear from the findings in the literature study, Chapter 2, it is the green propellant with the largest potential and the center of this study. More precisely, the exploitation of this chemical Section 2.3 has been primarily studied using chemicals called catalysts. The science behind catalysts effect on HTP is solid and relatively well understood, however catalysts are still a complex promoter to HTP exploitation, having troubles with life cycle, cost and capacity. To solve these issues and others hereby presented in this thesis, a new approach is looked into: thermal activation for HTP exploitation. This narrow research gap has only been timidly explored. This research aims at providing a more clear understanding of its nature through experimental study framing it within the option of using HTP as a monopropellant and as a bipropellant in a future dual-mode propulsion system.

1.3. Research questions and goals

The research is always marked by the direction taken set in the research objective and question. In this section, this is formulated. Throughout the duration of this research, the analysis and characterization of a catalyst-free ignition of green hydrogen peroxide with ethanol is researched, including the production of the chemical as well as innovative approaches to boost the performance through gelling. However, to narrow down the exact direction the following is set as a the research objective:

> *The research objective is to test and characterize the feasibility of a catalyst-free dual mode system with High Test Peroxide as monopropellant and including ethanol for a pseudo-hypergolic bipropellant mode with the sole application of thermal energy.*

This objective is achieved by making use of the laboratory facilities present at the Delft University of Technology, while investigating innovative approaches of chemical procurement as well as preparing an efficient set up for both the monopropellant and hypergolic test within the given budget of 500€. This leads to the following research question for this thesis:

[1] From accessed data in Scopus

Is the use of thermal energy sufficient to achieve High Test Peroxide decomposition to allow for dual-mode system, as monopropellant and as pseudo-hypergolic bipropellant with ethanol, and if so, under what conditions?

To this research question, there are several variables which must be identified in this study to properly answer the conditions under which this is possible. First is the concentration of High Test Peroxide, as not all may be valid. Next, is the temperature needed to achieved this. Last, is the need to do this for both monopropellant and bipropellant. To put it into words, the following are the research goals for this study:

- **Procurement of H_2O_2 :** to procure HTP under the given budget through acquisition or production.
- **Thermal decomposition of HTP:** to provide a comprehensive and detailed study of the conditions and results of this approach, if feasible.
- **Pseudo-hypergolicity:** to prove and characterize that pseudo-hypergolicity is possible without catalysts with only thermal energy.
- **Characterization:** to provide a rationale of the understanding of the process for its later application in combustion chambers.
- **Performance boosting:** to give a preliminary solution to boost the performance of HTP through gellation.

1.4. Report structure

To address the research objective presented in Section 1.3, a research road map was established from the start to navigate this new field. This road map can be seen in Figure 1.1. Incidentally, out of this large road map, the first steps have already been taken within this research. Consequently, this report is structure in a way which follows the aforementioned road map. Firstly, a literature study was performed prior to this thesis investigation, the main results are presented in Chapter 2. Subsequently, the results of the research performed on HTP procurement are discussed in Chapter 3, where the shortcomings of finding the chemical and the solutions implemented are discussed. Having successfully found a way to obtain the chemical, the characterization and demonstration of its decomposition is shown in Chapter 4, these results present the accomplishment of thermal decomposition without the use of catalysts and the characterization of the process. Achieved this milestone, the bipropellant mechanism is studied through a hypergolicity study in Chapter 5 where HTP will be ignited together with ethanol and the results analyzed. Lastly, in an effort to get the system to the performance levels of conventional hypergolic propellants, gel propellants are researched in Chapter 6. The results presented will ease the studies on gelled hypergolic systems with hydrogen peroxide and ethanol through the gel characterization.

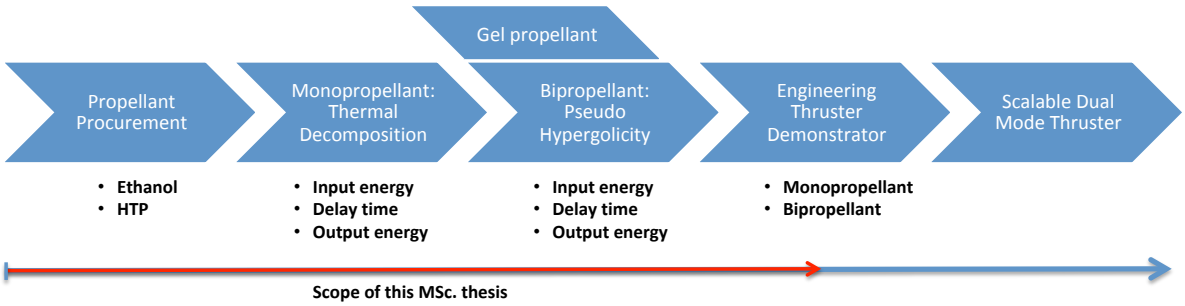

Figure 1.1: Roadmap in which this research fits in.

2

Literature study

In this chapter the results from the literature survey done to situate this research will be presented in a summarized manner. The full literature study is available upon request. Firstly, in Section 2.1 the paper of hydrogen peroxide within conventional oxidizers will be presented. Continuously, in Section 2.2 hydrogen peroxide will be looked into in more detail by providing its properties and background. After it, the processes needed to exploit the use of hydrogen peroxide as a space propellant will be summarized in Section 2.3. Later, the green effort to implement hydrogen peroxide with other fuel, in this case ethanol, will be presented by characterizing ethanol in Section 2.4. Lastly, the results of the literature discussing the benefits, mechanisms and approaches of gelling the propellants will be presented in Section 2.5.

2.1. Oxidizers: the green perspective

Following the literature study analysis of the green propellant initiative, a comparison of some conventional oxidizers with green options are provided in Table 2.1 under several criteria. The conventional oxidizers are White Fumming and Red Fumming Nitric Acid (WFNA/RFNA), which are blends with nitric acid with 90% excess of purity. Then Nitrogen TetraOxide (NTO) is a nitrogen oxide with hypergolic properties and extensively used as it is the case for the european space vehicles. Ammonium-based oxidizer includes ammonium perchlorate, ammodium dinitramide and ammonium nitrate, lastly another researched oxidizer in the past was the flour-containing oxidizers. These last include chlorine pentafluoride and chlorine trifluoride. On the green oxidizer side, two components are use as example, these are hydrogen peroxide and liquid oxygen [53]. In order to compile the main findings of the literature survey, 5 criteria are used. First, toxicity is understood as the possibility to incur into health issue both for humans and the environment. Performance refers to its ability as an oxidizer allowing combustion of a given (suitable) fuel. Availability refers to the possibility to obtain such an oxidizer for a potential thesis research on the topic. Safety refers with the measures needed to store and handle the oxidizer, lastly the cost is also a factor to take into account and it is thus represented in the comparison.

Table 2.1: Qualitative comparison of convenitonal oxidizers with green oxidizers. From [58], [12], Sigma Aldrich and Merck

	WFNA/RFNA	**NTO**	**Ammonium-based**	**Fluor-containing**	**Green oxidizers**
Toxicity	Toxic/Strong acid	Toxic Burn skin and toxic fumes	Moderately toxic	Highly toxic and lethal	Low toxicity
Performance	High and hypergolic	High and hypergolic	Medium	Very high	Medium (HTP) High (LOX)
Availability	Not easy, usually in-house formulated	Not easy	Relatively easy to obtain	Unavailable commercially	Relatively easy to obtain
Safety	High reactions with several daily components	Good as liquid, not flammable	Needs special handling	Extremely reactive and hazardous	Some may be explosive Some require cryogenics
Cost [FY2004 $/kg]	560 [per L]	40.8	300	Unavailable	0.01-0.13 (LOX) 2-3 (HTP)

As it can be seen from the qualitative comparison of the oxidizer in Table 2.1, the main disadvantage of

green oxidizers in general is the performance. Although for liquid oxygen the performance is high, the need for cryogenics makes it use quite complex. Moreover, exotic approaches for water propulsion using electrolysis prove to be a clear complexity barrier unrecoverable [19] Furthermore, the low toxicity, ease of availability, low cost and relative safety makes green propellants the best option to pursue for a thesis research. Previous research has focused on finding suitable monopropellant substitutes for hydrazine as well as bipropellant solutions [18]. The options which have been proposed and further researched are hydrogen peroxide, nitrous oxide fuel blends and ionic liquids.

When comparing these three, it is worth mentioning that hydrogen peroxide is the most researched of the three. Its use dates back to the V2 German rocket back during the WWII [47]. Since then, extensive studies have been done on its suitability as both a monopropellant fuel as well as an oxidizer in a bipropellant system. On the other hand, nitrous oxide fuel blends have been less researched than hydrogen peroxide although they have a large heritage as oxidizer for hydrazine and show potential as low cost, low toxicity and high performance bipropellant option. The last are the ionic liquids, the three most researched are: HNF (hydrazinium nitroformate), HAN (hydroxylammonium nitrates) and ADN (ammonium dinitramide) [18] [9]. These are by definition salts with melting point below 100°C, they usually incorporate fuel, a oxidizer salt and water, however they incur in higher costs of propellant and thruster. These complex organic molecule lead to larger molecular weights that ultimately increase the exhaust gases temperatures. This temperature increases result in drastic reductions in catalytic igniter lifetimes. At the same time, they require increase in manufacturing costs of valid materials that can incorporate cooling mechanisms [11]. Furthermore, when comparing ionic liquid salts with hydrogen peroxide, the only advantage of the former is shows larger performance [19]. On the other hand, when comparing hydrogen peroxide with NTO, it shows economic benefit on the propellant price as well as with the handling during launch at the expense of a 20% reduce in nominal propulsive performance [19]. Nonetheless, the volumetric specific impulse is larger given its higher density [11].

Thus, the easy handling, low toxicity and low cost of hydrogen peroxide makes it the most suitable candidate for a potential experimental research work at university level [56]. Moreover, the improvements in storability since it started being use as a propellant are large [54]. Nonetheless given that the performance of HTP in monopropellant mode (160-185s) [19] is relatively low, a fuel can be added to increase the performance. As it came from the literature study, ethanol is a suitable candidate for this approach, being easily accessible, non-toxic and with promising performance capabilities [56].

2.2. Hydrogen peroxide

In this section hydrogen peroxide as a chemical is looked into. First, a historic overview is provided. Subsequently, the properties of the chemical are summarized. Lastly, the legal framework for its accessibility is presented.

2.2.1. History overview

The characteristics of hydrogen peroxide as a high energetic liquid have been known for long time, dating its first application to WWII Germany. Then, 80% hydrogen peroxide was used to drive the turbo pumps of the V2, the first of its kind long-range ballistic missile, by decomposing it with potassium permanganate, a catalyst of HTP . Application of this technology after the war were only tested as exotic approaches within the US for their "AR" family of rocket-assisted planes, using over 90% concentrated HTP as well as for some turbo pumps. In the UK, the Black Knight program developed up to 10 engines which used HTP to be mixed with kerosene after decomposition through silver catalyst for launcher vehicle purposes [54]. Finally, the appearance of hydrazine and its improved performance with respect to HTP, displaced HTP from the cutting edge propellant world. Also for bipropellant systems, the appearance of liquid oxygen provided better performance. The last application was non-cryogenic bi-propellant systems, which also replaced HTP with the development of hypergolic reactions between NTO and hydrazine[54]. It is only recently that its green perspective, low toxicity and performance characteristics as an oxidizer for bipropellant systems starts gaining popularity.

2.2.2. Properties

Hydrogen peroxide (H_2O_2) is a chemical where three covalent bonds exist, one between the oxygen and 2 between hydrogen and oxygen atoms. When it comes to the chemical itself, the most important parameter is the concentration of the solution. Because pure hydrogen peroxide rarely exists in nature as such, hydrogen peroxide is most commonly measured in a percentage of concentration in aqueous solutions, where the

solvent is water (H_2O). Nonetheless, the properties for anhydrous hydrogen peroxide, at 100% concentration, can be seen in Table 2.2, where the physical properties are shown and should be taken with care as they are commonly extrapolations from lower concentration solutions. Consequently, it makes more practical sense to talk from the point of view of hydrogen peroxide *at a given concentration.* This parameter determines most of the properties of the final solution and most interestingly the energetic content of the chemical.

Table 2.2: List of general physical properties of anhydrous hydrogen peroxide at 1atm and 20°C. From [47].

H_2O_2 physical properties (pure)	
Property	**Value**
Formula	H_2O_2
CAS number	7722-84-1
Color	Pale blue
Odor	None
Molecular weight	34.016 g/mo]
Density	1.450 g/cm^3
Viscosity	1.245 x10^{-3} Pa·s
Melting point	-0.43 °C
Boiling point	150.2 °C
Standard heat of formation in vapor phase	136.15 kJ/mol
Vapor pressure	181.31 Pa
Refractive index	1.4084 -
Energetic content	6 MJ/L

Figure 2.1: H_2O_2 bond

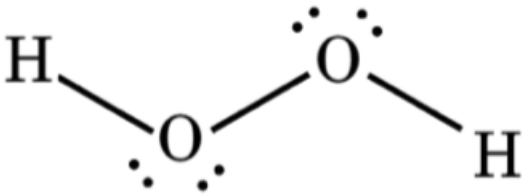

Another important characteristic of hydrogen peroxide is its degradation process, in which the concentration of the aqueous solution slowly reduces with time. For this, stability studies are carried in which the concentration decrease over time periods is studied. The accepted decomposition rate of HTP is around 1% per year at ambient temperature, however this value can be lowered down to 0.01-0.02% per year. A figure of merit to characterize this slow decomposition is the Active Oxygen Loss (AOL), Equation (2.1).

$$AOL = \frac{C_1 \cdot W_1 - C_2 \cdot W_2}{C_1 \cdot W_1} \cdot 100 \tag{2.1}$$

Where AOL is the active oxygen loss [%] C_1 and C_2 are the initial and final concentrations of hydrogen peroxide solution [%] and W_1 and W_2 are the initial and final weight [kg] of the hydrogen peroxide solution. The three factors affecting this rate are the initial concentration and impurities, the temperature and the characteristics of the container. In fact, for larger concentrations the rate of decomposition decreases, as purity is larger for higher concentrations, the rate of decomposition is 2.3 times as the temperature increases by 10K and the material of the contrainer has a significant effect on this parameter likewise [15]. Advancements by NASA and others are presenting a brighter future for the storability of this chemical for extended periods of time. In fact long-term periods are currently being pushed to up to 15 years without significant decomposition. It is argued that the increasing purity of the chemical can increase the storability to 2 to 10 times of the current levels [55] [1]. The most common materials employed for storage of HTP are aluminium alloys with low copper content such as 1060 and recent investigations for aluminum-magnesium alloys as well. The work with pyrex, borosilicates and teflon is also advantageous given their inert nature, being specially interested from the laboratory point of view. [47].

2.2.3. Accessibility status

Hydrogen peroxide is subject to many regulation agreements which affect its procurement, transport and packaging. These include rail transport (RID), road transport (ADR), sea transport (IMO) and air transport (ICAO) within the European Union. In terms of research, the quantity needed for experimentation is usually small, and thus road is the normal mean of transport. In this case, concentration of hydrogen peroxide

plays an important role on the exact regulation. The applicability can be seen summarized in Table 2.3. For concentrations below 8% no regulation applies, however as the value goes up the regulations becomes more strict. In fact over 60% a dedicated transport is needed. The investment for this kind of transportation is costly and dwells in time given the required bureaucratic measures. This is the first problem to overcome to perform research with this chemical product.

Table 2.3: Regulations applicable to hydrogen peroxide as a function of concentration. [41]

ADR		ICAO	
% by wt.	**Regulation**	**% by wt.**	**Regulation**
8-20	5.1, UN 2984, PG. III	8-20	5.1, UN 2984, PG. III
20-60	5.1, UN 2984, PG. II	20-40	5.1, UN 2984, PG. II
>60	5.1, UN 2984, PG. I	>40	Prohibited

2.3. The exploitation of hydrogen peroxide

Arguably the most interesting characteristic of hydrogen peroxide is its decomposition reaction. The capabilities of this process are well known and are the reason why this chemical is useful in a dual mode: as a monopropellant and as a bipropellant. This reaction can be seen in Equation (2.2). In this reaction two important elements are to be noticed, firstly the release of heat energy through an exothermic reaction, which allows for gaseous exhaust proving the system to be a possible monopropellant. Likewise, the exhaust of oxygen is a necessary supply for a bipropellant mode, making the chemical a valid oxidizer in this case.

$$H_2O_2(aq.) \longrightarrow H_2O(l) + \frac{1}{2}O_2(g) + \Delta H \tag{2.2}$$

This reaction is irreversible and exothermic liberating heat energy in accordance to a heat of decomposition (ΔH) of -23.45 ± 0.03 kcal/mol or -98.1 ± 0.13 kJ/mol for 100% hydrogen peroxide at 1atm and 25°C from linear extrapolation [22] [47]. In general the energy released is taken by the liquid water product to change phase, reducing the available energy liberated, but producing gaseous exhausts.

The question to pose now is how can this reaction be started and controlled. From the literature survey two main approaches are used: using catalyst and using thermal decomposition. Catalysts are chemicals which help the reaction to take place at lower activation energies. Their role is reducing the required activation energy to start the reaction without actively participating in it. The figure of merit used for catalysts is the as reaction rate constant, $k[-]$, defined within the Arrhenius equation Equation (2.3) as the value characterizing the rate of a chemical reaction. On the other hand, as it can be seen from Equation (2.3), temperature also has an effect on the final reaction rate constant. As the energy supplied to the reactants is larger, the speed of the reaction increases, which shows how with enough energy this reaction can also be started. Nonetheless, it has been mainly done with the use of catalysts, as thermal decomposition in comparison has been defined as much slower and unable to compete [5] [15].

$$k = A \cdot \exp\left(\frac{-E_a}{RT}\right) \tag{2.3}$$

Where k [-] is the reaction rate constant, A [-] is the pre-exponential factor which is a particular constant to each reaction, E_a is the activation energy [J/mol] and it is the energetic barrier to overcome to start the reaction, R is the universal gas constant [8.3145 J/K mol] and T [K] is the temperature at which the reaction takes place.

Several types of catalysts are used across literature. These includes MnO, MnO_2, $CuCl_2$, $CuCl_2H_2O$, Ag, Pd, Co, $C_10H_{14}MnO_4$, Pt, Ir among others. Being MnO and MnO_2 amongst the most popular ones given their elevated performance and relative low cost when compared to other more exotic options [5] [48]. In order to implement the use of catalysts within space propulsion systems, several were found. Firstly, the creation of catalytic beds are the most common approach used for HTP decomposition in propulsion systems. A catalytic bed is a web-like cylinder pipe at the beginning of the combustion chamber to force the HTP to flow through it and subsequently decompose before being injected, a exemplary design can be seen in Figure 2.2. In this

system, catalysts are placed in the form of coatings of the monolith or as pellets supported by a web-like structure. Catalytic beds have the advantage of allowing bi- and monopropellant propulsion at the expend of being the "most significant technology challenge in the realization of hydrogen peroxide" thrusters [11]. Moreover, they pose several performance disadvantages such as increase in size of combustion chamber, large pressure drops and capacity limitations for full decomposition of HTP. Conversely, adding the catalyst onto the fuel in a bipropellant case allows for pseudo-hypergolic system, where the HTP is decomposed at the same time it is provided with fuel to ignite. These approach was the first to be put into place with the famous case of Block 0 fuel, a mix of methanol and manganese (II) acetate tetrahydrate developed by the US Naval Air Warfare Center Weapons Division at China Lake [20]. This practice was also employed in recent studies with the use of gels, where the catalysts were better suspended [28] [29] [39] [48]. Although advances have been made in this field, poisoning of the fuel and catalysts due to extended time periods of contact is a notable disadvantage of this approach. Likewise, the addition of heavy molecular weight particles has a detrimental effect in the specific impulse, Isp [s]. The last approach found is more exotic, in which catalyst is released as third propellant to the combustion chamber in a catalytic igniter manner. This approach has only been contemplated as a possibility and not put into place [38].

Lastly, thermal activation has been proposed across literature with one special research effort performed at the Institute of Aviation in Poland. Researchers here studied thermal decomposition on 98% hydrogen peroxide with a closed chamber vessel [46]. However the publication leaves still numerous open questions and lacks proper characterization of the process in terms of decomposition time delay (DDT) as well as missing the bipropellant scope. The work they performed was further extended to the design of the first thermal decomposition monopropellant for 98% HTP [37], this can be seen in Figure 2.3. Their results are to be taken with caution, given the lack for specific information concerning the power supply which is suspected to be unfeasible for some designs.

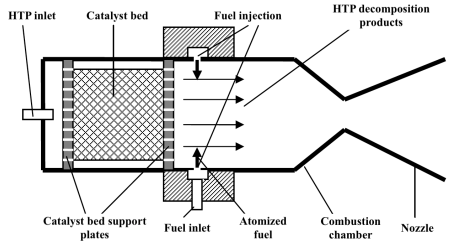

Figure 2.2: Catalytic bed schematic lay-out. From [56].

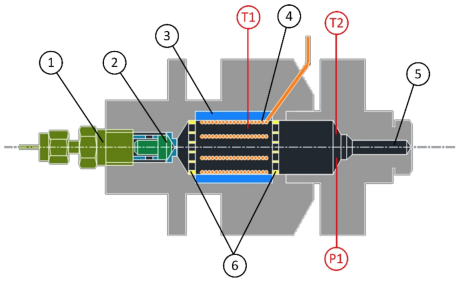

Figure 2.3: Schematic of thermal decomposition approach. From [37]. 1-HTP connector, 2-Injector, 3-Ceramic insulator, 4-Heating coil, 5-Nozzle, 6- Holding plates, T1, T2-Temperature ports, P1-Pressure port

2.4. Green effort: hypergolicity and ethanol

In this section, the green aspects and hypergolicity are discussed. Although they may seem as counter opposing concepts, the efforts to find their meeting points are gathered. Secondly, the properties of the fuel to use for this research, ethanol, are given.

2.4.1. Hypergolicity and green aspects

The study and search for green hypergolic propellant has lead to extensive research with hydrogen peroxide. Although most of it has focused on the properties of hydrogen peroxide as a pseudo-hypergolic. This is because hypergolicity of HTP has always been questioned to be rather marginal [15]. However it is due to its large temperature rise that it can achieve the autoignition temperature of some fuels, leading to their combustion. In this quest to replace the current hypergolic propellants such as NTO/Hydrazine, research is focusing in achieving hypergolicity with green propellants. In the case of HTP when used as an oxidizer, the search of fuels which have been used in combination with HTP are kerosene [50] [14] [24], ethanol [31] [26] [7] [32], methanol [23], JP-A [43], JP4 [52] or ethanolamine [36] among others. The final decision was to carry on exploring ethanol as the fuel, given its suitability as a green propellant, its possibility to be generated from biomass and, specially, the easiness of procurement for initial studies within this thesis.

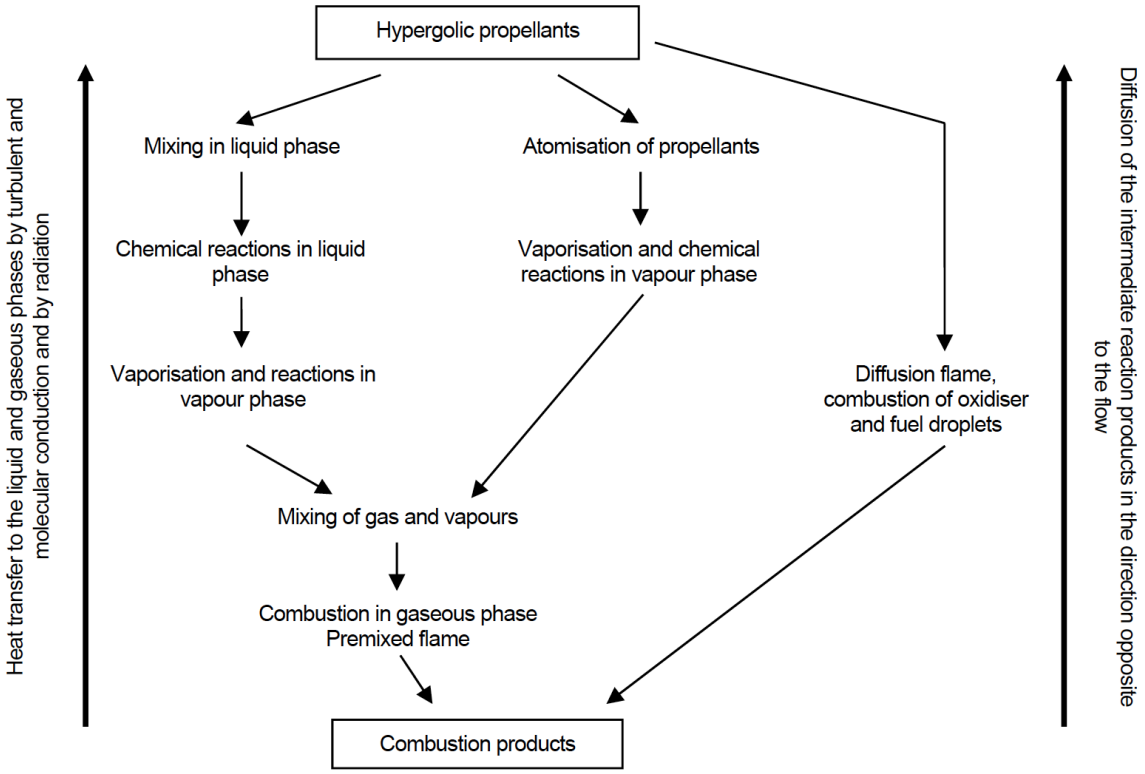

Figure 2.4: Hypergolicity processes involved in combustion of different hypergolic propellants. From [58].

Moreover, the understanding for hypergolic processes was researched. In Figure 2.4, the processes involved in the hypergolic ignition are presented as published by [58]. As it can be seen, hypergolicity does not require of igniter, instead the approaches are three. The first is by having the propellant mixing in liquid phase, when they start to react, vaporize due to the energy released in their reaction. At this stage, the reacting species mix in both liquid and gaseous which leads to combustion. The other approach is to atomize the propellant prior to mixing, when they already start to reach in both vapor and liquid phase right away. The next steps are similar to the first approach. The last approach, happens when the already started flame diffuses the energy back to the incoming propellant and starts the ignition of the droplets. This also leads to sustained combustion. In general, it is the unsteady nature of the chemicals involved in the propellant that allow for this reactions to take place. Unfortunately, this same unsteadiness responsible of hypergolicity is the cause of the dangerous effects of the propellants.

2.4.2. Ethanol properties

Ethanol is a hydrocarbon molecule with a clear color, distinctive odour and with volatile and flammable properties. The use of ethanol as a fuel for thruster applications dates back to the early days of rocketry, when the Germans would fuel their missiles with a mix of it and liquid oxygen as oxidizer, namely the V2. Since then, its use in combustion engines has been left aside given that its heat of combustion is less than 2/3 of that of kerosene/gasoline. However, due to the recent trends in green propellants its becoming increasingly researched as a possible fuel for thrusters. This couples up to the advances in its production which even enable the option to produce it from biomass sources. Some of the physico chemical properties of ethanol are given in Table 2.4.

Table 2.4: Ethanol physical and chemical properties at 1 bar and 293.15 K unless indicated. [58][21] [49]

Pure ethanol properties	
Property	**Value**
Molecular formula	C_2H_5OH
Molecular weight	46.069 g/mol
CAS number	64-17-5
Flash point	14°C
Boiling point	78.3-78.5 °C
Density	789-792 kg/m^3
Heat of vaporisation	842-930 kJ/kg
Autoignition temperature	365-425 °C
Flame temperature	1930 °C
Enthalpy of combustion (LHV)	1366.95 kJ/mol 26800-27000 kJ/kg
Viscosity	0.0017 Pa·s
Thermal conductivity	0.14 W/(m K)
Energetic content	26.8 MJ/kg

In the field of space propellants, the term green makes reference to the non-toxic, non-carcinogenic and non-corrosive nature of the propellants. In this context, the exhaust of combustion products such as CO_2 or H_2O are within the green scope, as opposed to other fields such as automotive. The magnitude of this green approach is twofold, first, the toxic impact is substantially reduced, but secondly, the resource investment required to work with this chemical is also largely reduced [2].

2.5. Performance booster: gelling

Unfortunately, hydrogen peroxide has in general a medium to low performance, achieving and Isp maximum of 150s [58] and with ethanol of up to 270s in best case scenario circumstances [56]. A solution to overcome this problem would be the addition of energetic nanoparticles, which unfortunately resembles dangerously the situation of blending catalysts into fuel, which leads to poisoning effects. The other solution hereby researched is the change of phase of the fuel, namely by gellation. Gel is the term used to refer to a viscoeslastic fluid which exhibits behavior of both a solid-elastic material and a highly viscous liquid. The reason why gels can behave in this dual way is due to the cross-linking existing within its molecules which leads to a 3D network. In order to achieve this, gels are composed of two main elements: the solvent and the gelling agent. The solvent is the chemical which will be gelled and the gelling agent is the chemical which allows to create the aforementioned 3D cross-linking network. The gelling agents can be inorganic, being silica the most common on propulsion applications, and organic which tend to be derivatives of cellulose, an example is HPC (hydroxy propyl cellulose) [35].

The addition of gelling agent to the liquid is normally indicated as percent weight of the parent liquid. Normal percentage weights vary from 2% to 10%. As expected, the larger the weight percentage, the more intense the solid-like properties. In fact, there exist what is known as the critical concentration, at which the liquid is no longer flowing and it resembles more a gel than a liquid. This distinction is done qualitatively in most cases as no strict boundary exists common to all solvent [59]. When it comes to gelling agents, the main distinction to make is their nature. Gelling agents can be organic or inorganic. The difference between the two is the presence of carbon atoms in their formula or not, however the implications are of more importance. While organic gelling agents can be burned together with the fuel in the reaction, the inorganic agents cannot be and thus do not contribute to the combustion energy release. It has also been pointed out that the fact that inorganic gelling agents do not burn, can clog the catalyst bed [48]. This effect can even be detrimental if it deposits on the walls of the combustion chamber. Thus organic gelling agents are in principle preferred over inorganic. An overview of some gelling agents can be found in Table 2.5. A large compilation of the combinations of gelling agents and fuels is given in [22].

Table 2.5: Overview of some organic and inorganic gelling agents used through literature

Organic		Inorganic	
Name	**Used where**	**Name**	**Used where**
Hydroxypropyl cellulose (HPC)	[35] [39]	Fumed Silica	[35] [29] [3]
Hydroxyethyl cellulose (HEC)	[35]		
Hydroxypropyl Methylcellulose	[34] [25]		
Polyvinylpyrrolidone (PVP)	[29]		
Methyl cellulose (MC)	[27] [29]		
Propylcellulose	[28]		

After the results of the literature study, it is clear that the molecular weight of the gelling agent plays an important role in the gelling agent concentration. It is thus decided to use a high molecular weight. Also alcohol family chemicals work well with cellulose derivative gelling agents. The use of HydroxyPropylCellulose (HPC) was finally chosen for this study. It will form a gel easy to tear apart during a future injection process and making the gel more viscous easily. For future work, HTP should be gelled with an inorganic gelling agent, namely SiO_2.

3

H_2O_2 acquisition and procurement

In this chapter, the first step in the roadmap of Figure 1.1 is presented. Acquiring this chemical was the first step in the research work and proved to be a vital one as well. As it was found from the literature study Section 2.2.3, HTP is a dangerous chemical highly regulated and hard to obtain. Consequently, the steps taken to procure it finally were a substantial part of this research now laid-out. Firstly, the apparent approach of obtaining it from commercial suppliers was explored in Section 3.1. After it was found not to be possible, in-house refining processes started, where the first technique is presented in Section 3.3, unsuccessful. It was not until an innovative solution was discovered, Section 3.4, that HTP was obtained; this approach resulted in a patent filing. Lastly, a stability study was performed along with the research to characterize the decomposition of HTP Section 3.5.

3.1. Suppliers

The production and commercialization of hydrogen peroxide at propulsion levels in the European Union is scarce. Although several suppliers exist for lower hydrogen peroxide concentrations: Solvay Interox and Arkema in France, Degussa in Belgium, or Kemira in Sweden, the higher concentration levels are harder to find and acquire due to stringent regulation (ADR, ICAO). Fortunately, the European Commission had already funded a large project where HTP was needed; this is Project GRASP. During the development of Project GRASP, the supplier of HTP was Evonik Industry AG. a German chemical producer that supplied the hydrogen peroxide for the research in the project at a concentration of 87.5%. The supplied HTP was under the brand name Propulse, which bears a specific combination of stabilizers, nonetheless Evonik now also supplies HTP in other quantities to specific customers. They are the first point of contact for the procurement of the chemical. After contact with the company, two products were available from their end: PROPULSE®825 HTP with a purity of 99.999% and a concentration of 82.5% and PROPULSE ®875 at a concentration of 87.5%. Both chemicals were only offered in 1.25L aluminum bottles. However, we initially inquired for small quantity 0.15-0.2 L. Additionally, the regulations were introduced (UN2015) as well as the German "Chemikalienverbotsverordnung" by which an explanation of the intended final use and a stamp of the company are required. The final quotation rose to a minimum sampling cost of 2500€ including packaging and freight transport in a dedicated vehicle.

Fortunately, there is another supplier with a lower profile and more affordable cost. A laboratory in Poland which now commercializes under the name Jakusz Spacetech [1] also supplies hydrogen peroxide in concentrations ranging from 85-98%. They were the second point of contact for the procurement of hydrogen peroxide. After the contact with their sales office, they provided a quotation of just 119€/kg of up to 98% HTP. Nonetheless, they pointed out that due to ADR regulations, HTP transportation is costly and that even for 1 kg an entire truck is normally needed. They rated transportation costs at around 1000€ to The Netherlands. Similarly, they offered a chemical analysis of the HTP for an extra 1000€. Consequently, in this case, the HTP at 98%, which we could later reduce in concentration for our desired levels, was a more attractive option as opposed to Evonik. However it was still unaffordable within the budget limitations of this thesis set at 500€.

Lastly, the option to inquire to research institutions who had worked with HTP was explored. For this, Toegepast Natuurwetenschappelijk Onderzoek (TNO) was contacted through one of its employees who pre-

[1] http://jakusz-spacetech.com/en/offer/hydrogen-peroxide/. Accessed on 15/07/2019.

viously worked on a similar topic within his thesis at Delft University of Technology. Unfortunately, the inquiry was not fruitful. Leftover HTP from past years (87.5-90%) could not be readily given away without taking ADR into account, and the inquiry did not make it any further[2]

Finally, the supplier option was turned down as being unfeasible within the framework of this thesis. A summary of the supplier options can be found in Table 3.1. Instead, the in-house refining of commercially available 30% hydrogen peroxide was chosen as the path to move through. 30% hydrogen peroxide was already available from the Logistic and Environment chemical storage upon request and payment.

Table 3.1: Summary of supplier possibilities.

Supplier	Possible?	Min. quantity	Total price
Evonik Industry AG	End-use certificate required	1.25L	2500 €
Jakusz Spacetech	Yes	1kg	1190 €
TNO	No	-	-

3.2. Instrumentation for in-house refinement

Given the unaffordability of the purchasing HTP from European suppliers nor research institutions, an in-house approach was taken. Although HTP is highly regulated, lower concentrations of hydrogen peroxide are common and relatively easily accessible. Consequently, refining hydrogen peroxide from available concentrations (30%) to propulsive concentrations (>70%) was explored. The work performed for the refining of hydrogen peroxide, as well as subsequent testing, was done in the Delft Aerospace Structures and Materials Laboratory (DASML). The DASML has access to chemical, physics lab as well as diverse instrumentation, which helped perform this study. The involved instrumentation in this phase was: hydrogen peroxide at 30% from Merck/Sigma-Aldrich, a Data Acquisition Card (DAQ) National Instruments 9219, one k-type thermocouple, liquid nitrogen, a handheld, and an Abbe refractometer.

Table 3.2: Instrumentation items used for refining and stability study

Instrumentation inventory			
ID	**Item**	**ID**	**Item**
PP	30% H_2O_2	KTH	K-type thermocouple
DAQ	DAQ NI-9219	LN2	Liquid N_2
HRE	Handheld refractometer	ARE	Abbe refractometer

The hydrogen peroxide used was procured from the Logistics and Environment building within the Delft University of Technology. Merck, previously known as Sigma-Aldrich, manufactures the chemical. It is at a concentration of 30% and is commercialized under the Perhydrol® trademark in volumes of 1L, and it will be used as the parent propellant (PP). After an inquiry to Merck, they indicated that it has an estimated 25 - 30 ppm of 2,6-Pyridinedicarboxylic acid, a conventional stabilizer for temperature effects on hydrogen peroxide. The k-type thermocouple (KTH) was procured from the available thermocouples within the laboratory. The general specifications for k-type thermocouple are a temperature range from -270 to 1260 $°C$ with an accuracy of around 2 $°C$. In particular, this thermocouple was calibrated to 100$°C$ and 0$°C$ with boiling and melting water with successful accordance to $\pm 3°C$. Moving on to the DAQ, it is a necessary piece of equipment to read the thermocouple voltage variation with temperature. The procured DAQ was available in the lab and is a National Instruments 9219, with up to 4 channels of thermocouple readings and a maximum reading rate of 60Hz. It is managed through LabView 2017 on Windows 10 running on a 2.6GHz Intel Core i5 of a MacBookPro 2013. The liquid nitrogen (LN2) is also available within the lab and is class 5, with a purity of 99.999%. Moving on to the refractometers. These are instruments that measure the refractive index of fluids. The handheld refractometer (HRE) was used initially. The HRE is commonly used to determine the sugar content in honey. It has a range of 0-32 Brix with a resolution of 0.1 Brix, and this translates to 0-72.8% and 0.2% of H_2O_2 concentration and resolution, respectively. A similar approach has been used by other

[2] It was later heard that TNO had trouble discarding the leftover HTP, which was there from previous bulk orders to other suppliers, due to its regulated nature. Even the transport from their old to a new location was troublesome.

researchers to characterize H_2O_2 concentration[17]. Lastly, an Abbe refractometer (ARE) offers a more scientific approach to determining the refractive index of substances. It was provided by the Applied Sciences faculty and included a thermometer also to measure the temperature of the sample investigated. The Abbe refractometer has a measuring range of 1.30-1.71 [-] with scale division of 0.0005 [-] and reading accuracy of 0.0002 [-] This translates to the full scale of concentrations (0-100%) and a resolution of 0.2%. Both refractometers have been calibrated to 1.3333 for distilled H_2O. Consistently, the measurements were taken at 20° C, as the temperature has a noticeable effect on the refractive index. An image of the HRE and the ABE can be seen in Appendix C.

3.3. Refining approach 1: freezing method

After extensive research done on the physiochemical characteristics of hydrogen peroxide and the possible approaches, action was taken. The first found solution is the freezing method.

3.3.1. Theory

The freezing method is no new approach, already discussed in early literature for small quantities [47]. The theory behind is to exploit the difference in melting temperature between water and H_2O_2 and freeze the water within the solution, leaving the hydrogen peroxide in liquid form. While water freezes at 0°C at 1 atm, H_2O_2 freezes slightly below at -0.43°C; this is the temperatures for pure substances, however, when in aqueous solution, their freezing values vary. Making use of this melting point difference, water can be frozen and removed while keeping the liquid H_2O_2. For this, it is necessary to look into the phase diagram of the chemical Figure 3.1. As it can be seen the freezing point varies with concentration starting at 0°C for pure H_2O to -0.43°C for pure H_2O_2 . It shows a dip in freezing point, which goes down to around -52.5°C at 46% H_2O_2 before reducing the slope of reduction in freezing point. It still decreases down to a minimum of -62.5°C for 61% H_2O_2 . Passed this point, the freezing point increases to the freezing point of pure H_2O_2 (-0.43°C). Different phases of the aqueous solution coexist together for a different combination of concentration and temperature; the white boxes indicate these. Here is of particular interest the crystal formulation of $H_2O_2 \cdot H_2O$, which happens in the region marked with a red cross as well as when the aqueous solution is supercooled below -62.5°C. This ideal behavior is, of course, for a pure substance without the presence of stabilizers, this is unfortunately never the case. These have an unknown effect on the phase diagram freezing line.

The importance of the crystal is superlative, as it means that the two chemicals, H_2O_2 and H_2O, will be fused in solid form, making it impossible to separate them physically. In this case, it is of interest to know what exactly would the concentration of a fluid with only this crystal. The final solution will have one molecule of H_2O_2 per 2 molecules of H_2O, from which we can calculate the final concentration. The final concentration is found to be 48.5%, as shown in Equation (3.1). This represents the theoretical maximum achievable with this approach.

$$\text{Final}\%wt. = \frac{\text{mol weight}\,(1 \cdot H_2O_2)}{\text{mol weight}\,(1 \cdot H_2O_2 + 2 \cdot H_2O)} = \frac{34.0147[g]}{34.0147 + 2 \cdot 18.0152[g]} = 48.5\% \tag{3.1}$$

3.3.2. Application

Moving on to the application of the theoretical background, the procedure is numbered in Figure 3.1. The feedstock chemical to which there is access is 30% hydrogen peroxide Perhydrol® from Merck. The Material Safety Data Sheet (MSDS) can be found in Appendix C. Consequently, the initial concentration of the feedstock is 30%. This is number one in Figure 3.1. In order to start eliminating water, the temperature of the liquid has to be brought down to -25°C, at point 2. Below this temperature, the solution will have floating traces of frozen H_2O to be removed manually with the help of a glass rod. This way, the concentration of the solution itself will differentially increase as so will the freezing point up until point 3, where the first crystal forms. Consequently, this approach can only reach to 48.5% hydrogen peroxide according to its phase diagram and Equation (3.1). From here, the next steps are unclear, but this first effort was deemed necessary.

To achieve the decrease in temperature to such low values, liquid nitrogen was used. Liquid nitrogen (N_2) boils at a temperate of -195.79°C, which is below the temperature we need; consequently, the application must be in a controlled manner. For this, a small quantity of H_2O_2 30% is placed in a sample vessel. For the initial experiments, a quantity of around 20mL was used. The vessel is later placed inside a container where the liquid N_2 is poured in a Bain-Marie manner. During this process, an ordinary k-type thermocouple attached to a DAQ NI9219 ran through LabView on a PC is used to monitor the temperature of the H_2O_2 . The

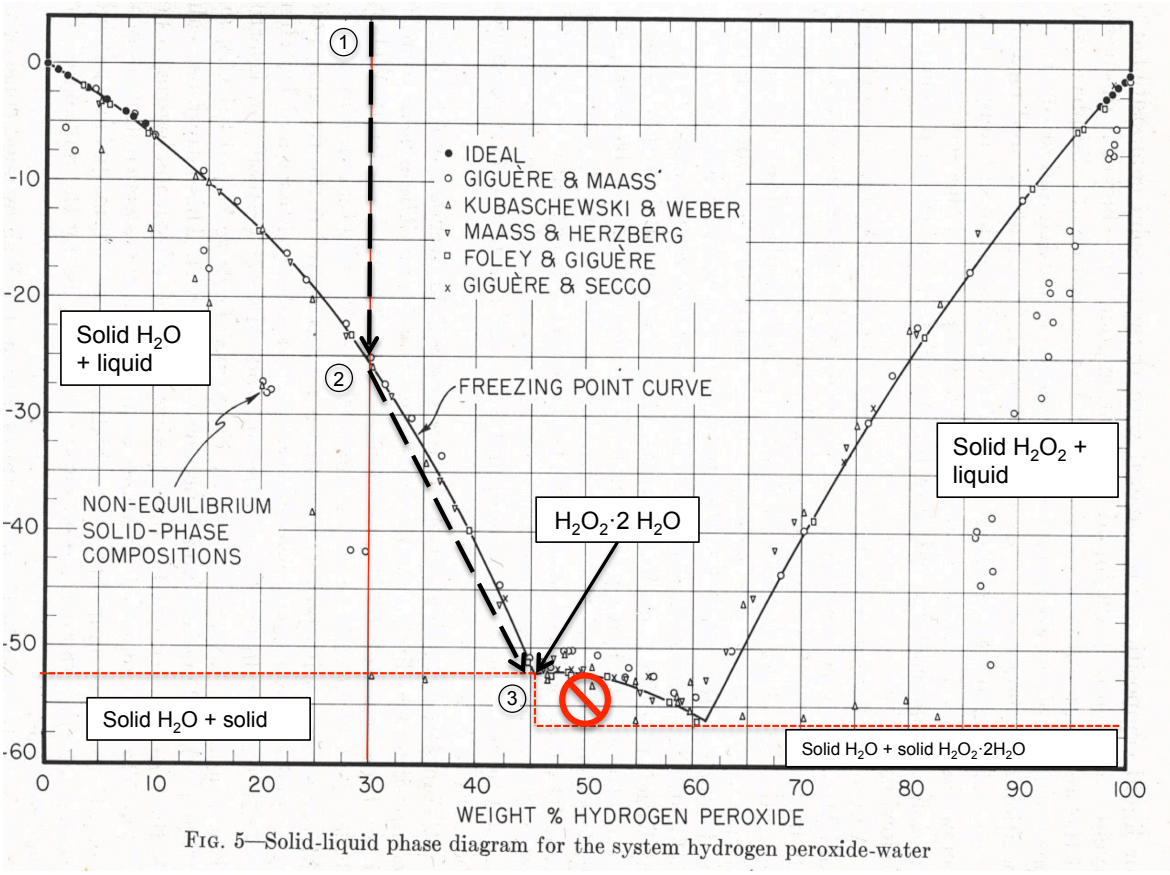

Figure 3.1: Phase diagram of hydrogen peroxide solution, adapted from [47]. The black dotted lines represent the path to follow to concentrate hydrogen peroxide and the solid line is the solid-phase line. The red dotted lines denote division between different aqueous phases.

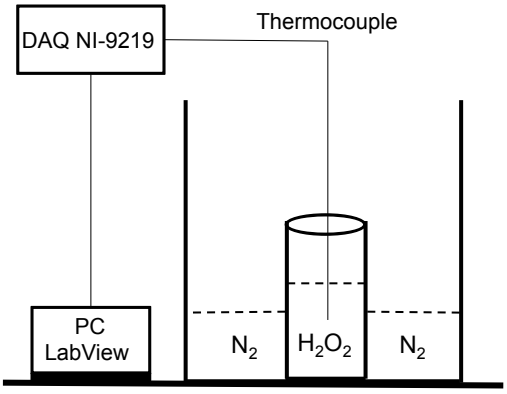

Figure 3.2: Schematic for the freezing method approach.

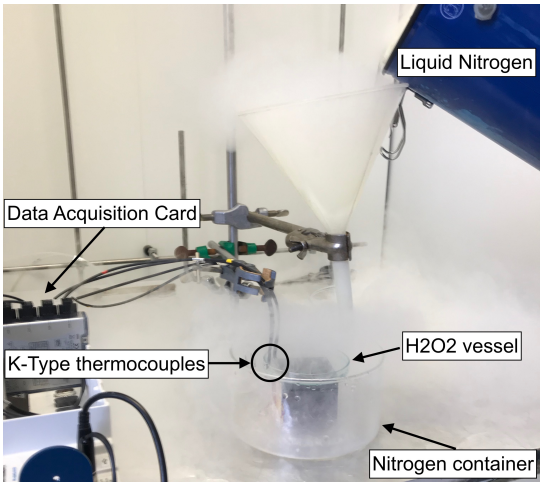

Figure 3.3: Final application of freezing method in laboratory facilities.

refresh rate is 1Hz. The thermocouples were calibrated to 100°C and to 0°C with boiling and melting water with successful accordance to ±3°C. A schematic of the approach used can be seen in Figure 3.2 and the final implementation in Figure 3.3

3.3.3. Results and discussion

Following the implementation previously discussed, a total of 4 tests were performed, none of which were successful. Along the course of the tests, improvements were made for the upcoming tests, given that no literature on the exact implementation of this method was available. Firstly, it was found that controlling the temperature to the precision required was not possible. Because of the initial setup, Figure 3.3, the liquid nitrogen was not lowering the temperature enough to the vessel. Thus it was decided to use a different vessel more similar to the one presented in Figure 3.2 for H_2O_2 . It was found that when the temperature was around -30°C, the initial signs of freezing were happening. This value is lower than what it should be according to the phase diagram, it is believed to be a consequence of the presence of stabilizers. In fact, the solution was acquiring a slushy-type of consistency, which made it impossible to separate the frozen H_2O from the rest. Although in tests 2 and 3, it was tried to steadily go to temperature points along the line joining points 2 and 3 in Figure 3.1, the appearance of this slushy-phase was not possible to overcome. Consequently, a different technique was used for test 4. Instead of steadily dropping the temperature, it was decided to go to a low temperature below the minimum value in the phase diagram, and remove the liquid N_2 supply to raise the temperature slowly. This way, test 4 would allow to drip off a block of the solid solution of H_2O_2 droplets of aqueous solution at composition close to point 3 in Figure 3.1.

The temperature measured in this test 4 can be seen in Figure 3.4 and the final look of the implementation is presented in Figure 3.5. This approach was also unfruitful. As can be seen from Figure 3.4, the temperature was brought down to around -120°C, from where it was allowed to stabilize to room temperature. There is an unusual plateau at around -55°C, which coincides with the eutectic zone in the phase diagram of Figure 3.1, this would mean that the solid part left in the melting process is the crystal $H_2O_2{\cdot}H_2O$, while the liquid is the remaining water of the parent solution. Unfortunately, the application of even this approach was troublesome. As it can be seen in Figure 3.5, the thermal conductivity of the parent solution was not good enough to evenly freeze the entire vessel. In fact, while one half was being supercooled, the upper part was still liquid. Not being the worst situation, it was decided to check still whether the concentration of the leftover ice would match the crystal composition. Unfortunately, the concentration varied, but it is not possible to determine whether the concentration rose as it was within the resolution limits of the instrument used. It is speculated that the cooling took place in such a short duration that the crystal formed, but it also entrapped the leftover water. This approach was unfeasible.

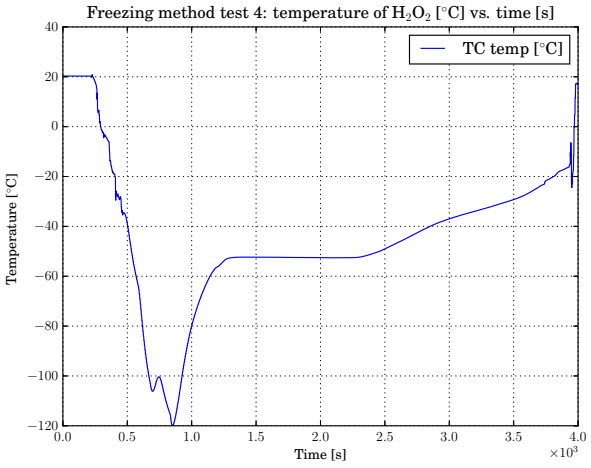

Figure 3.4: Freezing method test 4 results. Temperature measured by the k-type thermocouple [°C] vs. time duration of experiment [s].

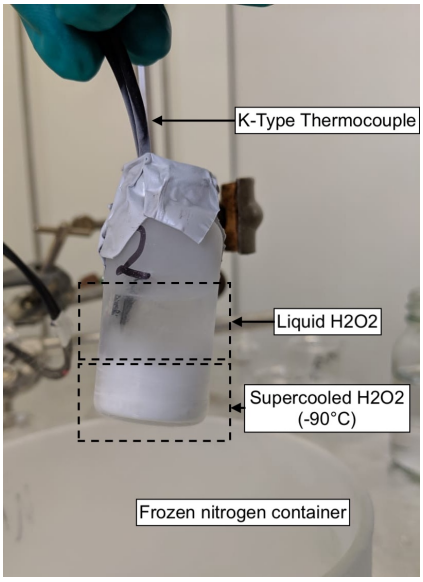

Figure 3.5: Result of freezing method application on test 4.

3.4. Refining approach 2: an innovative approach

Having found that the freezing method implementation could not be achieved with the equipment available, another look was thoroughly taken to the physiochemical properties of hydrogen peroxide. Luckily, another exciting capability of the chemical was found to be exploitable. This approach led to the successful refining of hydrogen peroxide to any desired concentration, from any starting parent concentration, in a significantly cost-effective manner and in a surprisingly minute time period. Unfortunately, **the technique has been filed for patent**[3]**, and no information about the theoretical background pertaining to this invention can be shared.** Instead, this section will present the results attained by the patent.

3.4.1. Test plan

Initially, when this technique was first discovered, no collection of data was being made. Only when it was proved to be a functioning approach, a test plan was put in place for the data collection. With a standard data collection approach, tests were performed on a requirement-basis. When HTP was required for further experiments, a new concentration test was performed. At the end of the study, a total of 9 tests were performed, for which 2 data points are normally taken in the data collection standard shown in Table 3.3. In all the tests, the relevant conditions affecting concentration were kept constant, including the temperature and size of the container. Only the initial quantity of feedstock H_2O_2 was varied.

Table 3.3: Data collection for concentration tests.

		Concentration by refractometer [%]						
Date	**Duration [h]**	**Honey [± 0.2%]**	**Abbe [± 0.2%]**	**Average**	**Tot. weight[g]**	**H_2O_2 weight [g]**	**H_2O_2 volume [mL]**	**Yield [%]**
dd/mm/yy hh:mm	hh	% (if applicable)	%	%	g	g	mL	%

The data collection was performed as shown in Table 3.3. In it, the times of sampling were recorded in *Date*, from where the *Duration [h]* was found with the experiment starting time. The readings of concentration were performed with the handheld refractometer, *Refractometer 1* and the *Abbe refractometer*. When the handheld refractometer was within range, this reading was used to find the average as a more accurate result. However, the concentration for the sample is not the only important parameter; in fact, in any chemical process, the efficiency or yield is of utmost importance. For this, the sample was weighted on a weight scale, recorded in *Weight raw [g]*. Subtracting the containers' weight, the H_2O_2 weight can be found, *H_2O_2 weight [g]*. With the help of Equation (3.3) the density of H_2O_2 can be found, from where the volume left of

[3] Patent was filed 13/11/19 under patent reference number: N2024229

H_2O_2 is recorded, *H_2O_2 Volume [mL]*. Then knowing the initial weight and concentration and final weight and concentration the yield can be found with Equation (3.2). The density of H_2O_2 is found from the code presented in Appendix D.

$$\text{Yield}[\%] = \frac{C_1 \cdot W_1}{C_0 \cdot W_0} \cdot 100 \tag{3.2}$$

Where C_0, C_1 [%] are the initial and final concentrations respectively and W_0, W_1 [g] are the initial and final weights of H_2O_2 , giving the yield in %.

$$\rho = a + b \cdot w + c \cdot w^2 + d \cdot w^3 \tag{3.3}$$

Where ρ [kg/m^3]is the density of the H_2O_2 solution for a concentration w [%] at a selected temperature which affects the other factors in this equation. a is the density of H_2O [kg/m^3] at a selected temperature. b, c and d [kg/m^3] are empirically fitted values which are dependent on temperature only. These values are subsequently presented:

$$b = J_b + K_b \cdot T + L_b \cdot T^2 + M_b \cdot T^3$$
$$c = J_c + K_c \cdot T + L_c \cdot T^2 + M_c \cdot T^3$$
$$d = J_d + K_d \cdot T + L_d \cdot T^2 + M_d \cdot T^3$$

Table 3.4: Density parameters. From [47].

Factor	**J [kg/m^3]**	**K·10^{-3} [kg/m^3°C]**	**L·10^{-5} [kg/m^3°C^2]**	**M·10^{-7} [kg/m^3°C^3]**
b	0.39763	-2.78132	3.2488	-1.6363
c	0.002206	3.5357	-6.0947	3.6165
d	0.05187	-1.9414	3.9061	-2.5500

Where T is the temperature selected [°C], the factors J [kg/m^3], K [kg/m^3°C], L [kg/m^3°C^2] and M [kg/m^3°C^3] are the coefficients relating these parameters to temperature. These can be found in Table 3.4.

3.4.2. Results and discussion

Throughout the thesis development, tests have been performed, up to 9 have been recorded. The findings in terms of concentration and yield, as a function of time, can be seen in Figure 3.6 and Figure 3.7. A total of 19 points have been used, from which 2 points per test and 1 point for the initial concentration is present. As it can be seen in Figure 3.6, there is a clear relation between the increase in concentration and duration of the refining process. Most of the points seem to follow a second-order parabolic fitted line, as presented in Equation (3.4). It provides insight into an optimum amount of time we need to refine the feedstock before concentration gets lost. The optimum point seems to lie around 60h of duration. In this graph, an outlier can be seen, which was not used for the fitting of the curve; this is the point at 22.8h and which will be discussed subsequently. In the case of the yield, the relation is as expected, it decreases with time and with concentration achieved. The fitted relation is also a polynomial of second order, Equation (3.5), with a worse coefficient of determination.

$$C_1/100[\%] = -1.96 \cdot 10^{-4} + 2.38 \cdot 10^{-2} \cdot t + 2.78 \cdot 10^{-1} \cdot t^2 \text{ for } t \in [0, 70].\ R^2 = 0.9119 \tag{3.4}$$

$$Y_1/100[\%] = -1.91 \cdot 10^{-4} + 6.24 \cdot 10^{-5} \cdot t + 9.84 \cdot 10^{-1} \cdot t^2 \text{ for } t \in [0, 70].\ R^2 = 0.7806 \tag{3.5}$$

Where C_1 [%] is the concentration of H_2O_2 after a certain duration of refining time t [h]. The fit is done through a 2nd order polynomial with a coefficient of determination of 91.19%. For the yield of the result, Y_1 [%], also time t [h] is the independent variable and is agreed with a coefficient of determination of 78.06%. These empirical relations only serve for an initial indicator of the dynamics of the process.

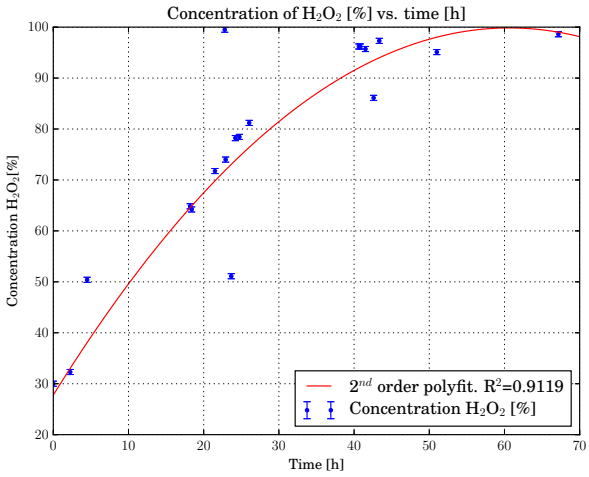

Figure 3.6: Concentration with time for filed invention.

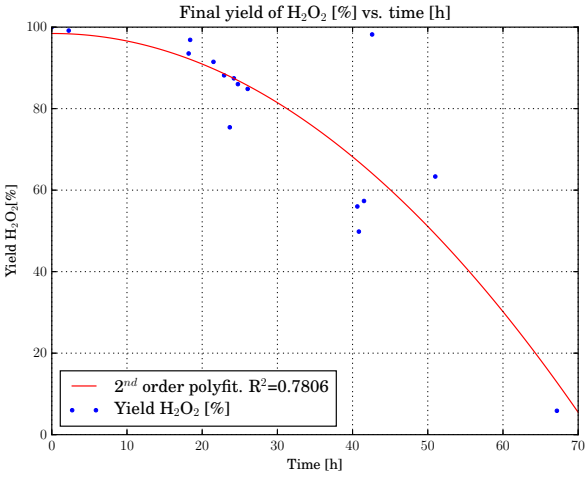

Figure 3.7: Yield with time for filed invention.

Several points were concluded from these results. The maximum achieved with the patent work was 98.6%±0.2% within 67h of duration. This sample had a worrisome yield of just 5.86%. The fastest sample recorded was 96.1%±0.2% in the span of 40h, with a yield of 49.83%. This means an average of 1.9% increase in concentration per hour. This value is unrivaled with current patents and opens a big door to on-site refining with a cost-efficient approach and fast turnover. It is also interesting to note that there seems to be a relation between concentration and yield, for values of concentration at 60-80%, the yield is quite high, around 85-95%. However, as soon as the concentration is boosted to over 90%, the yield goes down to 50-60%. Moreover, during the experimentation, several parameters were identified as having positive effects on the concentration value and speed. These were varied for discovery purposes. It was then found the outlier point in Figure 3.6, at high concentration for only 22.8h. It was achieved superior effectiveness with a maximum concentration of 99.5%±0.2% after a duration of 22.8 h and a superior yield of 70%. Lastly, to add value to the approach, changing the feedstock concentration was studied successfully. Varying the concentration and starting from down to 10% concentration H_2O_2 shows similar results.

Table 3.5: General features of the innovative approach.

Max. concentration [%]	**Fastest achieved**	**Min. feedstock conc. [%]**	**Average conc. speed [% /h]**
99.5	99.5% in 22.8h	10%	1.9

It is important to view these results from a critical standpoint. Although they have been proven to be true, also with the upcoming findings in this thesis, it is unsure how the role of stabilizers is affecting these values. Refractive index is a valid, studied and generally accepted technique for H_2O_2 concentration characterization, however, the value used as well as the fitting done, presented as a code for Python 2.7 in Appendix D, come from "pure" H_2O_2 [47]. The role of stabilizers in the refractive index cannot be mimicked theoretically due to lack of data of the stabilizer, and only a more in-depth experimental study can find how they are affecting concentration and even yield. They may also affect the exact density of the fluid, which was assumed to not be significant in Equation (3.3).

3.5. Stability and chemical study

The decay in concentration with time is an essential parameter for the future design of storage tanks and a valid time frame for the usage of the propellant. To study this, in this section, a small-scale stability study is presented. In order to study it, three samples of 10mL of 90% H_2O_2 were placed in a borosilicate vessel sealed at different temperatures, Table 3.6. The samples were tested at different times until they were depleted. The analyses were carried through 2 weeks and they are presented in Figure 3.8 shown as decrease in concentration in absolute value from the initial 90%. The temperatures tested were standard temperature (20°C), refrigerated sample (2°C) and freezer sample (-30°C). For the last sample, it was expected to have a solid sample following the phase diagram in Figure 3.1. The samples were measured with the Abbe refractometer, due

to the inability to measure this concentration with the handheld refractometer.

For the measurements, a standard process was followed:

1. **Preparation of ARE**: bring the temperature of the Abbe refractometer to 20°Cand measure it through its internal thermometer. Clean with distilled water its measuring prism to eliminate foreign particles.

2. **Perform calibration test:** take measurements of distilled water (n_D = 1.3300) at 20°C, clean measuring prism. Test 30% H_2O_2 (n_D = 1.3528) at 20°C, clean the measuring prism.[4]

3. **Test sample 1 of 20°C:** check its refractive index and note it down. Clean with distilled water.

4. **Test sample 2 of 2°C:** place some drops of the sample on the measuring prism and wait for the temperature to stabilize to 20°C. Then, check its refractive index and note it down. Clean with distilled water.

5. **Test sample 3 of -30°C:** place some drops of the sample on the measuring prism and wait for the temperature to stabilize to 20°C. Then, check its refractive index and note it down. Clean with distilled water.

6. **Collect data:** write down data on data collection Table 3.7

Table 3.6: Samples on study. Each with a volume of 10mL.

Sample	**Initial concentration [%]**	**Storage temp [°C]**
1	90	20
2	90	2
3	90	-30

Table 3.7: Table entries for data collection.

Date	**H_2O calibrated [Y/N]**	**PP calibrated [Y/N]**	**Sample 1 [-]**	**Sample 2 [-]**	**Sample 3 [-]**
dd/mm/yy hh:mm	Y/N	Y/N	n_D	n_D	n_D

The results were taken through a total of 14 days or over 330h, with a total of 8 measurements until sample 3 ran out first. The results have been processed in a more comprehensible format, as shown in Figure 3.8. The processing of the data comes from presenting the absolute decrease of concentration [%] with time. The decrease in concentration, ΔC, is found as given in Equation (3.6) at a given moment in time from the initial concentration C_0 [%].

$$\Delta C \pm 0.4\% = C_i \pm 0.2\% - C_0 \pm 0.2\% \tag{3.6}$$

Where ΔC [%] is the variation in concentration after a certain time given initial concentration C_o [%] and final concentration C_i [%].

[4] From the Abbe refractometer user manual

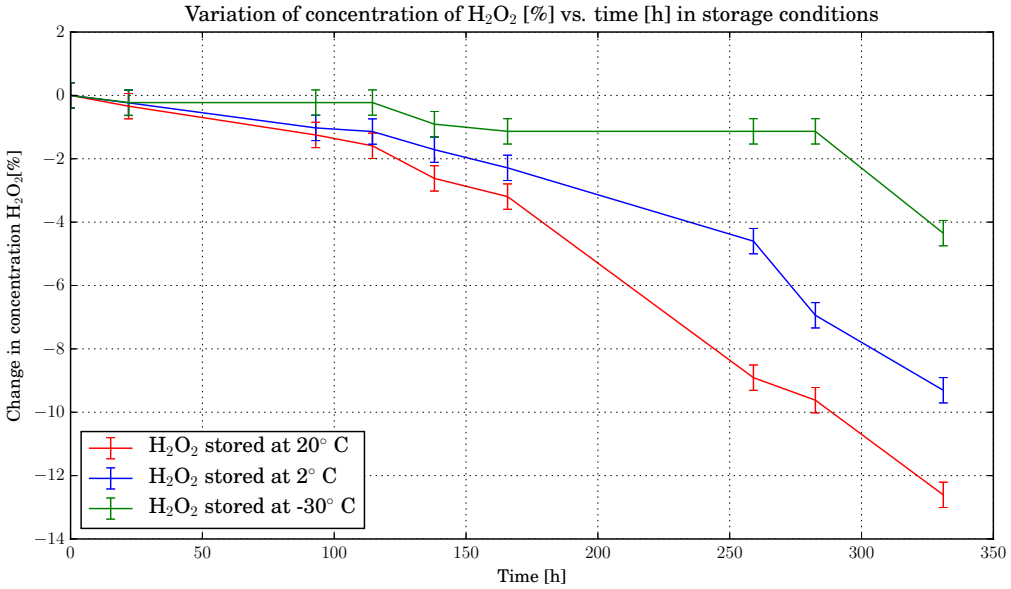

Figure 3.8: Stability study results. Initial concentration of 90% divided into 3 vessels and stored at different conditions through 330 h or 14 days.

Several conclusions are drawn from this stability study. Firstly, the rate of decrease in concentration is clearly higher than what literature states, as presented in Chapter 2, where 1% is considered the accepted independent decomposition rate per annum. It is believed that the presence of stabilizers has a detrimental effect in this aspect. When the refining of the parent propellant is done, the concentration of stabilizers grow. This increase of stabilizers may be the cause of the large drop in concentration through time. It is out of the scope of this research to characterize the effect of amount of stabilizers on the stability of the fuel. However, it can be argued that this is possible explanation as the concentration of the purchased parent propellant remaining did not change its concentration throughout the extend of 5 months of research. Consequently, another issue was identified. For the samples 2 and 3, there could be seen some condensation happening inside the walls of the vessel. Once they were opened in ambient air, new air would come in so that when they were returned to the storage place, the low temperature would condensate the water in the air and precipitate to the liquid they were storing. The exact effect of this phenomena is not known. Moreover, another interesting observation was that sample 3 did not freeze. This came as a big surprise, as H_2O_2 at 90% should freeze at -12.5°C. However no signs of freezing nor floating frozen parts were found all along the experiment. The hypothesis is that the stabilizers not only have a conservation effect on higher temperatures, but also on lower temperatures. Moving on to the sample study, a clear conclusion can be drawn, lowering temperature of storage of the chemical at concentration has a positive effect in retaining the concentration of the parent propellant for longer. This is as expected and found in the literature[15] [47]. The total decrease in concentration for the samples was:

- **Sample 1:** decrease of 12.6±0.4 % in the span of 331 h.
- **Sample 2:** decrease of 9.3±0.4 % in the span of 331 h.
- **Sample 3:** decrease of 4.3±0.4% in the span of 331 h.

During this experiment, a second longer-term stability study was carried in parallel. Instead of testing the samples continuously, the samples were only tested initially and the end of a long period of time. This way no sample would be lost during the testing and a longer period result could be found, as presented in Table 3.8. As presented, the stability of the HTP is still lower than what literature suggests. Nonetheless, the effect of temperature is still noticeable.For the case of -30 °C, the decrease is of 4% as opposed to 6% for 2°C and almost 10% for room temperature. When compared to the conventional testing approach presented in Figure 3.8, the conservation of concentration not only is better but also longer. Moreover,it is this case that represents a relevant case for the application in space, where the chemical might have to be stored for long in containers.

Table 3.8: Long-term stability study of the concentrated hydrogen peroxide at different storage temperatures for a duration of 37 days.

Date [dd/mm/yy hh.mm]	26/11/19 11.31		02/01/2020 16.40	
Duration [dd hh]	0		37d 5h	
	Parameter			
Temperature of conservation	$\mathbf{n}_D$ [-]	**Concentration** [%±**0.2%**]	$\mathbf{n}_D$ [-]	**Concentration** [%±**0.2%**]
20 °C	1.4050	96.3	1.3970	87.3
2 °C	1.4050	96.3	1.3997	90.4
-30 °C	1.4050	96.3	1.4012	92.0

Techniques to further reduce this fast decrease in concentration include providing a more comprehensive analysis of the suspended particles, such as the stabilizers. Likewise, the use of more passivized storage materials, such as aluminium or passivized stainless steel have a positive impact on the preservation of concentration. Moreover, the option to gelate the HTP will further reduce this decomposition. However this lays out of the scope of this thesis for the moment.

4

Thermally decomposing H_2O_2

In the past, HTP has been used for propulsion purposes. Either as monopropellant to drive turbopumps in the early days of rocketry [6]. Or as a bipropellant in dedicated and dual-mode propulsion systems [17] [11] [30]. However, they all have one common denominator: the use of catalysts as activators for HTP. In this chapter, the investigation of a different approach to decomposing hydrogen peroxide is looked into, namely thermal activation. Some work has been done in this respect [45] [37], but failed to characterize and give a sufficiently broad understanding of the range of applicability in terms of concentration or temperature needed. For this, an experiment is put into place where HTP droplets are released on a heating plate and recording temperature values and decomposition time delay (DDT). This chapter present the results to cover this gap. To do so, a brief theory overview is given in Section 4.1 on the feasibility of the approach. Then, in Section 4.2, the materials used as well as the setup is presented. Moving on, in Section 4.3, the goals and information to gather from this test are presented. The protocol to maintain scrupulous cleaning and repeatable results is presented as well. After it, the results of the study are presented and discussed Section 4.4. Later, for illustrative purposes a small comparison with some test run with catalysts, MnO_2 are presented in Section 4.5. Finally in Section 4.6, some conclusion are drawn which are later used for the incoming Chapter 5.

4.1. Theory

In this section, first a look into how to activate the reaction is taken, Section 4.1.1 and subsequently an analysis of the expected energy released in terms of temperature is looked into prior to the experiment, Section 4.1.2.

4.1.1. Activation of HTP

Activating HTP is the key that enables the use of the energy stored in the chemical. For the activation of HTP there exists two main approaches: the use of catalysts and thermal activation. Since the early days of the chemical, catalysts has been a favored approach opposed to thermal. The reason being that thermal has been said to be slower compared to catalysts, Moreover, authors argue that thermal decomposition is a heterogeneous process started by foreign particles [47]. Nonetheless, the past application of HTP, such as driving turbopumps, did not require complex geometries for the catalysts to work on the HTP. It has only been relatively recently, with the application of HTP on thrusters, that the appearance of catalytic beds has increased the complexity of the design exponentially. Catalytic beds are considered the hardest technological challenge to overcome in the realization of HTP thrusters [11]. This is partly the reason why catalyst is generally really well understood and characterized. Catalysts work as reducers of activation energy of the decomposition reaction, allowing the process to take place at reduced temperatures without actively participating in the reactions, an illustration of this can be seen in Figure 4.1. Consequently, the first question to raise is how much energy are catalysts reducing to start the decomposition. Moreover, whether this energy can be matched with thermal activation to avoid catalysts but still start the decomposition.

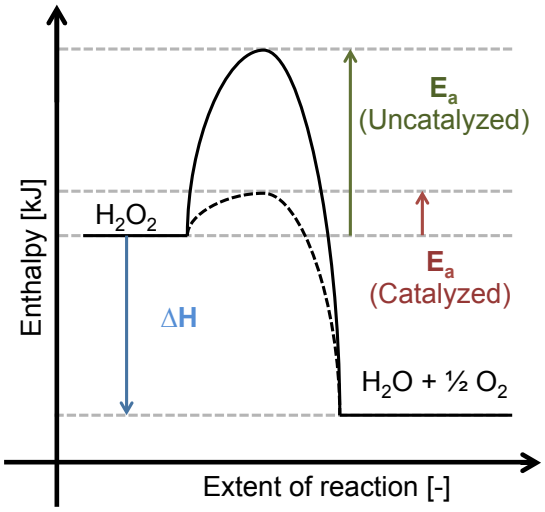

Figure 4.1: Illustration of the catalysts effect on chemical reaction

Table 4.1: Summary of the thermodynamic value of several species at standard conditions 1 atm 25°C.

Enthalpy [kJ/mol]		**E_a [kJ/mol]**	
H_2O_2	-187.8	Uncatalyzed	75
H_2O+1/2 O_2	- 285.8	MnO_2	58
		Pt	49

When analyzing the chemical reaction Equation (2.2) under the eyes of the Arrhenius equation Equation (2.3), it is possible to equate the rate of reaction achieved with catalysts to a given temperature. That given temperature shall return the same rate of reaction as the catalysts in order to be feasible to use. For uncatalyzed reaction at 25°C and 1 atm, the activation energy is 75kJ/mol, while with the use of MnO_2 this value drops to 58kJ/mol, with Pt down to 49kJ/mol and with catalase, a biological enzyme, down to 8kJ/mol. A way to compare the rate of reaction of different approaches is to compare their k values. For instance, the use of MnO_2 leads to a rate of reaction of 1073 [-], which means the reaction would develop 1073 times faster than in standard conditions. To achieve similar reaction speeds with only thermal energy, the reaction would require to reach a temperature of 105.87°C, Equation (4.1). At the end of the day, the energy released coincides with the difference in enthalpy of the products and reactants, in this case, adding up to 98.1 kJ/mol for 100% H_2O_2 at 25°C and 1 atm.

$$\frac{k_{T_{high}}}{k_{T_{293}}} = 1 = exp\left(\frac{-75000}{8.3145\cdot(273.15+T_{high})} + \frac{75000}{8.3145\cdot 293}\right) \Rightarrow T_{high} = 379.02K = 105.87°C \tag{4.1}$$

Where T_{high} [K] is the temperature need to attain that speed of reaction, T_{293} is the rate of reaction achieved at room temperature of 293 K. Consequently, for pure hydrogen peroxide, i.e. at 100% concentration, a temperature of 105.87°C at 1 atm would have the same speed of reaction as MnO_2 at 25°C. However, this value only serves as a theoretical minimum, as in reality, HTP has water content and stabilizers that affect the effect of temperature on this reaction and only through experimentation the real value can be approximated. Nonetheless, the reaction is indeed not for 100% H_2O_2 , but for an aqueous solution with water as shown in Equation (4.2).

4.1.2. Adiabatic flame temperature

In reality, the reaction to look at is Equation (4.2), where the concentration is taken into account, and it is further assumed that the products are already in gaseous phase after energy acquisition from the standard reaction. By varying the concentration of H_2O_2 the energy released also varies. Subsequently, the energy released in terms of adiabatic temperature is looked into. The approach is nicely laid approximately in [51].

$$2\cdot H_2O_2 + N\cdot H_2O(aq.) \longrightarrow (2+N)\cdot H_2O(g) + O_2(g) + \Delta H \tag{4.2}$$

Several assumptions must be presented. Assuming that no heat is lost in mixing purposes and that the temperature is 25°C at 1 atm, the following are the values for enthalpy of formation $\Delta_f H$ and molar weights of the involved products and reactants, Table 4.2. The procedure is to calculate the enthalpy released after the decomposition as a function of z; the solution's mass fraction of H_2O. z is defined as the mass fraction

of water in hydrogen peroxide as shown in Equation (4.3). Once the energy released is calculated, taking the evaporation of water into account, the temperature of the product gases can be found. For doing this, it is assumed to have ideal gas behavior at constant pressure and no heat loss to the environment. A summary of the assumptions are presented subsequently. The formulas that related the specific heat at constant pressure, C_p [J/mol K] are presented in Equation (4.5).

- **Standard conditions:** the temperature at 25°Cand 1 atm.
- **Pure H_2O_2 solution:** the presence of any other chemical, such as stabilizers or foreign articles is assumed be non-existent.
- **Adiabatic conditions:** no loss of energy to the surrounding, all the energy is transferred to the exhaust gases.
- **No mixing energy:** no energy is taken by the mixing of the reactants.

Table 4.2: Molecules involved in the decomposition of H_2O_2 with their formation enthalpy and molecular weight. From NIST Chemistry Webbook.

Species	Δ_f **H [kJ/mol]**	**M [g/mol]**
H_2O_2 (l)	-187.69	34.015
H_2O (l)	-285.83	18.015
H_2O (g)	-241.83	18.015
O_2 (g)	0	31.999

$$z = \frac{N \cdot M_{H_2O}}{N \cdot M_{H_2O} + 2 \cdot M_{H_2O_2}} = \frac{N \cdot 18.015}{2 \cdot 34.015 + N \cdot 18.015} \rightarrow N = \frac{z \cdot 3.776}{1 - z} \tag{4.3}$$

Where z is the mass fraction [-], N is the number of moles of water in the initial solution [-] and $M_{species}$ is the molecular weight of the given molecule [g/mol].

From the reaction, we can find the enthalpy released as a function of the mass fraction by subtracting the enthalpies of formation of the products minus the reactants. First, we look at the process before the evaporation of water, namely, 2 mol of H_2O_2 decompose into 1 mol of O_2 and 2 mol of H_2O . This is shown in Equation (4.4)

$$\Delta_r H = \Delta_f H_{products} - \Delta_f H_{reactants} = (2 \cdot -241.83) - (2 \cdot -187.69) = -108.28 \tag{4.4}$$

Where $\Delta_f H$ [kJ/mol] is the enthalpy of formation of a given molecule and $\Delta_r H$ [kJ/mol] is the enthalpy of reaction. Nonetheless, a total of 44 kJ is lost in vaporizing the water per molecule. Thus from the -108.28 kJ, $N \cdot$ 44 [kJ] goes to evaporation and is not released anymore. Leaving released energy of $108.28 - N \cdot 44$ [kJ] released. The specific heats at constant pressure for O_2 and H_2O are hereby given:

$$\begin{aligned}
[C_p]_{H_2O} &= 30.092 + 6.832 \cdot t + 6.793 \cdot t^2 - 2.534 \cdot t^3 + \frac{0.082}{t^2} \quad \text{for} t \in [373.15 - 1700] \\
[C_p]_{O_2} &= 31.322 - 20.235 \cdot t + 57.866 \cdot t^2 - 36.506 \cdot t^3 + \frac{-0.007}{t^2} \quad \text{for} t \in [100 - 700] \\
[C_p]_{O_2} &= 30.032 + 8.773 \cdot t - 3.988 \cdot t^2 + 0.788 \cdot t^3 + \frac{-0.741}{t^2} \quad \text{for} t \in [700 - 2000]
\end{aligned} \tag{4.5}$$

Where C_p is the specific heat at constant pressure [J/mol K] for the different species and t is the temperature of the species [K] divided by 1000. For now, constant values will be used at a temperature of 100°C/373.15K in order to find the adiabatic temperature. The relations in Equation (4.5) must be used for an accurate result of the adiabatic flame temperature [42]. Now to find the temperature, the energy released to the ambient, $108.28 - N \cdot 44$, must be equated to the increase in energy as temperature of the products at a constant pressure. A symbolic manipulator and a numerical solver implemented in Python 2.7 was used to find the solution, varying the valid C_p for the adequate limits to solve Equation (4.6), this can be found in Appendix D.

$$\int_{T_0}^{T_{adb}} \left(C_{p,O_2} + (2+N) \cdot C_{p,H_2O} \right) dT = 108 - N \cdot 44 \rightarrow T_{abd}(z) \tag{4.6}$$

Where T_0 [K] is the ambient temperature 298.15 K, T_{adb} [K] is the adiabatic flame temperature of the exhaust gases and the rest of the variables have been introduced already. The units for the specific energy must be set to kJ to match the energy released.

The results can be visualized in Figure 4.2, where the maximum temperature happens for anhydrous H_2O_2 , as expected with a total temperature of 1276.8 K or 1003.7 °C. The decrease in adiabatic flame temperature with concentration is linear from 100% H_2O_2 to 64.5% H_2O_2 concentration or $z = 0.355$. At that concentration the temperature released is enough to start the vaporization of water. This change of phase takes place from 10% H_2O_2 to 64.5% H_2O_2 concentration at the boiling point of water, 373.15 K. From 10% H_2O_2 to 0% or pure water, the decrease is linear from the ambient temperature 25°C. It is important to bare in mind that the adiabatic flame temperature represents an upper limit of the maximum temperature achieved.

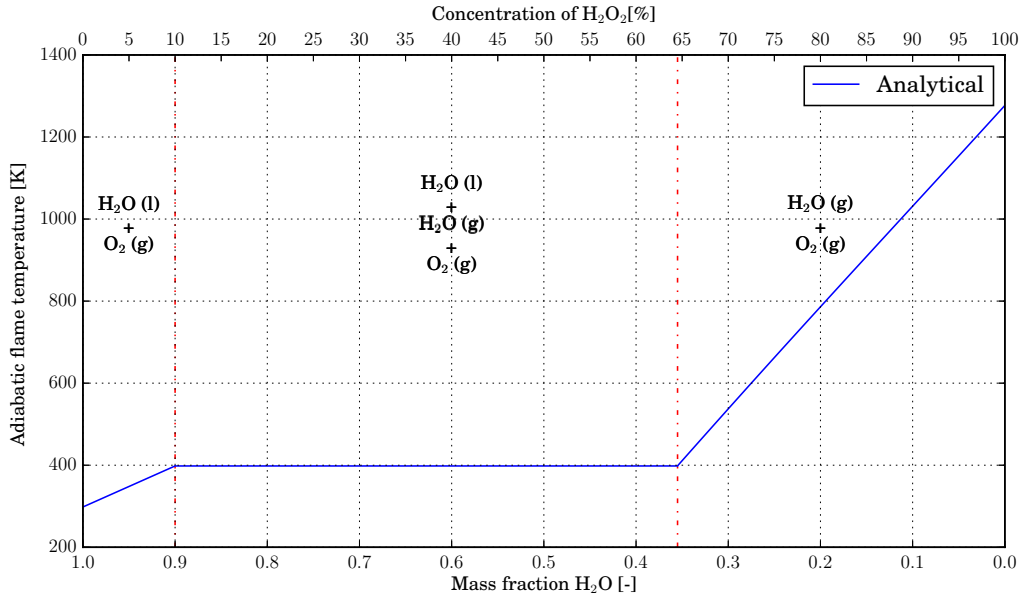

Figure 4.2: Analytical adiabatic flame temperature. Presentation design adapted from [17].

4.2. Experimental setup and materials

For the preparation of the drop-test experiment to characterize the thermal decomposition of HTP, a experimental setup was prepared. The inventory of the items used is presented in Table 4.3, a description of their specifications in given subsequently.

Table 4.3: Inventory for setup of experiment.

Inventory			
ID	**Item**	**ID**	**Item**
FM	Fumehood	SYP	Syringe pump
LIS	Light source	HP	Heating plate
DAQ	DAQ NI-9219	HSP	High-speed camera
FTK	Fine K-thermocouples	PC	Personal computer
SYR	Syringe	CAT	Capillary tube
HTP	High test peroxide	VES	Borosilicate vessel

Most items used for this experiment were found within the DASML in the TUDelft faculty of Aerospace Engineering. The fumehood, FM, was a large fumehood with enough space to be accessed by two scientists for the setup of the experiment. It was mainly used for the tests to have the safety of the glass screen protection, as the exhaust gases were innocuous its role as air sucker was not as relevant. The syringe pump, SYP, used is a Quality In Sensing syringe pump model NE-1000 programmable for rate of discharge as well as internal diameter of the syringe used, in this case a discharge rate of 7.1 mL/min for a syringe of 2 mL. The light

source, LIS, is a LED special light system for the HSC. It provides a short pulse duration, monochromatic and low-coherence light and intensity in excess of 10,000 lm (this was regulated as required). The heating plate used, HP, was a Ikatherm HCT heating plate, DIN 12878 class 1. It runs on 220V AC current 50/60Hz and consumes a maximum power of 600W. Its specifications state that it can regulate temperature on the plate from 0-300°C, although no temperature over 280°C was ever recorded, and has a diameter size of 13.5 cm. In order to record the temperatures, a DAQ was used, as introduced in Section 3.2. The DAQ is a National Instruments DAQ model 9219. It has 4 input channels which can be used for thermocouples with a specified maximum 60Hz refresh rate. It is ran through LabView on the PC, Windows 10 running on a MacBookPro 2.6GHz i5 processor. Unfortunately, the DAQ was only retrieved values on up to 55Hz. The high speed camera used is a Photron Mini AX200, available in DASML. This HSP can record up to 900000 fps at a reduced resolution and 6400 fps at the maximum resolution of 1024x1024 px. It interfaces through Gigabit Enthernet with the PC. Unfortunately, it only allowed to record in black and white, more information can be found in its information sheet in Appendix C. For this experiment, the thermocouples used are different from the thermocouples used previously. This time the thermocouples are still k-type, but they are finer bead size. The thermocouples are manufactured by OMEGA and are unsheathed fine diameter; they are just 0.125mm. These are among the smallest available in the market. It is desired to have such small bead sizes to reduce the influence of radiation effects on the readings and only to record the exact thermal energy released to the environment. They have a service temperature of 593°C given their fine size, however they can withstand substantial temperatures for shorter times, over 982°C. The time constant of the response time is below the 0.1 s, meaning that 63.2% of the temperature will be sensed 0.1 s after. They are advised not to be placed on oxidizing environments, however this did not pose any problems along the development of the studies. They were also calibrated to 100 and 0 °C prior to the start of the study. The syringe used was a 2 ml with internal diameter of 18 mm made of plastic. The capillary tube used is made of borosilicate and has a internal diameter of 1.25 mm or 19 Gauge, moreover, it has a wider cylindrical section of 0.5 cm of diameter. Also, a vessel where the droplets fell on as used. It is made of borosilicate and has a size of 2.5 cm diameter and 5 cm of height with a small throat-like closing at the top. Finally, the hydrogen peroxide used was produced in-house and 5 concentration levels were used 75, 80, 85, 90 and 95 %. The parent H_2O_2 has been previously intruded in Section 3.2

4.2.1. Set up

The setup presented in this subsection is also the setup used for the ignition study of Chapter 5. The setup consists of a borosilicate vessel with four k-type thermocouples placed on top of a heating plate, which lays 17cm away from the droplet generator. The droplet generator, in this case, a capillary tube, is fed HTP from a continuous source thanks to a syringe pump. A high speed camera in collaboration with a light source is placed to record the process dynamics and visualize after on a PC. The choice of 17cm comes from previous work on these experiments and it is kept constant for the entirety of the experiment [28]. The schematic and final implementation can be seen in Figure 4.3 and Figure 4.4, respectively.

The VES has holes poked at regular distances of 0, 3, and 6 mm away from the top for the FTK to be placed in. On top of the VES, a fourth thermocouple is placed for the ignition tests and is not used for this particular setup. The thermocouple placement is selected as such to be able to monitor at three locations of interest:

- **FTK1:** located at 0 mm from the bottom, it is placed such that it can monitor the temperature of the droplet once it falls.
- **FTK2:** located at 3 mm from the bottom of the vessel, it is located such as it can measure what happens exactly on the surface of the HTP drop.
- **FTK3:** located at 6 mm from the bottom, will monitor the effects of the ambient air close to the drop, but not directly on its surface.

Behind the heating plate setup a mesh of regular squares (1x1 cm) was placed to have a background for the HSP frames. The HSP is placed arbitrarily and focused on the FTK beads in the center of VES. The CAT are separated 1cm apart from each other and are used one for HTP and for EtOH. In this particular experiment, the EtOH was unused. To keep the FTK in place given their fine gauge, two rods had to be implemented, as it can be seen in Figure 4.4, these are plastic and non-conductive, having thus no effect on the TKH reading. The FTK were tensed with the rods help and later directed to the DAQ channel entries, situated in the back close to the VES, given the FTK short length of only 30cm.

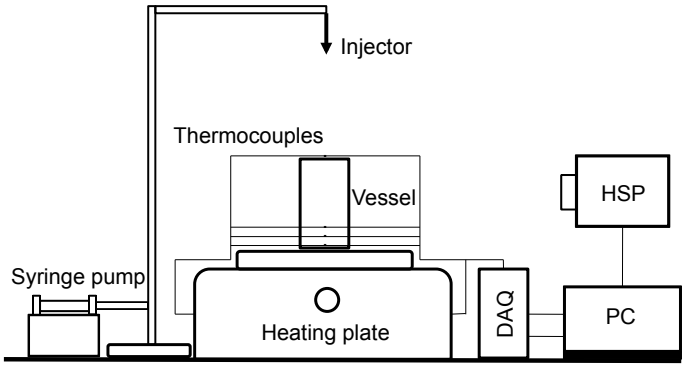

Figure 4.3: Schematic for drop-test experimentation.

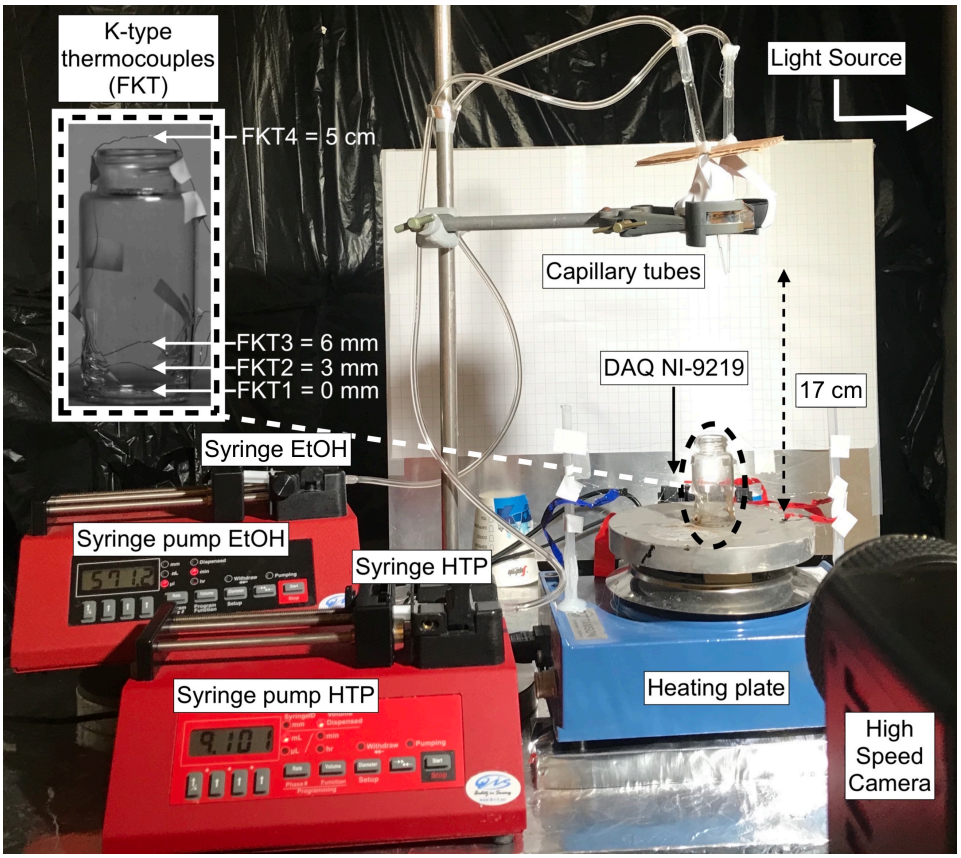

Figure 4.4: Setup for drop test experimentation.

4.3. Methodology/Test Plan

In this section, the overall methodology is provided, as well as the information to find from this test. Moreover, the definitions used for the upcoming result section are given. The entire test plan, on the other hand, is a comprehensive chapter included in Appendix B. This test plan was followed throughout the entire test campaign and the reader is encouraged to go through it as well to familiarize with the test approach.

4.3.1. Test order

The decomposition for HTP will be tested for a total of 30 HTP concentration / temperature combinations. The temperature of the HP will be varied from 50 to 300 °C in steps of 50 °C, (50, 100, 150, 200, 250, 300°C). These are the minimum and maximum achievable temperatures of the HP. From Section 4.1.1 it is known that theoretically, for 100% H_2O_2 , a temperature of about 105°C is needed to have a good decomposition, however this temperature is expected to significantly vary when reducing the concentration or adding stabilizers. Coming to the concentration tested, given that the HTP is required to be used as a monopropellant and as an oxidizer in the upcoming section, it is required to produce at least the autoignition temperature of EtOH around 360°C or 640 K.. This will be discussed in more depth in the upcoming Chapter 5. From the analysis in Section 4.1.2, the adiabatic temperature produced by 75% HTP is of 660 K, this is why the starting concentration to test was set at 75%. From there, concentrations up to 95% in steps of 5% were selected (75, 80, 85, 90, 95%). The order followed to cover these test experiments is presented in Table 4.4, also presented in Appendix B.

Moreover, several margins of acceptability were set before the experiments. Firstly, the concentration of the used HTP was allowed to be within ±1%. From the procurement analysis, it was found that the ARE has a resolution and error of 0.2%, however, the additional 0.8% was required as setting the HTP at a particular concentration is a tedious and challenging process. For the HP, a temperature margin of ±10°Cis used to allow for small fluctuations. The fluctuations are because the HP is a old-piece of equipment without feedback loop system. Consequently, the setting for the temperature comes from reading of FTK1 on the PC and varying the knob of the HP itself. Furthermore, the volume used for all droplets will be constant of 0.13 mL and generated with the syringe pump mechanically. A more elaborate explanation can be found in in Appendix B

Table 4.4: Order of test to do for decomposition. Based on the results of the decomposition, the ignition order follows. Each test, if successful, should be repeated 3 times.

T [°C±10 °C]	**Conc [%±1%]**	**75**	**80**	**85**	**90**	**95**
50		1	7	13	19	25
100		2	8	14	20	26
150		3	9	15	21	27
200		4	10	16	22	28
250		5	11	17	23	29
300		6	12	18	24	30

4.3.2. Expected results from the test

In short, the goal of the test is two-fold: obtain the Decomposition Delay Time (DDT) [ms] and measure the exhausted temperature. The DDT is a required value to characterize how long does the HTP take to decompose from the moment it is thermally activated. It is a crucial parameter for the ignition tests and for design of an upcoming combustion chamber in monopropellant mode. On the other hand, the importance of the exhaust temperature is also significant. By measuring how much the temperature rises from decomposition, it will be possible to estimate whether pseudo hypergolicity can be achieved or not, it will also play an important role in determining material and cooling methods, if needed, for a new design. More formally, the test goals are the following:

- **Temperature profile characterization:** to measure the temperature [°C] of the exhaust gases after decomposition of HTP through the use of 3 k-type thermocouples for the proposed combinations of HTP-HP temperature. FTK1 in contact with the HTP, FTK2 3 mm above and FTK3 6 mm above.
- **Decomposition Delay Time characterization:** to find the values of the DDT [ms] for the proposed combinations of HTP-HP temperature. This will be possible through the use of HSP and FTK/DAQ at 55Hz.

- **Visual understanding:** to investigate the dynamics of the process from a visual standpoint with the use of the HSP. Any discoveries related to the dynamics of the process should be reported.

In a bit more depth, it is essential to define properly DDT. For the purposes of this study, the DDT will be defined a the time taken from the moment of first visual droplet deformation, as result of impinging with HP, to the moment of initiation of visual shock wave in the HSP or to the moment of increase in temperature in any of the FTK1-3 above the HP temperature set for that experimentation. This means that two sources of DDT information are available, namely HSP and FTK/DAQ. The HSP as a DDT resolution of 1/6,400 s, or about 0.16 ms. On the other hand, the DAQ has a resolution for DDT of 1/55 s, or about 18 ms.

When it comes to the data acquisition, the temperature profile for FTK1-3 will be saved, the DDT from the HSP will be saved and the DDT form the DAQ will be saved. For more exact information on the process and data to find, the reader is referred to Appendix B. For each experiment, some processed data is required, after the raw data of the test, the following are the results used for the upcoming study. For every test with ID Equation (B.3), it must be found:

- **HTP concentration [%±1%]**
- **T_{HP} [°C±3°C]:** temperature of the heating plate that the HTP droplet will feel. This is not the heating plate temperature strictly speaking, but the temperature of the floor of the vessel. This value is given by the FTK1 and it is expected to be roughly equal to the HP. It is not expected that this value will have an impact on the maximum attained temperature, as this is only dependent on the chemical properties and the energy of the chemical itself.
- **$T_{decomposition}$ [°C±3°C]:** this is the temperature of the fluid when it undergoes decomposition. Attention must be paid to this value as it is not the temperature achieved on the decomposition, but rather the temperature at which the HTP is when it starts to decompose. This is the parameter expected to be about 105°C. This value is also provided by FTK1. This value is expected to be a constant among the same concentrations, as the point of decomposition should be a chemical-related property.
- **T_{max} [°C±3°C]:** this is the maximum temperature achieved at any point of the decomposition and at any FTK. The FTK at which it happens will also be monitored for qualitative analyses.
- **DDT_{DAQ} [ms±18ms]:** this is the DDT from the DAQ reading. As previously mentioned, it will be defined from the moment the DAQ feels a drop in temperature, caused by the droplet touching it, to the moment any of the 3 FTK feels a temperature which is above the HP set temperature.
- **DDT_{HSP} [ms±0.15ms]:** this is the DDT from the HSP. It has been previously defined and an only be identified visually and in some shots, consequently, when the data from the HSP is not available, the data from the DAQ will be used.

4.4. Results and discussion

In this section, the results of the study presented as well as discussion of their meaning. To do so, firstly, the results concerning the achievement of decomposition are presented in Section 4.4.1. Subsequently, the temperature results, profile and maximum values are given in Section 4.4.2. Lastly, the DDT results are discussed in Section 4.4.3.

4.4.1. Achievement of decomposition

Defining decomposition is a key step in this study. For the purposes of this work, decomposition is achieved when the HTP undergoes a recordable reaction in which a thermal, visual and auditive action occurs. As explained, the thermal aspect is the rapid increase in the exhaust gases temperature upon decomposition. For the DAQ analysis, the thermal decomposition is said to have taken place when the temperature measured is larger than the heating plate temperature. This will show that there is indeed energy being liberated. The visual aspect is when the HSPC recording can be analyzed and seen that there is a small shock wave occurring in it. A problem found with this, is that the shock wave recorded is specially subtle and hard to visualize for the experienced eye. An example can be seen in Figure 4.6, where the shock wave is barely noticeable in frame 4. For most of the DDT in this study, the information is based on DAQ readings only, as they are easier to find than the HSPC recording, this is not the case for ignition as a bright flame can be seen. Lastly, concerning the auditive effect, the volume expansion of decomposing HTP is over 4500 [47], consequently a small banding sound can be heard. If this sounds is not heard, then no decomposition took place.

After the test campaign, several main conclusions can be drawn. First and foremost, a clear picture of the possibility to use thermal decomposition is constructed after the tests in Figure 4.5. As explained, decomposition is achieved when the H_2O_2 is exploited and the energy is liberated and recorded in terms of temperature in the DAQ and visual explosion in the HSP. Coming to the expected decomposition activation temperature of 105°C, this proved not to be the case. In fact, the lowest temperature recorded to produce decomposition of HTP is 200±10°C. This first finding came up as surprising, as the difference with the expected value is double. However, the analysis provided in Equation (4.1) is based on several assumptions which do not relate to our case. Firstly, the presence of thermal stabilizers is a possible cause of larger temperature requirements. They may be preventing the effect of temperature on its decomposition, as they were intended to be used. Quantifying this effect is out of the scope of this analysis, so only the experimental data is analyzed. Moreover, the analysis of Equation (4.1) was meant for an ideal case of pure 100% H_2O_2 , this was not the case studied in this work and, thus, the addition of water is expected to quench this process. These two effects may contribute to this temperature gap.

Table 4.5: Matrix of achieved decomposition. Y-Yes, decomposition was achieved upon droplet precipitation on HP. N-No, decomposition was not achieved. Tests were performed at atmospheric conditions of 1 atm.

	Conc [%±1%]				
T_{HP} [°C±10°C]	**75**	**80**	**85**	**90**	**95**
50	N	N	N	N	N
100	N	N	N	N	N
150	N	N	N	N	N
200	N	N	Y	Y	Y
250	N	Y	Y	Y	Y
300	N	Y	Y	Y	Y

Furthermore, as it can be seen, the concentration of 75% did not achieve decomposition in any of the five temperature cases. Not even in the largest temperature of 270 °C. This shows that HTP at concentration of 75% has a too large content of water to be thermally decomposed and water absorbs too much of the thermal energy. Out of the tested droplets, no explosion was ever witnessed, except a timid boiling after some time at temperatures over 150°C. However, no homogeneous decomposition took place ever. Similarly, out of the recorded droplets, one per temperature in this case, no reaction was seen whatsoever, expect a timid boiling of the fluid after some time on the HP. At the end of the day, the energy left is not enough to spark the decomposition. 75% H_2O_2 is eliminated as a possibility for thermal decomposition.

Likewise, the temperatures of 50, 100 and 150°C, were not enough to start the decomposition on any of the concentrations. Although 150°C is over the boiling temperature for the four concentrations at 1 atm, none of them exhibited rapid decomposition. Boiling was appreciated only after a certain time on the heating plate for 150°C. Moreover, the combination of 85%±1% with 150°C±10°Cwas also unsuccessful. As expected, higher concentrations of water in the samples will require larger energies to achieve the thermal decomposition and will also experience a lower energy released. At that HP temperature of 200°C±10°C, the concentrations of 85, 90 and 95 %±1% had successful decomposition. At the temperatures of 250 and 270 °C±10°C, the HTP at 80, 85, 90, 95%±1% had successful decomposition.

For the successful cases, three droplets were done and recorded as discussed in the test plan. The processed output in presented in Table 4.6 for the data entries shown in Section 4.3.2. These include the temperature of decomposition [°C], the maximum temperature achieved [°C], the DDT [ms] and the thermocouple at which the maximum temperature was achieved. Moreover, all the successfully decomposed HTP have achieved upon decomposition a temperature in excess of the autoignition temperature of EtOH, which makes them suitable for the upcoming study of ignition. The analysis of the results is presented in the upcoming subsections.

4.4.2. Temperature profile and maximum values

In this subsection, the temperature results will be analyzed. The first and foremost finding is that the decomposition of HTP achieves the autoignition of EtOH, this is positive and will be exploited for the ignition cases. With this in mind, knowing how the decomposition works is of utmost importance to understand the behavior for later implementation in the combustion chamber arena. As it was observed from the majority of the test droplets, the decomposition temperature profile follows the same qualitative profile, with different

Table 4.6: Drop test values for decomposition temperature, maximum temperature attained and DDT. Three droplets per successful combination of HTP concentration and temperature of the heating plate. The * symbolizes that HSP recordings were possible to use to analyze the DDT, so the error is ±0.15 ms. The rest were taken from the DAQ data.

HTP [%±1%]	T_{HP} [°C±10°C]	Drop [#]	T_{Decomp} [°C±3°C]	T_{max} [°C±3°C]	DDT [ms±18ms]	FTK of T_{max}
80						
	200					
		1	NA	200.0	NA	1
	250					
		1	137.0	704.0	327.0	2
		2	140.0	709.0	36.3	2
		3	130.0	805.0	90.9	2
	270					
		1	137.4	666.0	75.5	3
		2	140.0	815.0	181.0	3
		3	130.0	792.0	54.5	2
85						
	200					
		1	174.0	462.0	91.0	1
		2	136.0	595.0	345.0	2
		3	130.	629.0	90.0	2
	250					
		1	180.0	794.0	54.5	2
		2	132.0	776.0	109.0	2
		3	130.0	843.0	90.9	2
	270					
		1	137.0	708.0	54.0	2
		2	137.0	672.0	72.0	3
		3	154.0	629.0	90.0	2
90						
	200					
		1	138.5	781.0	461.0*	2
		2	141.0	683.0	690.0	3
		3	131.0	989.7	390.0	2
	250					
		1	143.1	766.0	200.	2
		2	142.0	865.0	472.0	2
		3	129.0	853.0	36.36	3
	270					
		1	144.0	1038.3	45.7*	2
		2	145.5	995.0	18.2	3
		3	152.0	447.4	272.0	2
95						
	200					
		1	143.2	830.0	233.43*	2
		2	112.0	652.0	138.75*	2
		3	145.7	984.0	54.5	2
	250					
		1	143.4	847.0	145.5	2
		2	144.8	895.0	109.9	2
		3	107.7	813.3	54.5	2
	270					
		1	145.0	778.9	90.9	2
		2	145.7	857.0	18.2	2
		3	144.3	901.0	145.5	3

temperatures but the same shape overall. For illustration purposes a nominal case scenario is presented in Figure 4.5. This is the temperature profile measured for the droplet 2 of 95±% HTP on the HP at 200±10°Cand will subsequently be discussed.

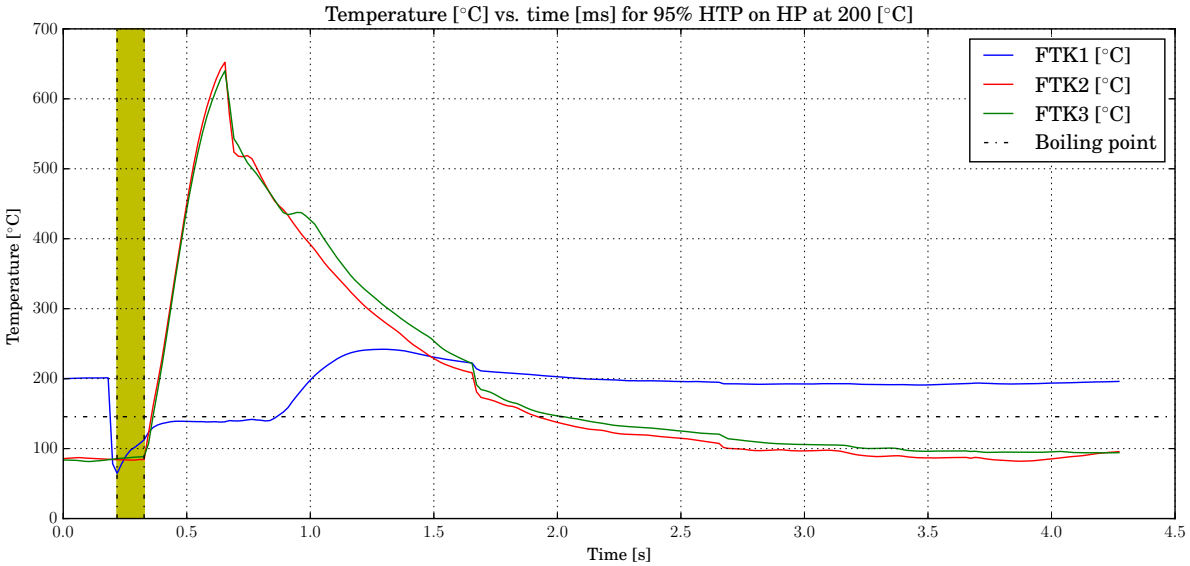

Figure 4.5: Temperature profile for droplet 2, 95% HTP on HP at 200°C. The test took place over a total of 4.5 seconds at a reading rate of 55Hz. The maximum attained temperature was 652±3°C.

The profile of Figure 4.5, shows the temperature recorded with 3 FTK located at 0 mm, 3 mm and 6 mm for a total of 4.5 s at a reading speed of 55Hz. Several features can be identified in this profile. Firstly, the temperature of the FTK1 is significantly larger than the FTK2 and FTK3 at the beginning of the graph, until around 0.2 s. In this case, FTK1 is in contact with the bottom of the glass, meaning that this is the HP temperature felt by the falling droplet. At around 0.25 s a large drop of over 130°Ctakes place. This is the signal that the droplet of HTP, kept at room temperature, has fallen onto the vessel and lowers the temperature of the surroundings up to the first dotted vertical line where the minimum temperature occurs. From this moment on, the droplet is starting to get the energy of the glass and warming up in the yellow-painted zone. In some cases, it has also been seen that FTK2 and 3 pick up a small increase in temperature prior to decomposition and it has been attributed to starts of evaporation and small boiling of gases which raise the FTK2 and 3 temperature. A close look to this region of interest is presented, together with images from the HSPC on Figure 4.6 and Figure 4.7. After the end of the yellow-painted zone, the sign of decomposition happens. FTK2 and FTK3 pick up an immense increase in temperature, of over 600°Cin the span of 0.5 s. This particular profile peaked at 652±3 °C. During this increase in temperature, FTK1 also increases up to a semi-constant value which holds from 0.25 s to 0.85 s. This plateau is common in all the temperature profiles. It is believed that FTK1 is immersed in the HTP fluid, thus, although decomposition is happening at the surface of the fluid, FTK1 does not feel that high temperature and only feels the fluid boiling. This plateau temperature is close to the boiling temperature and this is most likely what is being measured. However, although this is sustained for a while, the depletion of HTP starts to be felt by FTK1 at around 0.9 s, where it feels a larger temperature due to the decomposition location getting closer to it. This start of the depletion is also felt by the subtle drop in temperature for FTK2 and FTK3. At some point another interesting common feature takes place. At around 1.7 s, the three FTK feel a sudden drop of over 30 °C at the same time, this is believed to be the full depletion of HTP. From that moment the temperature at FTK1, 2, 3 stabilizes to the initial values.

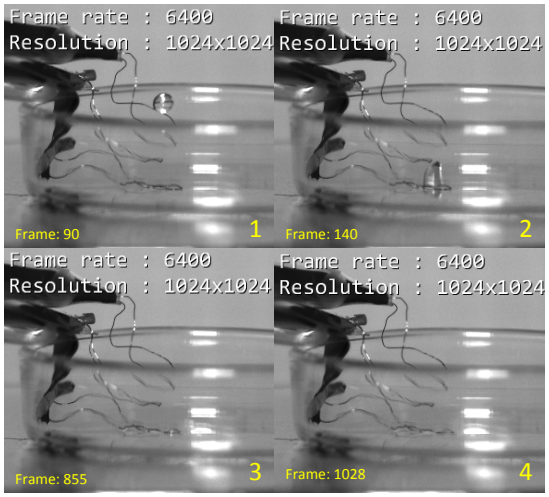

Figure 4.6: Decomposition sequence of frames captured by HSP for 95% HTP on 200°CHP. The respective profile positions are shown in Figure 4.7. 1- 95% HTP falling (*Frame 90*). 2- HTP touching FTK1, DDT starts now (*Frame 140*). 3- HTP warming up (*Frame 855*). 4- Decomposition of HTP starts, DDT calculated until here. (*Frame 1028*)

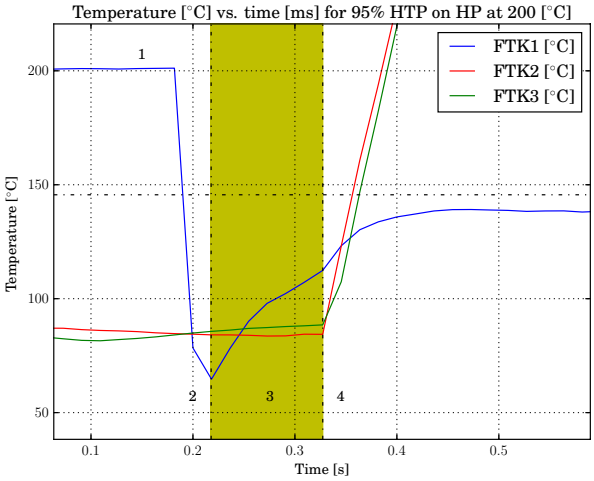

Figure 4.7: Zoom in of profile from Figure 4.5 for 95% HTP precipitating on HP at 200°C. Numbering refers to sequence of Figure 4.6 and the horizontal dotted line represents the boiling point of HTP at 95%. 1- Temperature of the HP prior to drop falling. 2- Droplet touches FTK1. 3- Increase in temperature from HTP. 4- Decomposition starts.

A closer look is now taken to the moment of decomposition in Figure 4.6 and Figure 4.7. The numbering presented matches the HSPC recording to the DAQ recording. As can be seen, the HSPC recording is hard to be used for DDT purposes, this is the reason why only a few cases were used to prove that DAQ and HSPC match on this aspect. In Figure 4.6, the first frame showed, frame 1 corresponds to the moment of HTP droplet precipitation. At this moment, the profile is still unaltered. It can be seen how the droplet form is spherical as expected. In picture 2, frame 140, the droplet has made contact with FTK1, its deformed shape seems to be an optical effect of the glass. This moment matches with number 2 in the graph next to it. At this very moment, the DDT starts ticking. Next, on the picture 3, frame 855, the HTP is starting to warm up on the glass, not much can be appreciated in this picture. Lastly, picture 4, frame 1028, shows the start of the shock wave. As previously mentioned it is extremely hard to see this and only with the video becomes clear, however this is the frame at which it started to happen. It is also shown in the graph next to it. In fact, the HSPC measures for HTP a DDT of

$$DDT = \frac{(1028-140)}{6400} = 0.13875 \pm 0.00015 = 138.75 \pm 0.15 ms \tag{4.7}$$

While the DAQ measured 127.27 ms ±18 ms, which cover the right value of 138.75 measured by the HSP, this was found to be the case for the decomposition where it was possible to see the shock wave.

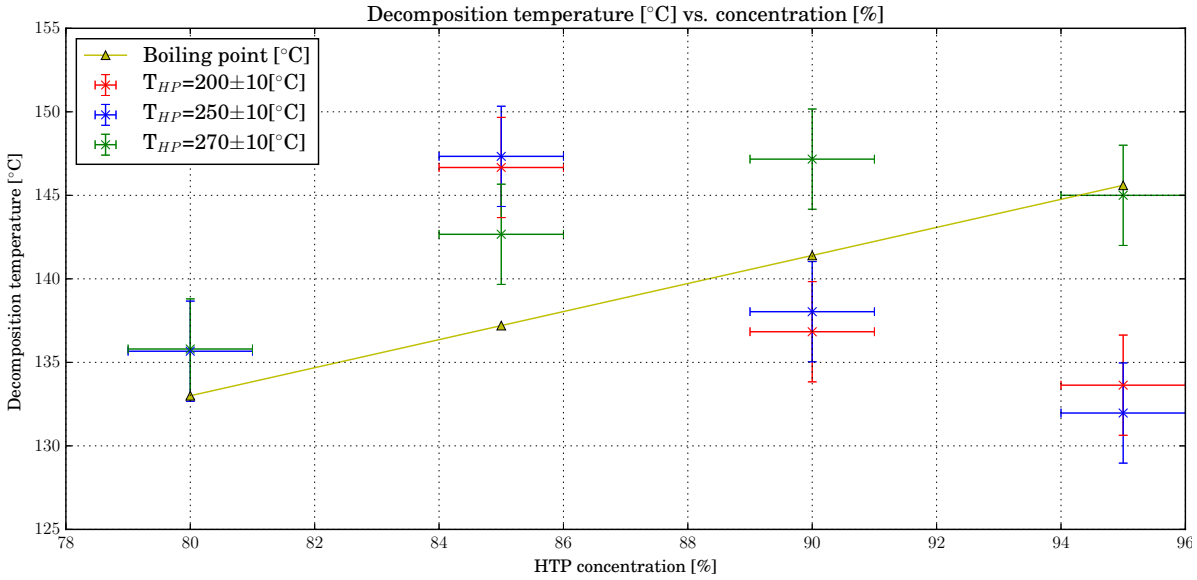

Figure 4.8: Temperature of HTP at the moment of decomposition for different concentrations. Three cases are presented for different HP temperatures of 200, 250 and 270 °C. For 80%, 200°Cis not included as no decomposition was attained. The boiling point at atmospheric conditions is included from [47].

Nonetheless, when looking at the data presented in Table 4.6, other parameters can be investigated. This is done in Figure 4.8 for the temperature at which the decomposition took place. The values presented are the average of the values in Table 4.6. In the plot, the decomposition temperature is presented vs. the concentration cases for different temperatures of the HP, represented in different colors. The error bars refer to the precision of the instrument used. As can be seen most all the values lay between 130-150 °C. It was interesting to find that this is also the case for the boiling point of HTP at those concentrations, thus it has been included into the graph for reference. This does not mean that the decomposition temperature should be the boiling point, this is unknown. As can be seen from the values, it seems like there is a point of maximum decomposition temperature somewhere between 85% and 90% HTP. Nonetheless, in general, the values are close to the boiling point. It can further be seen how the effect of the HP temperature is not apparent. In fact, the decomposition temperature is a property which could be either attributed to the energy provided to the system as well as to the chemical. This is because it could be argued that more energetic concentrations may require of less energy before undergoing decomposition, thus attained a lower decomposition temperature. However, it can also be argued that some gaseous H_2O_2 is needed to start the decomposition and propagate it to the liquid, this would require of the fluid to be boiling. These two counteracting processes may be the reason why there is a maximum laying somewhere between the concentrations. For 85% the values lay close to each other and T$_{HP}$=270°Cis below the lower temperatures. However, this scenario is entirely different for 90 and 95%.

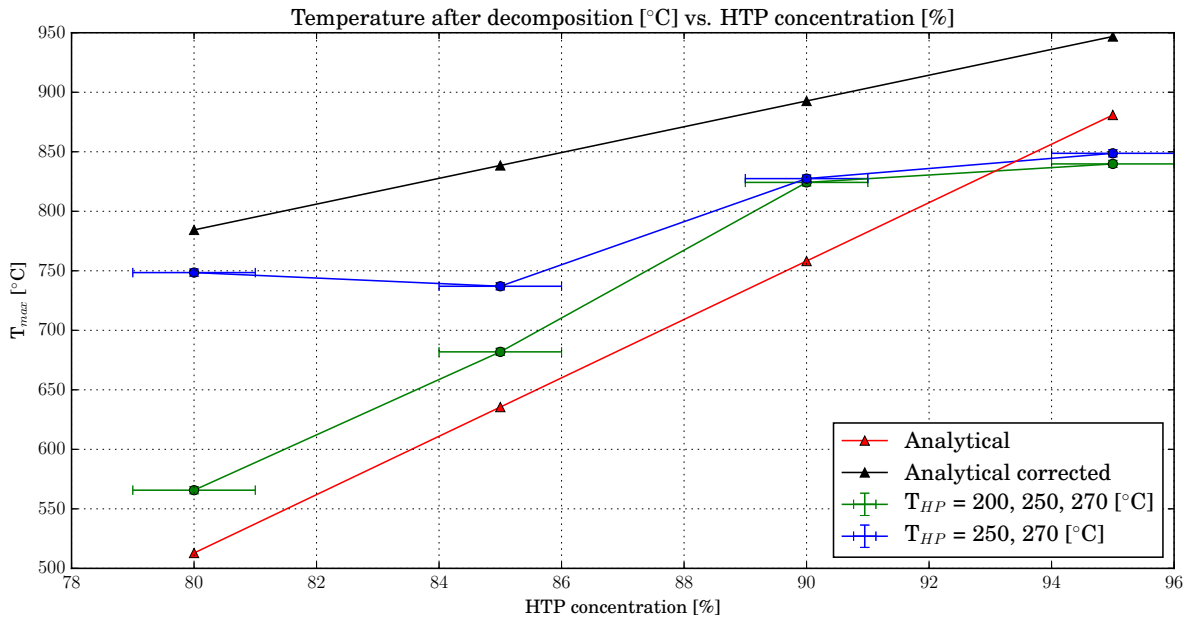

Figure 4.9: Maximum temperature achieved after decomposition for different concentrations and heating plate configurations. Analytic solution found in Section 4.1.2 is presented, and a corrected version where water is not evaporated is presented. The green data is presented for the average of the three HP situations, for 80% because no decomposition was attained at 200°C, the value of 200°Cis used for the average. The case in which the HP is at 250 and 270°Cis also presented where decomposition data is available for all concentrations.

Another critical aspect of characterizing decomposition is the maximum temperature achieved. It is also interesting to compare with the analytical analysis done in Section 4.1.2. In Figure 4.9, the maximum values of the temperature after decomposition are shown for different concentrations, and different heating plate temperatures. Likewise, the values found in the theoretical analysis are shown in red. Firstly, the values of the maximum temperature should, in theory, be heavily influenced by the concentration of the HTP and in less quantity by the heating plate temperature. The maximum temperature achieved is a chemical property above all and, in general, this trend can be seen in the figure. It is important to note that for 80% at 200°C, no decomposition took place, thus the value used for it is 200°C, which is the maximum it was attained. Bearing this in mind, 80% HTP has a slightly larger maximum temperature than 85% for the case of 250, 270°C. Apart from this, the trend is clear. The maximum temperature grows with concentration up to 850°C from the lowest of around 670 °C. Of course, the presented values are averages, so if we look for maximum and minimums, the highest achieved was 1038.3±3 °Cfor 90±1% at 270°Cand the lowest 447±3 °Calso in this combination. This is showing that this particular combination has a broad dynamic range.

Another clear fact from Figure 4.9, is that the values attained of maximum temperature are over the theoretical adiabatic flame temperature. This is shocking as the adiabatic flame temperature is the theoretical maximum to be attained, and the heat loss to the environment should significantly decrease this value. Consequently, a revision of the theory was taken, and it was further assumed that the water would not take energy to vaporize as the temperature of decomposition is 140 °C, meaning that almost all water will have evaporated. Saving this energy increases the temperature of the exhaust gas, as shown in the corrected temperature values. Nonetheless, a more extended look should be taken to it, as there are values which were recorded which did exceed the black line, such as the maximum temperature recorded. To explain how this is possible, there are uncertainties still; this include the increase in the starting temperature as well as the fact that some H_2O_2 will already be in gaseous form, this will alter its enthalpy of formation as well, having more energy to liberate. The impossibility to know how much H_2O_2 is already in gaseous form and how much is liquid make modeling this exact reaction a complex task out of the scope of this research. These results mean in terms of combustion design, that a temperature between 1000 to 600°C can be expected and that 95% HTP and 90% seem to give a similar temperature under atmospheric conditions, this means that EtOH can be used in combination with this chemical to produce a pseudo-hypergolic reaction. It is expected that under combustion chamber conditions, the increase in pressure will have an effect on these values by increasing them.

4.4.3. Decomposition Time Delay analysis

In this subsection, the results on the DDT are presented in a more digestible way. The raw data is provided in Table 4.6, however, a comparison to fully understand its meaning is necessary.Firstly, concerning the measuring of the DDT, it was found that not all the HSP recordings were useful to find the DDT, given the how subtle the shock wave is, partly due to the lack of color in the images. Consequently, it was confirmed that the HSPC and the DAQ both would read the same DDT for the same droplet to the best of their resolution, ±18 ms for the DAQ and ±0.15 ms for the HSP. This meant that for the majority of the DDT values, the DAQ was the most reliable system to find the DDT, and that only in some concrete cases, presented with a start in Table 4.6, the DDT could be taken for the HSP recording.

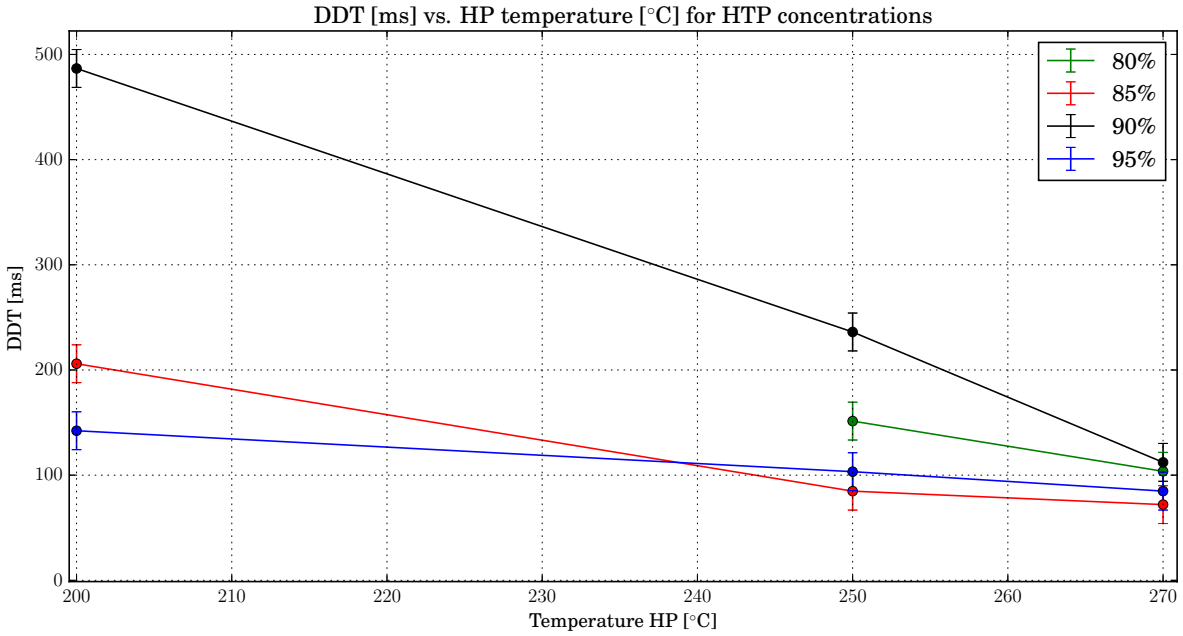

Figure 4.10: Decomposition time delay [ms] vs heating plate temperature [°C] for different concentrations of HTP. No data is available for decomposition for 80% given that it did not decompose. The data presented in the average of the droplets recorder for each concentration and HP temperature.

In Figure 4.10, the decomposition delay time [ms] is given against the temperature of the heating plate for the four successful concentrations (80, 85, 90, 95%), the data presents the averaged values for the three droplets per combination of heating plate temperature and HTP concentration. The raw data lays within the 700 and the 80 ms range. The lowest recorded was 18.2 ms±18.2ms, the resolution for the DAQ, for the cases of 95 %±1% and 90 %±1% at maximum HP temperature of 270 °C±10°C. This matches the understanding that larger concentrations have more energetic content and also that higher energy supplied will result in a shorter time to decomposition. On the other side, the longest took place at 90% ±1% for the lowest temperature of 200°C±10°C. However, when looking at the averaged values in Figure 4.10, a clear trend is identified. This is the significant decrease in DDT with the temperature of the heating plate. This trend is stronger that the trend of the larger concentration vs. lower concentration. The data is more scattered at lower temperatures than it is at higher temperatures. In fact, it is seen how the variability in DDT at 100°C is reduced from a margin of over 300ms to less than 100 ms. It is thus expected that a more precise setup, including a more powerful HP, would allow recording these values at higher temperatures, which would mean a total convergence of the results. Nonetheless, in this case, it must be asked why this large variability at low temperatures. As expected, the effect of stabilizers was going to be noticed in this parameter. At lower temperatures, the effect of stabilizers is more pronounced than at higher temperatures, where the stabilizers are overcome easily. This is translated into a more significant variability of the DDT at lower temperatures. It is still unclear how these values will vary when EtOH is applied to them, as it should quench the reaction and slow it, but the high volatility of EtOH may also induce ignition faster. To put it into perspective, in general the value of 100 ms is used as the benchmark for RCS systems to be able to meet their mission requirements [28]. This means that within our tested combinations, on average at 270°C±10°C, the concentrations of 95% and 85% would make it. The question then remains whether this would mean that 90% would also make it if further droplets would have

been made. At 250°C±10°C, 85% HTP, on average, would suit this requirement.

4.5. Comparison with catalysts

In this section, a comparison with MnO_2 as a catalyst against the thermal decomposition method is made. As introduced in Section 4.1.1, catalysts are chemicals which allow reducing the activation energy of a given reaction. By reducing this energy, they promote the start of the reaction at lower temperatures. This is the case for MnO_2 (manganese dioxide), on HTP. Although out of the scope of this study, the reaction which involves the decomposition of HTP through MnO_2 activity is understood to be a oxidation-reduction cycle [47]. Fortunately, some MnO_2 was available at DASML and could be used to test the HTP. It is important to bear in mind, that MnO_2 is a low-end catalyst and is not comparable to more exotic catalysts used in other approaches with HTP [40]. The results concerning the DDT, based on DAQ, and the maximum temperature, are gathered in Table 4.7, and a sample f the heating profile is presented in Figure 4.11. To measure these, the setup did not need to be adapted. Only the catalyst was thinned down and placed on top of FTK1.

Table 4.7: Catalyst results for one drop experiment performed at standard conditions of 25°Cand 1 atm.

Concentration [%±1%]	**T_{max} [°C±3°C]**	**DDT [ms ±18ms]**	**FTK of T_{max}**
80	119	18.2	1
85	201	18.2	1
90	230.6	72.7	1
95	302	36.4	1

As can be seen from the data in Table 4.7, the effect of MnO_2 on the decomposition of HTP is twofold. On the one hand, the temperature maximum achieved is significantly lower than for the thermal counterpart. As can be seen, there is an increase in temperature max as the concentration enlarges, which also matches with the understanding we have of HTP decomposition. However, the values are lower than what is expected from the theoretical analysis in Section 4.1.2. In fact, none of the droplets achieved a maximum temperature, which could be possible to use with EtOH for ignition. Consequently, on this end, the catalyst approach is not effective. The reasons behind it can be several. Firstly, the presence of stabilizers may influence the effectiveness of the catalyst, reducing its decomposition power. Moreover, the visual information of the experiments revealed that the decomposition did not take place in an "explosion" manner, meaning that no sudden rapid decomposition of the totality of the HTP was present in this work. Instead, the rise to maximum temperature took longer. This can be appreciated in the Figure 4.11, where the temperature is risen for a longer time than in Figure 4.5. At the end of the day, the temperature achieved through this specific catalyst is unrivaled with the thermal decomposition, even if the ΔT is looked into. Given that the catalysts tests were done at room temperature, the maximum ΔT achieved was for 95% being less than 300°C. While for 95% in the thermal case, the increase in temperature is about 600 °C. To solve this problem, warming up the catalyst is always an approach proposed, however when faced with the need to warm the catalyst, the question remains: why not to simply warm up the HTP and decompose it?

When it comes to the DDT, the values were taken from the readings of the DAQ, and as can be seen, the values are in general lower than what thermal attained. In fact, the values were within the resolution of the DAQ, meaning that in one reading the droplet is measured, and right in the next reading the decomposition is started to be measured. When comparing within these values, an interesting feature is that higher concentrations have a larger DDT, a larger sample case size is recommended to study this in more detailed. The readings of the HSP also showed an interesting phenomenon, as opposed to the case of the thermal activation, no shock wave was found. Instead, a more step-wise process was witnessed in which the HTP was progressively consumed from the catalyst.

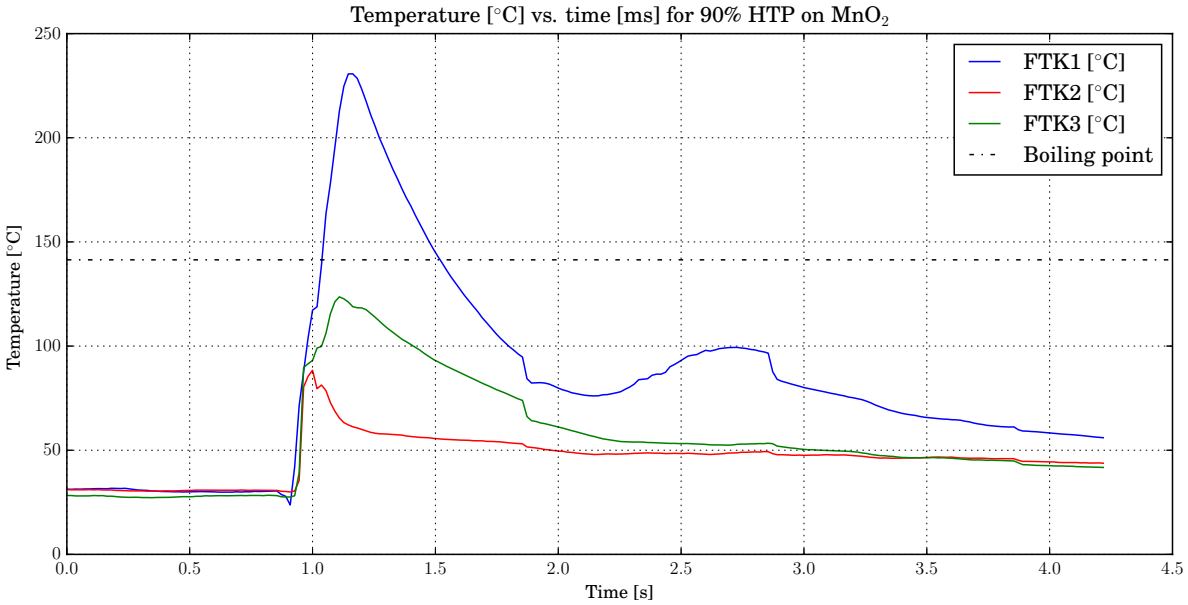

Figure 4.11: Temperature profile for 90%±1% HTP falling on meshed MnO_2 at room conditions of 25°Cand 1 atm.

4.6. Conclusions

In this chapter, a new approach to work with HTP is presented. To achieve this, thermally decomposing HTP is studied. The steps to set up the experiment and the methodology followed were given. Moreover, initial theoretical work on the heat needed and the heat released are presented. Subsequently, the results of the drop test study are presented and discussed. For completeness, a small insight into the decomposition with catalyst was also provided. After the presented results, several conclusions are drawn.

First and foremost, this study has shown that thermally decomposing HTP is possible for the proved combinations of concentrations and supplied temperatures of 80%±1% with 250±10 and 270±10°C, 85%±1% with 200±10, 250±10 and 270±10°C, 90%±1% with 200±10, 250±10 and 270±10°Cand lastly 95%±1% with 200±10, 250±10 and 270±10°C. The thermal decomposition was found to be a highly exothermic process, which surpassed the theoretical estimation based on adiabatic flame temperature. It was later found with the help of the HSPC that the phase of the reactants in the process is not fully liquid, which may be a reason why the mismatch between these two. Likewise, the required temperature to start decomposition was found not to be the same as the theoretically expected, instead, the value laid significantly over it and it was found to be close to the boiling point for HTP.

For each of the successful decomposition combinations, a total of three droplets were analyzed through the drop test method. It is clear after this study that the maximum temperature achieved after the decomposition lays above the autoignition temperature of EtOH, which opens the door to a future dual-mode system. The maximum temperature laid close to the 850°C for the cases of 90 and 95% HTP, for the concentrations of 85% and 80%, the successful decomposition are around the 700°C. When it was compared with the activity of a selected low-end catalyst, MnO_2

When looking at the DDT, a clear trend was found which shows that more significant temperature equals shorter DDT. In fact, for the benchmark of the 100 ms, 270°C as supplied HP temperature is needed. The concentration had a less significant effect on this parameter. It was also found that visual characterization of the DDT is involved on the HSP, given the lack of color recording. However, it was possible in some cases to identify the decomposing shock wave, which lead to a subsequent depletion of HTP in a self-sustained reaction.

Nonetheless, several question marks are still open. The effect of stabilizers is only inferred in the results of this study. The DDT at low temperature is more diverse due to this effect which prevents the decomposition from happening as fast as at higher temperatures. The decomposition required temperature, found to be 105°C in the theoretical study was significantly raised to around the boiling point, 140-150°C. This may be a result of the stabilizers. Moreover, the stabilizer may also be playing a role in the catalyst decomposition. Lastly, a larger test study with a more robust equipment is envisioned to be needed for future work on this topic. A more powerful heating plate and a HSPC in color are examples of this.

5

Igniting of H_2O_2 and Ethanol

In this chapter, the findings of the decomposition of H_2O_2 of the previous chapter will be put to use. This chapter will deal with the analysis of the bipropellant mode of a future thruster. Now that the understanding of the monopropellant mode use of HTP is solid, research on whether this can be applied for a bipropellant mode follows. In this chapter, a drop test study similar to the one in the previous chapter will be done, where HTP and EtOH will be subsequently shortly precipitated onto a heating plate. To do so, theory is presented in Section 5.1 for the process involving pseudo-hypergolicity, as well as a look into the analytical reaction and the expected temperature through more detailed analysis in NASA CEA. Subsequently, a brief touch on the experimental setup will be done in Section 5.2, as most has already been presented in Section 4.2. Afterward, a summary of the methodology followed in general is presented in Section 5.3 for the ignition drop test experiment. The entire test plan is presented in Appendix B. After, the full test results will be presented, analyzed and discussed in Section 5.4, including the trial cases for gel. Lastly, a set of conclusions and a reflection on the limitations of the study are given in Section 5.5.

5.1. Theory

When it comes to the ignition of fuel in collaboration with HTP, much work has already been done and is even in place by some start-ups such as Skyrora who uses hydrogen peroxide and kerosene for microlaunchers, or Dawn aerospace who uses it for their green propulsion systems. It is an obvious step, as hydrogen peroxide can be used as highly energetic chemical, but also as an oxidizer supplying of oxygen for the fuel. Nonetheless, when it comes to hypergolicity, it is also important to know what to expect from the ignition process. When it comes to hypergolic the processes involved in the combustion are well-known and taught at university level. These were discussed in Chapter 2. However, HTP in combination with ordinary chemicals is not strictly hypergolic. Instead, the high energetic content of HTP is released to allow for ignition without the help of an igniter. This is known as pseudo-hypergolicity, as the ignition truly happens upon contact of the propellants and not the action of the igniter. From the findings in the previous chapter, it was found that certain combination for heat supply and concentration of HTP lead to complete decomposition and high exhaust temperature. This high exhaust temperature can be used to ignite the fuel. From these, the pseudo-hypergolic process can be inferred and is presented in a flowchart manner in Figure 5.1.

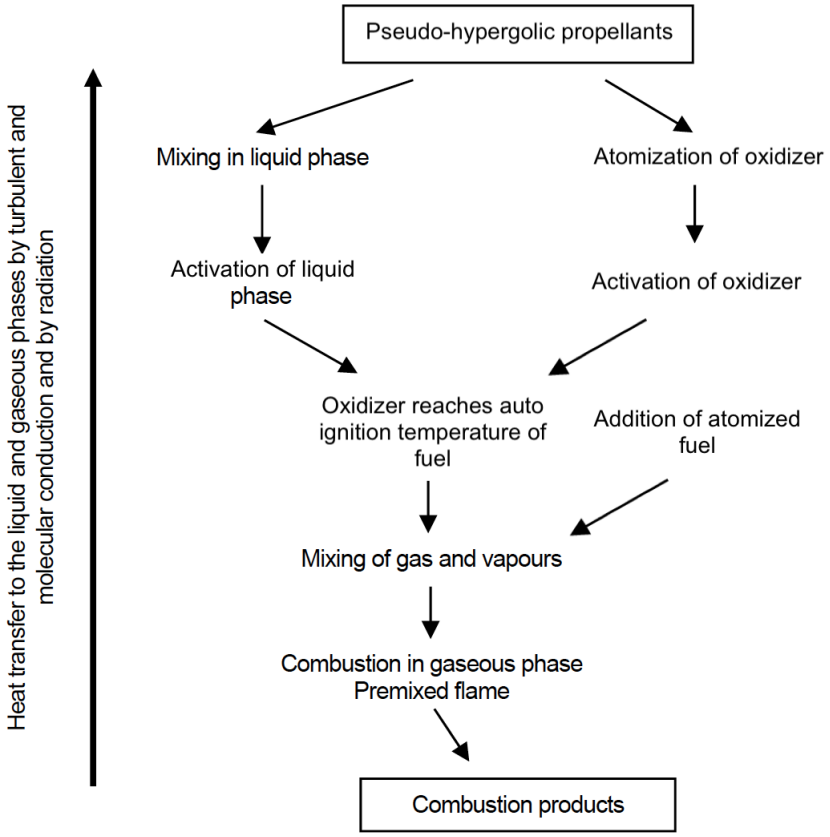

Figure 5.1: Expected processes for pseudo-hypergolic propellant combustion of H_2O_2 . Adapted from [58]

The critical step that differentiates pseudo-hypergolic propellants from hypergolic is the activation of one of the chemicals. In this case, the process is presented for HTP. The ignition of HTP with EtOH comes from reaching the EtOH autoignition temperature rather than starting a chemical reaction that leads to ignition, as in the case of NTO or UMDH/MMH. To reach this final state and start ignition, two approaches are envisioned. Firstly, as presented in Figure 5.1, the process on the right of the figure shows the obvious process. HTP would be atomized into the combustion chamber, where it would be activated in a similar manner to the presented in the previous chapter. Some heating device would start its decomposition so it would reach the autoignition temperature of the paired fuel. Then the fuel would be added after atomization. In the mixing, the HTP would autoignite the EtOH and provide the oxygen to it for full combustion. This would finally lead to the combustion of the EtOH in gaseous phase and the energy release would, in turn, allow for faster evaporation and ignition of the upcoming propellants through radiation and molecular conduction. On the other hand, the process presented on the left of the figure also should be tested. This is, whether the liquid phase of the propellants can be mixed prior to the activation of one of them. If this is the case, then the process would look the same as in the previous one, with the exception that the EtOH and HTP would already be in contact and thus no timing of which would come first is required. This process could not be possible with the use of catalyst, as fuel in contact with catalyst can have a poisoning effect on the catalyst pack [37].

5.1.1. Combustion reaction and expected temperature

As opposed to the reaction for decomposition of HTP, combustion reactions are common to most hydrocarbon fuels. The process always involves a hydrocarbon as a fuel in collaboration with oxygen to lead to a final exhaust of water and CO_2, provided that the all reactants are consumed. In the case of HTP and EtOH, the reaction is similar, as the only outcome of the decomposition of HTP is water and oxygen, where water would not interact with EtOH, but oxygen would allow for combustion. Although this process can be modeled in two steps: decomposition of HTP and combustion of EtOH, is more illustrative to have the full reaction together, as shown in Equation (5.1). In fact, according to Hess's law, no matter the number of steps present in a reaction, for energy/enthalpy, only the initial and final states are relevant. This makes enthalpy a state function. In Equation (5.1), the reactant HTP is set at 90% for illustrative purposes, however this number can

be varied as long as the reaction is balanced afterward. The reaction is highly exothermic and non-reversible.

$$3 \cdot C_2H_5OH + 20 \cdot [0.9 \cdot H_2O_2 + 0.1 \cdot H_2O] \longrightarrow 6 \cdot CO_2 + 29 \cdot H_2O + \Delta H \tag{5.1}$$

Where H_2O_2 is the hydrogen peroxide molecule, C_2H_5OH is the ethanol molecule, CO_2 is the carbon dioxide molecule, and Δ H is the change in enthalpy or energy liberated which in this case would be negative, meaning that the reaction is exothermic.

In this case, to model the temperature release after this reaction, the use of NASA Chemical Equilibrium with Applications (CAE) is used. For it, an important parameter is needed, this is the oxidizer to fuel ratio (OF). In fact, this parameter now plays an important role as the reactants are only fully burned if the reaction is fulfilled stoichiometrically. This means that the ratio of initial molecules of HTP to EtOh must be exactly the one shown in Equation (5.1) so that no leftover EtOH or O_2 happens. In the case of 90% the stochiometric OF ratio is:

$$OF_{stoch} = \frac{20 \cdot \left[0.9 \cdot M_{H_2O_2} + 0.1 \cdot M_{H_2O}\right]}{3 \cdot M_{C_2H_5OH}} = \frac{20 \cdot [0.9 \cdot 34.01 + 0.1 \cdot 18.01]}{3 \cdot 49.403} = 4.403 \tag{5.2}$$

Where OF_{stoch} is the stoichiometrically oxidizer to fuel ratio, M is the molecular weight [g/mol] for the presented molecules. Consequently, the optimum OF for the reaction is 4.403. However, due to limitations int he setup as presented in Appendix B and as it will become apparent in the upcoming sections, the fuel and oxidizer quantities are limited by the system used to generate the droplets. In fact, the limitation is set at generating HTP droplets of 0.13 mL and EtOH droplets of 0.06 mL. These values are setup limited and cannot be changed, consequently to predict the final temperature we must take them into account. The final OF ratio would then be calculated as follows:

$$OF_{\text{tested}} = \frac{m_{HTP}}{m_{EtOH}} = \frac{v_{HTP} \cdot \rho_{HTP}}{v_{EtOH} \cdot \rho_{EtOH}} = \frac{0.13mL \cdot \rho_{HTP}}{0.06mL \cdot 0.789(g/mL)} \tag{5.3}$$

Where OF_{tested} [-] is the oxidizer to fuel ratio that will be tested given the droplet generation limitation, m_{HTP} and m_{EtOH} [g] are the weights of the droplets for HTP and EtOH that will fall on the heating plate for the experimentation. To find the weight, known the volume for the droplets and represented as v [mL] in the equation, the density, ρ [g/mL] is used. The density for HTP, ρ_{HTP} [g/mL], is found through the presented theory of Section 3.4.1 and implemented in the code of Appendix D. The results of the tested OF for the different concentrations are shown in Table 5.1.

To find the expected values of temperature after the combustion, NASA CEA was used. The output logs for the simulations are presented in Appendix D. Although CEA is used to simulate the conditions inside a combustion chamber, for elevated pressure and high speeds, in this case it was only used to provide with data on the expected adiabatic temperatures after combustion and to find the exhaust products of the reaction. To do so, the simulation was set for 1 atm at 25°C for the reactants and HTP was forced to be decomposed by selecting the only products possible after combustion" water, carbon dioxide and ethanol (as a possible leftover given the lower OF for the test cases).

Table 5.1: Results from the combustion of EtOH with HTP of different concentrations at an initial temperature of 25°C performed in NASA Chemical Equilibrium with Applications (CAE). The OFR was varied to match the setup OFR, for which the HTP density is provided.The presented results are in terms of output temperature and chemical products weight percentage. Results from NASA CEA shown in Appendix D

				Products [% wt.]		
Concentration [%]	**Density [g/cm^3]**	**OF ratio used [-]**	**Temperature [K]**	**CO_2**	**H_2O**	**C_2H_5OH**
80	1.333	3.684	2292.3	27.2	65.7	7.2
85	1.359	3.756	2481.3	28.9	65.2	5.9
90	1.386	3.83	2675.1	30.8	64.6	4.6
95	1.413	3.9	2873.1	32.6	64.1	3.3

As it can be seen, the adiabatic temperature greatly exceeds the adiabatic flame temperature or the temperature found for the HTP decomposition case. In fact, it goes beyond the 200°C mark. As expected, the result exhibits a linear trend for the increase in concentration of HTP. This values also represent an upper limit, not only because of their condition of adiabatic, but also because CAE does not integrate the Cp with varying temperature, instead sets it at 2000 K. A clear consequence of this adiabatic preliminary values is that

the FTK which are rated to up to 1200°C or 1475 K, would be out of their rated region. FTK can measure outside these values and past their melting point, set by the manufacturer (OMEGA) at 1430 °C. Another expected result is that there will be leftover EtOH not combusted as the OF is below the optimum OF.

5.2. Experimental setup and materials

In this section, an introduction to the materials used for the experimental setup is presented. The setup is similar to the one sued for the decomposition of HTP, Section 4.2, with the difference of the addition of a second droplet generation system for the fuel. Given that two different syringe pumps, syringes, capillary tubes and a fourth thermocouple will be used, the identifiers should be changed accordingly. The involved materials with their ids are given in Table 5.2.

Table 5.2: Inventory for setup of ignition experiment.

Inventory			
ID	**Item**	**ID**	**Item**
FM	Fumehood	SYPH	Syringe pump HTP
SYPE	Syringe pump EtOH	PC	MacBookPro
LIS	Light source	HP	Heating plate
DAQ	DAQ NI-9219	HSP	High-speed camera
FTK1	Fine K-thermocouple 0mm	FTK2	Fine K-thermocouple 3mm
FTK3	Fine K-thermocouple 6mm	FTK4	Fine K-thermocouple 5cm
SYRH	Syringe HTP	SYRE	Syringe EtOH
CATH	Capillary tube HTP	CATE	Capillary tube EtOH
HTP	High Test Peroxide	ETOH	Ethanol

Most of the materials are introduced in Section 4.2, consequently FM, LIS, HP, HSP, DAQ, HTP and the PC will not be discussed. In the case of the previous SYP, CAT, SYR are now renamed to SYPH, CATH and SYRH, and will not be discussed again. Instead, the addition of a second droplet generation systems includes the addition of another syringe pump, SYPE, a new syringe SYRE, and a second capillary tube CATE. For the SYPE, the syringe pump is also manufactured by Quality in Sensing, but only a microsyringe pump was available. The SYPE is a NE-1002x, a syringe pump used for microsyringes, which only allows for a slower discharge rate, set at a maximum of 0.571 mL/min. This slower rate of discharge when compared to the SYPH, forces to have a slower droplet generation, which affects the droplets test, this is also discussed in the full test plan in Appendix B. When it comes it the CATE, it is the same model as the CATH. They are made of borosilicate glass, with an internal diameter of 1.25 mm or 19 gauge. They have a cylindrical narrowing section, which goes down to 0.5 cm from where the droplets precipitate. Because of the difference in density and surface tension of EtOH as opposed to HTP, the droplet volume for EtOH that can be made prior to precipitating of 0.06 mL, as opposed to the 0.13 mL of HTP. The SYPE, on the other hand, is the same as SYPH, made of plastic, and holding a total capacity of 2 mL. These 2 mL will be filled with ethanol which was purchased from VWR international. It has a purity of 99.5% and CAS number 64-17-5. Lastly, when it comes to the FTK, a fourth FTK is used, FTK4 at 5 cm, right on top of the throat of the vessel. It is part of the same batch as the other FTK1-3, fine k-type thermocouple of 0.125 mm width, unsheathed. They are all connected to the DAQ NI-9219 into its 4 thermocouple channels.

5.2.1. Set up

The setup is identical to what was presented in Section 4.2.1. The only difference is the addition of the second SYPE and CATE. The two CATE and CATH are separated by each other a distance less than 2.5 cm, so that the droplet generated can fall into the vessel. The CATE and CATH are situated 17 cm above the HP were the VES lays. The HSP is situated at a distance where the FTK1 can be in focus and connected to the PC. The used vessels had three holes poked on each side at heights of 0, 3 and 6 mm, so that FTK1-3 could be placed. They were later secured with tape to the sides. The location for the FTK1-3 is identical to the decomposition test, but the FTK4 is now used at a location for 5 cm above the HP, where the throat of the vessel is. The images of the schematic and final setup of the thermocouples are presented in Figure 4.3 and Figure 4.4, respectively.

5.3. Methodology

In this section, an overview of the methodology followed to do this test is given. The entire test plan followed is presented in Appendix B. In this section, the test order followed is given. Moreover, the expected results are presented as well as a new dimension on the input variables: the time between droplets of EtOH and HTP.

5.3.1. Test order

As discussed during the theory lay-out, the ignition of EtOH will only take place once the autoignition temperature of about 365°Cis achieved. Based on the results form the HTP decomposition study, this will only take place at selected combinations of HTP concentration and HP temperature. These combinations are the only ones studied, reducing the need for resource investment. The order to follow for the tests is presented in Table 5.3.

Thus, the HTP concentrations that will be used are 80, 85, 90 and 95 %±1% for the HP temperatures of 200, 250, 270 °C±10°C, except for 80%, where 200°Cwill not be tested. As for the previous experiments, the margins of acceptability are 1% for the concentration and 10°Cfor the HP temperature. The droplet are fixed at 0.13 mL for the HTP and 0.06 mL for the EtOH. For each combination, a total of 3 experiments are needed for repeatability. It is prescribed to have at least one video to check the matching between DAQ and HSP, but also to verify that the ignition sequence is similar in all the cases and that the increased energetic content of the higher HTP concentrations does not alter it. In most cases at least two videos per combination are desired.

Table 5.3: Order for the tests of the ignition campaign, based on the successful HTP decomposition from the previous test campaign.

T [°C±10°C]	**Conc [%±%]**	**80**	**85**	**90**	**95**
200		X	3	6	9
250		1	4	7	10
270		2	5	8	11

5.3.2. Expected results from the test

The aim of this test is to characterize in the way possible the ignition, through the pseudo-hypergolic process presented in the theory section, of HTP with EtOH without the presence of catalysts. The characterization is expected to take place through the finding of two key parameters: the Ignition Delay Time (IDT) and the ignition temperature. The IDT value is of importance for the sizing of the combustion chamber. Too short times, below the 20 ms margin, may be dangerously close to the injectors, while too long IDT has the problem of gas buildup in the combustion chamber with the risk of a hard-start. The maximum temperature is an important parameter as well, it serves to understand the amount of energy released and to put to context the temperature profile in terms of rising temperature. In any case, it is expected that the value of maximum temperature will increase as the pressure in the combustion chamber increases. The test goals are the following:

- **Temperature profile characterization:** to measure the temperature [°C] of the exhaust gases after ignition through the use of 4 k-type thermocouples for the proposed combinations of HTP-HP temperature. FTK1 in contact with the floor of the vessel, FTK2 3 mm above, FTK3 6 mm above and FTK4 at 5cm positioned on the throat section of the vessel.
- **Ignition Delay Time characterization:** to find the values of the IDT [ms] for the proposed combinations of HTP-HP temperature. This will be possible through the use of HSP and FTK/DAQ at 55Hz.
- **Visual understanding:** to investigate the dynamics of the process from a visual standpoint with the use of the HSP. Any discoveries related to the dynamics of the process should be reported.

In this experiment, the IDT is more complicated to define, as two droplets will be used. First and foremost, the use of two different syringe pumps working at different discharge rates makes it difficult to have an exact timing of the droplet precipitation. This added a degree of complexity to the test. It is always prescribed for safety purposes to have the HTP droplet precipitating first. This avoids having the EtOH in the gaseous phase before HTP comes in, which could result in an explosion hazard. This new dimension of input variables was also recorded. Bearing this in mind, the IDT is defined by the purposes of this study in two manners depending on whether DAQ or HSP is used. For the HSP, the IDT starts the moment the two droplets touch

each other, until the moment the first ethanol ignition takes place. For the case of the DAQ, the droplets leave a small dip in temperature in the FTK1; they mark the precipitation of the droplets. However, for the DAQ, ignition is achieved when a sudden increase in temperature in FTK2,3 and 4 take place. The reason being that FTK1, being immersed in HTP with volatile EtOH, can sustain heterogeneous decomposition of HTP, which does not mean ignition, as ignition will spread all along the vessel and reach all thermocouples equally. For the design of a combustion chamber, the addition of the DDT may also be need. Only tests in a more relevant environment can tell. The resolution of the HSP is of 1/64,00 = 0.15 ms, while the DAQ at 55Hz would have a resolution of 18.2 ms. The drop test is designed to acquire the following parameter data:

- **HTP concentration [%±1%]**
- **Inter-droplet timing [ms±0.15ms]:** the time in between the droplets of ethanol and HTP. If the value is negative, it means that the EtOH fell first.
- **T_{HP} [°C±3°C]:** temperature of the heating plate that the propellant droplets will feel. This is not the heating plate temperature strictly speaking, but the temperature of the floor of the vessel. This value is given by the FTK1 and it is expected to be roughly equal to the HP. It is not expected that this value will have an impact on the maximum attained temperature, as this is only dependent on the chemical properties and the energy of the chemical itself.
- **$T_{ignition}$ [°C±3°C]:** this is the temperature of the fluid at the moment when ignition takes place. Attention must be paid to this value as it is not the temperature achieved on the ignition, but rather the temperature at which the propellants are when they start to ignite. Although unknown, it is expected that the value should be somewhere close to the found decomposition temperature on the previous experiment. This value is also provided by FTK1. This value is expected to be a constant among the same concentrations.
- **T_{max} [°C±3°C]:** this is the maximum temperature achieved at any point of the ignition and at any FTK. The FTK at which it happens will also be monitored for qualitative analyses. The maximum temperature is resulting from solely thermal purposes as the FTK was chosen to be as slim as possible to reduce the radiation effects.
- **IDT_{DAQ} [ms±18ms]:** this is the IDT from the DAQ reading. In some cases, it might be easier to identify it than in others. The IDT starts from the moment the second drop in temperature takes place, meaning that the EtOH has fallen.
- **IDT_{HSP} [ms±0.15ms]:** this is the IDT from the HSP. It has been previously defined and an only be identified visually and in some shots, consequently, when the data from the HSP is not available, the data from the DAQ will be used.

5.4. Results and comparison

In this section, the results achieved through the campaign test are presented. The results are divided into three main subsections. Initially, the characterization of the ignition process will be presented in Section 5.4.1. These are visual results together with the understanding of the temperature profile. Subsequently, a more thorough look is taken to the temperature attained at ignition and after ignition in Section 5.4.2. Lastly, the IDT results are discussed in Section 5.4.3.

Before diving into the results, the final valid data used for the analysis is presented. For this, the values used are presented into the Appendix A. As a summary of the data used, Table 5.4 includes the number of droplets valid for the subsequent analysis.

Table 5.4: Number of valid droplets used for the ignition study. All combinations of HTP concentration and HP temperature have the minimum of 3 points.

	Concentration [%±1%]			
HP temperature [°C±10°C]	80	85	90	95
200	NA	3	6	7
250	4	4	3	6
270	6	3	3	3

Table 5.5: Number of valid droplets with IDT HSP. *-The short DDT of the HTP made it hard to time the EtOH and HTP falling, so the only recording is a mid-air ignition, non-valid for this study.

	Concentration [%±1%]			
HP temperature [°C±10°C]	80	85	90	95
200	NA	3	3	4
250	2	2	1	1
270	2	2	2	0*

As presented in Table 5.4 and Table 5.5, the number of valid points which can be used for this study is over the minimum set in the test plan, Appendix B, of 3 data points. Nonetheless, the points caught on camera proved to be a more challenging task. As it happens with the decomposition analysis, the number of points caught on camera this time was 3, however upon close reinspection, some of them were not valid: either the EtOH had fallen first, or the temperature of FTK1 upon droplet precipitation was not the one for that temperature range and had to be moved or discarded. Special mention deserves the combination of 95% and 270°C, as the timing was the most challenging step. A proper precipitation mechanism is envisioned to be essential for further studies. The moment HTP fell on the HP, it was almost instantaneous that the decomposition took place, this is the reason why the only recording video filmed a mid-air ignition rather than a proper droplet fall. This video is thus invalid, but interesting as a case of special mention, thus, its sequence is presented in Figure 5.11. Nonetheless, as it happened with the HTP decomposition, the matching between the DAQ and HSP was within the resolution of the DAQ, meaning that the analysis with data from the DAQ is equally valid for this study.

5.4.1. Profile and visual characterization

The first outcome to discuss is the characterization of the ignition from a visual and temperature point of view.

After carefully reviewing the recorded HPS videos at 6400 fps, a shared process of ignition was identified. Firstly, the HTP falls onto the bottom of the VES, this first part is similar to the decomposition first steps. Once the HTP falls, it starts taking energy from the heated VES and slightly from the FTK1. The energy rapidly rises the temperature of the HTP which appears to start releasing bubbles almost immediately. The release of bubbles corresponds with the initial boiling of HTP. This does not take place for too long, as EtOH is falling within 200 ms, typically below 100 ms, after HTP. Once the EtOH touches the already boiling HTP, it appears to quench the boiling momentarily. Then, another differentiated process starts, in which the bubbles are not seen anymore, but instead a wave-like pattern can be seen right above the propellant mixture. This pattern seems to be caused by the refraction of light in a similar way to really warms surfaces do. In the meanwhile, the gases of HTP, EtOH and water fill the container. A subtle hissing sound can be heard. This does not take place for too long until the ignition happens, depending on the HTP concentration and especially the heating energy supplied. At some point, decomposition of HTP takes place similar to the only decomposition case. It is then when the shockwave of decomposed HTP touches any molecule of EtOH that the ignition takes place. In most cases, the initial HTP decomposed shockwave cannot be seen, but the ignition is seen first, however it is known that the shockwave must have happened prior to the ignition,as the necessary autoignition temperature must be achieved. It is only then when a small fireball can be identified in the camera, this marks ignition. The small fireball spreads fast, a speed analysis could be put into place given the proper resources. The ignition burns the entirety of the propellants and a subtle combustion chamber-like behavior can be seen with the expulsion of ignited propellants through the throat. The propellants are fully ignited and then strong radiation disappears and the camera picks up the FTKs glowing. This process is sound-characteristic as well, as a strong explosion-like sound can be identified and be surprising for the unprepared ear.

As an example of the nominal temperature profile, the case of the 95% HTP with EtOH at 250°Cis presented in Figure 5.2, which corresponds to the frames presented in Figure 5.3. After reviewing multiple temperature profiles, the profiles all seem to have the same characteristic points, these are indicated in the figure. The profile goes from the beginning prior to HTP dropping, to the complete combustion of all the propellants and the slow decay in temperature. 4 FTKs are presented, these are FTK1 in blue (touching the bottom of the VES), FTK2 in red (placed at 3 mm above the VES bottom), FTK3 in green (placed at 6 mm) and FTK4 placed at 5cm on top of the throat of the vessel in black, plus these are visible in the frames of Figure 5.3. The figure includes a numbering that corresponds with the numbering presented in the frames of Figure 5.3 for the same drop test, from 1-7, where 3 cannot be adequately identified, only by HPS camera. In Figure 5.3, the frame number of the video is presented, from where the IDT [ms] and the time in between droplets can be found [ms]. The numbering is as follows:

- **Point 1:** location 1 is the vessel awaiting the droplet to come. In this case, the temperature is 243°C±3°C. At this stage, the HSP is started to film. This is frame 19 in the HSP recording. As can be seen in the frame image, both droplets of HTP and EtOH can be seen, where the HTP has more volume, is larger in

size and is falling before the EtOH. The EtOH is still outside the vessel when HTP is about to touch the bottom, it can be also seen how it is smaller in size as expected.

- **Point 2 [t=-33.75 ms]:** at location 2, the temperature felt by FTK1 declines as the HTP touches it in frame 43 of the recording. FTK2 and FTK3 also feel this drop in temperature resulting from almost instantaneous initial boiling of the HTP, whose gases should be at about 145 °C, which is the boiling point for 95% HTP. In this frame, the EtOH still has not reached the bottom of the HP. The time in between droplets can be found by calculating the amount of frames between droplets and with the frame rate: $t = (259-43)[frames]/(6400)[fps] = 33.75[ms]$. Drawn in yellow in Figure 5.2 is the period of HTP and propellant energy absorption, similar to what is presented for the decomposition case.
- **Point 3 [t=0 ms]:** this location is where the EtOH falls in contact with HTP at the bottom of the plate. Here is when the IDT starts. In most of the cases, identifying the second droplets in the temperature reading of Figure 5.2 is complex, due to the short separation in between the droplets and the smaller impact on the temperature EtOH has after HTP has already fallen. Consequently, this value is normally obtained from the valid HSP recordings, if no recording is available, visual confirmation of HTP falling first is used alone.
- **Point 4 [t=IDT=96.1 ms]:** ignition takes place. Normally, the ignition starts by an initial decomposition of HTP, which in contact with the gaseous molecules of EtOH ignites, as it is over the autoignition temperature. The ignition takes the shape of a small fireballs which indicated the start of ignition. This increase in temperature is quickly felt by FTK1 and subsequently FTK2, 3 and 4. The rapid increase in temperature, in this case, of over 900 °C. The location where the ignition starts is normally close to the bottom of the VES, which is the warmest in the vessel. Nonetheless, some cases of aerial start of the decomposition were also found.
- **Point 5:** the small fireball is spreads quickly to the entire fuel and oxidizer combustion. It can, moreover, be seen how a combustion chamber-like behavior appears at the throat of the vessel. The maximum temperature is quickly achieved.
- **Point 6:** a common temperature decay takes place; it is believed that the oxidizer runs out. The OF ratio used is below the optimum OF ratio, meaning that extra fuel is present for which no oxidizer will be left. Once the HTP runs out, still some EtOH is present to burn, but the reduced oxygen available reduces the temperature drastically.
- **Point 7:** the second more subtle temperature decay is not visible in all the temperature profiles. Nonetheless, it is attributed to the final consumption of all the EtOH present in the propellant mixture.

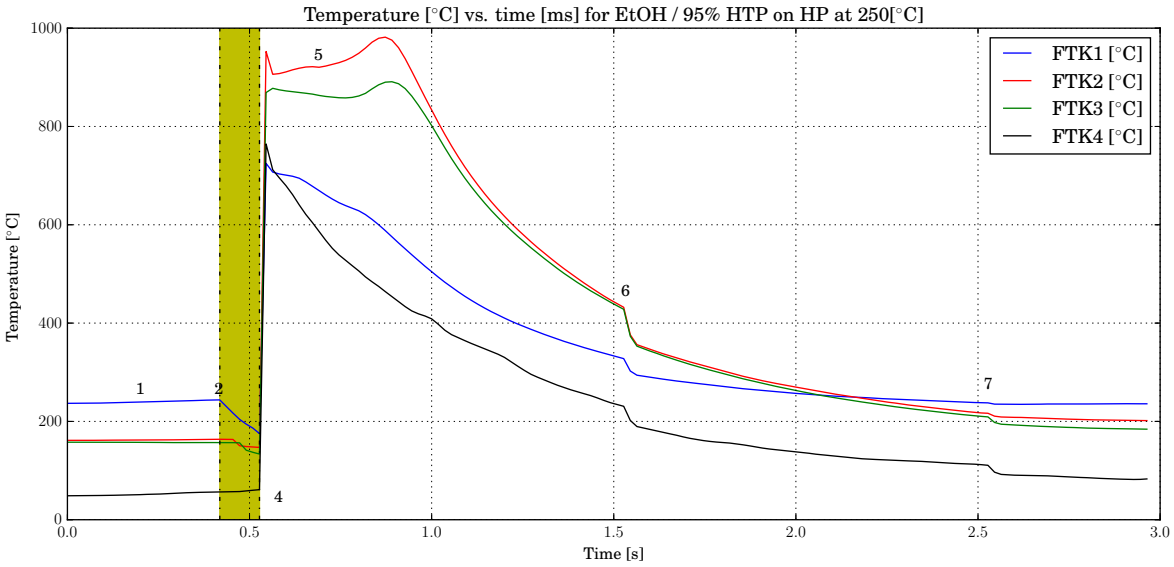

Figure 5.2: Temperature profile for test combination 95%±1% HTP and EtOH precipitating on the HP at 250°C±10°C. Legend for numbering is done in accordance with frame pictures of Figure 5.3. Rest of numbering is discussed in-text.

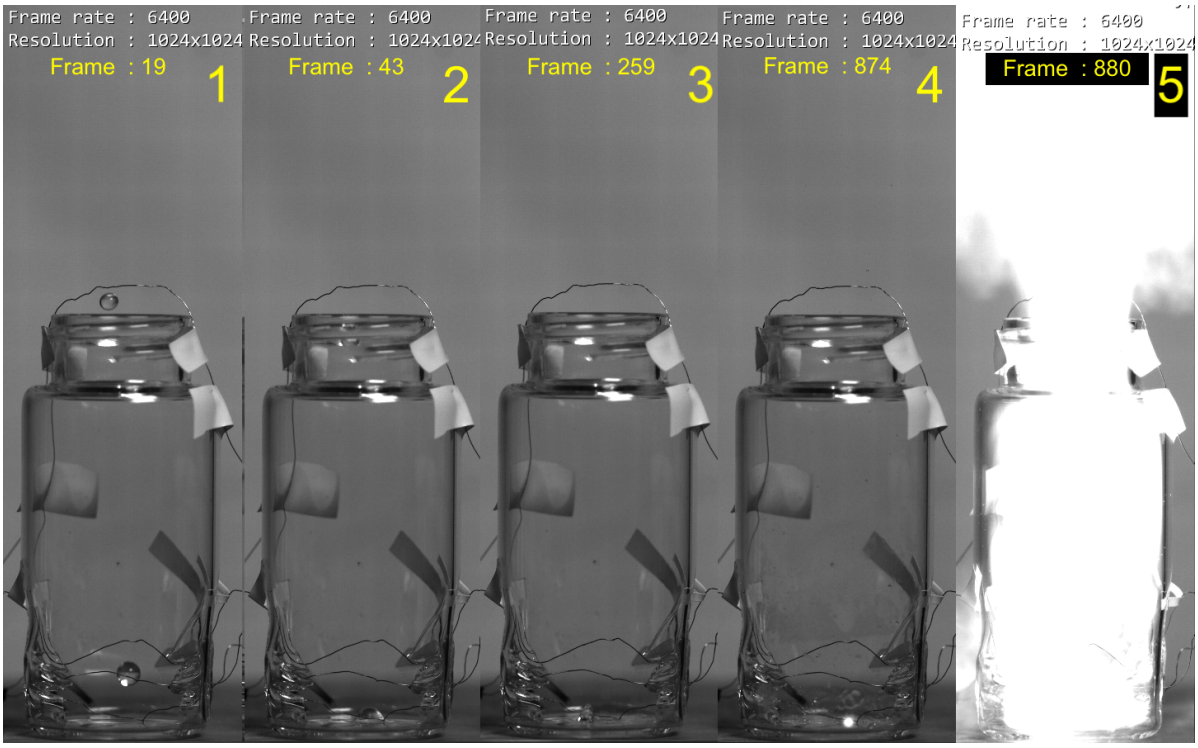

Figure 5.3: Valid ignition sequence for 95% HTP with EtOH. The frames are indicated as well as the image sequence. 1- HTP and EtOH droplets falling, HTP first (*Frame: 19*). 2-HTP touching FTK1 (*Frame:43*). 3- EtOH touching FTK1, IDT starts now(*Frame: 259*). 4- Ignition starts, IDT calculated until here (*Frame: 874*). 5- Rapid full ignition. (*Frame: 880*).

Given the initial difficulty of precipitating the HTP droplet before the EtOH droplet, a few failed tests were recorded. It is learned the hard way what is understood as a "hard-start". When EtOH falls significantly before HTP in the vessel, it undergoes rapid evaporation, given its high volatility, and it fills the entire vessel with its gas. Then, the decomposition of HTP, once it falls, promotes a rapid expansion and combustion of gaseous ethanol. This combustion has an explosive nature, which can even lead to breaking the vessel. This can be seen in the sequence of Figure 5.4. In this case 95% HTP on 250°CHP fell $(2466-223)[frames]/(6400)[fps] = 350.5[ms]$ after the EtOH. In this time, the EtOH was fully evaporated. The ignition starts on the side of the vessel and the spread is fast and explosive, as it can be seen in the image 4 of Figure 5.4, the explosion breaks the vessel. The resulting vessel was later examined in Figure 5.5. It is clear that HTP must always appear before EtOH, in fact, this is what is required to avoid a hard-start in a future combustion chamber.

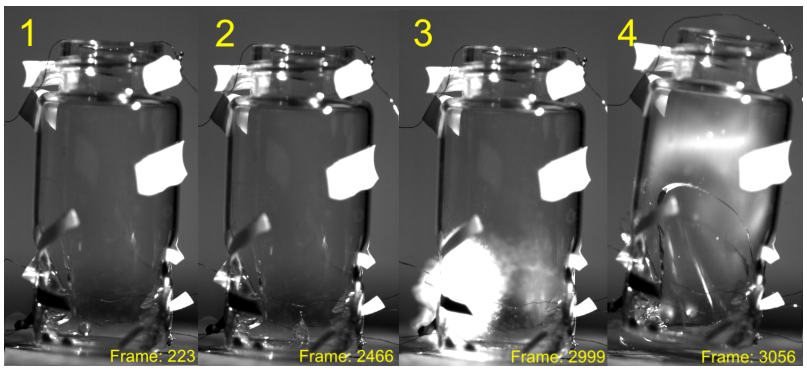

Figure 5.4: Ignition sequence for non-valid case when ethanol precipitates into the vessel substantially before the 95% HTP on a 250 °CHP. 1-EtOH falls in first into the vessel (*Frame:223*). 2-HTP precipitates 350ms after (*Frame:2466*). 3-Ignition takes place 83ms after (*Frame:2999*) 4-The ignition is explosive and cracks the vessel (*Frame: 3056*)

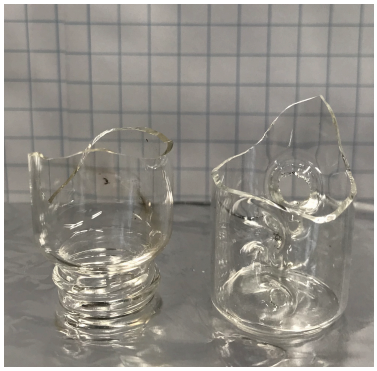

Figure 5.5: Cracked vessel resulting from erroneous precipitation order, as shown in Figure 5.4. It had to be discarded and a new vessel was prepared.

5.4.2. Temperature investigation: ignition and maximum

In this subsection, the temperature results from the droplets are processed and analyzed. Firstly, the ignition temperature will be looked into, subsequently, the increase of temperature after ignition will be analyzed.

In Figure 5.6, the averaged temperature achieved at the moment of ignition is presented for the varying temperatures of the HP and of the 4 HTP concentrations. The data points are also presented in a tabular form in Table 5.6. Moreover, a linear fit to the unaveraged data is also present in the dotted line manner. In it, for valid data points of Appendix A, the average of the points per concentration and HP temperature is shown. The vertical error bars belong to the Inter Quartile Range (IQR). The IQR is found by assuming that the data points acquired are part of a normal distribution centered at the "real" value. This statistical perspective allows for more flexible and realistic results, given small variations in real-life experiments. Clearly, there is a positive correlation between the energy supplied to the system and the temperature of the propellant when it ignites. Moreover, a subtle trend within the concentration for the oxidizer is also present.

At lower temperatures of the HP, 200°C, the three tested concentrations (85, 90, 95%) lay very close to each other and close to the boiling point. The three are between 127-130°C, moreover, the three have a low variability expressed in terms of the IQR of the averaged values. It is speculated that in this case, the slower energy supply leads to a more steady result, giving a close to reality value. However, as the energy increases and the concentration decreases, the reaction becomes more unsteady and the results start varying more aggressively. When looking at 250°C, the low concentration of 80% manifests this aforementioned behavior. It displays a larger IQR and higher temperature of ignition. In fact, the temperature of ignition is entirely above the boiling point. It is speculated that the decomposition of HTP, in this case, is not homogeneous but heterogeneous and happening only at FTK1, as FTK2 and 3 do not record ignition temperature spiked until this temperature was reached in FTK1. For 80%, this is further found for 270°C, where the IQR grows to over 100°C. As larger energy supplied take place and lower concentrations of HTP are used, the larger the ignition temperature, but also the larger the variability. For the cases of larger concentrations and stronger energetic content, the temperature of the HP has a lower effect, this is expected as the more energetic content is less affected by the energy supply, at the end of the day the energetic nature comes from within the chemical. 90%±1% HTP shows an increase in ignition temperature with HP energy supply, but its variability is not affected as much by the HP. Finally, the highest concentration 95% HTP is the least affected by the energy supply. The values of ignition are close to the boiling point of 145°C, in fact, only at 250°C HP is above the boiling point, indicating the possibility of requiring to retake more samples. The trend lines indicate what was expected, lower concentrations are affected in a larger way by energy supply. The trend lines are linearly fitted to show an initial trend of how the ignition temperature is related to the energy supply. The fittings are far from perfect, however they show the relationship. The coefficients of determination [R^2] indicate that in the case of 95%, the fit is off and a linear fit might not be good for this case, however the values also seem to be independent of the HP temperature, thus the averaged distances affect this R^2 value more. The slopes of the linear fittings show how larger concentrations are less affected by the HP opposed to the lower concentrations.

Table 5.6: Ignition temperature recorded by FTK1 at the moment of ignition averaged with the valid data points and interquartile range from them. Based on the valid data points. The coefficients of determination for the linear fittings R^2 of the data points are indicated next to the concentrations. The ignition study was done at atmospheric pressure in a lab-controlled environment.

	Concentration [%±1%]							
	80 [R^2 = 0.27]		**85 [R^2 = 0.48]**		**90 [R^2 = 0.66]**		**95 [R^2 = 0.02]**	
HP temperature [°C±10°C]	**Average** T_{igni} **[°C]**	**±IQR** [°C]	**Average** T_{igni} **[°C]**	**±IQR** [°C]	**Average** T_{igni} **[°C]**	**±IQR** [°C]	**Average** T_{igni} **[°C]**	**±IQR** [°C]
200	NA	NA	127.3	5.3	143.5	1.1	139.2	7.7
250	580.3	59.9	202.0	33.3	186.4	35.8	160.9	14.3
270	657.7	118.0	522.3	104.3	266.9	10.8	140.3	1.25

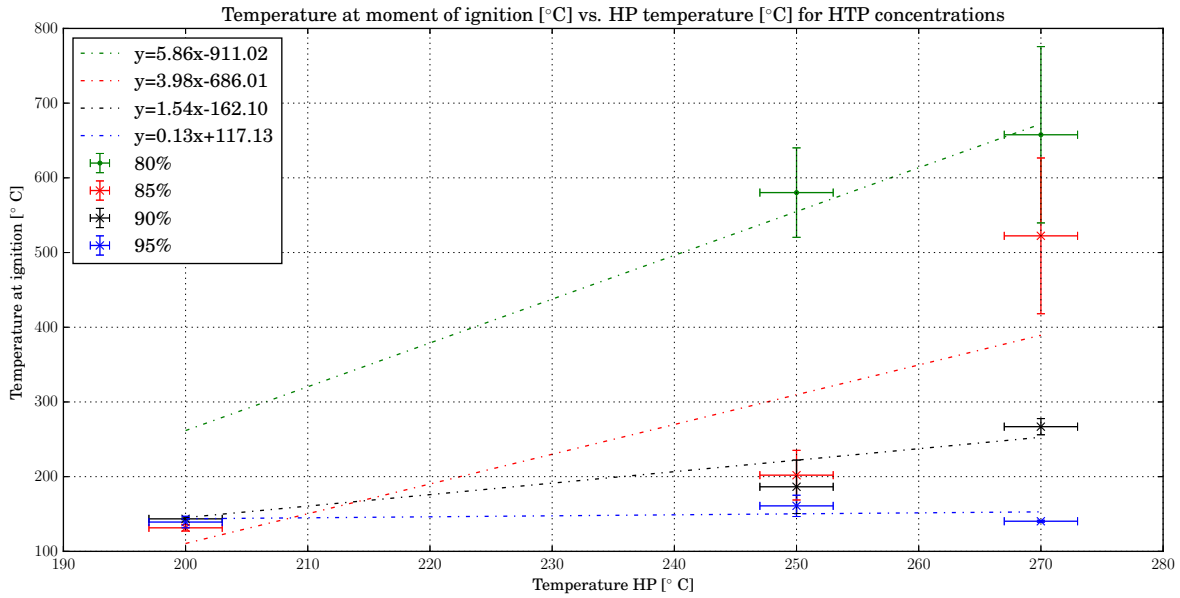

Figure 5.6: Temperature at the moment of ignition [°C] recorded by FTK1 immersed in propellant vs. HP temperature [°C±10°C] for different concentrations of 80, 85, 90, 95% ±1% HTP with EtOH. The presented values are the averages of the data points pertaining to that HP value. The y error bar is the IQR for the averaged set of values. Trend lines are fitted to the individual set of data points. The ignition study was done at atmospheric pressure in a lab-controlled environment.

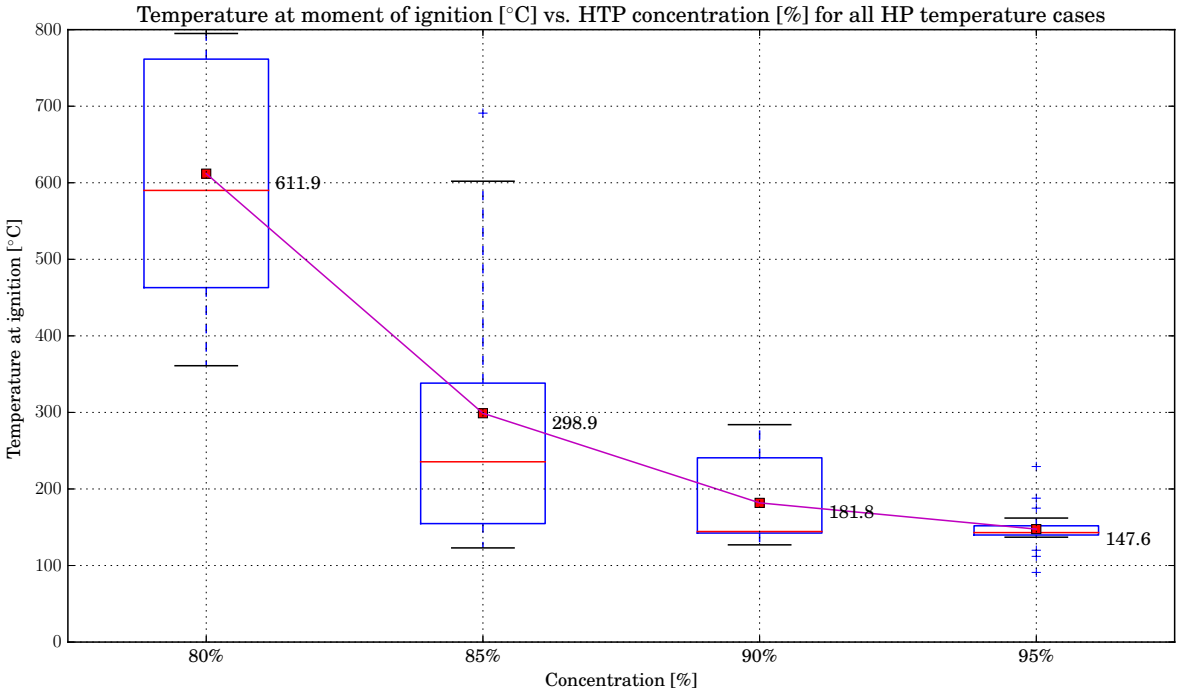

Figure 5.7: Box and whiskers plot graph of temperature at the moment of ignition [°C] measured by FTK1 immersed in propellant vs. concentration of HTP [%±1%]. All the tested HP temperatures are bundled together. The boxes represent the IQR, with the red line being the median and the red squares the average. Written in text are the average per concentration. The ignition study was done at atmospheric pressure in a lab-controlled environment.

Looking in more depth for the effect of concentration on the ignition temperature leads to exciting results. In Figure 5.7, a box and whiskers plot is presented to show the overall ignition temperatures per concentrations, these were measured with the FTK1, which is immersed in the propellant at the bottom of the VES. In this plot, the median is represented by the red line within the box, while the red square represents the average

value, which is indicated in text next to it. In this format, it can be easily appreciated how larger concentrations are favorable for their more stable behavior, showing a decrease of variability along the concentration axis, but also the ignition temperature decreases with concentration as well. The interaction of the HTP stabilizers with EtOH is unknown and might also play a role, as well as the water dilution of EtOH might be affecting its autoignition temperature.

Equally as illustrative, is the energy liberated after the ignition takes place. To fully characterize the efficiency of the ignition, the temperature achieved is of importance. For this the averaged maximum temperature is presented per combination of HP temperature and HTP concentration in Figure 5.8. In the graph, the plotted points are given with error bars in the Y-axis corresponding to the IQR of the averaged values. The averaged values and the IQR is also given in a tabular form in Table 5.7.

Table 5.7: Maximum temperatures [°C] achieved after the ignition of HTP at different concentrations with EtOH for different HP temperatures. The ignition study was done at atmospheric pressure in lab-controlled environment.

	Concentration [%±1%]							
	80		**85**		**90**		**95**	
HP temperature [°C±10°C]	**Average** T_{max} **[°C]**	**±IQR** [°C]	**Average** T_{max} **[°C]**	**±IQR** [°C]	**Average** T_{max} **[°C]**	**±IQR** [°C]	**Average** T_{max} **[°C]**	**±IQR** [°C]
200	NA	NA	666.1	32.6	663.3	54.4	946.1	231.5
250	825.9	22.8	833	99.5	839.3	47.8	797.8	145.25
270	914.33	59.9	860.6	69.8	1048.33	89.0	731.6	61.8

When looking at Figure 5.8, several interesting features can be noticed, some of which were not expected. Firstly, an expected behavior is the increase of T_{max} with increasing energy supplied, or T_{HP}. In all the concentrations with the exception of 95%, this was respected. More interestingly, the increase in T_{max} between the T_{HP} does not correspond with just the increase in temperature between the T_{HP}. Instead, the increase of T_{max} is significantly larger than that. In the case of 80%, passing from 250 to 270°Clead to an average increase of 90°C. It must also be said that if it were only the change in T_{HP}, the IQR of the results would include this possibility. For the concentration of 85% and 90%, this trend is also visible. Especially, the case of 90%, the increase of 250 to 270°Cof T_{HP} leads to an increase of over 200°C, which even with the IQR could not be explained solely by the increase in temperature supplied. This points to the fact that the energy released might not be linear with the energy supplied. This is not surprising, as other secondary effects can make this process non-linear, such as the timing to ignition or the percentage of gaseous HTP prior to EtOH falling. On the other hand, the case of 95% goes against the previous trends. The maximum T_{HP} leads to lower T_{max} by over 200°C. It is unclear whether this might be due to secondary effects or whether this is the real value, however, it does look suspicious. Moreover, for the maximum temperature at this concentration , there is a large variability of over 200°C, this also points at the need of re-going through the data in the future. More precisely, concerning T_{max}, 95% HTP shows a suspiciously large IQR, of up to 231°Cfor the lowest energy supplied (T_{HP} = 200°C). Although the ignition temperature was less variable, the maximum temperature is too variable, the quality of these results is less solid. Bearing in mind that the temperature readings comes from the temperature felt by the FTK, the only reason to this variability is that the FTK was not in contact with the points of maximum temperature across experiments. This raises another finding: the point of maximum temperature does not happen at the same location. This can be correlated to what was seen on the HSP, where it was found that the point of start of the decomposition/ignition is not constant and changes.

Adding to this analysis, the results point to a lack of correlation between concentration and energy released in terms of temperature, T_{max}. For T_{HP} =200°C, the temperature achieved is around the 600°C, excepting 95%, which displays an odd 946°Cwith a large IQR. A similar behavior happens with T_{HP} =270°C, where all the concentrations are around the 900°Cmark, with 90% slightly larger to 1000°C, but 95% at a low temperature of 700°C. Nonetheless, the trend is the clearest at T_{HP} =250°C. For this HP temperature, all the concentrations are centered at 800°C. As opposed to the case of HTP decomposition, the energy released in the case is mostly driven by the ethanol combustion, so it could be argued that the concentration does not play a role in it, thus this constant temperature across concentrations. However, it is known from the theory analysis that the extra release in oxygen from higher concentrations should lead to larger energy released in shorter time, increasing the temperature of the gases. Consequently, a more in-depth look has to be taken to the energy released alone, this is done in Figure 5.9 looking only at the increase in temperature. Still, the maximum temperature achieved is an important parameter when looking at the design of combustion chambers. According to the results hereby found, in what regards to the maximum temperature, the difference in con-

centration is not a critical aspect, this is not the case for the ignition temperature as shown and it is equally not irrelevant for the IDT.

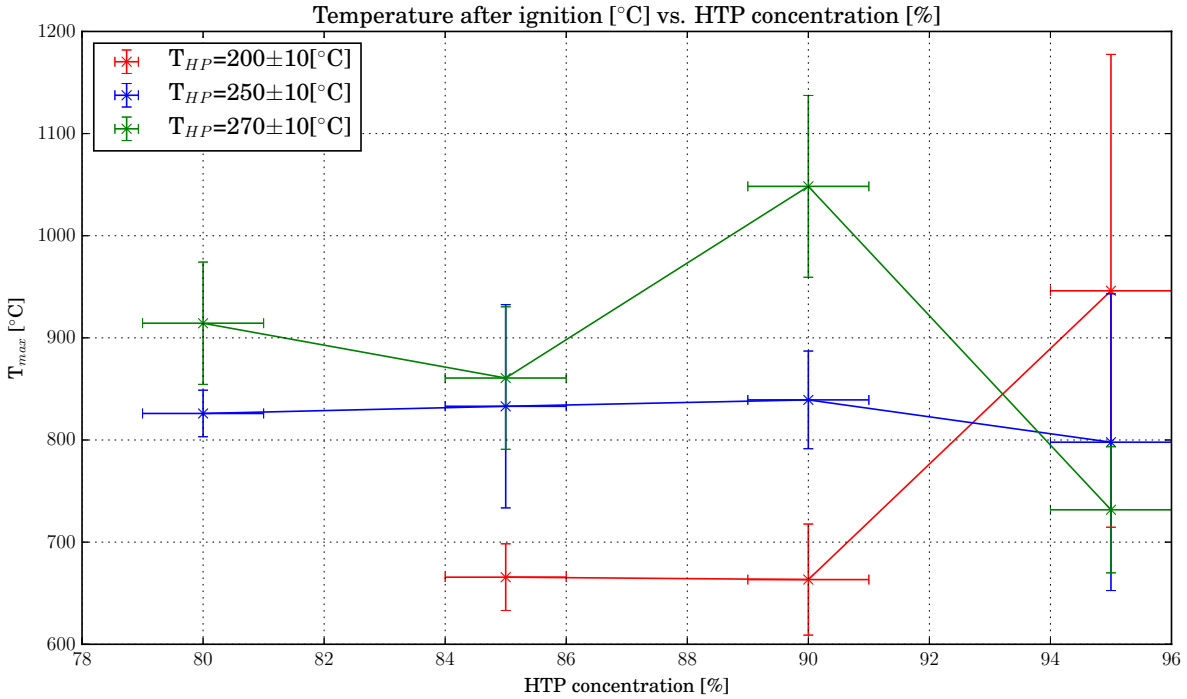

Figure 5.8: Averaged maximum temperature [°C] attained after ignition of EtOH and HTP vs. concentration of HTP [%±1%] used. The three used HP temperatures of 200, 250 and 270 ±10 [°C] are presented. The error bars in the y-axis are the IQR of the averaged values per concentration and HP temperature. The ignition study was done at atmospheric pressure in a lab-controlled environment.

When looking at the energy released alone, this is the increase in temperature from the moment of ignition to the moment of maximum temperature, the ΔT [°C] can be found. The results are presented in Figure 5.9 in a whiskers and box plot manner. Where the ΔT defined as the increase in temperature from ignition to maximum is presented, this is $\Delta T = T_{max} - T_{ignition}$. In the figure, all the data points, irrespective of the T_{HP} are used, as the $T_{ingition}$ already takes care of accounting for it. The read line is the median of the results and the red square the average. The box is the IQR as in a common boxplot graph. As it can be seen, there is a clear correlation of increase in temperature with concentration. For larger concentration the energy released becomes more. This has to do with the speed at which EtOH gets burned and the amount of energy taken by the water. For larger concentrations, the available oxygen is more, this promotes a faster combustion which in turn leads to more energy released in a shorter time span. Moreover, lower concentrations offer larger quantities of water, which takes away part of the energy to increase its own temperature. This trend is not linear, however it is more pronounced at lower concentrations that at higher. While from 80% to 85%, there is an increase of over 200°C, the increase from 90% to 95% is somewhere about 80°Con average. The medians of 85, 90 and 95% lay close to each other, but they still represent this trend. Lastly, in terms of variability, it is mostly translated from $T_{ignition}$ and T_{max}. 95% presents a similar large IQR as from T_{max}, pointing at the need to re-study this process.

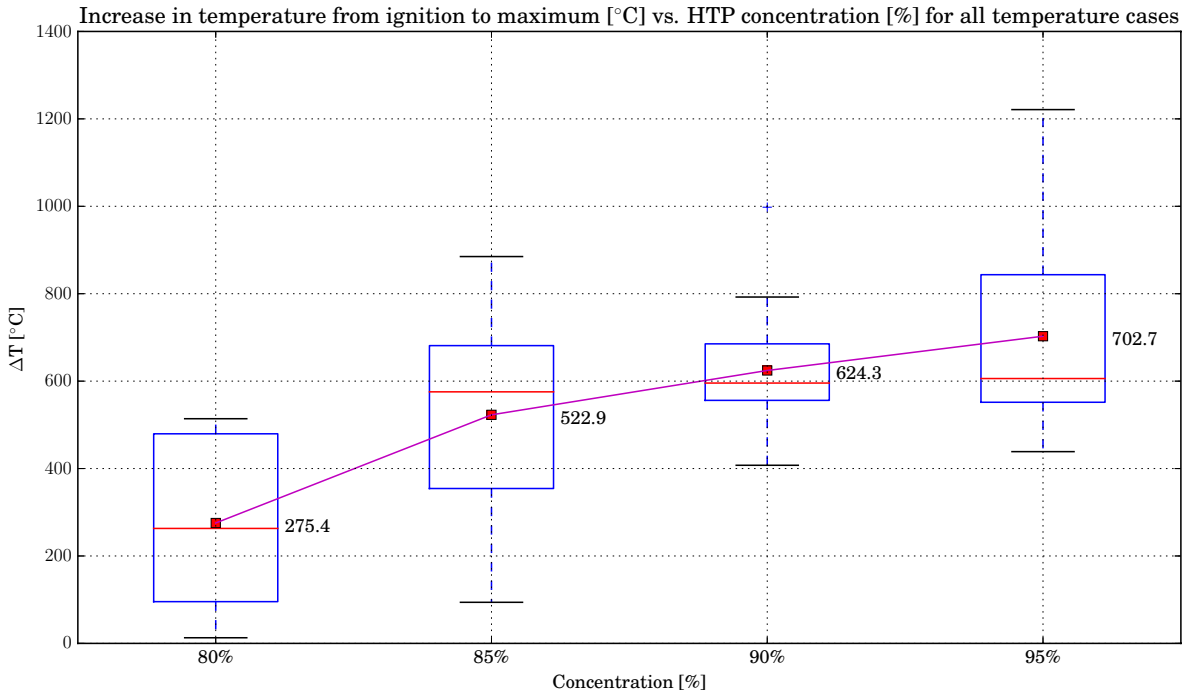

Figure 5.9: Box and whiskers plot of increase in temperature ΔT [°C] vs. Concentration of HTP [%±1%] used in the ignition with EtOH. All HP temperatures are bundled together. The increase in temperature results from the maximum attained temperature per point minus the temperature at the moment of ignition. The blue boxes represent the IQR, the red line the median and the red squares the average, which is annotated in black next to it. The ignition study was done at atmospheric pressure in lab-controlled environment.

5.4.3. Ignition Delay Time investigation

The last analysis from the acquired data refers to the Ignition Delay Time [ms]. The results used are taken co-jointly from the HSP and the DAQ. It has been found that the DAQ and HSP agree with each other in terms of IDT to the extent of their resolution for what is defined as IDT in this study given the novelty of the ignition sequence. As expressed previously, the IDT is defined from the moment the EtOH droplet precipitates onto the already precipitated HTP droplet to the moment a first fireball can be found in the HSP or the sudden increase in temperature in FTK2, 3 and 4 can be seen in the DAQ.

The results of the averaged IDT and the IQR are presented in Table 5.8 and plotted in Figure 5.10. As shown in the tabular format, the values all lay below the 400 ms mark and the variability is lower on average than for other parameters, where the maximum IQR is 80 ms. Comparing to the 100 ms benchmark, normally used as requirement for hypergolic systems, it can be seen how some several of the combinations would succeed this requirement. These are the concentrations of 90 and 95% at high T_{HP}. 90% at 250°Cis just at IDT of 97 ms, which would suffice. It decreases to even 66.7 ms for an increase of 20°Cin HP energy supply. For the larger concentration for 95%, the trend in similar, achieving around 90 ms for 250°Cand just 22.7 ms for 270°Cof T_{HP}. It is important to bare in mind that the atmospheric conditions used for this experiment have a large impact on the IDT value. In fact, authors in [10] performed drop test studies with 90% HTP and catalyst-promoted fuels in both atmospheric and pressurized conditions. Their assessment indicates that the increase in pressure can substantially reduce the IDT and even halve it at 10 bar, meaning that several more combinations from this study can achieve the 100 ms mark. Looking at the individual datapoints, the lowest IDT achieved happened at 90% HTP at 276°C. The ignition took place at 17.2 ms after the EtOH touched the HTP as seen in the HSP, it also achieved a large maximum temperature of 1200°C. On the other end of the spectrum, a droplet with 80% HTP falling on the HP at 259°Ctook 490 ms to ignite, almost half a second.

As seen in Figure 5.10, some clear trends are found. This figure presents the average of the IDT recorded pertaining that HP temperature slot. While 80% avoids 200°C, as setup, 85, 90 and 95% include it as well as 250 and 270°C. The error bars in the y axis represent the IQR of the data used for the average. The strongest visible trend is the effect of the energy supplied through the HP to the propellants. As T_{HP} increases, the IDT goes down for all except one of the concentrations. For the case of 80%, the step from 200°Cto 250°Clead to an increase in the average IDT. This is due to the large weight that droplet 7 has, given that it gave a total of 381 ms of IDT, largely affecting the average IDT. Apart form it, all the other concentrations and combination with

Table 5.8: Ignition Delay Time (IDT) [ms] achieved after the ignition of HTP at different concentrations with EtOH for different HP temperatures. The variability in terms of IQR is presented as well. The ignition study was done at atmospheric pressure in lab-controlled environment.

	Concentration [%±1%]							
	80		**85**		**90**		**95**	
HP temperature [°C±10°C]	**Average IDT [ms]**	**±IQR** $[ms]$	**Average IDT [ms]**	**±IQR** $[ms]$	**Average IDT [ms]**	**±IQR** $[ms]$	**Average IDT [ms]**	**±IQR** $[ms]$
200	NA	NA	371.8	22.1	190.1	31.8	152.8	40.9
250	270.4	65.2	135.1	57.5	97	22.8	91.6	48.4
270	215.3	57.7	217.5	79.4	66.7	22.7	54.6	9.0

HP temperature result in a decrease of IDT. For 80%, it decreases a 20%, 1% per 1°C. While for 90 and 95%, the decrease is 40% on average around 1.15% decrease in IDT per 1°C. The reduction in percentage is more pronounced at larger temperatures, where an increase in temperature results in a larger decrease in IDT as opposed to lower heating plate temperatures.

Adding to this, an expected result from the analysis is the effect of concentration of HTP on the IDT. The increased energetic content of larger concentrations in this case also means lower IDT. In a similar way to what was found with the HTP decomposition, the concentrations of 90 and 95% return the lowest IDTs. This is respected with exception to the IDT of 85% at 270 °C. The decrease in IDT with concentration is not linear and it gives the impression of being larger at lower concentrations than at higher. From 80 to 85%, there is a large decrease at 250°Cof around 50% in IDT. From 85% to 90%, the decrease is more than half the IDT at T_{HP}=270°C, but around half at T_{HP}=200°C. From 90% to 95%, the decrease in IDT is less, meaning that at higher concentrations the IDT is less sensitive to the concentration of the oxidizer.

Lastly, the variability of the results also raises questions on the need of repeatability. As it can be seen from the data, there is a point which seems specially out of place, this is the 85% at T_{HP}=270°C. It also has the largest variability. This points to the fact that this combination may have been contaminated at some point and the result is questionable. From the statistical analysis performed on the 3 data points available, half of the results would fall within the bracket of 297 to 138 ms, which means a large variability for the design of a future injector plate. On the other hand, the largest concentration of 95% is overall quite solid around its average, specially for the largest temperature is only differs ±9 ms from its average.

With the gathered data, an attempt was made at reconstructing a trend line for the IDT as a function of concentration through a function in the Arrhenius form as presented in [13]. However the work done by researchers trying to fit this trend is done at auto ignition temperatures range, which greatly surpasses the temperature given in this test. Likewise, the range of temperatures supplied is not broad enough to fit this trend.

Lastly, an interesting case worth mentioning apart was made found when a mid-air autoignition took place and was timed to take 1.64 ms as recorded with the HSP. It happened with 95%HTP, which fell significantly before EtOH and was undergoing decomposition by the moment EtOH fell. The decomposition shockwave was traveling upward when the EtOH droplet just crossed the throat of the vessel. The shockwave got into contact with EtOH which was repelled and pushed while slightly atomized and ignited at the same time. The ignition transferred quickly and consumed the EtOH while pushing it out of the vessel. The sequence was recorded and analyzed. It is presented in Figure 5.11. As indicated in the caption, the sequence presents the autoignition in mid-air in different phases. Interesting ot notice is the timeline. In the span of 3 frames, from 883 to 885, the EtOH goes from sensing the upcoming shockwave without entering into contact with it to be ignited. In fact, the IDT would be 1 frame or 0.16 ms, as from the moment of contact of HTP to ignition only 1 frame is apart. This translates to an important consequence for the design of a combustion chamber: if only HTP i being decomposed in the mono-propellant mode, addition of EtOH will almost instantaneously lead to combustion given proper atomization.

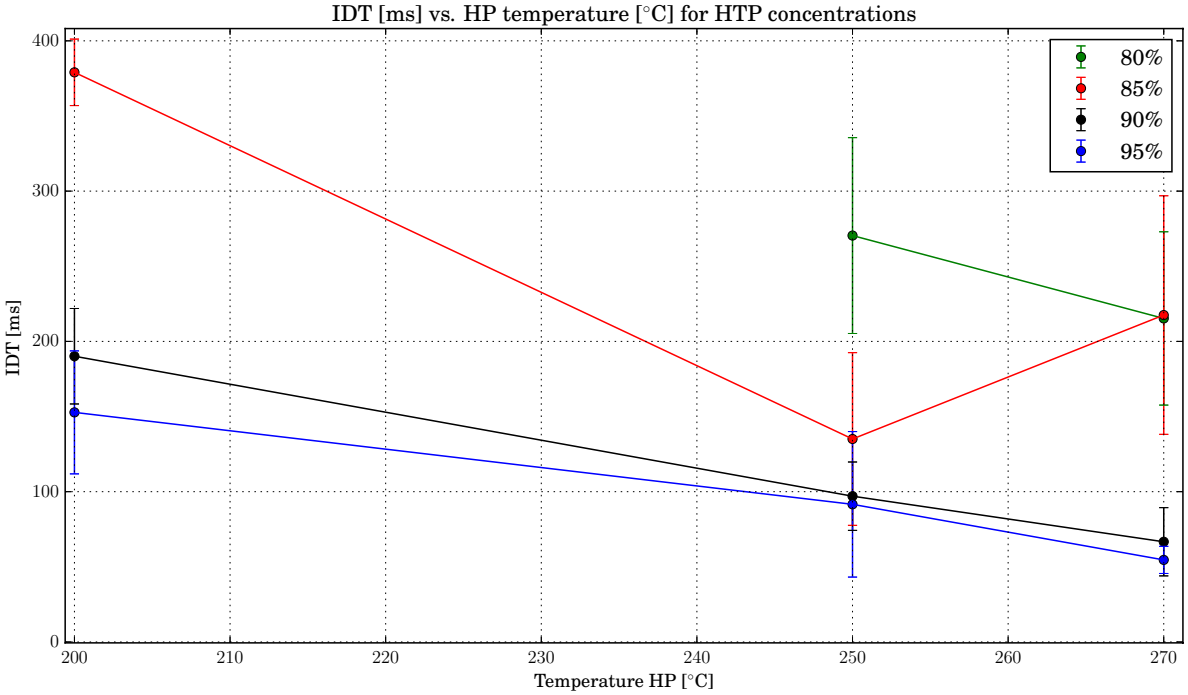

Figure 5.10: Ignition Delay Time [ms] vs. HP temperature [°C±10°C] for different concentrations of HTP as oxidizer with EtOH. The error bars in the y-axis are the IQR for the averaged values of IDT. The IDT comes from both sources: HSP and DAQ, when HSP IDT is available it is used, when it is not,the DAQ IDT is used. The ignition study was done at atmospheric pressure in lab-controlled environment.

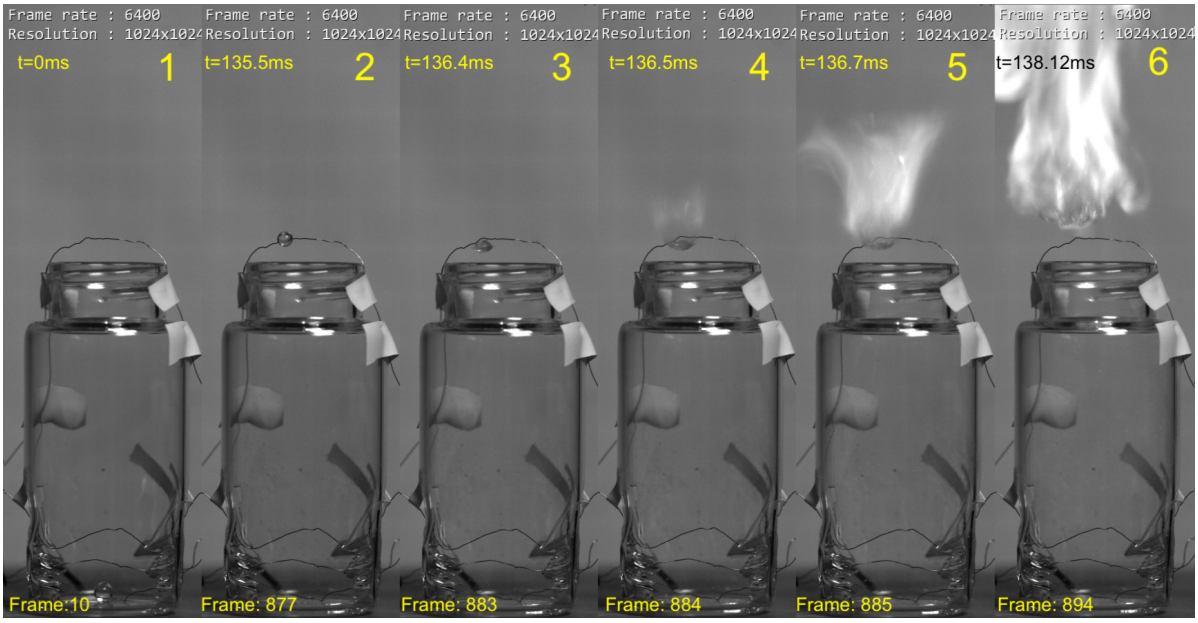

Figure 5.11: Sequence of frames recorded for mid-air ignition for the trail case of 95% HTP at T_{HP}=270|celsius. 1-HTP falls onto the bottom of the VES (*frame:10*). 2-EtOH is about to cross the throat, butthe HTP is starting to decompose (*frame:877*). 3-The shockwave of the decomposed HTP starts to push the air of the vessel and the EtOH drop0.letys starts to deform (*frame:883*). 4-The shockwave of superheated decomposed gases now reaches the EtOH and starts to atomize the EtOH droplet, no ignition is present yet (*frame:884*). 5-Ignition takes place, the EtOH reaches the autoignition temperature promoted by the exhaust decomposed gases and ignition happens (*frame:885*). 6-Full ignition of the EtOH starts to take place and EtOH starts to get consumed (*frame:894*)

5.4.4. Gel trial

In this subsection, the findings of the trial done with gelled EtOH will be presented. The range of extent of this experiment was shorter than for the liquid case, given the need to only prove the feasibility of ignition with gel

at this stage of the research. More information about the gel nature is presented in Chapter 6. Nonetheless, as an introduction to it, the gel used for the experimentation was EtOH with hydroxypropyl cellulose at 1.8% wt. The gelling agent was procured from Sigma Aldrich with CAS number 9004-64-2. The tests were performed with 95% HTP on a 200°C HP. As opposed to the liquid case, for the gelling approach, generating a droplet is more tedious and complex to achieve on demand, given the highly viscous nature of the gel. Instead, the gel was dropped prior to HTP falling in. This allows to start the filming with the HSC easily, as HTP droplet generation is easy and on-demand. Two results are presented in this trial test: the first one, a large temperature was achieved after ignition, which melted one of the FTK as shown in Figure 5.12. The second, avoiding the use of the melted FTK presents the case that was filmed Figure 5.13 and recorded in the DAQ Figure 5.14.

As can be seen in Figure 5.12, the profile of the gel case is completely different to the liquid case. First and foremost, the length of the increased temperature felt is larger. This means that the energy contained in the gel is more durable than in the liquid case. However this is not the most interesting feature of the graph. This case was the largest ever recorded temperature across all of the experiments. The largest temperature measured was of 3252 °C. However, this result should be taken with caution. According to the manufacturer, the range of validity of these k-type thermocouple is 900°C and, moreover, their melting point is 1430°C. However, as it can be seen, at the point of measuring these values, the FTK was not melted yet, because the melting death-signal or open-voltage of the FTK would measure the constant of 948°C. The IDT was measure to be 90±18.2 ms, given the lack of video for it. In general, the profile is less neat than the liquid counterpart. More wobbly signal are sensed by the FTKs. Moreover, the temperature is significantly higher than for the normal liquid cases. FTK4 measures a value well over the 100°C mark for around 0.9 s and FTK for 0.25 s. FTK1 senses an increased temperature around the 500°C for an extended period of time as well, however the depletion of the oxidizer (HTP) quenches the ignition substantially after the large sudden dip of 1.4 s. Then is the surrounding air that is being used as oxidizer, leading to a reduced temperature after ignition. After the complete combustion of the gelled EtOH no rests of the EtOH or gelling agent were present in the vessel, indicating that he gelling agent precipitates in the combustion as well.

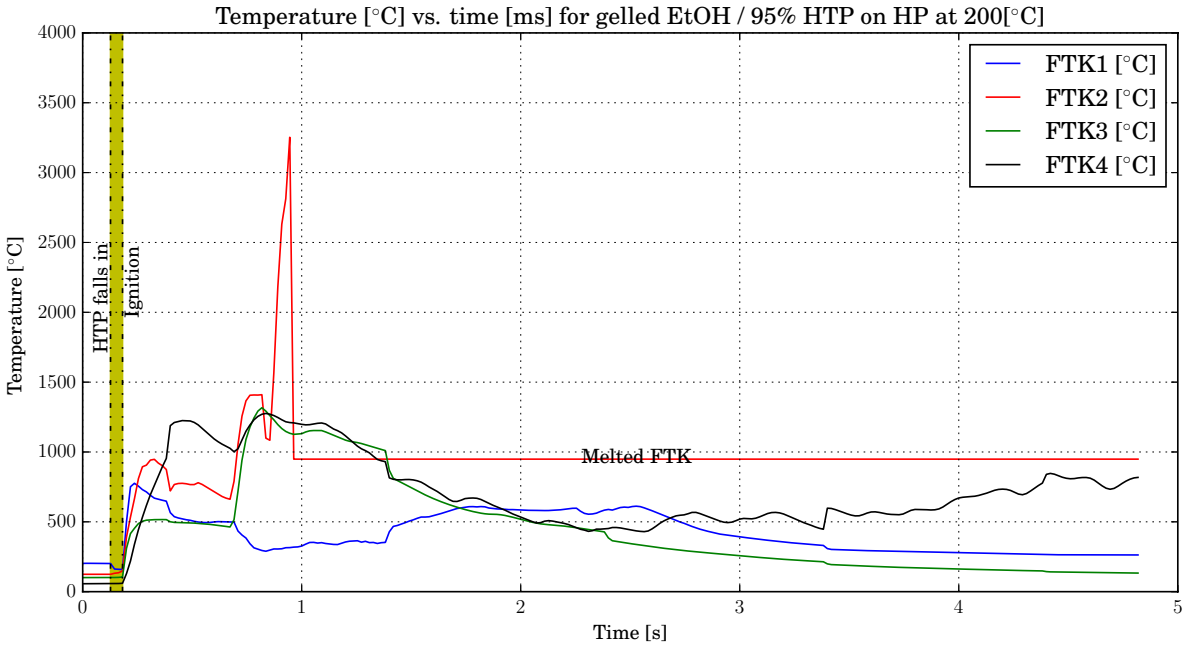

Figure 5.12: Temperature profile [°C] recorded with the DAQ through 5 s and 4 FTK situated at 0, 3, 6 and 500 mm from the bottom of the vessel at a rate of 55 Hz. The ignition was with 95% HTP and gelled EtOH with 1.8% gelling agent. The large spike in temperature lead to the melting of FTK2, leading to a constant death-signal at 948°C. The ignition took place at atmospheric conditions in lab-controlled setup.

The positive on the feasibility of ignition of gel lead to the need to film it in camera and a second drop-test with a new EtOH sample was prepared on the vessel with the melted FTK. The image sequence can be seen in Figure 5.13 and the temperature profile in Figure 5.14. As it can be seen in the sequence, the procedure is similar to the liquid case with some variations. The fuel in this situation is place prior to the HTP falling onto

the HP. While it is laying there, the HTP is released at 0.13 mL, as in the liquid case. The volume of the fuel lays around the 1 mL, given its complicated nature it is harder to measure than the liquid. When the HTP falls in, prior to the ignition, a phenomena known to gel ignition takes place: caging [28] [48]. During caging the ethanol entrapped in the carbon chain network of the gelling agent starts to evaporate and form bubbles of caged ethanol. The temperature also raises as the HTP evaporates. This phenomena cannot be seen in the temperature profile unfortunately. It is speculated that if the FTK bead is exactly inside one of the entrapped bubbles, it would feel a slight increase in temperature, however this cannot be said from the profile presented. At some point, decomposition takes place and it instantaneously ignites the ethanol, entrapped with it in the small bubbles. This is the image 3 in the figure. The ignition fully spreads and it leaves an accelerated burned gas exiting the vessel as shown in image 4. These two phenomena happen only 4 frames or 0.625 ms apart and are felt at the same time in the DAQ, as shown. In the temperature profile, the increase in temperature is felt by the 3 FTK at the same time, meaning that the gel was not exactly on top of the bead of the FTK. The ignition of the gel remains even after the full depletion of the oxidizer, which takes place at 1.1 s in the profile shown, where FTK1 and FTK4 feel a sudden dip in temperature. From there the oxidizer used in the oxygen present in the air, this means that the system is also valid for ignition of the system and later continuous combustion.

Figure 5.13: Image sequence recordedd with High Speed Camera at 6400 fps of ignition sequence of 95% HTP falling on gelled EtOH with 1.8% wt. gelling agent for gellation. The temperature profile as well as the numbering can be seen in Figure 5.14. FTK2 was melted in the previous experiment and can be seen cut in two. 1- 95% HTP falling onto the bottom of the VES, gelled EtOH is already there on the left on the HTP droplet (*frame:96*). 2- Caging phenomena typical of gels starts to take place after HTP starts to interact with it (*frame:1673*). 3- Ignition takes place, IDT calculated until here and equal to 253.9 ms (*frame:1821*). 4-Full spread of ignition across the entire vessel, signs of throat=like behavior can be seen (*frame:1825*). 5-Signs of continued combustion of the ignited gelled EtOH, as the FTK still glow due to the heat released of the remaining gel (*frame:4252*).

At the end of the day, the tests performed with the gelled ethanol with gelling agent at 1.8% wt. hydroxypropyl cellulose are successful and return a valid ignition for a future use. Specially, given the added energetic content of the gel versus the liquid fuel, distinguishable from the increase in average temperature during ignition, it can serve as a performance booster for a future combustion chamber design.

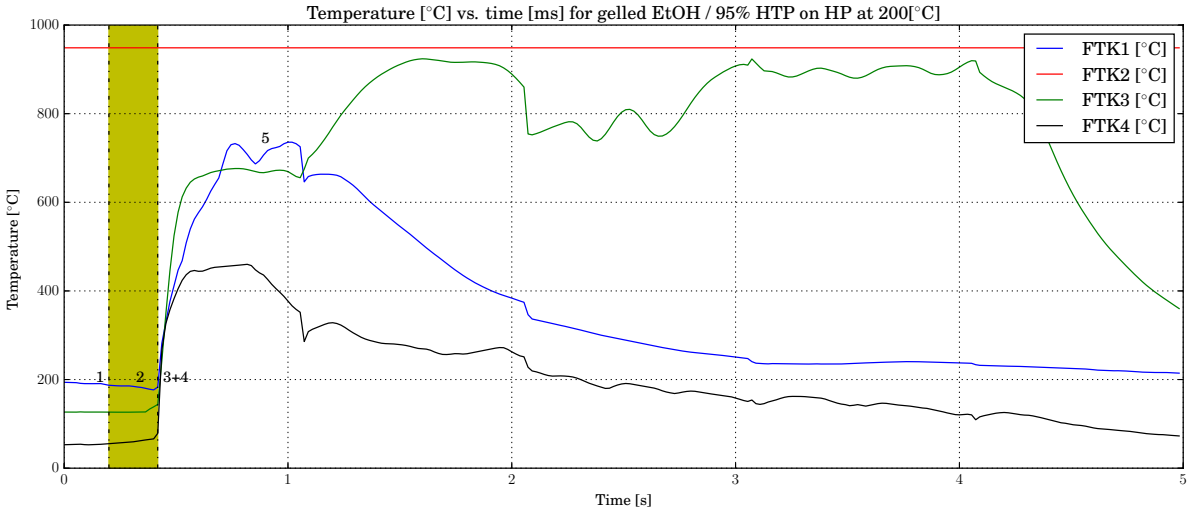

Figure 5.14: Temperature profile [°C] vs. time measured with DAQ and 4 k-type thermocouples throughout 5 s. The ignition recorded was between 95% HTP and gelled EtOH containing 1.8% wt. of gelling agent. FTK2 gives a death signal at 948°C due to being melted in a previous experiment. The sequence was recorded with a HSC and the numbering relates to them in Figure 5.13. The ignition took place at atmospheric pressure and controlled laboratory conditions.

5.5. Conclusions

In this chapter, the results of the ignition through psuedo-hypergolic approach of EtOH and HTP at different concentrations through sole thermal activation are presented. Several aspects have been tested and investigated always at the constant of 0.13 mL of HTP per 0.06 mL of EtOH, both precipitating at 17 cm from the vessel. These includes:

- **Oxidizer concentration:** varying the concentrations of the oxidizer HTP at 80, 85, 90 and 95% ±1%.
- **Energy supply to activate:** varying the temperature provided to the HTP to activate it between 200, 250 and 270 °C ±10 °C.
- **Phase of fuel:** tests were performed to validate ignition can also happen with gelled EtOH.

Throughout these tests, valuable information to characterize the ignition and feasibility of the test were recorded. The data saved included:

- **Temperature:** measuring the temperature [°C] every 55 Hz through a DAQ NI-9219 with four k-type thermocouples of fine gauge placed at 0, 3, and 6 mm and one at the throat-like section at 5 cm above the bottom of the vessel.
- **Filming:** filming the ignition and droplet precipitation with a high-speed camera at 6400 fps in black and white.
- **Logging:** keeping a logbook of all the visual and felt results of the experiments, such as hearing and other consequences of ignition.

In Section 5.4.1, the initial characterization of the ignition process is given. Here pseudo-hypergolicity is described as being the consequence of decomposing HTP and entering into contact with EtOH, where the autoignition temperature is reached and ignition quickly spreads. The process is similar in all droplets studied and a nominal representative case is presented for 95% HTP falling into a HP of 250°C. It was found that the ignition can only take place once the HTP decomposes and this is the critical step. Moreover, it was found that the order of the droplet precipitation matters greatly. In the case that EtOH falls in first, the risk of explosion is significant as expected. A vessel was lost due to this problem. This translates for future combustion chamber design to the need to assuring that HTP is decomposed prior to EtOH flow into the chamber.

In Section 5.4.2, the ignition temperature is explored in the first place. The ignition temperature is defined to be the temperature at which the bottom fluid is when it undergoes ignition, which is measured by

the massive spike in temperature in a short time in all FTKs. It was found that the ignition temperature is sensitive to concentration of oxidizer. For increased concentrations, the ignition temperature is less variable and lower than for the lower concentrations counterparts. This is attributed to the increased energetic content of the HTP at high concentrations, which quickly decomposes upon contact with the HP. For the higher concentrations the value resembled a lot the behavior of the decomposition of HTP, values close to the boiling temperature of 140-150°C. However, for lower concentrations the value could rise up to even 500°Cbefore a large spike in temperature was felt in all the FTKs. Moreover, it was found that energy supplied also played a role. Larger energy supplies, measured in terms of the T_{HP}, lead in general to larger and less constant ignition temperatures. It is believed that the unsteadiness of the process with larger energies is the cause of this behavior. For all the concentrations the increase in temperature of ignition with energy supplied was positive, being even about 6°C per 1°C of increase in T_{HP} for 80% HTP. All the tested concentrations laid around the boiling point of 140-150°C for the 200°C HP provided.

In the second part of Section 5.4.3, the energy released after ignition is discussed in terms of maximum temperature and increase in temperature, Δ T [°C]. The first clear output of the results is that there is a definite trend between energy supplied to the system and maximum temperature. In all but 95% concentration, the maximum temperature increased when the T_{HP} did. Meaning that for larger energy supplied to the system, also more thermal considerations will be required. It was also found that the increase is not linear, instead, increasing the T_{HP} leads in all the cases but 95% to larger increase on average of T_{max}. However, the values found proved to be significantly below the theoretically predicted by CEA, which estimated over 2000°C while the values never exceed 1000°C on average. This large difference is attributed to the atmospheric pressure and open chamber conditions, which deem the adiabatic assumption invalid. Secondly, it was found that the maximum achieved temperature behaves roughly constant for a given T_{HP}. With the exception of 95% which returned inconclusive results. For T_{HP}=200°C the temperature is around the 670°C for 250°Cis rises to around 800°Cand lastly for the maximum of 270°C is around 900°C on average. This trend clashed against the understanding of increasing HTP concentration, thus a look into the ΔT, from the ignition to the maximum temperature. It was found that there is a clear trend of increased ΔT with concentration, going from 275 °C for 80% all the way to 702°C for 95% on average. This means that larger concentrations will inevitably lead to larger thermal strains in a future combustion chamber, but the maximum temperature will be mostly dictated by the activation energy supplied to the propellants.

In Section 5.4.3, the IDT is looked into. After review of the droplet results, it was found that only concentrations of 90 and 95% achieve on average less than 100 ms of IDT at heating plate temperatures over 250°C. On general terms, higher heating plate temperatures lead to reduced IDTs on all the cases except 85% at maximum temperature of 270°C. It is believed that further tests are needed for it as only 3 data points are present. The reduction of IDT with increasing HP temperatures is a trend that was also found for HTP decomposition. This means that for a combustion chamber, the increase in temperature during combustion may lead to variations in the point of starts of ignition as temperature builds up. It was also found that the IDT at larger concentrations is less sensitive and tends to vary less around its average than the lower concentrations. In the future, this less variable behavior can be beneficial for increased reliability on the design of combustion chamber. The data could not be used for reconstructing an IDT fit in the Arrhenius form. This is attributed to the short range of temperatures tested as well as the low temperature values as opposed to other autoignition fits found in literature. The findings of explosiveness risks when EtOH falls in first or the possibility to ignite EtOH mid air, were also discussed as being exotic cases which could be exploited in the future.

Lastly, a smaller-scale feasibility test was performed with gels in Section 5.4.4. The used gel was EtOH with 1.8% of hydroxypropyl cellulose. The results were conclusive in that gel also ignited with HTP at the same temperature ranges as the liquid counterpart. Moreover, the gelling agent participated in the combustion and left no residue, showing incredible potential for a future propellant. The values attained with gel lead to larger energy released to the point that a thermocouple was melted.The different phases of gelled EtOH prior to ignition are presented and should be taken into account for the combustion chamber design.

6

Gelling the propellants

In this chapter, a concise rheological study of the gel is made. The use of gelled propellants in space propulsion is still novel, but it already has is adepts as discussed in the introduction and literature study of this thesis. This chapter will not deal with the advances in the field, but rather with the characterization of the ethanol gel with hydroxypropyl cellulose. To do so, firstly the critical concentration at which the liquid starts being a gel will be presented in Section 6.1. Subsequently, the rheology study tests are introduced in Section 6.2, as well as their importance for gel characterization. Lastly, the results are presented in Section 6.3 and summarized in the conclusion of Section 6.4

6.1. Critical concentration

In this section, the critical concentration used for the gel study is presented. As introduced in the literature study, the gellation process includes the addition of a gelling agent to a solvent. The gelling agent can be organic or inorganic, depending on the presence of carbon-chain groups. For this study a large carbon-chain cellulose group was selected: hydroxypropyl cellulose (HPC) at a quite large molecular weight unseen previously in literature. It is expected that this large molecular weight will reduce the need to add extra gelling agent in the future The solvent, in this case is the ethanol present at the DASML lab, 99.5% purity from VWR international with CAS number: 64-17-5.

The critical concentration of gelling agent is the weight percentage needed of gelling agent on a given solvent to take the liquid state to a visco-elastic/gel-like state. This concentration varies with type of solvent, type of gelling agent, but also with the molecular weight of the gelling agent. The importance of the critical concentration is paramount. This is because in general , the solvent wants to be as little disrupted as possible. Thus the addition of gelling agent is always desired to be minimal, but the benefits of gelling are needed as well. Consequently, the critical concentration is the optimum point for gelling preparation. Although numerous combination are found in literature, the combination of HPC and EtOH was not found. Instead, other combination with EtOH and other solvents with HPC were found to start finding the right concentration. These can be found in Table 6.1. As it can be seen, the concentration varies greatly between the different gelling agents. For ethanol it seems like the concentrations lays around 5-10% wt., however for HPC as little as 3% wt. was needed for a larger molecule as monomethyl hydrazine, so there is possibility that for ethanol even less is needed.

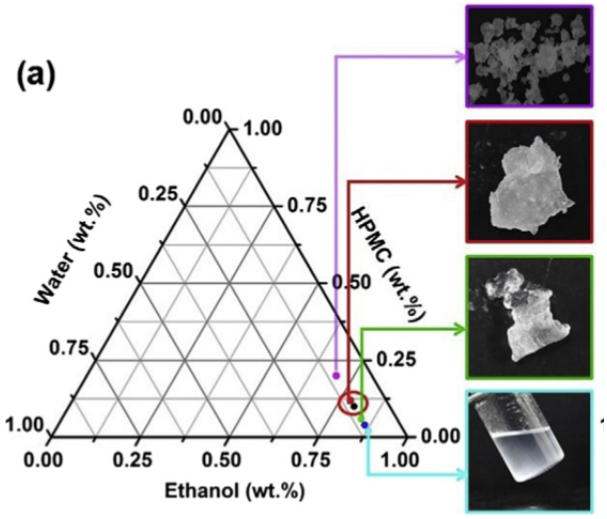

Figure 6.1: Illustration of change in variation of critical concentration for Ethanol and hydroxypropyl methylcellulose, from [25]. The concentration of water, ethanol and HPMC is given in a triangle graph. From bottom to top: 1- not enough gelling agent, to liquid. 2- Critical concentration reached. 3- Addition for further gelling agent makes the gel more solid like. 4- Granulation starts to happen as the critical concentration is exceeding by too much.

Table 6.1: Critical concentrations for ethanol solvent with different gelling agents and HPC with monomethylhydrazine.mw is the molecular weight.

Solvent	**Gelling agent**	**Critical concentration** [%]	**Ref.**
Ethanol	Methyl cellulose (mw = 40,000)	8	[48]
Ethanol	Hydroxypropyl methyl cellulose	10	[25]
Ethanol	Propyl cellulose (mw = 370,000)	6	[27]
Monomethyl hydrazine	Hydroxypropyl cellulose	3	[16]

At the critical concentration, the solvent starts to behave like a gel, exhibiting visco-elastic behavior which situates it between a solid and a liquid. As shear is applied, the gel thins down, and its viscosity reduces resembling like a liquid. However, this behavioral is also impacted by the quantity of gelling agent present. When the gelling agent concentration exceeds the critical concentration, it starts to have like a solid and increased shear is required to thin it, this impacts the pressure need in the pipelines or the atomization. On the other hand, not adding enough gelling agent leads to a liquid with a larger viscosity, but doe not exhibit the benefits of the gel. An illustration of this can be seen in Figure 6.1.

6.1.1. Critical concentration finding for EtOH and HPC

The critical concentration was searched within the lab by varying the concentration of HPC in ethanol. To do so, the weight of the ethanol solvent was measured and the required HPC weight was later found form the desired weight percentage to be used as shown in Equation (6.1). Because of the need to have as little as possible gelling agent, it is always desired to start testing the concentration of the gelling agent from lower values. These low values required of a microgram-scale weight scale present at the DASML. The gel was prepared by slowly adding the gelling agent to the solvent in a borosilicate vessel with a rotational pellet to make the fluid spin on top of a rotational plate. The addition of the gelling agent must be done slowly and making sure the gelling agent fully dissolves in the ethanol before adding more and more. When all the gelling agent was added, the solution was left to mix with the rotational plate for about 15 minutes. After this time,

the pellet was removed and the gel was let to form the remaining 3d network by resting in a dark cool place for 5 days.

$$W_{GA} = \frac{C \cdot W_S}{100 - C} \tag{6.1}$$

Where W_{GA} [g] is the weight of the gelling agent to be added to the solvent of weight W_S [g] for a given concentration C [% wt.]

Initially, it was started with as little gelling agent as possible to test the efficacy of the selected gelling agent and growing. The prepared samples are presented in Table 6.2 with remarks concerning their phase.

Table 6.2: Gel samples and their concentration tested as well as their remarks concerning their status as gels. The samples appreace is shown in Figure 6.2

Identifier	GA concentration [%]	Remarks
GS1	0.05	Too liquidy, not enough consistency.
GS2	0.08	Too liquidy, not enough consistency.
GS3	1	Too liquidy, not enough consistency. First signs of impact behaviour of the entire fluid together moving as one.
GS4	1.5	Close-to-solid like behaviour, still dripping could be found and more similar to liquid than viscoelastic behaviour.
GS5	1.8	First possible critical concentration. All-in-one movement. Unseen dripping and more solid-like feeling than 1.5%.
GS6	1.98	More solid consistency than GS5, although almost inappreciable. The gain with respect to GS5 is not clear.
GS7	2	Exactly as with GS6. Inappreciable difference.

After going through the possibilities several conclusions were found. First an foremost, the large molecular weight of the chosen gelling agent was not enough to work with lower concentrations than 1%. This is why GS1 and GS2 exhibited liquid-like behavior. Although a certain level of network creation could be found and the viscosity was increased, the phase was still liquid and flowing when tilted. Consequently, the next concentration tried was 1% at GS3. It started to exhibit the conditions of a fused chunk, flowing more like a connected piece. However, it would still exhibit excessive dripping and it would not pose any benefits as opposed to a liquid. Thus, the increase to 1.5% was done at GS4. This started to present more viscoelastic appearance, while presenting dripping still. The behavior was close to the optimum, so the step wise was reduced to achieve 1.8% in GS5. This sample was already a possible solution. No dripping was found even after large acceleration. The behavior was of a solid-like all-in-one piece. This option posed itself as valid. After it, two more samples were tried to compared how much it would increase given additional GA. GS6 and GS7 proved to be quite similar to each other. This would potentially favor GS7 as a candidate given that 2% is a better rounded number than 1.98%. Because, the benefit from GS5 to GS7 was not as substantial as it was from GS4 to GS5, it was decided to go with GS5 for the rheological study. This meant that the increase in molecular weight lead to a final decrease of 1.2% in GA concentration from what was found in [16], although for a shorter molecular as ethanol is. This decrease in GA translates into further fuel presence in the propellant, leading to a more efficient combustion.

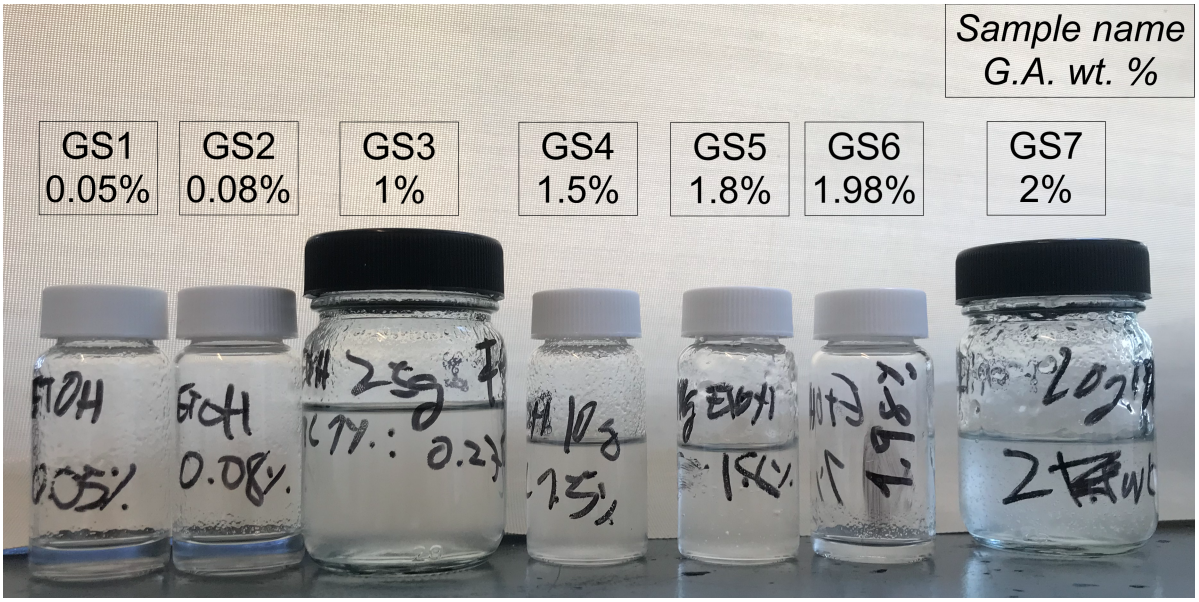

Figure 6.2: Gel samples at different tried concentration of gelling agent. The remarks concerning their phase is presented in Table 6.2

6.2. Initial rheology study: setup and materials

In this section, the experimental setup used for the rheology study will be presented as well as the exact test performed on the gel sample. The study was performed in the available rheometer at the DASML, a HAAKE MARS III rheometer from Thermo Scientific. The test was performed on parallel plates of 5 cm diameter. The characterization performed was done through a set of 4 main tests devised to characterization in a preliminary manner the behavior of the sample used. For the characterization, the sample GS5 was used which comprises of:

- **Solvent:** ethanol (CAS number: 64-17-5) 99.5% from VWR international in a presence of 98.2% of the total of the gel.
- **Gelling agent:** hydroxypropyl cellulose from Sigma Aldrich with CAS number: 9004-64-2, 99% through in powder and 20 mesh size.

The tests were all performed at atmospheric conditions and room temperature of about 20°C, with the exception of the temperature oscillation study. The size gap used was 1 mm for all the tests and the procedure always comprised of a through clean of the rotational pates, addition of the gel with a spatula, press until the gel dripped from the sides and removal of the surplus on the sides. Only then, the test was started. The tests are the following:

- **Test 1:** Strain sweep for yield stress characterization through static study.
- **Test 2:** Viscosity variation with shear stress through static study.
- **Test 3:** Hysteresis loop analysis of viscosity and stress through static study.
- **Test 4:** Temperature oscillation for viscosity characterization through static study.

In Test 1, the yield stress is searched for by varying the strain from 0.1 [-] to 100 [-] in 1000 steps. The test is performed at 20.5°C at a frequency of 1.59Hz. These study are normally carried at low and constant frequencies, this is why they are called static. Through these study, the behavior of the gel through the pipelines can be characterized in terms of its storage modulus (G'). Moreover, this study returns information about the point in which the gel network starts to break down and it flows. At that point, known as the critical stress, happening at the critical strain, the gel would flow in a pipe. This minimum shear stress is thus needed inside the pipe for continuous flow of the gel in the pipe. It is found when the storage modulus (G') [Pa], a quantity which measures the consistency of the gel drastically breaks down and decays exponentially. At that critical strain, the shear stress (τ) [Pa] felt by the gel is the stress needed to make the gel flow. At this stress, normally,

a following test to characterize the behavior of the gel in storage would be done. This would imply a dynamic study through frequency sweep, where the storage (G') and the loss modulus (G") [Pa] would be plotted and the behavior of the gel in terms of viscoelastic properties would be found for different frequencies to be later related to different phases of the launch/atomization or lifetime of the gel.

For Test 2, the information searched is different. Identifying the viscosity (η) [Pa] change with shear stress is of importance to demonstrate the nature of gels. This gel would exhibit a viscoelastic behavior, where at low shear stresses the gel is elastic-dominated, but as stress increases the gel is more similar to a viscous material. This is studied by performing a strain rate (GP) [s^{-1}] sweep from 0.001 to 1000 [s^{-1}] during 2 min in 100 steps. As the shear stress increases with strain rate, an important characteristic of gel is presented: the shear thinning. The increase in shear stress in the gel induces a reduction in viscosity typical of gels. This is the characteristic which allows for liquid-like behavior at the atomization step.

For Test 3, the approach is similar to Test 2, however the goal of the test is to identify another key characteristic typical is gels: thixotropy. Thixotropy is a time-dependent characteristic in gels by which the viscosity of a gel is not only affected by the shear stress applied. but also by the history of the shear stress applied. Normally, as shear is applied the gel exhibits shear thinning, however this phenomena is further amplified at gels which have recently been sheared, this is due to the 3D network breakage. Once the network is broken, it needs some recovery time prior to returning to its original state, if no time is given to the gel to recover, then the viscosity will be lower than initially. Normally, this behavior is measured through a hysteresis loop, in which the strain rate is increased and then decreased, measuring the variation in viscosity. Normally in the ramping down, the viscosity is lower, meaning a more liquid-like behavior. This test was performed by varying the strain rate from 0.001 to 20 to 0.001 [s^{-1}] subsequently in 2 min for ramping up and 2 min for ramping down.

For Test 4, the effect of temperature is tested. It is known that gels thin as temperature is increased. To characterize and demonstrate this effect, temperature is varied for a constant strain, demonstrating the decrease in viscosity. In this case, the test was performed by varying the temperature from 25°Cto 50°Cin a duration of 10 min in steps of 0.3°C. The complex viscosity is recorded as for this test a constant frequency of 10 rad/s is used. Nonetheless, by the Cox-Merz theorem[57], this would equate to the real apparent viscosity at a stress of 62 Hz. The temperature is kept constant by the rheometer which incorporates a thermocouple in its lower plate. The result is normally presented in terms of the viscosity vs the inverse of the temperature. Moreover, an exponential fit of the Arrhenius equation-form is normally fitted [44] to the results as follows:

$$\eta = A \cdot exp\left(\frac{E_a}{RT}\right) \tag{6.2}$$

Where η [Pa s] is the (apparent) viscosity, A is a constant which measures the viscosity of the molecular motion [Pa s], E_a [J/mol] is the activation energy, R is the universal gas constant 8.314 J mol^{-1} K^{-1} and T is the absolute temperature [K]. [4]

6.3. Results and analysis

In this section the results of the study are presented and serve to prove that indeed the gel behaved as expected. The results showed that the gel is a thixotropic, shear thinning viscoelastic material. The presented results correspond to the presented tests in the previous section.

As it can be seen in Figure 6.3, the results from Test 1 are presented in terms of storage modulus and shear stress. When looking at the storage modulus, two main regions can be identified, the first between 10^{-1} and about 70^{-1} , is an almost constant value at 40 Pa presented by the parallel dotted red line. As the strain increases, the storage modulus starts to experience a exponential decay, meaning that the gel is no longer together and bond breaking starts to take place and spread exponentially. The secant red dotted line represents this behavior. The point at which this change takes place is the critical strain at which a certain shear stress is the cause of this sudden network breakage. The yield stress can be found and in this case is This is the minimum shear pressure needed to make the gel flow and it impacts the design of a later pipeline system. The found yield stress is of around 36.7 Pa.

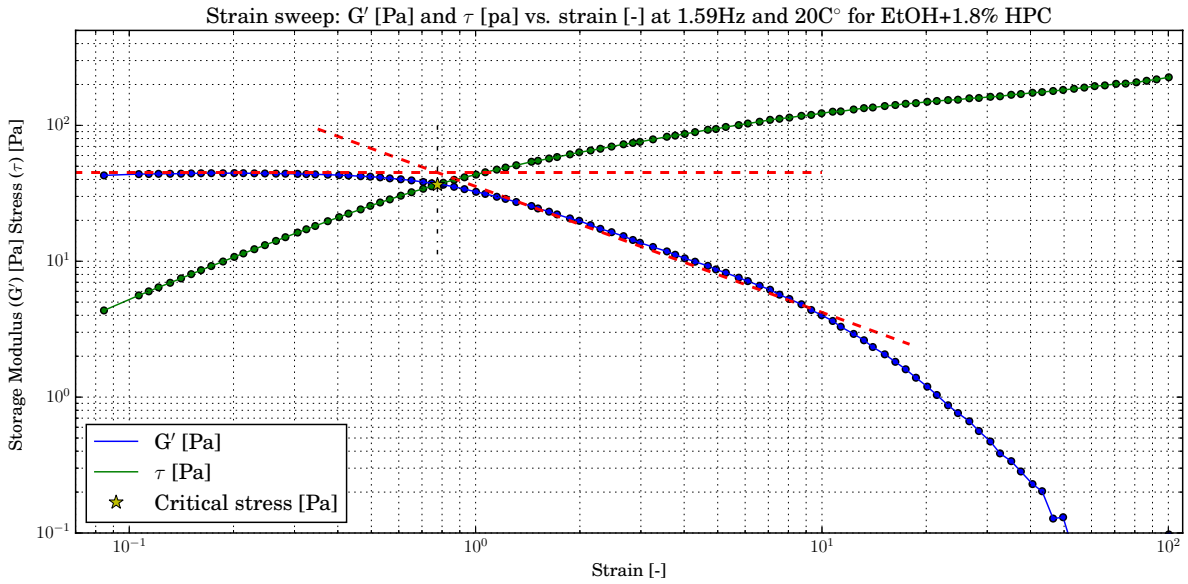

Figure 6.3: Test 1. Strain sweep for critical stress identification of the gel EtOH+1.8% HPC. Storage modulus (G') [Pa] and shear stress (τ) [Pa] are presented versus strain. The test was performed at atmospheric conditions and 20°C.

In Figure 6.4, the results from test 2 are presented. The variation in shear rate is presented by plotting the variation of the viscosity of the gel with the shear stress it felt. The test confirms the gel behaves as a linear elastic solid and as a viscous liquid. The viscous liquid presents a clear shear thinning characteristic.

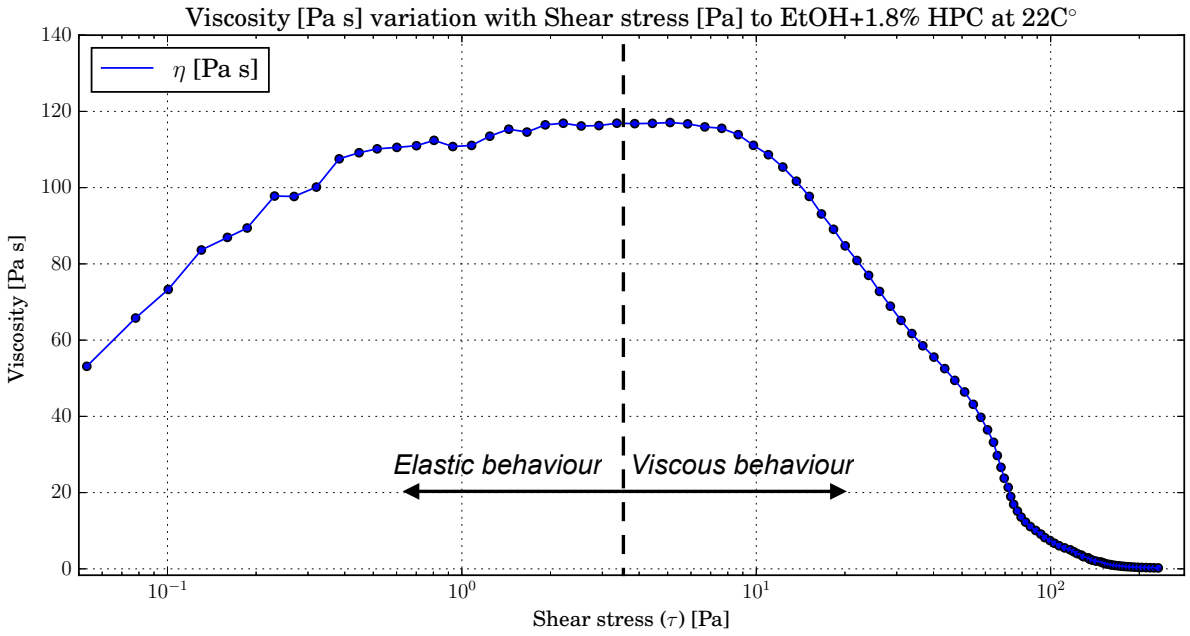

Figure 6.4: Test 2. Viscosity variation with shear stress felt by the gel EtOH+1.8% HPC. Two regions are identified a linear elastic and viscous region, the differentiation is the yield stress. The test was performed at atmospheric conditions and 22°C.

In Figure 6.5, the viscosity and shear stress are presented as a function of the shear rate. In this case a shorter range is tested up to 20 s^{-1}. The plot shows that the gel is thixotropic by nature. The ramping down or decrease in shear rate demonstrates that lower viscosity levels are achieved, meaning that the gel is more liquid once it has been previously sheared for a similar shear rate. This behavior is also present in the shear stress. For a similar shear rate, the ramping down returns a lower shear stress, meaning a less solid-like material is being sheared. The hysteresis loop, quantified by the area of the loop has only qualitative

relevance. The effects of the test procedure also play a role in it, thus it only serves to prove this characteristic of the gel

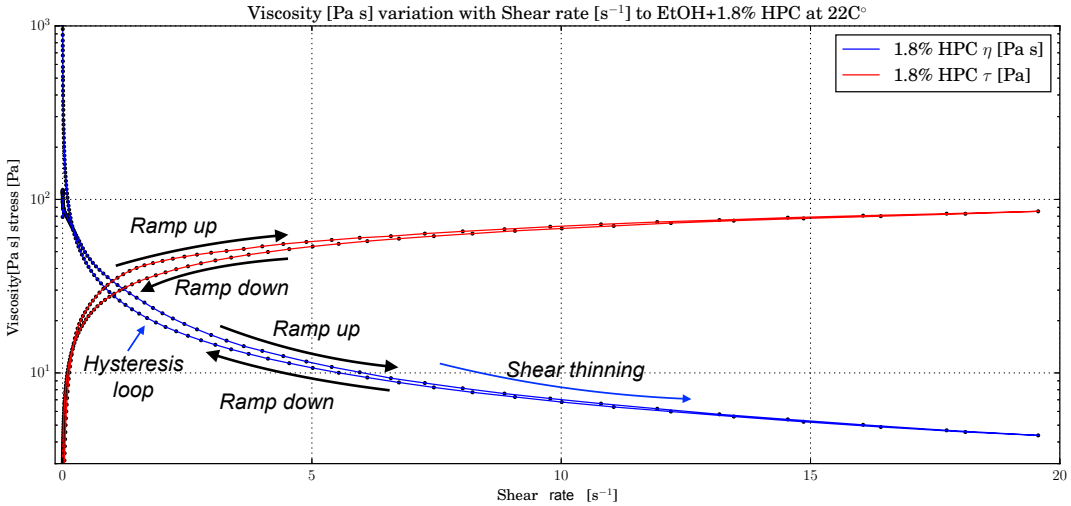

Figure 6.5: Test 2. Viscosity and shear stress as a function of shear rate. Ramp up and ramp down are presented and show the effects of thixotropy on the gel EtOH+1.8% HPC through hysteresis identification.

In Figure 6.6, the temperature oscillation test results are presented. As expected, the impact of temperature of the gel leads to viscosity reduction. Although the complex viscosity is presented, the values match the apparent real viscosity at a constant shear stress of 62 Pa, which is the frequency used for this test 10 rad/s. The fitted equation was found to be:

$$\eta^* = 5.45 \cdot 10^{-5} \cdot exp\left(\frac{28931.6}{RT}\right) \qquad R^2 = 0.99786 \tag{6.3}$$

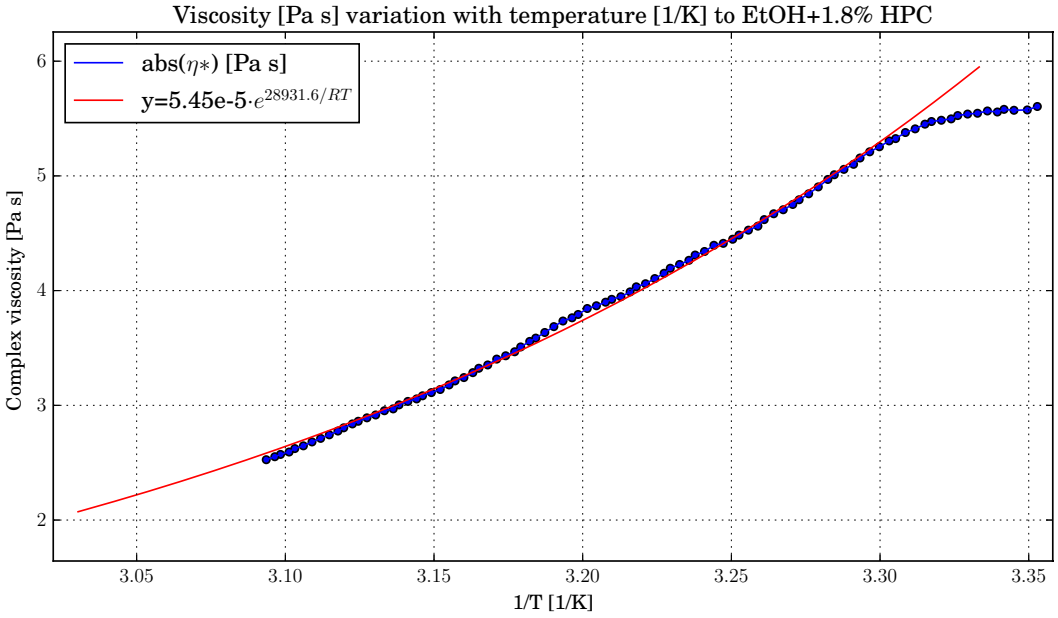

Figure 6.6: Test 4. Temperature oscillation and its effect on the viscosity of the gel EtOH+1.8% HPC. The temperature was varied from 20°Cto 50°C. A exponential Arrhenius-like function is fitted. The activation energy matches with the slope of the curve. Test was performed at atmospheric pressure conditions.

6.4. Conclusion

In this chapter, a comprehensive look into the characteristic of the gelled fuel has been taken. In order to make ethanol gel, several concentration of hydroxypropyl cellulose at high molecular weight have been used. After trying with different combinations spanning from 0.05% up to 2% wt., it was found that around 1.8% wt. of gelling agent in the fuel, leads to gellation. Thus, this was used as the critical concentration for gelling ethanol. For this critical concentration, a rheological study was perform to determine whether the final gel behaved as expected. In order to test this, four rheological test were done and the result analyzed. Firstly, during a dynamic test of strain sweep, in which a constant frequency of 1.59 Hz was used, showed that the gel exhibited a yield point at about 36.7 Pa of shear stress. This gave information of the needed pressure to maintain the flow on gel in a future pipeline. Subsequently, a static test was performed by varying the shear rate. The results indicated that the gel indeed behaves as a solid-elastic material at low shear stresses, but it presented viscous-like characteristics and the stress was increased. The reduction of viscosity with increasing pressure is known as shear-thinning and is innate to visco-elastic materials such as gels. Moreover, a test to characterize the time-dependency through the thixotropic property of the gel was performed. The results showed that a clear hysterics loop demonstrates that ethanol with 1.8% HPC is thixotropic. Lastly, the results of a temperature oscillation test were presented. The gel behaved as expected by thinning its viscosity as temperature increased. The result was fitted to an Arrhenius-like equation, demonstrating solid match between theory and results. To conclude, the gel behaved as a visco-elastic material, presenting thixotropic characteristics and temperature-dependent viscosity.

7

Conclusion and recommendations

This chapter gathers the conclusions and recommendations after the research questions and the work performed for this thesis work.

In this thesis work, a study of the possibility of exploiting the energy content of hydrogen peroxide was conducted. Hydrogen Peroxide was first studied as a monopropellant and then also as a bi-propellant with ethanol without the use of catalyst, making the system pseudo-hypergolic. The drop-test study returned valuable information on the conditions needed to achieve the hydrogen peroxide decomposition phenomena, but also information about the ignition in terms of temperatures and times.

Thus, taking the initial research question, the study conducted herein now provides an answer. The research question of this thesis work is as follows:

> *Is the use of thermal energy sufficient to achieve High Test Peroxide decomposition to allow for dual-mode system, as monopropellant and as pseudo-hypergolic bipropellant with ethanol, and if so, under what conditions?*

After the findings in this thesis, the answer is yes. Decomposition of High Test Peroxide (HTP) can be achieved with the sole use of thermal energy, and its application is not only valid as a monopropellant, but its combination with ethanol also leads to a pseudo-hypergolic ignition as well. The answer to this question is expanded subsequently by addressing the research goals

First and foremost, for experimentation, the procurement of hydrogen peroxide was not possible through vendors or other research institutions. This is because of the highly regulated legal framework surrounding the chemical at high concentrations above 60% wt. Its energetic content makes it expensive to transport and tedious to obtain legally. Instead, an innovative approach to refine hydrogen peroxide in-house from commercially available lower concentrations was achieved. The approach which came after other failed approaches, is now patented[1]. This allowed us to achieve in-house concentrations of the chemical in excess of 99% wt., for one order of magnitude in cost less and in the span of less than 2 days. For this chemical, a characterization was made through stability study. The decrease of concentration with time is an intrinsic characteristic of hydrogen peroxide. It was found that the in-house refined chemical suffers a more significant degradation over time when presented against the literature. The degradation reduced the concentration from 96.3% to 92.0% in 37 days when kept refrigerated at -30°C, and was larger for increased temperature.

The thermal decomposition approach was investigated through a drop test study. Where a droplet of HTP fell onto a heating plate, and three thermocouples were measuring the temperatures. It was found that only certain combinations of HTP concentrations and temperature of the heating plate would lead to full decomposition. These combinations were 80, 85, 90 and 95% HTP with 200, 250 and 270 °C heating plate. It was found that 80% HTP and 200°C would not lead to full decomposition, also lower temperatures of 150°C and lower concentrations of 75% HTP returned no decomposition as well. This indicated that the need for high energetic concentration in HTP and the reduction in water content play an important role in this mechanism.

[1] Patent was filed 13/11/19 under patent reference number: N2024229

Similarly, the energy supplied, regulated through the heating plate temperature, heavily affected the process. The process of decomposition was recorded with a High Speed Camera at 6400 fps, and it was found that the droplet undergoes a certain level of boiling prior to the decomposition which, once started, spreads through the entirety of the fluid. This process was found to be irreversible and in most cases starting close to the surface of the droplet. With concentrations of 90 and 95%, the achieved maximum temperatures were around 850°C, which was lower for 80 and 85% laying around 700°C. These are well above the autoignition temperature of ethanol, and thus can be implemented as bipropellants as well. The decomposition was found to always begin at a temperature close to the boiling point of that HTP concentration, which points at the need to have some evaporated HTP prior to its energetic decomposition. The time they took to decompose was influenced largely by the concentration as well as the heating plate temperature. The Decomposition Delay Time (DDT), showed a reduction of over 400 ms with the increase in heating plate temperature for some concentrations. For all the concentrations, the lowest DDT always took place at 270°C, which is also the heating plate temperature needed to reach the benchmark of 100 ms normally used for hypergolic RCS systems. Furthermore, when compared with the catalyst action of MnO_2, it was found that the thermal approach led to larger temperatures increases, but showed a faster DDT for heterogeneous decomposition.

Following this, the ignition with ethanol and HTP was analyzed to serve as the bipropellant mode in a dual-mode propulsion system. It was found that ethanol and HTP can be considered to be pseudo-hypergolic, given that HTP decomposition in touch with fuel will ignite it, as was found in this research. The combinations of HTP concentration and heating plate temperature testing were the same as for the HTP monopropellant mode. The recordings on the high speed camera showed that the process always involves the decomposition of HTP, and then later contact with ethanol in gaseous forms ignites the fuel while the rest of the liquid on the heating plate gets quickly consumed. The initial combustion is quite bright and sonorous, due to the suspension of some gaseous ethanol. After, because the oxidizer gets consumed before the fuel is totally depleted, a less bright and more reddish ethanol flame is all that could be seen. The properties of the propellants only allowed the production of droplets of 0.13 mL for HTP and 0.06 mL for ethanol, which gives a lower OF ratio (about 3.8 average) than the optimum 4.4. Moreover, it was found that the fuel should never fall before the HTP, due to the substantial risk of explosion. This risk should be taken into account when designing the combustion chamber and always start the combustion chamber with HTP in monopropellant mode prior to the bipropellant mode. Conversely to the HTP decomposition case, the ignition showed a different temperature at the moment of ignition. As the concentration of HTP increased, the reaction was more oxidizer-dominated and the temperature got closer to the boiling point of 150°C and was less sensitive to the energy supplied. However at lower concentrations, the temperature of the heating plate greatly affected its temperature at ignition, increasing variability of the result by a significant margin. This points to the fact that lower concentration of HTP are more mixture-dominated and that the role of ethanol, which is less understood, is significant. The maximum temperatures are, in general, larger than the decomposition-only case. It was found that larger concentrations have a tremendous impact on the amount of extra energy liberated, being in excess of 700°C on top of the boiling temperature for 95% HTP. The difference of these values with what was theoretically expected show that the assumption of adiabatic is not applicable in this case and that open-air testing has an impact on it as well. When it comes to the Ignition Delay Time (IDT), ethanol and HTP achieved values under 100 ms for the largest concentrations of 90 and 95% at the largest energy supplies of 250 and 270 °C of heating plate temperature. In general, the IDT of all decreased with increasing temperature of heating plate and with concentration of HTP provided, due to its energetic nature. The open-air conditions of the test are quite promising and the testing in a more relevant environment will further increase its appeal, as shorter IDT can be achieved. In fact, some exciting cases were filmed in which already decomposed HTP collided in mid air with ethanol igniting it in less than 1 ms. Moreover, the ignition with gelled ethanol proved to be a success, as the IDT was below the 100 ms for both tested cases and the energy significantly released surpassed its liquid counterpart, even melting one of the thermocouples. Due to the organic nature of the gelling agent, the gel left no residue in the vessel, showing tremendous potential for an application in the combustion chamber.

The gel used to boost the performance was analyzed for characterization through a rheology study. The gelling agent hydroxypropyl cellulose with a large molecular weight was used to find the critical concentration, which was placed at 1.8% wt. The resulting gel was characterized through four independent test studies in the rheometer. It exhibited a viscoelastic nature with a yield point at 36.7 Pa, a thixotropic behavior characteristic of gels and temperature-dependent viscosity.

The possibility to implement the decomposition of HTP as a monopropellant and the ignition of HTP with ethanol as a bipropellant with only thermal energy activation has been proven to be possible and is promising. Several aspects of this work will further impact the design of green propulsion approaches in the future. The innovative refining of hydrogen peroxide will open the door to hypergolic studies for students at Masters levels. The decomposition of HTP will allow for low-performance required propulsion, such as sounding rocket orbit correction or small-sat orbit raising. The pseudo-hypergolic ignition with ethanol paves the path for green and safe large propulsion systems, such as micro-launchers. However, the combination of the two can be applied to other systems, such as large satellites, cube-sats with stringent requirements, or rockets with special orbit needs.

7.1. Recommendations for future work

Due to the nature of the work in this thesis, mainly experimental, numerous unexpected setbacks have been found along the way. Mostly related to the physical problems of experimentation. In this section, recommendations for these problems and future work on this area are given.

Concerning the procurement of HTP, for future scientist I recommend them to have a solid procurement supplier and to not have to struggle with the procurement. If this is not possible, I encourage them to contact me for help on the matter. The research institutions will do little to help, given the stringent regulations, and the commercial suppliers and scarce and expensive. Having surpassed the problem of procuring the chemical, for future work, it is need to perform a detailed analysis of the particles present in the refined HTP. This can be done by using a mass spectrometer, however the need to vaporize the chemical make this task dangerous. Liquid chromatography, on the other hand, may give a qualitative insight into the chemical present in the solution. Other solutions may imply specialized equipment such as the IBM excursion [33]. Knowing the particles is key to understanding the degradation with time suffered for the samples in this study. Moreover, to limit this degradation, gelling the HTP with an inorganic gelling agent, such as fumed silica (SiO_2), may reduce the degradation and it is recommended to investigate. Furthermore, the container material is also interesting to examine. Borosilicate is considered a class 1 material with HTP, however exploring other class 1 materials such as aluminum 95% pure, or polyethylene is recommended. Likewise, increasing the length of the stability study to 1 year is of interest, to prove the statement that 1% over a year is the normal HTP loss. Lastly, having access to a more precise instrument to measure the concentration of hydrogen peroxide. The L-Dens 7400 available by Anton Paar is a good candidate. It can measure up to 95% with a resolution of $\pm$ 0.7 %

For the drop test experiment, several recommendations are made for future researchers. First and foremost there is a need to improve the overall setting of the droplet system. A close-chamber system where to make the droplets fall and ignite is recommended, such as [45]. This allows to also measure the pressure of the ignition and decomposition, but can also improve the poor thermal control of the used heating plate. By improving this heating plate, the analysis done can be finer, which is recommended to fully understand the location of the decomposition line. Such a chamber, with a quartz view-through part should also incorporate a system to generate the droplets on demand in terms of time and volume. This was a clear limitation faced in this study and its implications for future research is of importance for design of combustion chambers. For the decomposition approach, only MnO_2 was used at unconventional size, for the future other catalysts such as manganese acetylacetonate ($C_{10}H_{14}MnO_4$) or platinum and silver are recommenced to have a more relevant comparison. As a future improvement in the setup, the use of a thermal camera is also interesting to include. The locations where maximum temperature take place are interesting for the injection and combustion chamber design. In fact, the theory of adiabatic flame temperature is also recommended to be explored in more depth. There seems to be a great effect coming from the phase of the reactants, which ultimately affects the final temperature achieved. A more detailed study of this may better predict what percentage of HTP evaporates prior to decomposition, specially for different pressure cases.

The ignition test campaign also raised several recommendations for work in this area. Assuming that the setup is shared with the decomposition study, the recommendations of the setup also apply here. The main aspect of the setup is to regulate more precisely the time between droplets to also avoid the falling of ethanol prior to HTP and to also measure the pressure changes. Moreover, for the High Speed Camera, the future

researchers are recommended to work with a color-mode equipment, as the lack of color misses substantial information concerning the temperature at locations and the different consumption of propellants. For the ignition, it is known that increase in pressure would lead to lower IDT, it is of interest to study this phenomena at pressures ranging from 1 to 10 atm, or whatever pressure is more relevant for the future combustion chamber. Lastly, a laser to trigger the filming when the droplet passes through ti is interesting to add,. This would result is shorter and more precise filming. In fact, the shorter filming is needed, as the download speed of a single video is still in the 45 min, even after cropping part of it. For the future, this download speed is required to be shortened, the use of solid state drives may improve this, or faster PCs. Although this thesis only tested ethanol as a fuel, some small companies employ kerosene as their fuel, so researching into other fuels, such as kerosene, gasoline or larger carbon chains is an interesting next step. Lastly, for the use of gels, a system to create more precise droplets, such as a Eppendorf droplet generator are suggested for the future. For the theoretical part, the results at NASA CAE are a good first estimate, but a more detailed study is advised through thermal analysis and CFD as soon as a chamber sizing is available.

Finally, for the rheology side of this thesis. The upcoming scientist is encourage to perform a larger scale gel rheological study. Specially, once the combustion chamber is sizing is finished and the preliminary injector sizing is known. A more detailed study should include a dynamic study through frequency sweep at the critical strain. This is needed to understand the storage and loss modulus of the gel at its point of viscous phase-change. The use of other gelling agents, such as hydroxypropyl methyl cellulose are encouraged to try as well, in order to find the gelling agent with the lowest critical concentration. Moreover, for the future researcher, fitting the results to one of the models available, such as the extended Herschel-Buckley or a power-law is recommended.

Bibliography

[1] Rajan Ambat and ES Dwarakadasa. Effect of hydrogen in aluminium and aluminium alloys: A review. *Bulletin of Materials Science*, 19(1):103–114, 1996.

[2] Vittorio Bombelli, Dieter Simon, Jean-Luc Moerel, and Ton Marée. Economic benefits of the use of non-toxic mono-propellants for spacecraft applications. In *39th AIAA/ASME/SAE/ASEE Joint Propulsion Conference and Exhibit*, page 4783, 2003.

[3] Jyoti Botchu and Seung Baek. Rheological characterization of hydrogen peroxide gel propellant. *International Journal of Aeronautical and Space Sciences*, 15:112–121, 06 2014. doi: 10.5139/IJASS.2014.15.2.199.

[4] Jyoti Botchu and Seung Baek. Rheological characterization of ethanolamine gel propellants. *Journal of Energetic Materials*, 34, 01 2015. doi: 10.1080/07370652.2015.1061617.

[5] Cristina Bramanti, Angelo Cervone, Luca Romeo, Lucio Torre, Luca d'Agostino, Antony Musker, and Giorgio Saccoccia. Experimental characterization of advanced materials for the catalytic decomposition of hydrogen peroxide. 07 2006. doi: 10.2514/6.2006-5238.

[6] ME Bretschger and ES Shanley. Concentrated hydrogen peroxide. *Transactions of The Electrochemical Society*, 92(1):67–76, 1947.

[7] N.A. Brikner and J.M. Protz. Modeling of the decomposition and combustion of hydrogen peroxide and ethanol for design of a bipropellant microrocket engine. 2011. URL https://www.scopus.com/inward/record.uri?eid=2-s2.0-84880680228&partnerID=40&md5=11b70f44f380e68b9bb0812de4970d71. cited By 2.

[8] Claudio Bruno and Antonio G. Accettura. *Advanced Propulsion Systems and Technologies, Today to 2020*. American Institute of Aeronautics and Astronautics, Reston, UNITED STATES, 2000. ISBN 9781600864742. URL http://ebookcentral.proquest.com/lib/delft/detail.action?docID=3111453.

[9] H C. Ciezki, Christoph Kirchberger, Alexander Stiefel, P Kröger, Pedro Pinto, J Ramsel, K W. Naumann, and Volker Weiser. Overview on the german gel propulsion technology activities: Status 2017 and outlook. 07 2017.

[10] David A Castaneda and Benveniste Natan. Experimental investigation of the hydrogen peroxide–solid hydrocarbon hypergolic ignition. *Acta Astronautica*, 158:286–295, 2019.

[11] Angelo Cervone, Luca Romeo, Lucio Torre, Luca d'Agostino, Fausto Calderazzo, A Musker, Graham T Roberts, and Giorgio Saccoccia. Development of green hydrogen peroxide monopropellant rocket engines and testing of advanced catalytic beds. In *Proc. of the 3rd International Conference on Green Propellants for Space Propulsion*, pages 17–20, 2006.

[12] J.D. Clark and I. Asimov. *Ignition!: An Informal History of Liquid Rocket Propellants*. Rutgers University Press classics. Rutgers University Press, 2018. ISBN 9780813599199. URL https://books.google.nl/books?id=_JZcDwAAQBAJ.

[13] Meredith B Colket and Louis J Spadaccini. Scramjet fuels autoignition study. *Journal of propulsion and power*, 17(2):315–323, 2001.

[14] Y. Cong, T. Zhang, T. Li, J. Sun, X. Wang, L. Ma, D. Liang, and L. Lin. Propulsive performance of a hypergolic h2o2 and kerosene bipropellant. *Journal of Propulsion and Power*, 20(1): 83–86, 2004. URL https://www.scopus.com/inward/record.uri?eid=2-s2.0-1042277440&partnerID=40&md5=20bdcf5a6fffcf08153f61639bb8e402. cited By 20.

[15] M. T. Constantine, E. F. Cain, ROCKETDYNE CANOGA PARK CA CHEMICAL, and MATERIAL SCIENCES Dept. Hydrogen peroxide handbook., 1967. URL http://www.dtic.mil/docs/citations/AD819081.

[16] Jacob D Dennis, Jared D Willits, and Timothée L Pourpoint. Performance of neat and gelled monomethylhydrazine and red fuming nitric acid in an unlike-doublet combustor. *Combustion Science and Technology*, 190(7):1141–1157, 2018.

[17] Kevin Gagne, M McDevitt, and Darren Hitt. A dual mode propulsion system for small satellite applications. *Aerospace*, 5(2):52, 2018.

[18] Amir S. Gohardani, Johann Stanojev, Alain Demairé, Kjell Anflo, Mathias Persson, Niklas Wingborg, and Christer Nilsson. Green space propulsion: Opportunities and prospects. *Progress in Aerospace Sciences*, 71:128 – 149, 2014. ISSN 0376-0421. doi: https://doi.org/10.1016/j.paerosci.2014.08.001. URL http://www.sciencedirect.com/science/article/pii/S0376042114000797.

[19] Ulrich Gotzig. Challenges and economic benefits of green propellants for satellite propulsion. 01 2017.

[20] S.D. Heister, W.E. Anderson, T.L. Pourpoint, and R.J. Cassady. *Rocket Propulsion*. Cambridge Aerospace Series. Cambridge University Press, 2019. ISBN 9781108422277. URL https://books.google.nl/books?id=V96CDwAAQBAJ.

[21] T. Hiraiwa, T. Saito, T. Tomita, N. Azuma, K. Okita, K. Obase, and T. Kaneko. Research works of ethanol propulsion system for the future rocket-plane experimental vehicle. 2011. URL https://www.scopus.com/inward/record.uri?eid=2-s2.0-84880647990&partnerID=40&md5=5e000dbb29c1e29dfcc1da9ed2e842fe. cited By 4.

[22] Jeongmoo Huh, Jyoti Botchu, Yongtae Yun, Muhammad Naseem, and Sejin Kwon. Preliminary assessment of hydrogen peroxide gel as an oxidizer in a catalyst ignited hybrid thruster. *International Journal of Aerospace Engineering*, 2018:1–14, 12 2018. doi: 10.1155/2018/5630587.

[23] R.W. Humble. Bipropellant engine development using hydrogen peroxide and a hypergolic fuel. 2000. URL https://www.scopus.com/inward/record.uri?eid=2-s2.0-80054704164&partnerID=40&md5=1aa352344686c5e8aefbd41ff8b4c783. cited By 3.

[24] S. Jo, S. An, J. Kim, H. Yoon, and S. Kwon. Performance characteristics of hydrogen peroxide/kerosene staged-bipropellant engine with axial fuel injector. *Journal of Propulsion and Power*, 27(3):684–691, 2011. doi: 10.2514/1.B34083. URL https://www.scopus.com/inward/record.uri?eid=2-s2.0-79955960059&doi=10.2514%2f1.B34083&partnerID=40&md5=812a2c306b10b3fc88483e4ab576bb20. cited By 15.

[25] Jerin John, Purushothaman Nandagopalan, Seung Wook Baek, and Ankur Miglani. Rheology of solid-like ethanol fuel for hybrid rockets: Effect of type and concentration of gellants. *Fuel*, 209:96 – 108, 2017. ISSN 0016-2361. doi: https://doi.org/10.1016/j.fuel.2017.06.124. URL http://www.sciencedirect.com/science/article/pii/S0016236117308335.

[26] W. Jung, S. Baek, T. Kwon, J. Park, and S. Kwon. Demonstration of ethanol-blended hydrogen peroxide gas generator for ramjet combustor flow simulation. *Journal of Propulsion and Power*, 34(3):591–599, 2018. doi: 10.2514/1.B36633. URL https://www.scopus.com/inward/record.uri?eid=2-s2.0-85045762221&doi=10.2514%2f1.B36633&partnerID=40&md5=c4b980649c385a22ddd33c9a32223ba0. cited By 2.

[27] B.V.S. Jyoti and S.W. Baek. Formulation and comparative study of rheological properties of loaded and unloaded ethanol-based gel propellants. *Journal of Energetic Materials*, 33(2):125–139, 2015. doi: 10.1080/07370652.2014.939311. URL https://www.scopus.com/inward/record.uri?eid=2-s2.0-84911968458&doi=10.1080%2f07370652.2014.939311&partnerID=40&md5=1b3d8466d8e582aca9d822346ab857f5. cited By 10.

[28] B.V.S. Jyoti, M.S. Naseem, and S.W. Baek. Hypergolicity and ignition delay study of pure and energized ethanol gel fuel with hydrogen peroxide. *Combustion and Flame*, 176:318–325, 2017. doi: 10.1016/j.combustflame.2016.11.018. URL https://www.scopus.com/inward/record.uri?eid=

2-s2.0-85001946014&doi=10.1016%2fj.combustflame.2016.11.018&partnerID=40&md5=65f7ff81c1275eb646d36ee6257ac3f5. cited By 5.

[29] B.V.S. Jyoti, M.S. Naseem, S.W. Baek, H.J. Lee, and S.J. Cho. Hypergolicity and ignition delay study of gelled ethanolamine fuel. *Combustion and Flame*, 183:102–112, 2017. doi: 10.1016/j.combustflame.2017.05.007. URL https://www.scopus.com/inward/record.uri?eid=2-s2.0-85019617474&doi=10.1016%2fj.combustflame.2017.05.007&partnerID=40&md5=cb1b5a7191063121c5cc5a979afc7f8e. cited By 2.

[30] Hongjae Kang, Hyuntak Kim, and Sejin Kwon. Difficulties in dual-mode operation of nontoxic hypergolic thruster using decomposition of h2o2. *Journal of Propulsion and Power*, 35(4):780–786, 2019. doi: 10.2514/1.B37420. URL https://doi.org/10.2514/1.B37420.

[31] J. Lee and S. Kwon. Evaluation of ethanol-blended hydrogen peroxide monopropellant on a 10 n class thruster. *Journal of Propulsion and Power*, 29(5):1164–1170, 2013. doi: 10.2514/1.B34790. URL https://www.scopus.com/inward/record.uri?eid=2-s2.0-84885035457&doi=10.2514%2f1.B34790&partnerID=40&md5=8059d3b3a5f33500f61b64b3b8f9fdf6. cited By 8.

[32] J. Lee, D. Jang, and S. Kwon. Performance improvement of hydrogen peroxide monopropellant by blending ethanol. 2012. URL https://www.scopus.com/inward/record.uri?eid=2-s2.0-84880783216&partnerID=40&md5=9b1dc318d3d6502d2ddc963bac792db8. cited By 0.

[33] M. E. Lydon, J. P. Ritter, and J. K. Comeau. Trace analysis of hydrogen peroxide contamination. In *2015 26th Annual SEMI Advanced Semiconductor Manufacturing Conference (ASMC)*, pages 228–231, May 2015. doi: 10.1109/ASMC.2015.7164476.

[34] Klaus Madlener and Helmut Ciezki. Some aspects of rheological and flow characteristics of gel fuels with regard to propulsion application. 08 2009. doi: 10.2514/6.2009-5240.

[35] Jennifer Mallory, Sarah Jo DeFini, and Paul Sojka. *Formulation of Gelled Propellant Simulants*. American Institute of Aeronautics and Astronautics, 2019/02/18 2010. doi: doi:10.2514/6.2010-7142. URL https://doi.org/10.2514/6.2010-7142.

[36] B.M. Melof and M.C. Grubelich. Investigation of hypergolic fuels with hydrogen peroxide. 2001. URL https://www.scopus.com/inward/record.uri?eid=2-s2.0-84894296921&partnerID=40&md5=590e97e1bd784a7a5b03b838bc73b48f. cited By 11.

[37] Lukasz Mezyk, Zbigniew Gut, Przemysław Paszkiewicz, Piotr Wolanski, and Grzegorz Rarata. Possibility of using thermal decomposition of hydrogen peroxide for low thrust propulsion system application. 07 2017. doi: 10.13009/EUCASS2017-626.

[38] Antony Musker, Graham Roberts, Paul Chandler, John Grayson, and Joseph Holdsworth. Optimisation study of a homogeneously-catalysed htp rocket engine. In *ESA Special Publication*, volume 557, 2004.

[39] M.S. Naseem, B.V.S. Jyoti, S.W. Baek, H.J. Lee, and S.J. Cho. Hypergolic studies of ethanol based gelled bi-propellant system for propulsion application. *Propellants, Explosives, Pyrotechnics*, 42 (6):676–682, 2017. doi: 10.1002/prep.201700046. URL https://www.scopus.com/inward/record.uri?eid=2-s2.0-85016576963&doi=10.1002%2fprep.201700046&partnerID=40&md5=a26f05438a36143faec1fde3116b31d4. cited By 2.

[40] Benveniste Natan, Valeriano Perteghella, and Yair Solomon. Hypergolic ignition of oxidizers and fuels by fuel gelation and suspension of reactive or catalyst particles. In *46th AIAA/ASME/SAE/ASEE Joint Propulsion Conference & Exhibit*, page 7144.

[41] United Nations. European agreement concerning the international carriage of dangerous goods by road (adr)), 2019.
https://adrbook.com.

[42] National Institute of Standards and Technology (U.S.). *NIST Chemistry Webbook: NIST Standard Reference Database Number 69*. NIST, 2000. URL https://books.google.nl/books?id=dxM3ngAACAAJ.

[43] A. Okninski, B. Bartkowiak, K. Sobczak, D. Kublik, P. Surmacz, G. Rarata, B. Marciniak, and P. Wolanski. Development of a small green bipropellant rocket engine using hydrogen peroxide as oxidizer. 2014. doi: 10.2514/6.2014-3592. URL https://www.scopus.com/inward/record.uri?eid=2-s2.0-84913556464&doi=10.2514%2f6.2014-3592&partnerID=40&md5=34670d0276329d10620f152de382ab81. cited By 12.

[44] Shai Rahimi, Arie Peretz, and Benveniste Natan. On shear rheology of gel propellants. *Propellants, Explosives, Pyrotechnics*, 32(2):165–174, 2007. doi: 10.1002/prep.200700018. URL https://onlinelibrary.wiley.com/doi/abs/10.1002/prep.200700018.

[45] Grzegorz Rarata, Lukasz Mezyk, and Zbigniew Gut. Research on thermal decomposition of 98class. *Journal of Power Technologies*, 12 2016.

[46] FO Rice and ORLAND M Reiff. The thermal decomposition of hydrogen peroxide. *The Journal of Physical Chemistry*, 31(9):1352–1356, 1927.

[47] Walter C. Schumb, Charles N. Satterfield, and R. L. Wentworth. *Hydrogen peroxide*. Reinhold, New York, 1955.

[48] M.N. Shoaib, B.V.S. Jyoti, S.W. Baek, and J. Huh. Effect of alcohol carbon chain on enthalpy of combustion and ignition delay time for gelled hypergolic propellant system. *Propellants, Explosives, Pyrotechnics*, 43(5):453–460, 2018. doi: 10.1002/prep.201700268. URL https://www.scopus.com/inward/record.uri?eid=2-s2.0-85046895356&doi=10.1002%2fprep.201700268&partnerID=40&md5=1e6159240fcbdeb28d8b15f57123e991. cited By 0.

[49] Jerry E Sinor and Brent K Bailey. Current and potential future performance of ethanol fuels. Technical report, SAE Technical Paper, 1993.

[50] J.C. Sisco, B.L. Austin, J.S. Mok, and W.E. Anderson. Autoignition of kerosene by decomposed hydrogen peroxide in a dump-combustor configuration. *Journal of Propulsion and Power*, 21(3):450–459, 2005. doi: 10.2514/1.5287. URL https://www.scopus.com/inward/record.uri?eid=2-s2.0-19644394380&doi=10.2514%2f1.5287&partnerID=40&md5=42e806d5d6384c08e377d692f16890dd. cited By 27.

[51] George P. Sutton and Oscar Biblarz. *Rocket Propulsion Elements*. John Wiley & Sons, Incorporated, New York, UNITED STATES, 2016. ISBN 9781118753880. URL http://ebookcentral.proquest.com/lib/delft/detail.action?docID=4756773.

[52] N. Tsujikado, M. Koshimae, R. Ishikawa, K. Kitahara, A. Ishihara, Y. Sakai, and K. Konishi. An application of commercial grade hydrogen peroxide for hybrid/liquid rocket engine. 2002. URL https://www.scopus.com/inward/record.uri?eid=2-s2.0-84896878055&partnerID=40&md5=e53e58a31a0a90dfba8e7124f17a9840. cited By 2.

[53] Ferran Valencia-Bel. Green propulsion. *State-of-art, prospectives and roadmap*, 2015.

[54] M Ventura and G Garboden. A brief history of concentrated hydrogen peroxide uses. In *35th Joint Propulsion Conference and Exhibit*, page 2739.

[55] Mark Ventura. Long term storability of hydrogen peroxide. In *41st AIAA/ASME/SAE/ASEE Joint Propulsion Conference & Exhibit*, page 4551.

[56] W.P.W. Wieling. Preliminary design of a rghp/ethanol thruster for the advanced re-entry vehicle. Master's thesis, Delft University of Technology.

[57] H. Winter. Three views of viscoelasticity for cox–merz materials. *Rheologica Acta - RHEOL ACTA*, 48: 241–243, 04 2009. doi: 10.1007/s00397-008-0329-5.

[58] B.T.C. Zandbergen and Delft University of Technology. Faculty of Aerospace Engineering. *Thermal rocket propulsion (version 2.07): Ae4S01*. TU Delft, 2010. URL https://books.google.nl/books?id=2A2xnQEACAAJ.

[59] J. Zhang, Y. Hu, and Y. Li. *Gel Chemistry: Interactions, Structures and Properties*. Lecture Notes in Chemistry. Springer Singapore, 2018. ISBN 9789811068812. URL https://books.google.nl/books?id=C3BGDwAAQBAJ.

A

Data points of ignition test campaign

Table A.1: Droplet analysis and results from the test campaign of ignition for concentrations of 80 and 85%. Presented are the ignition temperature [°C], the maximum temperature [°C], the ignition delay time form the DAQ and the HSP [ms]. HTP is the concentration of H_2O_2 and Id the identifier or numbering for the droplet-test.

HTP[%±1%]	**T_{HP}[°C±10°C]**	**Id. [-]**	**$T_{Ignition}$[°C±3°C]**	**T_{max}[°C±3°C]**	**IDT_{DAQ} [ms±18ms]**	**IDT_{DAQ} [ms±0.16ms]**
80						
	250					
		1	361.0	813.0	54.5	NR
		2	464.0	971.0	18.2	32.1
		3	590.0	925.0	290.9	282.3
		4	575.0	758.0	254.0	NR
		5	795.0	807.9	490.9	NR
	270					
		1	727.0	851.0	181.8	NR
		2	446.0	955.0	472.0	NR
		3	756.0	823.0	200.0	NR
		4	788.0	851.0	272.7	256.8
		5	462.0	976.0	72.0	62.8
		6	767.0	1030.0	109.1	NR
85						
	200					
		1	119.0	666.9	309.0	357.3
		2	140.0	600.4	327.0	334.8
		3	123.0	731.0	436.0	423.3
	250					
		1	197.0	516.0	163.0	179.37
		2	157.0	934.0	18.8	18.5
		3	300.0	843.0	109.0	NR
		4	154.0	1039.0	250.2	NR
	270					
		1	602.0	696.0	381.0	357.8
		2	274.0	975.0	54.5	40.3
		3	351.0	973.0	181.0	NR
		4	691.0	911.0	254.5	NR

Table A.2: Droplet analysis and results from the test campaign of ignition for concentrations of 90% and 95%. Presented are the ignition temperature [°C], the maximum temperature [°C], the ignition delay time form the DAQ and the HSP [ms]. HTP is the concentration of H_2O_2 and Id the identifier or numbering for the droplet-test.

HTP[%±1%]	**T_{HP}[°C±10°C]**	**Id. [-]**	**$T_{Ignition}$[°C±3°C]**	**T_{max}[°C±3°C]**	**IDT_{DAQ} [ms±18ms]**	**IDT_{DAQ} [ms±0.16ms]**
90						
	200					
		1	143.0	837.6	309.0	NR
		2	142.0	586.0	145.5	NR
		3	127.0	715.0	218.6	218.6
		4	144.5	552.0	363.6	357.0
		5	143.2	670.0	54.5	NR
		6	144.4	741.0	200.0	NR
		7	160.0	716.0	145.5	165.2
	250					
		1	136.9	929.3	54.5	NR
		2	142.4	738.0	145.5	139.7
		3	280.0	850.5	91.0	NR
	270					
		1	240.7	926.0	109.0	129.0
		2	284.0	1282.0	18.2	17.2
		3	276.0	937.0	72.8	NR
95						
	200					
		1	120.0	1341.2	18.2	14.7
		2	91.0	654.0	145.5	147.0
		3	148.5	739.4	181.2	NR
		4	143.2	1144.9	182.0	180.2
		5	188.0	1223.4	54.5	NR
		6	143.0	816.6	145.0	NR
		7	140.8	703.0	345.0	365.0
	250					
		1	144.0	624.0	18.2	NR
		2	162.0	783.0	18.2	NR
		3	143.0	1099.0	182.0	NR
		4	229.3	668.0	145.5	NR
		5	112.0	632.0	90.1	NR
		6	175.0	981.0	109.0	95.5
	270					
		1	142.0	619.0	54.5	NR
		2	142.0	710.0	36.6	NR
		3	137.0	866.0	72.7	NR

B

Test plan for drop tests

In this appendix, the test plan used for the drop test experiments is presented. The similarity between the decomposition and igntion studies is such, that the test plan is easily interpreted for both only HPT and HTP/EtOH. The drop test experiments were the heart of this thesis work and thus a strict plan was put into place throughout the course of the tests. To cover it, firstly the test description is given in Appendix B.1, where the high level test logic is provided and the breakdown of it. Subsequently, the test procedures are provided in Appendix B.2. Lastly, safety surrounding the development of the test is presented in Appendix B.3.

Concerning the instrumentation, the involved materials have been presented in Section 4.2 and Section 5.2. So it will only be hereby presented with identifiers for the exact amount use and their application (HTP or EtOH), as shown in Table B.1.

Inventory			
ID	**Item**	**ID**	**Item**
FM	Fumehood	SYPH	Syringe pump HTP
SYPE	Syringe pump EtOH	PC	MacBookPro
LIS	Light source	HP	Heating plate
DAQ	DAQ NI-9219	HSP	High speed camera
FKT1	Fine K-thermocouple 0mm	FKT2	Fine K-thermocouple 3mm
FKT3	Fine K-thermocouple 6mm	FKT4	Fine K-thermocouple 5cm
SYRH	Syringe HTP	SYRE	Syringe EtOH
CATH	Capillary tube HTP	CATE	Capillary tube EtOH
HTP	High Test Peroxide	ETOH	Ethanol

Table B.1: Inventory for setup of experiment.

B.1. Test description

In this section the test description is presented. The high level test logic overview is provided in Figure B.1. Subsequently, the steps are discussed in more depth.

B.1.1. High level test logic

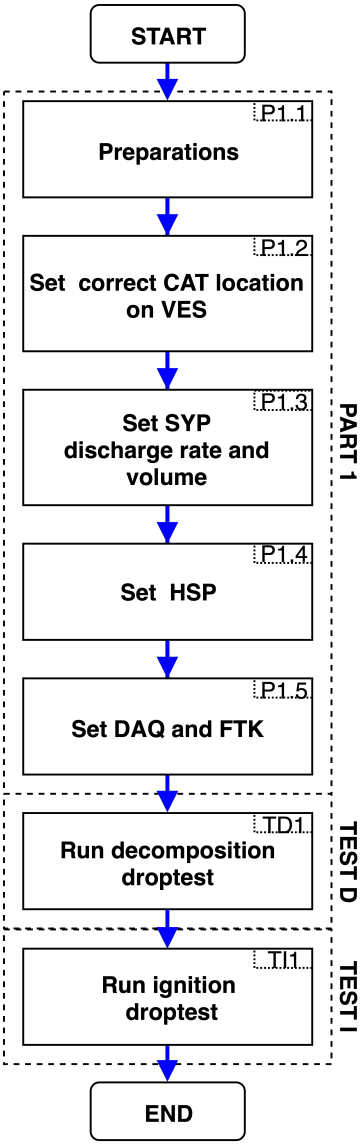

Figure B.1: High test level logic for full test campaign.

As it can be seen in Figure B.1, the test campaign will follow three parts. Part 1 covers the initial requirements to have the setup ready and working. Once these are covered, the tests can start for the decomposition of HTP and the data recorded. Once the decomposition is done, the ignition with EtOH follows. Using the same setup already prepared in part 1.

B.1.2. Preparations (P1.1)

The preparations prior to the start of the camping are the following.

Chemical preparation Given that for the tests HTP is used, its must be previously refined. For the tests the following concentrations are used as presented in Table B.2. For increasing HTP concentrations the preparation gets more complicated, as more feed stock is needed and low yield appear, so little sample were made for these. In the case of the EtOH, the chemical was readily available, so no preparations were made on it.

Decomposition		Ignition	
Concentration [% ±1%]	**Volume [mL]**	**Concentration [% ±1%]**	**Volume [mL]**
75	10	80	10
80	10	85	10
85	10	90	10
90	10	95	7
95	7	98*	5

Table B.2: Quantity of prepared HTP for the tests. (* this was only done for a 1-experiment tests and the results are not presented).

Programming the DAQ The data is acquired by means of a DAQ NI-9219 connected to the PC through an USB port. The DAQ is specific to work at a maximum of 60Hz for voltage input channels, such as for FTK. Nonetheless, the maximum possible frequency was set to 55Hz, as 60Hz was not possible to implement. The code was programmed in LabView which is the default controller for NI systems. The used software was LabView 2017 ran on Windows 10 on a i5 processor of 2.6GHz. The software can be found in **??**. The software was prepared to cover the following goals:

- To record k-type thermocouples reading at a reading rate of 55Hz.
- To allow for varied amount of thermocouple readings, choose between 3 and 4 thermocouples when FTK4 is used for ignition tests.
- To provide ON/OFF capability to write to file upon user clicking on it.
- To write to a .txt file solely the temperature of the used FTK.

B.1.3. Set correct CAT location on VES (P1.2)

The dropping of the chemicals onto the vessel is a delicate procedure. Given that the CAT are hanging at 17 cm distance from the VES, which has a narrow throat of about 2.5 cm, it is imperative to have a proper alignment. To check that the alignment is accurate, distilled after is loaded on both CAT, and drops are generated and the VES is moved as well as the support for the CAT. This iterative process is only finished once drops from CATE and CATH fall within the VES. Moreover, it is required that the drop coming from the CATH falls into contact with FTK1. By the naked eye this is challenging, thus the use of the HSC can be used in later stages to secure the dropping is perfect.

B.1.4. Set SYP discharge rate and volume (P1.3)

Within the facilities of the DASMl, two SYP were available. The SYPH is a syringe pump intended for normal syringes, with a large discharge rate and capacity for big syringes (model no. NE1000). Unfortunately, the other syringe pump, SYPE, is a syringe pump for application on micro syringes (model no. NE-1002X). This that SYPE will have normally slower discharge rates and it will be prepared for smaller syringes. SYRE and SYRH are the same size, 2 mL., consequently, the difference is discharge rate is a problem to deal with. For SYPE, the maximum discharge rate was used of 7.1 mL/min to have a fast dropping as possible in order to not waste recording time of the HSP. However, variations in the surface tension and gauge size of the injectors, in this case the CAT, affect how big the droplet will be before precipitating. Although this can be modeled theoretically, it is easier to test it and for this water cannot be used as the properties have a effect on it. Consequently, a small study is conducted to find the volume needed to pump to produce exactly one droplet for ethanol and HTP. The outcome can be found in Table B.3.

From it, it was decided to use a constant value of 0.13 mL for all HTP, as it would create one drop for all of the cases. The created drop will be smaller for lower concentrations, but the difference is below 10%. For EtOH the value found is 0.06 mL. This is in fact an important aspect about SYPE and SYPH. While SYPH was set to have a total volume to discharge of 0.13 mL at 7.1 mL/min, SYPE was too slow to set a finite volume to drop. Instead, a continuous flow of EtOH is set at a discharge rate of 571.2 μL/min, until one drop falls, which will have a volume of 0.06 mL, a constant value for the chemical. This eases the timing for the ignition study as it will be late introduced.

Chemical	1 drop volume [mL]
75%±1% HTP	0.12
80%±1% HTP	0.12
85%±1% HTP	0.12
90%±1% HTP	0.13
95%±1% HTP	0.13
EtOH	0.06

Table B.3: 1-drop volume from the CAT for different chemicals use.

Final SYP settings		
Item	Discharge rate [mL/min]	Volume [mL]
SYPH	7.1	0.13
SYPE	0.571	Manual stop

Table B.4: Settings for SYPH and SYPE.

B.1.5. Set HSP (P1.4)

Preparation of the HSP is more on a practical implementation level than physical. Photron has it sown software to control the high speed camera, this is the Photron FASTCAM Viewer (PFV), which was downloaded and implemented in the PC. It allows to control the camera recording start and the saved videos, as well as visualizing and saving from there. The program is only available for Windows environment and it was the reason why Windows environment was preferred for the development of this tests. Similarly, HSP only interfaces through Ethernet gigabit cable, thus a Ethernet to USB adapter is recommend to use. As with most Ethernet connections, it is necessary to configure the IP address of the camera to 192.168.0.1 or .2, and turn the firewall off. This process is tedious and not well explain in the instructions.

Once the HSP is ready to use, the lenses should be prepared to put into focus the bead of the thermocouple. This is the center of VES and the place where the droplets of HTP and EtOH will be falling. Familiarizing with the software is also recommended, it was found in the end that the recording speed at maximum resolution 1024x1024 px is 6400 fps. It was thus chosen. Moreover, it was also found that one video recorded at this speed can only save 3.1 s of video mounting to a total of 16 GB of data. This meant that the use of the HSP must be carefully selected. A summary of the final values can be seen in Table B.5

Property	Value
Speed [fps]	6400
Resolution [px]	1024x1024
Max. recording time [s]	3.14
Memory per video [GB]	32

Table B.5: Specifications of HSP for selected resolution and speed.

- table with final data

B.1.6. Set DAQ and FTK (P1.5)

The last step of the part 1 is to set the DAQ and the FTK to work correctly. This step aims at having the 4 thermocouples working properly, although for the decomposition test FTK4 is not required. Because FTK are unsheathed, they have no protection against voltage noise from the surroundings. To solve this problem, some insulation tape was place around it on the sides. With red marking the negative and blue marking the positive side. This prevents any conductive surface which is touching the FTK to not affect the reading coming from the temperature difference sensed in the bead. Moreover, FTK should not touch each other. The moment two FTK touch each other, or even two sides of the same FTK, the reading will be faulty. Generally, the response found in the PC from the reading is quite noisy, so it must be left to stabilize before proceeding. As a test, the heating plate was turned on to see variations in the readings and droplet of water were also precipitated to check on the decrease of temperature of FTK1.

To check whether the system complies with a low noise result. For each thermocouple the signal to noise ratio (SNR) is calculated for a total of 30 s of data points at room temperature as follows in Equation (B.1). An stringent limit value of 25 dB is chosen to represent a good signal and it is the minimum to proceed.

$$SNR_{dB} = 10 \cdot log_{10}\left(\frac{E[S^2]}{\sigma_N^2}\right) \tag{B.1}$$

Where SNR_{dB} [dB] is the SNR, an indicator of the level of noise, S [°C] is the value of the temperature signal, E[] is the expected value or average and σ_N^2 [°C^2] is the variance of the signal.

The result found on the tests is presented in Figure B.2, as the tabular data is significantly large (1650 points for 55Hz and 30s total). The final results are shown in Table B.6. As it can be seen, FTK 1 seems to be providing a more noisy result, however it still fits within the 25dB for a good signal. FTK2 is the clear example of a perfect FTK, this behavior is not attained in all FTK due to small imperfections such as unforeseen conductive surfaces touching, small particles present in the DAQ or even imperfections along the FTK.

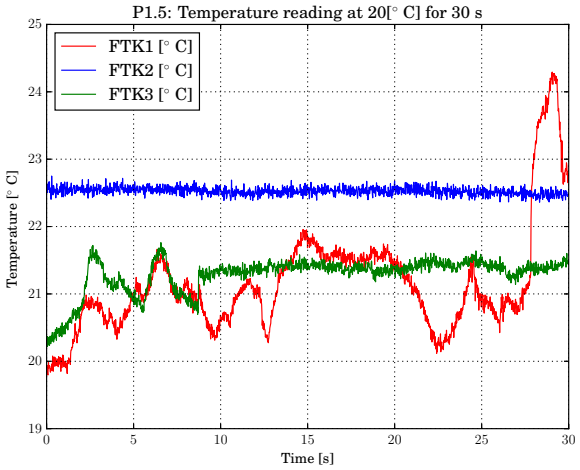

Figure B.2: Values of FTK1-3 for 30 s for a controlled environment of 20°C.

FTK	Mean [°C]	σ_N^2 [°C^2]	SNR [dB]
1	21.165	0.6541	28.355
2	22.526	0.003	51.92
3	21.283	0.0722	37.974

Table B.6: Results for initial test on P1.5.

B.1.7. Run decomposition tests (TD1)

The decomposition tests only require the use of HTP, as opposed to ignition where the EtOH is also used. The logic followed for the test can be seen in Figure B.3. This logic is the same followed for the ignition tests, with the difference that the procedures per step may vary. Subsequently, the steps will be briefly discussed and for each a procedure matrix is used, as presented in Appendix B.2.1. Moreover, the test combination order is presented in Table B.7. With this test matrix to follow, one question should come clear for the experimentation:

- Does that particular combination of HTP and temperature achieve decomposition?

Based on the answer to this question, the test matrix for the ignition study is prepared. Only successful combination of concentration and temperature are used for the ignition studies.

Table B.7: Order of test to do for decomposition. Based on the results of the decomposition, the ignition order follows.

T [°C±10 °C]	Conc [%±1%]	75	80	85	90	95
50		1	7	13	19	28
100		2	8	14	20	29
150		3	9	15	21	30
200		4	10	16	25	31
250		5	11	17	26	32
300		6	12	18	27	33

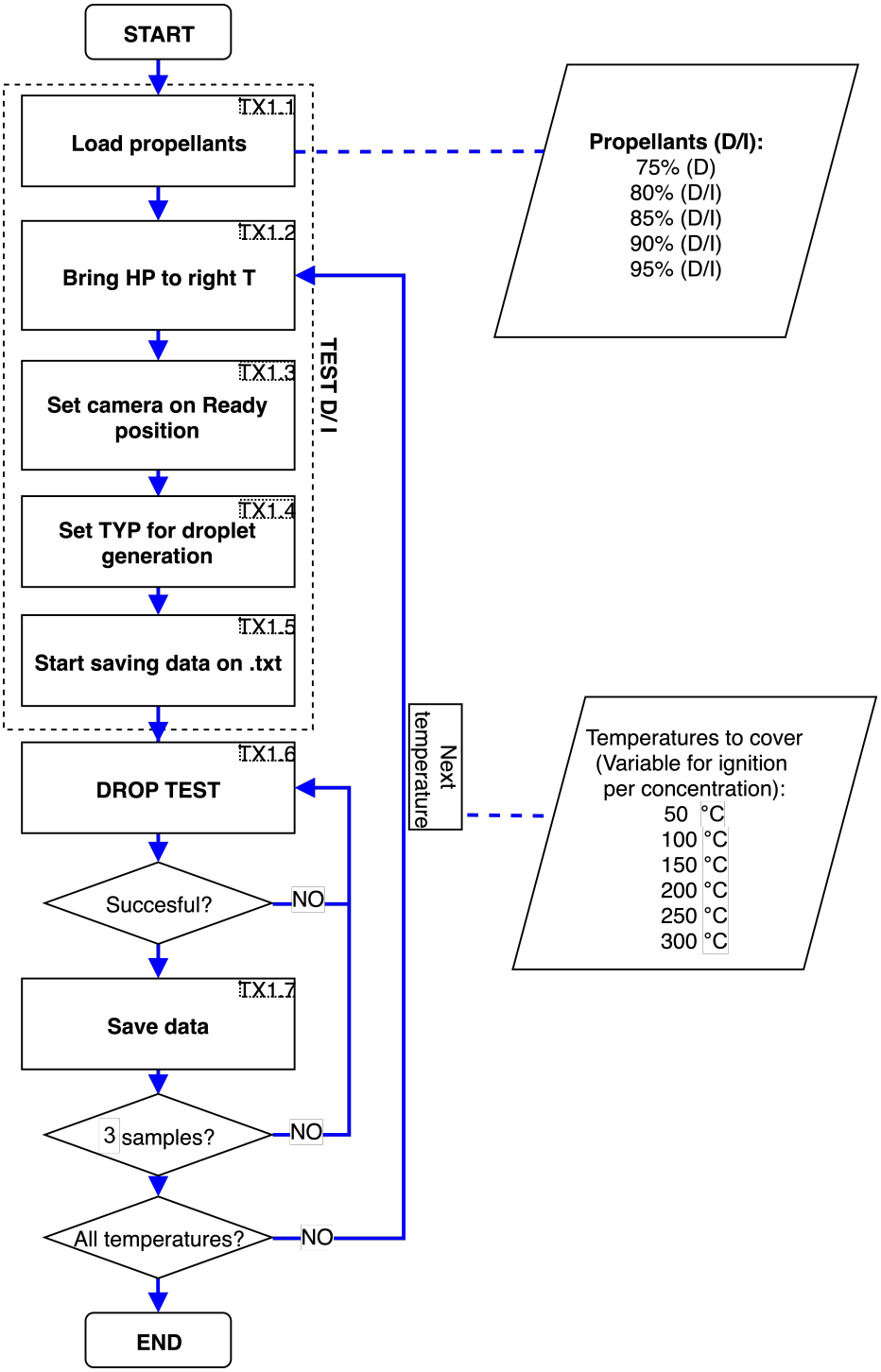

Figure B.3: Test logic for decomposition and ignition tests. Steps are the same, but the procedures vary per type of test: decomposition/ignition. Propellants and temperatures used also vary as a result of what is found in decomposition tests. The nomenclature TX refers to adaptable TD (decomposition) and TI (ignition).

Load propellants (TD1.1) Only HTP is used in this case. The concentrations were chosen to be from 75 to 95% in steps of 5%. The minimum level of 75% is chosen based on the findings in Section 4.1.2, as it would provide sufficient heat to auto ignite EtOH, as it is desired for the bipropellant ignition case. The maximum level of 95% was chosen as a realistic maximum attainable, as 100% HTP was never achieved and more concentrated samples decayed faster in time. As previously stated an error in the concentration of 1% is a valid margin for this values, as the error coming form the AR is only of 0.2%. The extra 0.8% is there for buffer

as selecting the exact concentration may sometimes be difficult. Refer to Table B.9 for the test procedure.

To load the HTP, the already prepared samples have to be withdrawn into the CATH with the help of the SYPH. For this, an amount in excess of 2 mL is normally withdrawn.

Bring HP to the right T (TD1.2) The Hp available is an old piece of equipment and unfortunately, it does not have feedback to be used, thus the temperature set is a really heuristic approach. To correct for this, the FTK1 is the indicator used for Hp characterization. It is in fact the temperature the Hp will feel when it is precipitated. The value of temperature is hard to set, thus an error margin of ±10 °Cis used for all experiments. It is varied in steps of 50°Cfrom 50 to around 300 °C, although 300 °Cas really never achieved due to instrument limitations. Refer to Table B.10 for the test procedure.

Set camera on Ready position (TD1.3) This step is necessary to assure a correct timing of the droplet generation and recording of the HSP. The software eof the HSP, PFV, has a 2-layer safety mechanism for filming. First, the camera must be armed to the ready position, then one click on the "Film" button will start the recording. Refer to Table B.11 for the test procedure.

Set SYPH to generate droplets (TD1.4) This step ensures the SYPH is prepared for generating the HTP droplet at the right volume (0.13 mL) and with the right discharge rate (7.1 mL/min). It should be in the "PUMP" mode. It should also be accessible, as the clicking button must be actioned by a human. Care must be taken when using the SYPH, as it shall not be mixed with the SYPE, as it could result in decrease of HTP concentration. Refer to Table B.12 for the test procedure.

Start saving data on .txt (PD1.5) This step ensures the recording of temperature data from the FTK is checked before proceeding further. Equally, the identifier must be put into place before starting to save data to the .txt file. The identifier is as follows:

$$\text{Tm-DDMM-CC-SAMPLE-TTT-i.txt} \tag{B.2}$$

Where Tm stands for Temperature measurement, DDMM is the day and month of the recording, CC is the concentration of the sample use [%], SAMPLE is the internal name given to the refined sample, TTT is the temperature target [°C] and i is the trial number. The sample name are only internally used for logistic purposes and generally include nomenclature in terms of TEST-Number (T-Number) or OXIDIZER-Number (O-Number). This identifier must be set before starting to save data and has to be set in the LabView environment. Refer to Table B.13 for the test procedure.

DROP TEST (TD1.6) Once steps TD1.1 - TD1.5 are covered, as well as their procedures. The drop test can be started. This step encompasses the dropping and correct timing of the HTP onto the heated VES. This procedure requires of two scientists. Coordination is required between the scientist behind the computer and the scientist pressing the SYPH. Refer to Table B.10 for the exact test procedure.

The success of the drop is dictated by the fact that it decomposed, it was filmed and it was recorded with the FTK. This means, that those droplets that did not decompose will not be saved. They will be reviewed in search of faults that may have played a role, but if there were none, the video will not be saved. The DAQ data is always saved regardless, given its low file weight.

Save data (TD1.7) Once the resulting video and data is proved to be valid/sucessful. This is, there is a decomposition going on and it was filmed within the 3 seconds of the HSP. Then the file can be atored. It is recommended to crop the video to the only frames where the droplet precipitates and decomposes, also crop the size of the image to only the vessel. This ways, the weight of the data file from the HSP can be significantly reduced making the data transfer faster.The identifier used for the files of the HSP is as follows:

$$\text{HSPC-DDMM-CC-SAMPLE-TTT-i.bmp} \tag{B.3}$$

Where HSPC stands for high speed camera, DDMM is the day and month, CC is the concentration of the HTP [%], SAMPLE is the names given internally to the samples of HTP and TTT is the temperature used for that video. If the video is not valid, it can be discarded.

B.1.8. Ignition tests

Once the decomposition test campaign is over, the ignition test campaign can start. As opposed to the decomposition, in the ignition tests, the use of 100% EtOH is used. The logic followed for the test can be seen in Figure B.3. This logic is the same followed for the decomposition tests, with the difference that the procedures per step may vary. Subsequently, the steps will be briefly discussed and for each a procedure matrix is used, as presented in Appendix B.2.2. Moreover, the test combination order is presented in Table B.8. For the ignition cases, only the successful combinations of the decomposition case are explored. As it was found, no concentration of HTP decomposed under 200 °C, equally, the concentration of 75% did not decompose at any temperature. Likewise, the combination of 80% and 200°C, did not ignite in any of the minimum 3 experiments carried leading to the following test order, Table B.8.

T [°C±10°C]	Conc [%±%]	80	85	90	95
200		X	3	6	9
250		1	4	7	10
300		2	5	8	11

Table B.8: Order for the tests of the ignition campaign.

Load propellants (PI1.1) Similarly to the decomposition case, the propellants must be loaded into the CATH and CATE. For this, the process is the same, except that EtOH should be loaded in first. Once EtOH is loaded into the CATE, then HTP can be loaded at the required concentration. EtOH can be loaded in large quantities, exceeding the marked 2 mL of the syringe. EtOH does not decompose, so it can be placed without any problems. As expressed previously, the minimum concentration of HTP used is 80%. Also, the ranges of valid concentration lay again within the ±1%. For it, a total of 2 mL is normally withdrawn for the specific test.

Bring HP to the right T (TI1.2) Using FKT1, the temperature is set on the HP. The value of temperature is hard to set as previously mentioned, thus an error margin of ±10 °Cis used for all experiments. It is varied in steps of 50°Cfrom the minimum temperature of decomposition, 150°Cfor 85% and 200°Cfor 80% to around 300 °C, although 300 °Cas really never achieved due to instrument limitations. Refer to Table B.10 for the test procedure.

Set camera on Ready position (TI1.3) This step is the same as for PD1.3.

Set SYPH to generate droplets (TI1.4) This step ensures the SYPH and SYPE are prepared for generating the HTP/EtOH droplets at the right volume, 0.13 mL for HTP and 0.06 mL for EtOH, and with the right discharge rate 7.1 mL/min for HTP and 0.571 mL/min for EtOH. They should be in the "PUMP" mode. They should both be close to each other and accessible for the scientist to press the buttons and perform the timing. Care must be taken when using the SYPH, as it shall not be mixed with the SYPE, as it could result in decrease of HTP concentration. Refer to Table B.16 for the test procedure.

Start saving data on .txt (PI1.5) This step is the same as in PD1.5 with a slight variation on the identifier and the addition of FTK4. The identifier for the ignition case is as follows:

$$\text{Tm-DDMM-OF-CC-SAMPLE-TTT-i.txt} \tag{B.4}$$

Where Tm stands for Temperature measurement, DDMM is the day and month of the recording, OF stands for OxidizerFuel, CC is the concentration of the sample use [%], SAMPLE is the internal name given to the refined sample, TTT is the temperature target [°C] and i is the trial number. The sample name are only internally used for logistic purposes and generally include nomenclature in terms of TEST-Number (T-Number) or OXIDIZER-Number (O-Number). This identifier must be set before starting to save data and has to be set in the LabView environment. Refer to Table B.17 for the test procedure.

DROP TEST (TI1.6) Once steps TI1.1 - TI1.5 are covered, as well as their procedures. The drop test can be started. This step has an extra layer of complication as two droplets have to be generated and timed manually. It is imperative that the HTP falls in first, as this is used for the definition of IDT. In order to time it, the SYPE must be switched on and pumping while having the hand prepared to click on SYPH at any moment. When the EtOH droplet is forming from the CATE, the SYPH must be activated and the difference in time between droplets should be such that HTP does not decompose prior to EtOH falling in. Coordination from the side of the scientist working with the SYP is need, also communication is required with the scientist behind the computer in order to film from the moment the first droplet starts to precipitate. As it can be anticipated, the repeatibility is a complex case scenario. Consequently, the dimension of time difference between droplets is also recorded by the HSP. Refer to Table B.18 for the exact test procedure.

An important disclaimer prior to the experiment is that special caution is taken in the case that EtOH falls in first, or int he case that several droplets of EtOH fall in first. The problem is that the volatility of EtOH will make the fuel almost instantly to evaporate, filling the vessel with gaseous EtOH. Once the autoignition temperature is achieved, the gas will instantaneously ignite and this can lead to explosion, serious bang noise and possible rupture of the VES. IN the case that the EtOH falls in first. HTP shall not be precipitated and instead, purging to he VES is recommended.

The success of the ignition in this case is defined as the scenario where the HTP falls in first, but does not decompose before EtOH comes into contact with it. Then if the ignition takes place the video is saved. The data is not saved if the ignition does not take place. These non-ignited scenarios will be reviewed to find any faults. The measurements form the FTK will be saved in any case.

Save data (TI1.7) Once the resulting video and data is proved to be valid/sucessful, the file can be stored. It is recommended to crop the video to the only frames where the droplets precipitate and ignition happens. Also crop the size of the image to only the vessel. This ways, the weight of the data file from the HSP can be significantly reduced making the data transfer faster.The identifier used for the files of the HSP is as follows:

$$\text{HSPC-DDMM-OF-CC-SAMPLE-TTT-i.bmp} \tag{B.5}$$

Where HSPC stands for high speed camera, DDMM is the day and month, OF stands for OxidizerFuel, CC is the concentration of the HTP [%], SAMPLE is the names given internally to the samples of HTP and TTT is the temperature used for that video. If the video is not valid, it can be discarded.

B.2. Test procedures templates

In this section, the tests procedures for the decomposition tests, ignition tests and safety flushing of the system are presented. The decomposition and ignition procedures are quite similar, with the difference of the addition of a second chemical. The flushing procedure includes a simple procedure for he flushing of the system when needed for safety purposes purposes.

B.2.1. Decomposition tests

As presented in Figure B.3, this subsection encompasses the test procedures for the decomposition side of the experiments in an orderly manner.

Step	Action	Criteria	Remarks	X
	TD1.1 LOAD PROPELLANTS			
1	Empty the fluids in CATH if any			
2	Prepare the HTP to be withdrawn		At concentration: [%]	
3	Check the SYPH is in withdrawn mode	Y/N		
XX			Answer must be yes, otherwise correct	
4	Select 2 mL to withdraw			
5	Proceed to withdraw with the CATH immersed in the HTP sample		Withdraw until 2mL or the HTP runs out	
XX	END OF LOADING PROPELLANTS PROCEDURE			

Table B.9: Procedure for TD1.1 Loading propellants.

Step	Action	Criteria	Remarks	X
	TD1.2 BRING HP TO RIGHT TEMPERATURE			
1	Turn HP on and connect the FTK		FTK 1 minimum	
2	Bring knob to similar temperature as desired		Slightly over the mark in the HP	
3	Wait for HP to heat up and for the heating indicator light to go off			
4	Check if T is within 10°C from required temperature	Y/N		
XX			Answer must be yes, otherwise correct on step 2	
XX	END OF HEATING PLATE PREPARATION PROCEDURE			

Table B.10: Procedure for TD1.2 Preparation of heating plate.

Step	Action	Criteria	Remarks	X
	TD1.3 SET HSP ON RIGHT POSITION			
1	Connect ethernet adaptor to PC and turn camera ON			
2	Start PFV software and assure camera is recognised in PC		Refer back to P1.4	
3	Is the camera recognised and properly connected	Y/N		
XX			Answer must be yes, otherwise refer to P1.4	
4	Select recording at 6400 fps			
5	Is the focus and the light sufficient	Y/N		
XX			Answer must be yes, otherwise correct	
6	Set camera on READY option in the FPV filling tab			
XX	END OF HSP PREPARATION PROCEDURE			

Table B.11: Procedure for TD1.3 Set HSP on ready position.

Step	Action	Criteria	Remarks	X
	TD1.4 SET TYPH FOR DROPLET GENERATION			
1	Connect SYPH to the power			
2	Are SYR and tubing in place?	Y/N		
XX			Answer must be yes, otherwise correct	
3	Set SYPH to discharge mode and to correct volume		Rate: 7.1 mL/min Volume: 0.13 mL	
4	Put a cloth under the CATH			
5	Is the SYPH generation one droplet when activated?	Y/N		
XX			Answer must be yes, otherwise correct	
6	Remove cloth			
XX	END OF TYPH FOR DROPLET GENERATION			

Table B.12: Procedure for TD1.4 Droplet generation from SYPH.

Step	Action	Criteria	Remarks	X
	TD1.5 DATA SAVING .TXT PROCEDURE			
1	Connect DAQ to PC via USB			
2	Start LabView and start task of data collection			
3	Are the FTK1-3 properly placed in VES?	Y/N	FTK1 - Touching bottom FTK2 - 3 mm FTK3 - 6 mm	
XX			Answer must be yes, otherwise correct	
4	Is the task/code selected running at 55Hz and for the required FTK?	Y/N	Decomposition is FTK1, FTK2 and FTK3	
XX			Answer must be yes, otherwise correct	
5	Input ID name on file title		Refer to PD1.5 explanation	
6	Click on saving			
XX	END OF DATA SAVING ON .TXT PROCEDURE			

Table B.13: Procedure for TD1.5 data saving on .txt files.

Step	Action	Criteria	Remarks	X
	TD1.6 DROPTEST PROCEDURE			
1	Are procedures TD1.1-TD1.5 correctly covered?	Y/N		
XX			Answer must be yes, otherwise go back to them	
2	Place scientist close to SYPH			
3	Scientist behind the computer gives first OK			
4	Scientist close to SYPH starts countdown from 3			
5	On 0, SPH is activated and the HSP is activated to film			
XX	END OF DROPTEST PROCEDURE			

Table B.14: Procedure for TD1.6 Drop test.

B.2.2. Ignition tests procedures

Step	Action	Criteria	Remarks	X
	TI1.1 LOAD PROPELLANTS			
1	Empty the fluids in CATH and CATE if any			
2	Prepare EtOH to be withdrawn			
3	Check the SYPE is in withdrawn mode	Y/N		
XX			Aswer must be yes, otherwise correct	
4	Select 3 mL to withdraw			
5	Proceed to withdraw with the CATE immersed in the EtOH		Withdraw until 3mL	
6	Prepare HTP to be withdrawn		At concentration: [%]	
7	Is the SYPH in withdrawing mode	Y/N		
XX			Answer must be yes, otherwise correct	
8	Select 2 mL to withdraw			
9	Proceed ti withdraw with CATH immersed in the HTP			
XX	END OF LOADING PROPELLANTS PROCEDURE			

Table B.15: Procedure for TI1.1 Loading propellants.

Step	Action	Criteria	Remarks	X
	TI1.4 SET TYPH/TYPE FOR DROPLET GENERATION			
1	Connect SYPH/SYPE to the power			
2	Are the SYR and tubing in place?	Y/N		
XX			Aswer must be yes, otherwise correct	
3	Set SYPH and SYPE to discharge mode and correct volume		Refer to Table B.4	
4	Put a cloth under the CATE and CATH			
5	Is the SYPH/SYPE generation 1 droplet when activated?	Y/N		
XX			Answer must be yes, otherwise correct	
6	Remove cloth			
XX	END OF SET TYPH/TYPE FOR DROPLET GENERATION PROCEDURE			

Table B.16: Procedure for TI1.4 Droplet generation from SYPH and SYPE.

Step	Action	Criteria	Remarks	X
	TI1.5 DATA SAVING .TXT PROCEDURE			
1	Connect DAQ to PC via USB			
2	Start LabView and start task of data collection			
3	Are the FTK1-4 properly placed in VES?	Y/N	FTK1 - Touching bottom FTK2 - 3 mm FTK3 - 6 mm FTK4 - throat	
XX			Answer must be yes, otherwise correct	
4	Is the task/code selected running at 55Hz and for the required FTK?	Y/N	All FTK are required	
XX			Answer must be yes, otherwise correct	
5	Input ID name on file title		Refer to PI1.5 explanation	
6	Click on saving			
XX	END OF DATA SAVING ON .TXT PROCEDURE			

Table B.17: Procedure for TI1.5 data saving on .txt files.

Step	Action	Criteria	Remarks	X
	TI1.6 DROPTEST PROCEDURE			
1	Are procedures TI1.1-TI1.5 correctly covered?	Y/N	TI1.2 is TD1.2 TI1.3 is TD1.3	
XX			Answer must be yes, otherwise go back to them	
2	Place scientist close to SYPH/SYPE			
3	Scientist behind the computer gives first OK			
4	Scientist close to SYPH/SYPE starts countdown from 3			
5	On 0, scientist close to SYPH/SYPE starts SYPE and prepares to click SYPH			
6	When EtOH is forming from CATE, click on SYPH and notify scientist at PC		Timing is key, practice is needed to time well	
7	On 0, SPH is activated and the HSP is activated to film			
XX	END OF DROPTEST PROCEDURE			

Table B.18: Procedure for TI1.6 Drop test.

B.2.3. Flushing procedure

Step	Action	Criteria	Remarks	X
	FLUSHING THE VES PROCEDURE			
1	Is the experiment stopped?	Y/N		
XX			Answer must be yes, otherwise go back to them	
2	Stat the flow of N2 on the knob			
3	Direct the hose of N2 to the VES from on top		Care must be taken with CATE and CATH	
4	Leave the flow for at least 30 s		Regulate the flow as needed	
5	Close the flow of N2			
XX	END OF FLUSHING PROCEDURE			

Table B.19: Procedure for flushing the vessel with purged nitrogen.

B.3. Safety overview

In this section, the overview of the safety features to bear into account when performing the experiment are presented. The use safety is paramount and in line with the requirement for working in the Chemical lab facilities of the DASML. For this two safety tours were taken, one for safety in DASML and one for safety in the chemical lab. The need of sfaety must be present at all times during and prior to the experiment as well as the post-handling. The safety regarding the ethanol Appendix B.3.1, HTP Appendix B.3.2 and the decomposition with the HP Appendix B.3.3 are hereby provided.

B.3.1. Ethanol handling

- The use of protective clothes is necessary when working with ethanol. The protection includes gloves, lab coat and goggles.
- The experiments must take place inside the fumehood.
- The handling of ethanol must take place in a separated are in the lab as HTP.
- Only designated new syringes must be used. No reusing of syringes for ethanol handling in allowed.
- Ethanol should only be stored in a dry, cool and well-ventilated place.
- A large enough water barrel should be close to he ethanol in case dilution is need for any spillage.
- A medical kit should be available in the vicinity of the experiment.
- Safety showers and access to running water should be in the vicinity of the experiment.
- In case of accidental ignition, access to a fire extinguisher is needed.
- A telephone should be available at all times with the number of the internal safety of the TUDelft.
- 2 scientist are required at all times when working with ethanol.

B.3.2. HTP handling

- The use of protective clothes is strictly necessary when working with HTP. The protection includes gloves, lab coat and goggles. HTP causes a deep itching sensation if it falls on skin and can cause severe damage tot he eyes as well.
- The experiments must take place inside the fumehood.
- The handling of HTP must take place in a separated are in the lab as ethanol. Also no foreign particles should be available nearby, for this the fumehood makes the perfect place to work with HTP.
- It is not recommended to wear leather when working with HTP, as a simple spill can easily cause a fire.

- Only designated new syringes must be used. No reusing of syringes for HTP handling in allowed. Thus a new syringe and needle must be used when working with HTP.
- HTP should only be stored in an isolated, dry, cool, inaccessible and well-ventilated place. The fumehood is the best location.
- A large enough water barrel should be close to he ethanol in case dilution is need for any spillage.
- A medical kit should be available in the vicinity of the experiment.
- Safety showers and access to running water should be in the vicinity of the experiment.
- In case of accidental ignition, access to a fire extinguisher is needed.
- A telephone should be available at all times with the number of the internal safety of the TUDelft.
- 2 scientist are required at all times when working with HTP.

B.3.3. HP handling

- The heating plate must always be handled with heat gloves, even when it is turned on as it might still be hot from before.
- When performing the drop test experiments, whenever ethanol falls on the heating plate first, extra attention must be paid as gaseous ethanol is easily explosive. It must be purged if this happens.
- The use of the safety glass screen of the fumehood must always be down. The ignition of EtOH with HTP may break the VES and result in small glass particles.
- For the drop tests on the heating plate, the use of ear plugs is recommended, as the noise may get high.
- A medical kit should be available in the vicinity of the experiment.
- Care must be taken with the heating plate as it is an old piece of equipment, so it may give small electroshocks, based on previous experiences.
- In case of accidental ignition, access to a fire extinguisher is needed and the power must be cut off from the entire set of electrical apparatus.
- A telephone should be available at all times with the number of the internal safety of the TUDelft.
- 2 scientist are required at all times when working with HTP.

C

Instrumentation specification sheets and images

In this chapter, images of the instruments are provided in Appendix C.1. Also the material safety data sheets (MSDS) are provided for different used chemicals. For 30% H_2O_2 in Appendix C.2, for 90% H_2O_2 in Appendix C.3 and for ethanol in Appendix C.4. Moreover, the specification sheet for the high speed camera used in this research is also given for the reader to find its capabilities in Appendix C.5.

C.1. Instrumentation images

In this section, a few images of the process and the instruments used are presented.

Figure C.1: A- Fumehood used for the tests at the Chemical lab of the DASML. B- Lighting system for high speed camera. C-Syringe pump used for drop-test experiments

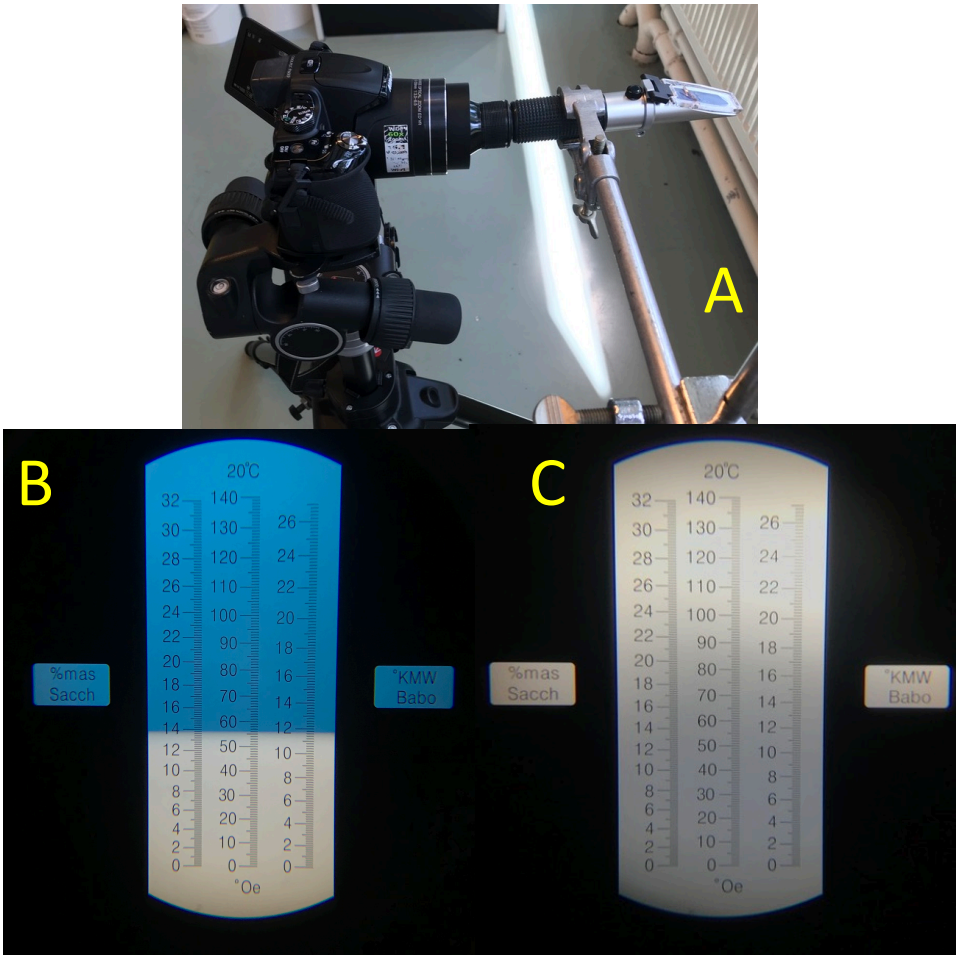

Figure C.2: A-Hand-held refractometer attached to camera to read off the result. B-Measurement for 30% H_2O_2 through the handheld refractometer, around 13 Brix. C- First time refining system worked and result was out of scale in handheld refractometer, meaning the concentration was over 70%.

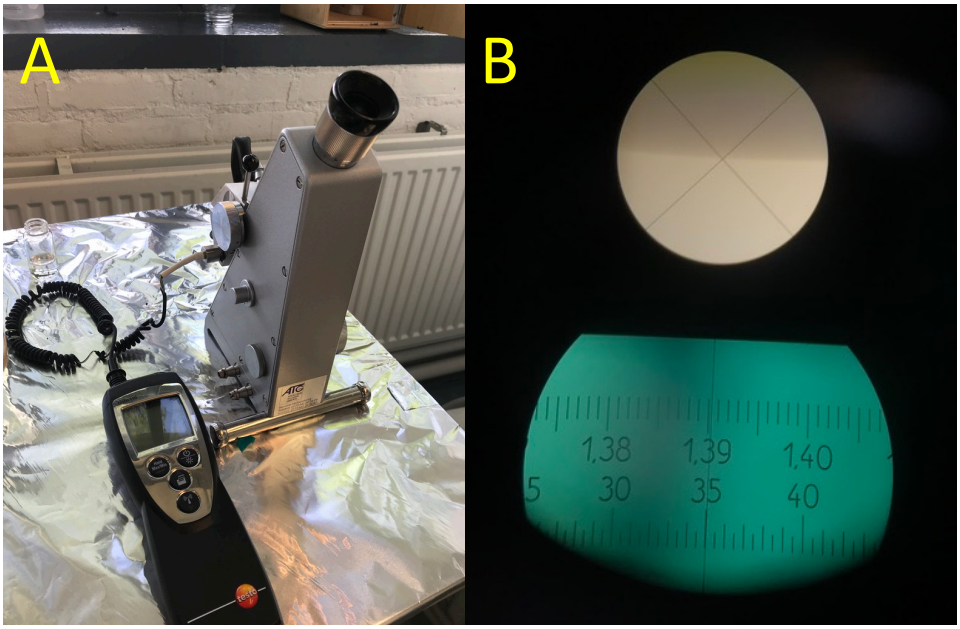

Figure C.3: A-Abbe refractometer with its thermometer attached. B-Reading inside the refractometer, in this case measuring 79% HTP.

Figure C.4: A-Parent propellant at 30% H_2O_2 from Merck. B-Accidental spill of highly concentrated H_2O_2 on finger, leaves white coloring and needle-like sensation. Dissipates in minutes and leaves no consequences.

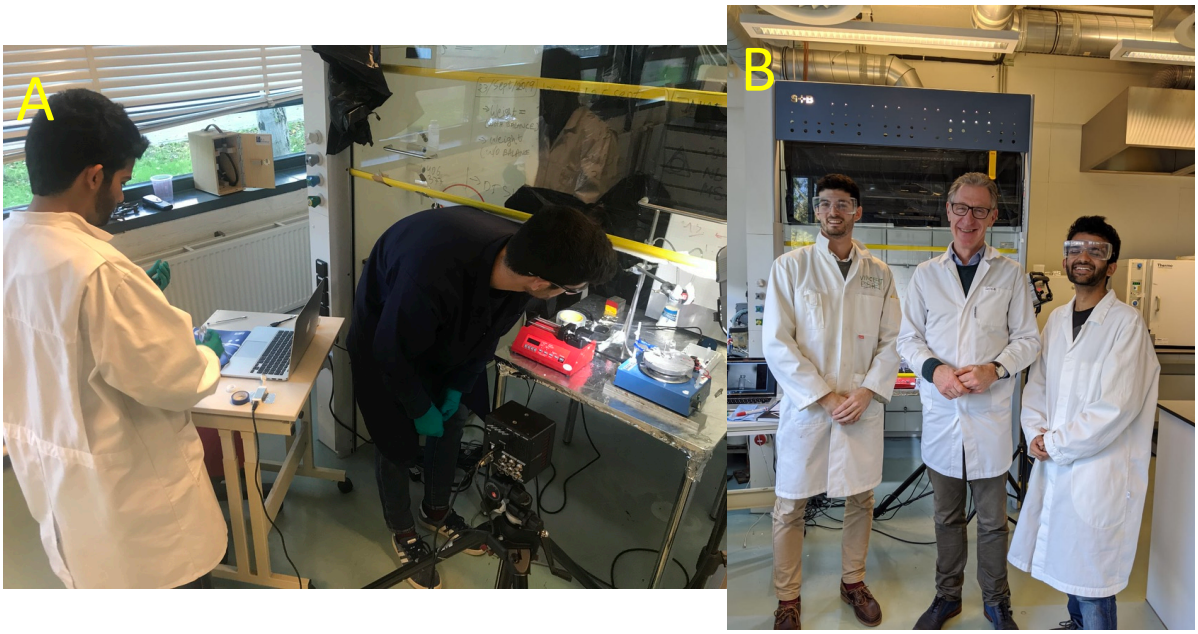

Figure C.5: A-Pranav and I working on setting an ignition drop test study. B-Visit of the Dean of Aerospace Engineering dr. Henry Werij to our research stand.

C.2. Material Safety Data Sheet of 30% H_2O_2

Here the material safety data sheet of the purchased hydrogen peroxide at 30% from Merck / Sigma Aldrich is presented.

SAFETY DATA SHEET

according to Regulation (EC) No. 1907/2006

Revision Date 17.07.2017 Version 19.2

SECTION 1. Identification of the substance/mixture and of the company/undertaking

1.1 Product identifier

Catalogue No.	107209
Product name	Hydrogen peroxide 30% (Perhydrol®) for analysis EMSURE® ISO
REACH Registration Number	This product is a mixture. REACH Registration Number see section 3.

1.2 Relevant identified uses of the substance or mixture and uses advised against

Identified uses	Reagent for analysis In compliance with the conditions described in the annex to this safety data sheet.

1.3 Details of the supplier of the safety data sheet

Company	Merck KGaA * 64271 Darmstadt * Germany * Phone:+49 6151 72-0
Responsible Department	LS-QHC * e-mail: prodsafe@merckgroup.com

1.4 Emergency telephone number **Please contact the regional company representation in your country.**

SECTION 2. Hazards identification

2.1 Classification of the substance or mixture

Classification (REGULATION (EC) No 1272/2008)

Acute toxicity, Category 4, Oral, H302
Serious eye damage, Category 1, H318
Chronic aquatic toxicity, Category 4, H413

For the full text of the H-Statements mentioned in this Section, see Section 16.

SAFETY DATA SHEET

according to Regulation (EC) No. 1907/2006

Catalogue No.	107209
Product name	Hydrogen peroxide 30% (Perhydrol®) for analysis EMSURE® ISO

2.2 Label elements

Labelling (REGULATION (EC) No 1272/2008)

Hazard pictograms

Signal word

Danger

Hazard statements

H302 Harmful if swallowed.

H318 Causes serious eye damage.

H413 May cause long lasting harmful effects to aquatic life.

Precautionary statements

Prevention

P273 Avoid release to the environment.

P280 Wear eye protection.

Response

P305 + P351 + P338 IF IN EYES: Rinse cautiously with water for several minutes. Remove contact lenses, if present and easy to do. Continue rinsing.

P313 Get medical advice/ attention.

Reduced labelling (≤125 ml)

Hazard pictograms

Signal word

Danger

Hazard statements

H318 Causes serious eye damage.

H413 May cause long lasting harmful effects to aquatic life.

SAFETY DATA SHEET

according to Regulation (EC) No. 1907/2006

Catalogue No.	107209
Product name	Hydrogen peroxide 30% (Perhydrol®) for analysis EMSURE® ISO

Precautionary statements
P280 Wear eye protection.
P305 + P351 + P338 IF IN EYES: Rinse cautiously with water for several minutes. Remove contact lenses, if present and easy to do. Continue rinsing.
P313 Get medical advice/ attention.

Contains: Hydrogen Peroxide

2.3 Other hazards

None known.

SECTION 3. Composition/information on ingredients

Chemical nature Aqueous solution

3.1 Substance

Not applicable

3.2 Mixture

Hazardous components (REGULATION (EC) No 1272/2008)

Chemical name (Concentration)

CAS-No.	Registration number	Classification
Hydrogen Peroxide *(>= 25 % - < 35 %)*		
Substance does not meet the criteria for PBT or vPvB according to Regulation (EC) No 1907/2006, Annex XIII.		
7722-84-1	01-2119485845-22-XXXX	Oxidizing liquid, Category 1, H271
		Acute toxicity, Category 4, H302
		Acute toxicity, Category 4, H332
		Skin corrosion, Category 1A, H314
		Specific target organ toxicity - single exposure, Category 3, H335
		Chronic aquatic toxicity, Category 3, H412

For the full text of the H-Statements mentioned in this Section, see Section 16.

SAFETY DATA SHEET

according to Regulation (EC) No. 1907/2006

Catalogue No.	107209
Product name	Hydrogen peroxide 30% (Perhydrol®) for analysis EMSURE® ISO

SECTION 4. First aid measures

4.1 Description of first aid measures

After inhalation: fresh air.

In case of skin contact: Take off immediately all contaminated clothing. Rinse skin with water/ shower.

After eye contact: rinse out with plenty of water. Immediately call in ophthalmologist. Remove contact lenses.

After swallowing: immediately make victim drink water (two glasses at most). Consult a physician.

4.2 Most important symptoms and effects, both acute and delayed

Dizziness, Unconsciousness, Diarrhoea, Nausea, Vomiting, Headache, Convulsions, muscle twitching, insomnia, shock, Irritation and corrosion, conjunctivitis
Risk of serious damage to eyes.

4.3 Indication of any immediate medical attention and special treatment needed

No information available.

SECTION 5. Firefighting measures

5.1 Extinguishing media

Suitable extinguishing media

Use extinguishing measures that are appropriate to local circumstances and the surrounding environment.

Unsuitable extinguishing media

For this substance/mixture no limitations of extinguishing agents are given.

5.2 Special hazards arising from the substance or mixture

Not combustible.
Ambient fire may liberate hazardous vapours.
Has a fire-promoting effect due to release of oxygen.

SAFETY DATA SHEET

according to Regulation (EC) No. 1907/2006

Catalogue No.	107209
Product name	Hydrogen peroxide 30% (Perhydrol®) for analysis EMSURE® ISO

5.3 Advice for firefighters

Special protective equipment for firefighters

Stay in danger area only with self-contained breathing apparatus. Prevent skin contact by keeping a safe distance or by wearing suitable protective clothing.

Further information

Prevent fire extinguishing water from contaminating surface water or the ground water system.

SECTION 6. Accidental release measures

6.1 Personal precautions, protective equipment and emergency procedures

Advice for non-emergency personnel: Do not breathe vapours, aerosols. Avoid substance contact. Ensure adequate ventilation. Evacuate the danger area, observe emergency procedures, consult an expert.

Advice for emergency responders: Protective equipment see section 8.

6.2 Environmental precautions

Do not empty into drains.

6.3 Methods and materials for containment and cleaning up

Cover drains. Collect, bind, and pump off spills.
Observe possible material restrictions (see sections 7 and 10).
Take up with liquid-absorbent and neutralising material (e.g. Chemizorb® H^+, Merck Art. No. 101595). Dispose of properly. Clean up affected area.

6.4 Reference to other sections

Indications about waste treatment see section 13.

SECTION 7. Handling and storage

7.1 Precautions for safe handling

Advice on safe handling

Observe label precautions.

Hygiene measures

Immediately change contaminated clothing. Apply preventive skin protection. Wash hands and face after working with substance.

7.2 Conditions for safe storage, including any incompatibilities

Requirements for storage areas and containers

Close containers in such a way to enable internal pressure to escape (e.g. excess pressure valve).

No metal containers.

Storage conditions

Tightly closed. Protected from light. Do not store near combustible materials.

Recommended storage temperature see product label.

7.3 Specific end use(s)

See exposure scenario in the Annex to this MSDS.

SECTION 8. Exposure controls/personal protection

8.1 Control parameters

Derived No Effect Level (DNEL)

Hydrogen Peroxide (7722-84-1)

Worker DNEL, acute	Local effects	inhalation	3 mg/m³
Worker DNEL, longterm	Local effects	inhalation	1,4 mg/m³
Consumer DNEL, acute	Local effects	inhalation	1,93 mg/m³
Consumer DNEL, longterm	Local effects	inhalation	0,21 mg/m³

Predicted No Effect Concentration (PNEC)

Hydrogen Peroxide (7722-84-1)

PNEC Fresh water	0,0126 mg/l
PNEC Marine water	0,0126 mg/l

SAFETY DATA SHEET

according to Regulation (EC) No. 1907/2006

Catalogue No.	107209
Product name	Hydrogen peroxide 30% (Perhydrol®) for analysis EMSURE® ISO

PNEC Aquatic intermittent release	0,0138 mg/l
PNEC Sewage treatment plant	4,66 mg/l
PNEC Fresh water sediment	0,47 mg/kg
PNEC Marine sediment	0,47 mg/kg
PNEC Soil	0,0023 mg/kg

8.2 Exposure controls

Engineering measures

Technical measures and appropriate working operations should be given priority over the use of personal protective equipment.

See section 7.1.

Individual protection measures

Protective clothing needs to be selected specifically for the workplace, depending on concentrations and quantities of the hazardous substances handled. The chemical resistance of the protective equipment should be enquired at the respective supplier.

Eye/face protection

Tightly fitting safety goggles

Hand protection

full contact:

Glove material:	natural latex
Glove thickness:	0,6 mm
Break through time:	> 480 min

splash contact:

Glove material:	Nitrile rubber
Glove thickness:	0,11 mm
Break through time:	> 480 min

SAFETY DATA SHEET

according to Regulation (EC) No. 1907/2006

Catalogue No.	107209
Product name	Hydrogen peroxide 30% (Perhydrol®) for analysis EMSURE® ISO

The protective gloves to be used must comply with the specifications of EC Directive 89/686/EEC and the related standard EN374, for example KCL 706 Lapren® (full contact), KCL 741 Dermatril® L (splash contact).
The breakthrough times stated above were determined by KCL in laboratory tests acc. to EN374 with samples of the recommended glove types.
This recommendation applies only to the product stated in the safety data sheet<(>,<)> supplied by us and for the designated use. When dissolving in or mixing with other substances and under conditions deviating from those stated in EN374 please contact the supplier of CE-approved gloves (e.g. KCL GmbH, D-36124 Eichenzell, Internet: www.kcl.de).

Other protective equipment
protective clothing

Respiratory protection
required when vapours/aerosols are generated.
Recommended Filter type: filter NO
The entrepeneur has to ensure that maintenance, cleaning and testing of respiratory protective devices are carried out according to the instructions of the producer. These measures have to be properly documented.

Environmental exposure controls
Do not empty into drains.

SECTION 9. Physical and chemical properties

9.1 Information on basic physical and chemical properties

Form	liquid
Colour	colourless
Odour	slight stinging
Odour Threshold	No information available.

SAFETY DATA SHEET

according to Regulation (EC) No. 1907/2006

Catalogue No.	107209
Product name	Hydrogen peroxide 30% (Perhydrol®) for analysis EMSURE® ISO

pH	<= 3,5 at 20 °C
Melting point	-25,7 °C
Boiling point/boiling range	107 °C at 1.013 hPa
Flash point	Not applicable
Evaporation rate	No information available.
Flammability (solid, gas)	No information available.
Lower explosion limit	No information available.
Upper explosion limit	No information available.
Vapour pressure	ca.18 hPa at 20 °C
Relative vapour density	No information available.
Density	1,11 g/cm3 at 20 °C
Relative density	No information available.
Water solubility	at 20 °C completely miscible
Partition coefficient: n-octanol/water	log Pow: -1,57 (calculated) Bioaccumulation is not expected. (External MSDS) (refers to pure substance)

SAFETY DATA SHEET

according to Regulation (EC) No. 1907/2006

Catalogue No.	107209
Product name	Hydrogen peroxide 30% (Perhydrol®) for analysis EMSURE® ISO

Auto-ignition temperature	No information available.
Decomposition temperature	> 100 °C
Viscosity, dynamic	No information available.
Explosive properties	Not classified as explosive.
Oxidizing properties	Oxidizing potential

9.2 Other data

none

SECTION 10. Stability and reactivity

10.1 Reactivity

Has a fire-promoting effect due to release of oxygen.

10.2 Chemical stability

heat-sensitive

Sensitivity to light

Stabilizer

2,6-Pyridinedicarboxylic acid

10.3 Possibility of hazardous reactions

Risk of explosion with:

Acetaldehyde, Acetone, Activated charcoal, Alcohols, formic acid, Ammonia, combustible substances, vinyl acetate, Organic Substances, Powdered metals, Dust., hydrazine and derivatives, hydrides, Ether, Potassium, anilines, metallic salts, acetic acid, Acetic anhydride, formaldehyde, furfuryl alcohol, oils, sodium, Lithium, lithium aluminium hydride, organic solvents, magnesium, metallic oxides, Methanol, Reducing agents, Oxides of phosphorus

butanol, with, Sulphuric acid

alkali hydroxides, with, Heavy metals

Exothermic reaction with:

alkali hydroxides, antimony sulfide, tin (II) chloride, Sulphides, THIOPHENE, nitric acid (conc.), ethanol, glycerol, Potassium hydroxide, phosphorus, metallic oxides, Sodium hydroxide, Aldehydes, nonmetals, nonmetallic oxides, strong alkalis, Amines, Acids, Oxidizing agents, alkali salts, Alkali metals, Alkaline earth metals, iodides, peroxi compounds, brass, organic nitro compounds

phenol, with, metal catalysts

Risk of ignition or formation of inflammable gases or vapours with:

potassium permanganate, Wood/Sawdust

vinyl acetate, with, Catalyst

10.4 Conditions to avoid

Heating.

10.5 Incompatible materials

Metals

10.6 Hazardous decomposition products

no information available

SECTION 11. Toxicological information

11.1 Information on toxicological effects

Mixture

Acute oral toxicity

Symptoms: Irritations of mucous membranes in the mouth, pharynx, oesophagus and gastrointestinal tract.

Acute toxicity estimate: 1.667 mg/kg
Calculation method

Acute inhalation toxicity

Symptoms: Possible damages:, mucosal irritations
Acute toxicity estimate: > 20 mg/l; 4 h ; vapour
Calculation method

SAFETY DATA SHEET

according to Regulation (EC) No. 1907/2006

Catalogue No.	107209
Product name	Hydrogen peroxide 30% (Perhydrol®) for analysis EMSURE® ISO

Acute dermal toxicity

This information is not available.

Skin irritation

After long-term exposure to the chemical: Causes skin burns.

Eye irritation

conjunctivitis

Mixture causes serious eye damage.

Sensitisation

This information is not available.

Germ cell mutagenicity

This information is not available.

Carcinogenicity

This information is not available.

Reproductive toxicity

This information is not available.

Teratogenicity

This information is not available.

Specific target organ toxicity - single exposure

This information is not available.

Specific target organ toxicity - repeated exposure

This information is not available.

Aspiration hazard

This information is not available.

11.2 Further information

Systemic effects:

Headache, Dizziness, Nausea, Vomiting, Diarrhoea, insomnia, muscle twitching, Convulsions, Unconsciousness, shock

Other dangerous properties can not be excluded.

Handle in accordance with good industrial hygiene and safety practice.

SAFETY DATA SHEET

according to Regulation (EC) No. 1907/2006

Catalogue No.	107209
Product name	Hydrogen peroxide 30% (Perhydrol®) for analysis EMSURE® ISO

Components

Hydrogen Peroxide

Acute oral toxicity

Acute toxicity estimate: 500,1 mg/kg

Expert judgement

Acute dermal toxicity

LD50 Rabbit: > 2.000 mg/kg

US-EPA

Repeated dose toxicity

Mouse

male

Oral

90 d

daily

NOAEL: 26 mg/kg

LOAEL: 76 mg/kg

OECD Test Guideline 408

Subchronic toxicity

Rat

male and female

inhalation (dust/mist/fume)

28 d

daily

NOAEL: 0,0029 mg/l

LOAEL: 0,0146 mg/l

OECD Test Guideline 412

Subacute toxicity

Germ cell mutagenicity

Genotoxicity in vivo

In vivo micronucleus test

Mouse

male and female

Intraperitoneal injection

Result: negative

Method: OECD Test Guideline 474

SAFETY DATA SHEET

according to Regulation (EC) No. 1907/2006

Catalogue No.	107209
Product name	Hydrogen peroxide 30% (Perhydrol®) for analysis EMSURE® ISO

SECTION 12. Ecological information

Mixture

12.1 Toxicity

No information available.

12.2 Persistence and degradability

Biodegradability

Readily biodegradable

12.3 Bioaccumulative potential

Partition coefficient: n-octanol/water

log Pow: -1,57

(calculated)

Bioaccumulation is not expected. (External MSDS) (refers to pure substance)

12.4 Mobility in soil

No information available.

12.5 Results of PBT and vPvB assessment

Substance(s) in the mixture do(es) not meet the criteria for PBT or vPvB according to Regulation (EC) No 1907/2006, Annex XIII, or a PBT/vPvB assessment was not conducted.

12.6 Other adverse effects

Surface tension

ca. 74,12 mN/m

at 20 °C

Additional ecological information

No interference with wastewater treatment plants are to be expected when used properly.

Discharge into the environment must be avoided.

Components

Hydrogen Peroxide

SAFETY DATA SHEET

according to Regulation (EC) No. 1907/2006

Catalogue No.	107209
Product name	Hydrogen peroxide 30% (Perhydrol®) for analysis EMSURE® ISO

Toxicity to fish
semi-static test LC50 Pimephales promelas (fathead minnow): 16,4 mg/l; 96 h
Analytical monitoring: yes
US-EPA

semi-static test NOEC Pimephales promelas (fathead minnow): 5 mg/l; 96 h
Analytical monitoring: yes
US-EPA

Toxicity to daphnia and other aquatic invertebrates
semi-static test LC50 Daphnia pulex (Water flea): 2,4 mg/l; 48 h
Analytical monitoring: yes
US-EPA

semi-static test NOEC Daphnia pulex (Water flea): 1 mg/l; 48 h
Analytical monitoring: yes
US-EPA

Toxicity to algae
IC50 Pseudokirchneriella subcapitata (green algae): 5,7 mg/l; 72 h
(ECOTOX Database)

Growth rate NOEC Skeletonema costatum (marine diatom): 0,63 mg/l; 72 h
(External MSDS)

Toxicity to bacteria
static test EC50 activated sludge: 466 mg/l; 30 min
Analytical monitoring: yes
OECD Test Guideline 209

static test EC50 activated sludge: > 1.000 mg/l; 3 h
Analytical monitoring: yes
OECD Test Guideline 209

Toxicity to daphnia and other aquatic invertebrates (Chronic toxicity)
flow-through test NOEC Daphnia magna (Water flea): 0,63 mg/l; 21 d

(ECHA)

Biodegradability
> 99 %; 0,5 h; aerobic
(ECHA)
Readily biodegradable

SAFETY DATA SHEET

according to Regulation (EC) No. 1907/2006

Catalogue No.	107209
Product name	Hydrogen peroxide 30% (Perhydrol®) for analysis EMSURE® ISO

Substance does not meet the criteria for PBT or vPvB according to Regulation (EC) No 1907/2006, Annex XIII.

SECTION 13. Disposal considerations

Waste treatment methods

See www.retrologistik.com for processes regarding the return of chemicals and containers, or contact us there if you have further questions.

SECTION 14. Transport information

Land transport (ADR/RID)

14.1 UN number	UN 2014
14.2 Proper shipping name	HYDROGEN PEROXIDE, AQUEOUS SOLUTION
14.3 Class	5.1 (8)
14.4 Packing group	II
14.5 Environmentally hazardous	--
14.6 Special precautions for user	yes
Tunnel restriction code	E

Inland waterway transport (ADN)

Not relevant

Air transport (IATA)

14.1 UN number	UN 2014
14.2 Proper shipping name	HYDROGEN PEROXIDE, AQUEOUS SOLUTION
14.3 Class	5.1 (8)
14.4 Packing group	II
14.5 Environmentally hazardous	--
14.6 Special precautions for user	yes **Not permitted for transport**

Sea transport (IMDG)

SAFETY DATA SHEET

according to Regulation (EC) No. 1907/2006

Catalogue No.	107209
Product name	Hydrogen peroxide 30% (Perhydrol®) for analysis EMSURE® ISO

14.1 UN number	UN 2014
14.2 Proper shipping name	HYDROGEN PEROXIDE, AQUEOUS SOLUTION
14.3 Class	5.1 (8)
14.4 Packing group	II
14.5 Environmentally hazardous	--
14.6 Special precautions for user	yes
EmS	F-H S-Q

14.7 Transport in bulk according to Annex II of MARPOL 73/78 and the IBC Code

Not relevant

SECTION 15. Regulatory information

15.1 Safety, health and environmental regulations/legislation specific for the substance or mixture

EU regulations

Major Accident Hazard	SEVESO III
Legislation	Not applicable
Occupational restrictions	Take note of Dir 94/33/EC on the protection of young people at work. Observe work restrictions regarding maternity protection in accordance to Dir 92/85/EEC or stricter national regulations where applicable.
Regulation (EC) No 1005/2009 on substances that deplete the ozone layer	not regulated
Regulation (EC) No 850/2004 of the European Parliament and of the Council of 29 April 2004 on persistent organic pollutants and amending Directive 79/117/EEC	not regulated

SAFETY DATA SHEET

according to Regulation (EC) No. 1907/2006

Catalogue No.	107209
Product name	Hydrogen peroxide 30% (Perhydrol®) for analysis EMSURE® ISO

Substances of very high concern (SVHC)	This product does not contain substances of very high concern according to Regulation (EC) No 1907/2006 (REACH), Article 57 above the respective regulatory concentration limit of ≥ 0.1 % (w/w).

National legislation

Storage class	5.1B

15.2 Chemical safety assessment

For this product a chemical safety assessment was not carried out.

SECTION 16. Other information

Full text of H-Statements referred to under sections 2 and 3.

H271	May cause fire or explosion; strong oxidizer.
H302	Harmful if swallowed.
H314	Causes severe skin burns and eye damage.
H318	Causes serious eye damage.
H332	Harmful if inhaled.
H335	May cause respiratory irritation.
H412	Harmful to aquatic life with long lasting effects.
H413	May cause long lasting harmful effects to aquatic life.

Training advice

Provide adequate information, instruction and training for operators.

Labelling

Hazard pictograms

Signal word

SAFETY DATA SHEET

according to Regulation (EC) No. 1907/2006

Catalogue No.	107209
Product name	Hydrogen peroxide 30% (Perhydrol®) for analysis EMSURE® ISO

Danger

Hazard statements

H302 Harmful if swallowed.

H318 Causes serious eye damage.

H413 May cause long lasting harmful effects to aquatic life.

Precautionary statements

Prevention

P273 Avoid release to the environment.

P280 Wear eye protection.

Response

P305 + P351 + P338 IF IN EYES: Rinse cautiously with water for several minutes. Remove contact lenses, if present and easy to do. Continue rinsing.

P313 Get medical advice/ attention.

Contains: Hydrogen Peroxide

Key or legend to abbreviations and acronyms used in the safety data sheet

Used abbreviations and acronyms can be looked up at www.wikipedia.org.

Regional representation

This information is given on the authorised Safety Data Sheet for your country.

The information contained herein is based on the present state of our knowledge. It characterises the product with regard to the appropriate safety precautions. It does not represent a guarantee of any properties of the product.

SAFETY DATA SHEET

according to Regulation (EC) No. 1907/2006

Catalogue No.	107209
Product name	Hydrogen peroxide 30% (Perhydrol®) for analysis EMSURE® ISO

EXPOSURE SCENARIO 1 (Industrial use)

1. Industrial use Reagent for analysis)

Sectors of end-use

SU 3	Industrial uses: Uses of substances as such or in preparations at industrial sites
SU9	Manufacture of fine chemicals
SU 10	Formulation [mixing] of preparations and/ or re-packaging (excluding alloys)

Chemical product category

PC21	Laboratory chemicals

Process categories

PROC1	Use in closed process, no likelihood of exposure
PROC2	Use in closed, continuous process with occasional controlled exposure
PROC3	Use in closed batch process (synthesis or formulation)
PROC4	Use in batch and other process (synthesis) where opportunity for exposure arises
PROC5	Mixing or blending in batch processes for formulation of preparations and articles (multistage and/ or significant contact)
PROC8a	Transfer of substance or preparation (charging/ discharging) from/ to vessels/ large containers at non-dedicated facilities
PROC8b	Transfer of substance or preparation (charging/ discharging) from/ to vessels/ large containers at dedicated facilities
PROC9	Transfer of substance or preparation into small containers (dedicated filling line, including weighing)
PROC10	Roller application or brushing
PROC14	Production of preparations or articles by tabletting, compression, extrusion, pelletisation
PROC15	Use as laboratory reagent

Environmental Release Categories

ERC1	Manufacture of substances
ERC2	Formulation of preparations
ERC4	Industrial use of processing aids in processes and products, not becoming part of articles
ERC6a	Industrial use resulting in manufacture of another substance (use of intermediates)
ERC6b	Industrial use of reactive processing aids

SAFETY DATA SHEET

according to Regulation (EC) No. 1907/2006

Catalogue No.	107209
Product name	Hydrogen peroxide 30% (Perhydrol®) for analysis EMSURE® ISO

2. Contributing scenarios: Operational conditions and risk management measures

2.1 Contributing scenario controlling environmental exposure for: ERC1, ERC2, ERC4, ERC6a, ERC6b

Amount used

Annual amount per site	1010 t
Remarks	(refers to pure substance)

Other given operational conditions affecting environmental exposure

Number of emission days per year	360
Emission or Release Factor: Air	0,10 %
Emission or Release Factor: Water	0,50 %
Emission or Release Factor: Soil	0,10 %

Technical conditions and measures / Organizational measures

Air	Use of air emission abatement equipments.
Water	Biological waste water treatment plant

Conditions and measures related to municipal sewage treatment plant

Type of Sewage Treatment Plant	Municipal sewage treatment plant
Flow rate of sewage treatment plant effluent	2.000 m3/d
Percentage removed from waste water	97 %

2.2 Contributing scenario controlling worker exposure for: PROC1, PROC2, PROC3, PROC8b, PROC15

Product characteristics

Concentration of the Substance in Mixture/Article	Covers the percentage of the substance in the product up to 70 %.
Physical Form (at time of use)	Medium volatile liquid
Process Temperature	< 70 °C

Frequency and duration of use

Frequency of use	8 hours/day

Other operational conditions affecting workers exposure

Outdoor / Indoor	Indoor with local exhaust ventilation (LEV)

Organisational measures to prevent /limit releases, dispersion and exposure

Covers daily exposures up to 8 hours.

Conditions and measures related to personal protection, hygiene and health evaluation

Wear suitable gloves (tested to EN374) and eye protection.

2.3 Contributing scenario controlling worker exposure for: PROC4

Product characteristics

Concentration of the Substance in Mixture/Article	Covers the percentage of the substance in the product up to 70 %.
Physical Form (at time of use)	Medium volatile liquid
Process Temperature	< 70 °C

Frequency and duration of use

Frequency of use	8 hours/day

Other operational conditions affecting workers exposure

Outdoor / Indoor	Indoor with LEV and good general ventilation

Organisational measures to prevent /limit releases, dispersion and exposure

Covers daily exposures up to 8 hours.

Conditions and measures related to personal protection, hygiene and health evaluation

Wear suitable gloves (tested to EN374) and eye protection.

2.4 Contributing scenario controlling worker exposure for: PROC5, PROC8a, PROC9

Product characteristics

Concentration of the Substance in	Covers the percentage of the substance in the product up to

SAFETY DATA SHEET

according to Regulation (EC) No. 1907/2006

Catalogue No.	107209
Product name	Hydrogen peroxide 30% (Perhydrol®) for analysis EMSURE® ISO

Mixture/Article	70 %.
Physical Form (at time of use)	Medium volatile liquid
Process Temperature	< 70 °C

Frequency and duration of use

Frequency of use	< 4 hours/day

Other operational conditions affecting workers exposure

Outdoor / Indoor	Indoor with LEV and enhanced general ventilation

Organisational measures to prevent /limit releases, dispersion and exposure

Avoid carrying out operation for more than 4 hours.

Conditions and measures related to personal protection, hygiene and health evaluation

Wear suitable gloves (tested to EN374) and eye protection.

2.5 Contributing scenario controlling worker exposure for: PROC10, PROC14

Product characteristics

Concentration of the Substance in Mixture/Article	Covers the percentage of the substance in the product up to 70 %.
Physical Form (at time of use)	Medium volatile liquid
Process Temperature	< 70 °C

Frequency and duration of use

Frequency of use	8 hours/day

Other operational conditions affecting workers exposure

Outdoor / Indoor	Indoor with LEV and enhanced general ventilation

Organisational measures to prevent /limit releases, dispersion and exposure

Covers daily exposures up to 8 hours.

Conditions and measures related to personal protection, hygiene and health evaluation

Wear suitable gloves (tested to EN374) and eye protection.

SAFETY DATA SHEET

according to Regulation (EC) No. 1907/2006

Catalogue No.	107209
Product name	Hydrogen peroxide 30% (Perhydrol®) for analysis EMSURE® ISO

3. Exposure estimation and reference to its source

Environment

CS	Use descriptor	Msafe	Compartment	RCR	Exposure Assessment Method
2.1	ERC1		Fresh water	0,61	EUSES
2.1	ERC2		Fresh water	0,61	EUSES
2.1	ERC4		Fresh water	0,61	EUSES
2.1	ERC6a		Fresh water	0,61	EUSES
2.1	ERC6b		Fresh water	0,61	EUSES

Workers

CS	Use descriptor	Exposure duration, route, effect	RCR	Exposure Assessment Method
2.2	PROC1	longterm, inhalative, systemic	< 0,01	ECETOC TRA, modified
2.2	PROC2	longterm, inhalative, systemic	0,35	ECETOC TRA, modified
2.2	PROC3	longterm, inhalative, systemic	0,71	ECETOC TRA, modified
2.2	PROC8b	longterm, inhalative, systemic	0,89	ECETOC TRA, modified
2.2	PROC15	longterm, inhalative, systemic	0,71	ECETOC TRA, modified
2.3	PROC4	longterm, inhalative, systemic	0,99	ECETOC TRA, modified
2.4	PROC5	longterm, inhalative, systemic	0,64	ECETOC TRA, modified
2.4	PROC8a	longterm, inhalative, systemic	0,64	ECETOC TRA, modified
2.4	PROC9	longterm, inhalative, systemic	0,64	ECETOC TRA, modified
2.5	PROC10	longterm, inhalative, systemic	0,91	ECETOC TRA, modified
2.5	PROC14	longterm, inhalative, systemic	0,91	ECETOC TRA, modified

The default parameters and -efficiencies of the applied exposure assessment model were used for the calculation (unless stated differently).
For (other) local effects risk management measures are based on qualitative risk characterisation.

4. Guidance to Downstream User to evaluate whether he works inside the boundaries set by the Exposure Scenario

Please refer to the following documents: ECHA Guidance on information requirements and chemical

SAFETY DATA SHEET

according to Regulation (EC) No. 1907/2006

Catalogue No.	107209
Product name	Hydrogen peroxide 30% (Perhydrol®) for analysis EMSURE® ISO

safety assessment Chapter R.12: Use descriptor system; ECHA Guidance for downstream users; ECHA Guidance on information requirements and chemical safety assessment Part D: Exposure Scenario Building, Part E: Risk Characterisation and Part G: Extending the SDS; VCI/Cefic REACH Practical Guides on Exposure Assessment and Communications in the Supply Chain; CEFIC Guidance Specific Environmental Release Categories (SPERCs).

For scaling of worker exposure assessments performed with ECETOC TRA, please consult the Merck tool SclDeEx® at www.merckmillipore.com/scideex.

SAFETY DATA SHEET

according to Regulation (EC) No. 1907/2006

Catalogue No.	107209
Product name	Hydrogen peroxide 30% (Perhydrol®) for analysis EMSURE® ISO

EXPOSURE SCENARIO 2 (Professional use)

1. Professional use Reagent for analysis)

Sectors of end-use

SU 22 Professional uses: Public domain (administration, education, entertainment, services, craftsmen)

Chemical product category

PC21 Laboratory chemicals

Process categories

PROC15 Use as laboratory reagent

Environmental Release Categories

ERC2 Formulation of preparations

ERC4 Industrial use of processing aids in processes and products, not becoming part of articles

ERC6a Industrial use resulting in manufacture of another substance (use of intermediates)

ERC6b Industrial use of reactive processing aids

2. Contributing scenarios: Operational conditions and risk management measures

2.1 Contributing scenario controlling environmental exposure for: ERC2, ERC4, ERC6a, ERC6b

Amount used

Annual amount per site	1010 t
Remarks	(refers to pure substance)

Other given operational conditions affecting environmental exposure

Number of emission days per year	360
Emission or Release Factor: Air	0,10 %
Emission or Release Factor: Water	0,50 %
Emission or Release Factor: Soil	0,10 %

Technical conditions and measures / Organizational measures

Air	Use of air emission abatement equipments.
Water	Biological waste water treatment plant

SAFETY DATA SHEET

according to Regulation (EC) No. 1907/2006

Catalogue No.	107209
Product name	Hydrogen peroxide 30% (Perhydrol®) for analysis EMSURE® ISO

Conditions and measures related to municipal sewage treatment plant

Type of Sewage Treatment Plant	Municipal sewage treatment plant
Flow rate of sewage treatment plant effluent	2.000 m3/d
Percentage removed from waste water	97 %

2.2 Contributing scenario controlling worker exposure for: PROC15

Product characteristics

Concentration of the Substance in Mixture/Article	Covers the percentage of the substance in the product up to 70 %.
Physical Form (at time of use)	Medium volatile liquid
Process Temperature	< 70 °C

Frequency and duration of use

Frequency of use	8 hours/day

Other operational conditions affecting workers exposure

Outdoor / Indoor	Indoor with LEV and good general ventilation

Organisational measures to prevent /limit releases, dispersion and exposure

Covers daily exposures up to 8 hours.

Conditions and measures related to personal protection, hygiene and health evaluation

Wear suitable gloves (tested to EN374) and eye protection.

3. Exposure estimation and reference to its source

SAFETY DATA SHEET

according to Regulation (EC) No. 1907/2006

Catalogue No.	107209
Product name	Hydrogen peroxide 30% (Perhydrol®) for analysis EMSURE® ISO

Environment

CS	Use descriptor	Msafe	Compartment	RCR	Exposure Assessment Method
2.1	ERC2		Fresh water	0,61	EUSES
2.1	ERC4		Fresh water	0,61	EUSES
2.1	ERC6a		Fresh water	0,61	EUSES
2.1	ERC6b		Fresh water	0,61	EUSES

Workers

CS	Use descriptor	Exposure duration, route, effect	RCR	Exposure Assessment Method
2.2	PROC15	longterm, inhalative, systemic	0,99	ECETOC TRA, modified

The default parameters and -efficiencies of the applied exposure assessment model were used for the calculation (unless stated differently).
For (other) local effects risk management measures are based on qualitative risk characterisation.

4. Guidance to Downstream User to evaluate whether he works inside the boundaries set by the Exposure Scenario

Please refer to the following documents: ECHA Guidance on information requirements and chemical safety assessment Chapter R.12: Use descriptor system; ECHA Guidance for downstream users; ECHA Guidance on information requirements and chemical safety assessment Part D: Exposure Scenario Building, Part E: Risk Characterisation and Part G: Extending the SDS; VCI/Cefic REACH Practical Guides on Exposure Assessment and Communications in the Supply Chain; CEFIC Guidance Specific Environmental Release Categories (SPERCs).

For scaling of worker exposure assessments performed with ECETOC TRA, please consult the Merck tool ScIDeEx® at www.merckmillipore.com/scideex.

C.3. Material Safety Data Sheet of 90% H_2O_2

This MSDS refers to 90% H_2O_2 which is the highest that could be found for MSDS. It does not refer to the exact solution we achieved in this thesis, however gives an indication of the precaution needed to work with highly concentrated hydrogen peroxide. Some of the advice are different from the 30% solution. The MSDS is produced by PeroxyChem.

SAFETY DATA SHEET
Hydrogen Peroxide 90% HTP

SDS # : 7722-84-1-90-60
Revision date: 2015-05-28
Format: NA
Version 1

1. PRODUCT AND COMPANY IDENTIFICATION

Product Identifier

Product Name Hydrogen Peroxide 90% HTP

Other means of identification

CAS-No 7722-84-1

Recommended use of the chemical and restrictions on use

Recommended Use: Monopropellant and bipropellant systems; fuel for rocket engines; rocket boosters / propellants / power source for aircraft; steam generation; rapid source of heat; electronics IC circuits and other military uses

Restrictions on Use: Use as recommended by the label.

Manufacturer/Supplier

PeroxyChem LLC
2005 Market Street
Suite 3200
Philadelphia, PA 19103
Phone: +1 267/ 422-2400 (General Information)
E-Mail: sdsinfo@peroxychem.com

PeroxyChem Canada
PG Pulp Mill Road
Prince George, BC V2N2S6
1+ 250/ 561-4200 (General Information)

Emergency telephone number

For leak, fire, spill or accident emergencies, call:
1 800 / 424 9300 (CHEMTREC - U.S.A.)
1 703 / 527 3887 (CHEMTREC - Collect - All Other Countries)
1 613/ 996-6666 (CANUTEC - Canada)
1 303/ 389-1409 (Medical - U.S. - Call Collect)

1 281 / 474-8750 (Bayport, Texas Plant)
1 250 / 561-4221 (Prince George, BC, Canada Plant)

2. HAZARDS IDENTIFICATION

Classification

OSHA Regulatory Status
This material is considered hazardous by the OSHA Hazard Communication Standard (29 CFR 1910.1200).

Acute toxicity - Oral	Category 4
Acute toxicity - Inhalation (Vapors)	Category 4
Skin corrosion/irritation	Category 1 Sub-category A

Serious eye damage/eye irritation	Category 1
Specific target organ toxicity (single exposure)	Category 3
Oxidizing Liquids	Category 1

GHS Label elements, including precautionary statements

EMERGENCY OVERVIEW

Danger

Hazard Statements
H314 - Causes severe skin burns and eye damage
H302 - Harmful if swallowed
H332 - Harmful if inhaled
H335 - May cause respiratory irritation
H272 - May intensify fire; oxidizer

Precautionary Statements - Prevention
P271 - Use only outdoors or in a well-ventilated area
P260 - Do not breathe mist, vapours or spray.
P280 - Wear protective gloves/ protective clothing/ eye protection/ face protection
P283 - Wear fire/ flame resistant/ retardant clothing
P210 - Keep away from heat/sparks/open flames/hot surfaces. - No smoking
P220 - Keep/Store away from clothing/flammable materials/combustibles
P221 - Take any precaution to avoid mixing with combustibles/flammables

Precautionary Statements - Response
P305 + P351 + P338 - IF IN EYES: Rinse cautiously with water for several minutes. Remove contact lenses, if present and easy to do. Continue rinsing
P310 - Immediately call a POISON CENTER or doctor
P303 + P361 + P353 - IF ON SKIN (or hair): Take off immediately all contaminated clothing. Rinse skin with water/ shower
P306 + P360 - IF ON CLOTHING: rinse immediately contaminated clothing and skin with plenty of water before removing clothes
P304 + P340 - IF INHALED: Remove person to fresh air and keep comfortable for breathing
P312 - Call a POISON CENTER or doctor if you feel unwell
P301 + P330 + P331 - IF SWALLOWED: rinse mouth. Do NOT induce vomiting
P310 - Immediately call a POISON CENTER or doctor
P370 + P378 - In case of fire: Use water for extinction
P371 + P380 + P375 - In case of major fire and large quantities: Evacuate area. Fight fire remotely due to the risk of explosion

Hazards not otherwise classified (HNOC)
No hazards not otherwise classified were identified.

Other Information

Keep container in a cool place out of direct sunlight. Store only in vented containers. Do not store on wooden pallets. Do not return unused material to its original container. Avoid contamination - Contamination could cause decomposition and generation of oxygen which may result in high pressure and possible container rupture. Empty drums should be triple rinsed with water before discarding. .

Hydrogen Peroxide 90% HTP

SDS # : 7722-84-1-90-60
Revision date: 2015-05-28
Version 1

3. COMPOSITION/INFORMATION ON INGREDIENTS

Formula HO - OH

Chemical name	CAS-No	Weight %
Hydrogen peroxide	7722-84-1	90
Water	7732-18-5	10

Occupational exposure limits, if available, are listed in section 8

4. FIRST AID MEASURES

Eye Contact Rinse immediately with plenty of water, also under the eyelids, for at least 15 minutes. Remove contact lenses, if present, after the first 5 minutes, then continue rinsing. Seek immediate medical attention/advice.

Skin Contact Take off contaminated clothing. Rinse skin immediately with plenty of water for 15-20 minutes. Call a poison control center or doctor for further treatment advice.

Inhalation Move to fresh air. If person is not breathing, contact emergency medical services, then give artificial respiration, preferably mouth-to-mouth if possible. Call a poison control center or doctor for further treatment advice.

Ingestion Rinse mouth. Do not induce vomiting. If conscious, give 2 glasses of water. Get immediate medical attention. Never give anything by mouth to an unconscious person.

Most important symptoms and effects, both acute and delayed Hydrogen Peroxide irritates respiratory system and, if inhaled, may cause inflammation and pulmonary edema. The effects may not be immediate In case of accidental ingestion, necrosis may result from mucous membrane burns (mouth, esophagus and stomach). Oxygen rapid release may cause stomach swelling and hemorrhaging, which may product major, or even fatal, injury to organs if a large amount has been ingested.
Corneal lesions and irreversible damage if contact with the eyes

Indication of immediate medical attention and special treatment needed, if necessary Hydrogen peroxide at these concentrations is a strong oxidant. Direct contact with the eye is likely to cause corneal damage especially if not washed immediately. Careful opthalmologic evaluation is recommended and the possibility of local corticosteroid therapy should be considered. Because of the likelihood of corrosive effects on the gastrointestinal tract after ingestion, and the unlikelihood of systemic effects, attemps at evacuating the stomach via emesis induction or gastric lavage should be avoided. There is a remote possibility, however, that a nasogastric or orogastric tube may be required for the reduction of severe distension due to gas formation.

5. FIRE-FIGHTING MEASURES

Suitable Extinguishing Media Water. Do not use any other substance.

Specific Hazards Arising from the Chemical In closed unventilated containers, risk of rupture due to the increased pressure from decomposition. Contact with combustible material may cause fire. Non-flammable but vapor phase decomposition occurs at 7.6 vol. % for 90% based on flash point.

Hazardous Combustion Products A severe detonation hazard when mixed with organics. Contact with combustibles will cause fire. While not flammable by OSHA and DOT definitions, contamination, contact with incompatible materials, or high temperatures could cause a rapid decomposition that yields heat and oxygen, which support combustion and will cause a rapid overpressure if confined.
.

Explosion data
Sensitivity to Mechanical Impact Not sensitive.
Sensitivity to Static Discharge Static discharge can potentially initiate decomposition in vapor mixtures.

Protective equipment and Use water spray to cool fire exposed surfaces and protect personnel. Move containers from

precautions for firefighters fire area if you can do it without risk. As in any fire, wear self-contained breathing apparatus and full protective gear.

6. ACCIDENTAL RELEASE MEASURES

Personal Precautions Avoid contact with skin, eyes and clothing. Wear personal protective equipment. Isolate and post spill area. Keep people away from and upwind of spill/leak. Eliminate all sources of ignition and remove combustible materials.

Other Combustible materials exposed to hydrogen peroxide should be immediately submerged in or rinsed with large amounts of water to ensure that all hydrogen peroxide is removed. Residual hydrogen peroxide that is allowed to dry (upon evaporation hydrogen peroxide can concentrate) on organic materials such as paper, fabrics, cotton, leather, wood or other combustibles can cause the material to ignite and result in fire.

Environmental Precautions Prevent material from entering into soil, ditches, sewers, waterways, and/or groundwater. See Section 12, Ecological Information for more detailed information.

Methods for Containment Dike to collect large liquid spills. Stop leak and contain spill if this can be done safely. Small spillage: Dilute with large quantities of water.

Methods for cleaning up Flush area with flooding quantities of water. Hydrogen peroxide may be decomposed by adding sodium metabisulfite or sodium sulfite after diluting to about 5%.

7. HANDLING AND STORAGE

Handling CONSULT PEROXYCHEM FOR APPROVED PERSONAL PROTECTIVE EQUIPMENTAND HANDLING AND STORAGE PROCEDURES. Wear chemical splash-type monogoggles and full face shield, Gortex®, polyester or acrylic full cover clothing and approved rubber or nitrile gloves and shoes. Do not use cotton, wool or leather for these materials react rapidly with hydrogen peroxide concentrations greater than 90%. Avoid contamination and heat as these will cause decomposition and generation of oxygen gas which will result in high pressures and possible container rupture. Hydrogen peroxide should be stored only in vented containers and transferred only in a prescribed manner (contact Peroxychem for procedures). Never return unused hydrogen peroxide to original container. Empty aluminum drums should be returned to Peroxychem. Utensils used for handling hydrogen peroxide should be made only of clean glass, pre-approved passivated aluminum or stainless steel, or approved plastics such as polytetrafluoroethylene. Do not discard 90% or higher concentrations without first diluting to less than 5%.

Storage Keep containers in cool areas out of direct sunlight and away from combustibles. Provide mechanical general and/or local exhaust ventilation to prevent release of vapor or mist into work environment. Containers must be vented. Keep/store only in original container. Store rooms or warehouses should be made of non-combustible materials with impermeable floors. In case of release, spillage should flow to safe area. Containers should be visually inspected on a regular basis to detect any abnormalities (swollen drums, increases in temperature, etc.).

Incompatible products Combustible materials. Copper alloys, galvanized iron. Strong reducing agents. Heavy metals. Iron. Copper alloys. Contact with metals, metallic ions, alkalis, reducing agents and organic matter (such as alcohols or terpenes) may produce self-accelerated thermal decomposition.

8. EXPOSURE CONTROLS/PERSONAL PROTECTION

Control parameters

Exposure Guidelines Ingredients with workplace control parameters.

Chemical name	ACGIH TLV	OSHA PEL	NIOSH	Mexico
Hydrogen peroxide 7722-84-1	TWA: 1 ppm	TWA: 1 ppm TWA: 1.4 mg/m^3	IDLH: 75 ppm TWA: 1 ppm TWA: 1.4 mg/m^3	Mexico: TWA 1 ppm Mexico: TWA 1.5 mg/m^3 Mexico: STEL 2 ppm

				Mexico: STEL 3 mg/m³
Chemical name	**British Columbia**	**Quebec**	**Ontario TWAEV**	**Alberta**
Hydrogen peroxide 7722-84-1	TWA: 1 ppm	TWA: 1 ppm TWA: 1.4 mg/m³	TWA: 1 ppm	TWA: 1 ppm TWA: 1.4 mg/m³

Appropriate engineering controls

Engineering measures Showers. Eyewash stations. Ventilation systems.

Individual protection measures, such as personal protective equipment

Eye/Face Protection Use chemical splash-type monogoggles and a full-face shield made of polycarbonate, acetate, polycarbonate/acetate, PETG or thermoplastic.

Skin and Body Protection For body protection wear impervious clothing such as an approved splash protective suit made of SBR rubber, PVC (PVC Outershell w/Polyester Substrate), Gore-Tex (Polyester trilaminate w/Gore-Tex), or a specialized HAZMAT Splash or Protective Suite (Level A, B, or C). DO NOT wear any form of splash suit or rainwear made of nylon or nylon-blends. For foot protection, wear approved boots made of NBR, PVC, Polyurethane, or neoprene. Overboots made of Latex or PVC, as well as firefighter boots or specialized HAZMAT boots are also permitted. DO NOT wear any form of boot or overboot made of nylon or nylon blends. DO NOT USE cotton, wool or leather as these materials react RAPIDLY with 90% or higher concentrations of hydrogen peroxide. Completely submerge hydrogen peroxide contaminated clothing or other materials in water prior to drying. Residual hydrogen peroxide, if allowed to dry on materials such as paper, fabrics, cotton, leather, wood or other combustibles, can cause the material to ignite and result in a fire.

Hand Protection For hand protection, wear approved gloves made of nitrile, PVC, or neoprene. DO NOT use cotton, wool or leather for these materials react RAPIDLY with higher concentrations of hydrogen peroxide. Thoroughly rinse the outside of gloves with water prior to removal. Inspect regularly for leaks.

Respiratory Protection If concentrations in excess of 10 ppm are expected, use NIOSH/DHHS approved self-contained breathing apparatus (SCBA) or other approved air-supplied respirator (ASR) equipment (e.g., a full-face airline respirator (ALR)). DO NOT use any form of air-purifying respirator (APR) or filtering facepiece (dust mask), especially those containing oxidizable sorbants such as activated carbon.

Hygiene measures Avoid breathing vapors, mist or gas. Clean water should be available for washing in case of eye or skin contamination. .

General information Protective engineering solutions should be implemented and in use before personal protective equipment is considered.

9. PHYSICAL AND CHEMICAL PROPERTIES

Information on basic physical and chemical properties

Appearance Clear, colorless liquid
Physical State Liquid
Color Colorless
Odor odorless
Odor threshold Not applicable
pH <= 1
Melting point/freezing point -12 °C
Boiling Point/Range 141 °C
Flash point Seta Closed Cup: (90%) 82 - 85°C. No visible flame observed. Reaction attributed to rapid decomposition.
Evaporation Rate > 1 (n-butyl acetate=1)
Flammability (solid, gas) Non-flammable but vapor phase decomposition occurs at 7.6 vol. % for 90 % based on flash point.
Flammability Limit in Air Not applicable
Upper flammability limit:

Lower flammability limit:	
Vapor pressure	5 mm Hg @ 30 °C
Vapor density	No information available
Density	1.39 g/cm³ @ 20ºC
Specific gravity	1.39
Water solubility	completely soluble
Solubility in other solvents	No information available
Partition coefficient	No data available
Autoignition temperature	ASTM E 659-78: 99% - 210°C (in air) 169°C (in oxygen). Reaction was attributed to rapid decomposition of vapors.
Decomposition temperature	740 °C
Viscosity, kinematic	1.15 cP @ 25 °C
Viscosity, dynamic	No information available
Explosive properties	No information available
Oxidizing properties	Powerful oxidizer
Molecular weight	34
Bulk density	Not applicable

10. STABILITY AND REACTIVITY

Reactivity Reactive and oxidizing agent.

Chemical Stability Stable under normal conditions. Decomposes on heating. Stable under recommended storage conditions.

Possibility of Hazardous Reactions A severe detonation hazard when mixed with organics. Contact with combustibles will cause fire. While not flammable by OSHA and DOT definitions, contamination, contact with incompatible materials, or high temperatures could cause a rapid decomposition that yields heat and oxygen, which support combustion and will cause a rapid overpressure if confined. .

Hazardous polymerization Hazardous polymerization does not occur.

Conditions to avoid Excessive heat; Contamination; Exposure to UV-rays; pH variations.

Incompatible materials Combustible materials. Copper alloys, galvanized iron. Strong reducing agents. Heavy metals. Iron. Copper alloys. Contact with metals, metallic ions, alkalis, reducing agents and organic matter (such as alcohols or terpenes) may produce self-accelerated thermal decomposition.

Hazardous Decomposition Products Oxygen which supports combustion. Liable to produce overpressure in container.

11. TOXICOLOGICAL INFORMATION

Product Information

LD50 Oral 50% solution: LD50: > 225 mg/kg bw (rat)
35 % solution:LD50 1193 mg/kg bw (rat)
70 % solution: LD50 1026 mg/kg bw (rat)

LD50 Dermal 35% solution: LD50 > 2000 mg/kg bw (rabbit)
70 % solution: LD50 9200 mg/kg bw (rabbit)

LC50 Inhalation 50% solution: LC50 > 170 mg/m³ (rat) (4-hr)
Hydrogen Peroxide vapors: LC0 9400 mg/m³ (mouse) (5 - 15 minutes)
Hydrogen Peroxide vapors: LC50 > 2160 mg/m³ (mouse)

Sensitization Did not cause sensitization on laboratory animals.

Information on toxicological effects

Symptoms Vapors, mists, or aerosols of hydrogen peroxide can cause upper airway irritation, inflammation of the nose, hoarseness, shortness of breath, and a sensation of burning or tightness in the chest. Prolonged exposure to concentrated vapor or to dilute solutions can

cause irritation and temporary bleaching of skin and hair. Exposure to vapor, mist, or aerosol can cause stinging pain and tearing of eyes.

Delayed and immediate effects as well as chronic effects from short and long-term exposure

Carcinogenicity

This product contains hydrogen peroxide. The International Agency for Research on Cancer (IARC) has conculded that there is inadequate evidence for carcinogenicity of hydrogen peroxide in humans, but limited evidence in experimental animals (Group 3 - not classifiable as to its carcinogenicity to humans). The American Conference of Governmental Industrial Hygienists (ACGIH) has concluded that hydrogen peroxide is a 'Confirmed Animal Carcinogen with Unknown Relevance to Humans' (A3).

Chemical name	ACGIH	IARC	NTP	OSHA
Hydrogen peroxide 7722-84-1	A3	3		

Mutagenicity

This product is not recognized as mutagenic by Research Agencies
In vivo tests did not show mutagenic effects

Reproductive toxicity

This product is not recognized as reprotox by Research Agencies.

STOT - single exposure

May cause respiratory irritation.

STOT - repeated exposure

Not classified.

Target organ effects

Eyes, Respiratory System, Skin.

Aspiration hazard

Aspiration risk: may cause lung damage if swallowed.

12. ECOLOGICAL INFORMATION

Ecotoxicity

Ecotoxicity effects

Hydrogen peroxide is naturally produced by sunlight (between 0.1 and 4 ppb in air and 0.001 to 0.1 mg/L in water). Not expected to have significant environmental effects.

Hydrogen peroxide (7722-84-1)				
Active Ingredient(s)	Duration	Species	Value	Units
Hydrogen peroxide	96 h LC50	Fish Pimephales promelas	16.4	mg/L
Hydrogen peroxide	72 h LC50	Fish Leuciscus idus	35	mg/L
Hydrogen peroxide	48 h EC50	Daphnia pulex	2.4	mg/L
Hydrogen peroxide	24 h EC50	Daphnia magna	7.7	mg/L
Hydrogen peroxide	72 h EC50	Algae Skeletonema costatum	1.38	mg/L
Hydrogen peroxide	21 d NOEC	Daphnia magna	0.63	mg/L

Persistence and degradability

Hydrogen peroxide in the aquatic environment is subject to various reduction or oxidation processes and decomposes into water and oxygen. Hydrogen peroxide half-life in freshwater ranged from 8 hours to 20 days, in air from 10 - 20 hours, and in soils from minutes to hours depending upon microbiological activity and metal contamination.

Bioaccumulation

Material may have some potential to bioaccumulate but will likely degrade in most environments before accumulation can occur.

Mobility

Will likely be mobile in the environment due to its water solubility but will likely degrade over time.

Other Adverse Effects

Decomposes into oxygen and water. No adverse effects.

13. DISPOSAL CONSIDERATIONS

Waste disposal methods	Dispose of in accordance with local regulations. Can be disposed as waste water, when in compliance with local regulations.
US EPA Waste Number	D001 D002
Contaminated Packaging	Dispose of in accordance with local regulations. Drums - Empty as thoroughly as possible. Triple rinse drums before disposal. Avoid contamination; impurities accelerate decomposition. Never return product to original container.

14. TRANSPORT INFORMATION

DOT

UN/ID no	2015
Proper Shipping Name	HYDROGEN PEROXIDE, AQUEOUS SOLUTION, STABILIZED
Hazard class	5.1 (Oxidizer)
Subsidiary class	8
Packing Group	I

TDG

UN/ID no	UN 2015
Proper Shipping Name	HYDROGEN PEROXIDE, AQUEOUS SOLUTION, STABILIZED
Hazard class	5.1 (Oxidizer)
Subsidiary class	8
Packing Group	I

ICAO/IATA Hydrogen peroxide (>40%) is forbidden on Passenger and Cargo Aircraft.

IMDG/IMO

UN/ID no	2015
Proper Shipping Name	HYDROGEN PEROXIDE, AQUEOUS SOLUTION, STABILIZED
Hazard class	5.1
Subsidiary Hazard Class	8
Packing Group	I

OTHER INFORMATION Protect from physical damage. Keep drums in upright position. Drums should not be stacked in transit. Do not store drums on wooden pallets.

15. REGULATORY INFORMATION

U.S. Federal Regulations

SARA 313
Section 313 of Title III of the Superfund Amendments and Reauthorization Act of 1986 (SARA). This product does not contain any chemicals which are subject to the reporting requirements of the Act and Title 40 of the Code of Federal Regulations, Part 372

SARA 311/312 Hazard Categories

Acute health hazard	Yes
Chronic health hazard	No
Fire hazard	Yes
Sudden release of pressure hazard	No
Reactive Hazard	No

Clean Water Act
This product does not contain any substances regulated as pollutants pursuant to the Clean Water Act (40 CFR 122.21 and 40 CFR 122.42)

CERCLA
This material, as supplied, contains one or more substances regulated as a hazardous substance under the Comprehensive Environmental Response Compensation and Liability Act (CERCLA) (40 CFR 302):

Chemical name	Hazardous Substances RQs	Extremely Hazardous Substances RQs	SARA RQ
Hydrogen peroxide 7722-84-1		1000 lb	

Hydrogen Peroxide RQ is for concentrations of > 52% only

International Inventories

Component	TSCA (United States)	DSL (Canada)	EINECS/ELINCS (Europe)	ENCS (Japan)	China (IECSC)	KECL (Korea)	PICCS (Philippines)	AICS (Australia)	NZIoC (New Zealand)
Hydrogen peroxide 7722-84-1 (90)	X	X	X	X	X	X	X	X	X

Mexico - Grade Serious risk, Grade 3

CANADA

WHMIS Hazard Class
C - Oxidizing materials
D1B - Toxic materials
E - Corrosive material
F - Dangerously reactive material




16. OTHER INFORMATION

NFPA	**Health Hazards** 3	**Flammability** 0	**Stability** 3	**Special Hazards** OX
HMIS	**Health Hazards** 3	**Flammability** 0	**Physical hazard** 3	**Special precautions** H

NFPA/HMIS Ratings Legend Severe = 4; Serious = 3; Moderate = 2; Slight = 1; Minimal = 0
Special Hazards: OX = Oxidizer
Protection = H (Safety goggles, gloves, apron, the use of supplied air or SCBA respirator is required in lieu of a vapor cartidge respirator)

Uniform Fire Code Oxidizer: Class 3--Liquid

Revision date: 2015-05-28
Revision note Initial Release

Disclaimer
PeroxyChem believes that the information and recommendations contained herein (including data and statements) are accurate as of the date hereof. NO WARRANTY OF FITNESS FOR ANY PARTICULAR PURPOSE, WARRANTY OF MERCHANTABILITY OR ANY OTHER WARRANTY, EXPRESSED OR IMPLIED, IS MADE CONCERNING THE INFORMATION PROVIDED HEREIN. The information provided herein relates only to the specified product designated and may not be applicable where such product is used in combination with any other materials or in any process. Further, since the conditions and methods of use are beyond the control of PeroxyChem, PeroxyChem expressly disclaims any and all liability as to any results obtained or arising from any use of the products or reliance on such information.

Prepared By:

PeroxyChem

End of Safety Data Sheet

C.4. Material Safety Data Sheet of ethanol

In this section, the safety information about 99.5% pure ethanol is presented.

Supelco®

www.sigmaaldrich.com

SAFETY DATA SHEET

according to Regulation (EC) No. 1907/2006

Revision Date 19.02.2019 Version 7.10

SECTION 1. Identification of the substance/mixture and of the company/undertaking

1.1 Product identifier

Catalogue No.	107017
Product name	Ethanol absolute for analysis EMPARTA® ACS
REACH Registration Number	01-2119457610-43-XXXX
CAS-No.	64-17-5

1.2 Relevant identified uses of the substance or mixture and uses advised against

Identified uses	Reagent for analysis In compliance with the conditions described in the annex to this safety data sheet.

1.3 Details of the supplier of the safety data sheet

Company	Merck KGaA * 64271 Darmstadt * Germany * Phone:+49 6151 72-0
Responsible Department	LS-QHC * e-mail: prodsafe@merckgroup.com

1.4 Emergency telephone number

Please contact the regional company representation in your country.

SECTION 2. Hazards identification

2.1 Classification of the substance or mixture

Classification (REGULATION (EC) No 1272/2008)

Flammable liquid, Category 2, H225
Eye irritation, Category 2, H319

For the full text of the H-Statements mentioned in this Section, see Section 16.

2.2 Label elements

Labelling (REGULATION (EC) No 1272/2008)

Hazard pictograms

Signal word
Danger

Hazard statements
H225 Highly flammable liquid and vapour.
H319 Causes serious eye irritation.

Precautionary statements
Prevention
P210 Keep away from heat, hot surfaces, sparks, open flames and other ignition sources. No smoking.
P240 Ground/bond container and receiving equipment.
Response
P305 + P351 + P338 IF IN EYES: Rinse cautiously with water for several minutes. Remove contact lenses, if present and easy to do. Continue rinsing.
Storage
P403 + P233 Store in a well-ventilated place. Keep container tightly closed.

Reduced labelling (≤125 ml)
Hazard pictograms

Signal word
Danger

Precautionary statements
P210 Keep away from heat, hot surfaces, sparks, open flames and other ignition sources. No smoking.

Index-No. 603-002-00-5

2.3 Other hazards
None known.

SECTION 3. Composition/information on ingredients

3.1 Substance

Formula	C_2H_5OH	C_2H_6O (Hill)
Index-No.	603-002-00-5	
EC-No.	200-578-6	
Molar mass	46,07 g/mol	

SAFETY DATA SHEET
according to Regulation (EC) No. 1907/2006

Catalogue No.	107017
Product name	Ethanol absolute for analysis EMPARTA® ACS

Hazardous components (REGULATION (EC) No 1272/2008)
Chemical name (Concentration)

CAS-No.	Registration number	Classification
ethanol (<= 100 %)		
Substance does not meet the criteria for PBT or vPvB according to Regulation (EC) No 1907/2006, Annex XIII.		
64-17-5	01-2119457610-43-XXXX	Flammable liquid, Category 2, H225 Eye irritation, Category 2, H319

For the full text of the H-Statements mentioned in this Section, see Section 16.

3.2 Mixture
Not applicable

SECTION 4. First aid measures

4.1 Description of first aid measures
After inhalation: fresh air.

In case of skin contact: Take off immediately all contaminated clothing. Rinse skin with water/ shower.

After eye contact: rinse out with plenty of water. Call in ophthalmologist. Remove contact lenses.

After swallowing: immediately make victim drink water (two glasses at most). Consult a physician.

4.2 Most important symptoms and effects, both acute and delayed
irritant effects, respiratory paralysis, Dizziness, narcosis, inebriation, euphoria, Nausea, Vomiting

4.3 Indication of any immediate medical attention and special treatment needed
No information available.

SECTION 5. Firefighting measures

5.1 Extinguishing media
Suitable extinguishing media
Carbon dioxide (CO2), Foam, Dry powder, Water

Unsuitable extinguishing media
For this substance/mixture no limitations of extinguishing agents are given.

5.2 Special hazards arising from the substance or mixture
Combustible.
Pay attention to flashback.
Forms explosive mixtures with air at ambient temperatures.
Vapours are heavier than air and may spread along floors.
Development of hazardous combustion gases or vapours possible in the event of fire.

5.3 Advice for firefighters

Special protective equipment for firefighters
In the event of fire, wear self-contained breathing apparatus.

Further information
Remove container from danger zone and cool with water. Prevent fire extinguishing water from contaminating surface water or the ground water system.

SECTION 6. Accidental release measures

6.1 Personal precautions, protective equipment and emergency procedures
Advice for non-emergency personnel: Do not breathe vapours, aerosols. Avoid substance contact. Ensure adequate ventilation. Keep away from heat and sources of ignition. Evacuate the danger area, observe emergency procedures, consult an expert.

Advice for emergency responders:

Protective equipment see section 8.

6.2 Environmental precautions
Do not let product enter drains. Risk of explosion.

6.3 Methods and materials for containment and cleaning up
Cover drains. Collect, bind, and pump off spills. Observe possible material restrictions (see sections 7 and 10). Take up with liquid-absorbent material (e.g. Chemizorb®). Dispose of properly. Clean up affected area.

6.4 Reference to other sections
Indications about waste treatment see section 13.

SECTION 7. Handling and storage

7.1 Precautions for safe handling

Advice on safe handling
Observe label precautions.

Advice on protection against fire and explosion
Keep away from open flames, hot surfaces and sources of ignition. Take precautionary measures against static discharge.

Hygiene measures
Change contaminated clothing. Wash hands after working with substance.

7.2 Conditions for safe storage, including any incompatibilities
Storage conditions
Keep container tightly closed in a dry and well-ventilated place. Keep away from heat and sources of ignition.

Recommended storage temperature see product label.

7.3 Specific end use(s)
See exposure scenario in the Annex to this MSDS.

SAFETY DATA SHEET
according to Regulation (EC) No. 1907/2006

Catalogue No.	107017
Product name	Ethanol absolute for analysis EMPARTA® ACS

SECTION 8. Exposure controls/personal protection

8.1 Control parameters

Derived No Effect Level (DNEL)

Worker DNEL, acute	Local effects	inhalation	1900 mg/m³
Worker DNEL, longterm	Systemic effects	dermal	343 mg/kg Body weight
Worker DNEL, longterm	Systemic effects	inhalation	950 mg/m³
Consumer DNEL, acute	Local effects	inhalation	950 mg/m³
Consumer DNEL, longterm	Systemic effects	dermal	206 mg/kg Body weight
Consumer DNEL, longterm	Systemic effects	inhalation	114 mg/m³
Consumer DNEL, longterm	Systemic effects	oral	87 mg/kg Body weight

Predicted No Effect Concentration (PNEC)

PNEC Fresh water	0,96 mg/l
PNEC Marine water	0,79 mg/l
PNEC Fresh water sediment	3,6 mg/kg
PNEC Soil	0,63 mg/kg
PNEC Aquatic intermittent release	2,75 mg/l
PNEC Sewage treatment plant	580 mg/l
PNEC oral	720 mg/kg

8.2 Exposure controls

Engineering measures
Technical measures and appropriate working operations should be given priority over the use of personal protective equipment.

See section 7.1.

Individual protection measures
Protective clothing needs to be selected specifically for the workplace, depending on concentrations and quantities of the hazardous substances handled. The chemical resistance of the protective equipment should be enquired at the respective supplier.

Eye/face protection
Safety glasses

Hand protection
full contact:

Glove material:	butyl-rubber
Glove thickness:	0,7 mm
Break through time:	> 480 min

splash contact:

Glove material:	Nitrile rubber
Glove thickness:	0,40 mm
Break through time:	> 120 min

The protective gloves to be used must comply with the specifications of EC Directive 89/686/EEC and the related standard EN374, for example KCL 898 Butoject® (full contact), KCL 730 Camatril® -Velours (splash contact).
The breakthrough times stated above were determined by KCL in laboratory tests acc. to EN374 with samples of the recommended glove types.
This recommendation applies only to the product stated in the safety data sheet, supplied by us and for the designated use. When dissolving in or mixing with other substances and under conditions deviating from those stated in EN374 please contact the supplier of CE-approved gloves (e.g. KCL GmbH, D-36124 Eichenzell, Internet: www.kcl.de).

Other protective equipment
Flame retardant antistatic protective clothing.

Respiratory protection
required when vapours/aerosols are generated.
Recommended Filter type: Filter A (acc. to DIN 3181) for vapours of organic compounds
The entrepeneur has to ensure that maintenance, cleaning and testing of respiratory protective devices are carried out according to the instructions of the producer.
These measures have to be properly documented.

Environmental exposure controls
Do not let product enter drains.
Risk of explosion.

SECTION 9. Physical and chemical properties

9.1 Information on basic physical and chemical properties

Form	liquid
Colour	colourless
Odour	alcohol-like
Odour Threshold	0,1 - 5058,5 ppm
pH	7,0 at 10 g/l 20 °C
Melting point	-114,5 °C
Boiling point/boiling range	78,3 °C at 1.013 hPa

SAFETY DATA SHEET
according to Regulation (EC) No. 1907/2006

Catalogue No. 107017
Product name Ethanol absolute for analysis EMPARTA® ACS

Flash point	12 °C Method: c.c.
Evaporation rate	No information available.
Flammability (solid, gas)	No information available.
Lower explosion limit	3,1 %(V)
Upper explosion limit	27,7 %(V)
Vapour pressure	59 hPa at 20 °C
Relative vapour density	1,6
Density	0,790 - 0,793 g/cm3 at 20 °C
Relative density	No information available.
Water solubility	at 20 °C completely miscible
Partition coefficient: n-octanol/water	log Pow: -0,31 (experimental) (Lit.) Bioaccumulation is not expected.
Auto-ignition temperature	No information available.
Decomposition temperature	No information available.
Viscosity, dynamic	1,2 mPa.s at 20 °C
Explosive properties	Not classified as explosive.
Oxidizing properties	none

9.2 Other data

Ignition temperature	425 °C Method: DIN 51794
Conductivity	< 1 µS/cm

SECTION 10. Stability and reactivity

10.1 Reactivity

Vapours may form explosive mixture with air.

10.2 Chemical stability
The product is chemically stable under standard ambient conditions (room temperature) .

10.3 Possibility of hazardous reactions
Risk of explosion/exothermic reaction with:

hydrogen peroxide, perchlorates, perchloric acid, Nitric acid, mercury(II) nitrate, permanganic acid, Nitriles, peroxi compounds, Strong oxidizing agents, nitrosyl compounds, Peroxides, sodium, Potassium, halogen oxides, calcium hypochlorite, nitrogen dioxide, metallic oxides, uranium hexafluoride, iodides, Chlorine, Alkali metals, Alkaline earth metals, alkali oxides, Ethylene oxide

silver, with, Nitric acid

silver compounds, with, Ammonia

potassium permanganate, with, conc. sulfuric acid

Risk of ignition or formation of inflammable gases or vapours with:

halogen-halogen compounds, chromium(VI) oxide, chromyl chloride, Fluorine, hydrides, Oxides of phosphorus, platinum

Nitric acid, with, potassium permanganate

10.4 Conditions to avoid
Warming.

10.5 Incompatible materials
rubber, various plastics

10.6 Hazardous decomposition products
no information available

SECTION 11. Toxicological information

11.1 Information on toxicological effects

Acute oral toxicity
LD50 Rat: 10.470 mg/kg
OECD Test Guideline 401

Symptoms: Nausea, Vomiting

Acute inhalation toxicity
LC50 Rat: 124,7 mg/l; 4 h ; vapour
OECD Test Guideline 403

Symptoms: slight mucosal irritations

Acute dermal toxicity
This information is not available.

Skin irritation
Rabbit
Result: No skin irritation
OECD Test Guideline 404

Repeated or prolonged exposure may cause skin irritation and dermatitis, due to degreasing properties of the product.

Eye irritation
Rabbit
Result: Eye irritation
OECD Test Guideline 405
Causes serious eye irritation.

Sensitisation
Local lymph node assay (LLNA) Mouse
Result: negative
Method: OECD Test Guideline 429

Germ cell mutagenicity
Genotoxicity in vitro
Ames test
Salmonella typhimurium
Result: negative
Method: OECD Test Guideline 471

In vitro mammalian cell gene mutation test
Mouse lymphoma test
Result: negative
Method: OECD Test Guideline 476

Carcinogenicity
This information is not available.

Reproductive toxicity
Application Route: Oral
Mouse
Method: OECD Test Guideline 416

Teratogenicity
This information is not available.

Specific target organ toxicity - single exposure
This information is not available.

Specific target organ toxicity - repeated exposure
This information is not available.

Aspiration hazard
This information is not available.

11.2 Further information
Systemic effects:
euphoria
After absorption:
Dizziness, inebriation, narcosis, respiratory paralysis
Other dangerous properties can not be excluded.
Handle in accordance with good industrial hygiene and safety practice.

SECTION 12. Ecological information

SAFETY DATA SHEET
according to Regulation (EC) No. 1907/2006

Catalogue No.	107017
Product name	Ethanol absolute for analysis EMPARTA® ACS

12.1 Toxicity

Toxicity to fish
flow-through test EC50 Pimephales promelas (fathead minnow): 15.300 mg/l; 96 h
Analytical monitoring: yes
US-EPA

Toxicity to daphnia and other aquatic invertebrates
EC50 Daphnia magna (Water flea): 9.268 - 14.221 mg/l; 48 h
(IUCLID)

Toxicity to algae
IC5 Scenedesmus quadricauda (Green algae): 5.000 mg/l; 7 d
(Lit.)

Toxicity to bacteria
EC5 Pseudomonas putida: 6.500 mg/l; 16 h
(IUCLID)

Toxicity to daphnia and other aquatic invertebrates (Chronic toxicity)
semi-static test NOEC Daphnia magna (Water flea): 9,6 mg/l; 9 d
(ECHA)

12.2 Persistence and degradability

Biodegradability
94 %
OECD Test Guideline 301E
Readily biodegradable

Biochemical Oxygen Demand (BOD)
930 - 1.670 mg/g (5 d)

(Lit.)

Theoretical oxygen demand (ThOD)
2.100 mg/g

(Lit.)

Ratio COD/ThBOD
90 %
(Lit.)

12.3 Bioaccumulative potential

Partition coefficient: n-octanol/water
log Pow: -0,31
(experimental)

(Lit.) Bioaccumulation is not expected.

12.4 Mobility in soil

No information available.

12.5 Results of PBT and vPvB assessment

Substance does not meet the criteria for PBT or vPvB according to Regulation (EC) No 1907/2006, Annex XIII.

12.6 Other adverse effects

Additional ecological information
No interference with wastewater treatment plants are to be expected when used properly.

Discharge into the environment must be avoided.

SECTION 13. Disposal considerations

Waste treatment methods
See www.retrologistik.com for processes regarding the return of chemicals and containers, or contact us there if you have further questions.

SECTION 14. Transport information

Land transport (ADR/RID)

14.1 UN number	UN 1170
14.2 Proper shipping name	ETHANOL
14.3 Class	3
14.4 Packing group	II
14.5 Environmentally hazardous	--
14.6 Special precautions for user	yes
Tunnel restriction code	D/E

Inland waterway transport (ADN)

Not relevant

Air transport (IATA)

14.1 UN number	UN 1170
14.2 Proper shipping name	ETHANOL
14.3 Class	3
14.4 Packing group	II
14.5 Environmentally hazardous	--
14.6 Special precautions for user	no

Sea transport (IMDG)

14.1 UN number	UN 1170
14.2 Proper shipping name	ETHANOL
14.3 Class	3
14.4 Packing group	II
14.5 Environmentally hazardous	--
14.6 Special precautions for user	yes
EmS	F-E S-D

14.7 Transport in bulk according to Annex II of MARPOL 73/78 and the IBC Code
Not relevant

SECTION 15. Regulatory information

15.1 Safety, health and environmental regulations/legislation specific for the substance or mixture

EU regulations

Major Accident Hazard Legislation	SEVESO III FLAMMABLE LIQUIDS P5c Quantity 1: 5.000 t Quantity 2: 50.000 t
Occupational restrictions	Take note of Dir 94/33/EC on the protection of young people at work.

Regulation (EC) No 1005/2009 on substances that deplete the ozone layer	not regulated
Regulation (EC) No 850/2004 of the European Parliament and of the Council of 29 April 2004 on persistent organic pollutants and amending Directive 79/117/EEC	not regulated
Substances of very high concern (SVHC)	This product does not contain substances of very high concern according to Regulation (EC) No 1907/2006 (REACH), Article 57 above the respective regulatory concentration limit of ≥ 0.1 % (w/w).

National legislation

Storage class	3

15.2 Chemical safety assessment

For this product a chemical safety assessment was not carried out.

SECTION 16. Other information

Full text of H-Statements referred to under sections 2 and 3.

H225	Highly flammable liquid and vapour.
H319	Causes serious eye irritation.

Training advice
Provide adequate information, instruction and training for operators.

SAFETY DATA SHEET
according to Regulation (EC) No. 1907/2006

Catalogue No.	107017
Product name	Ethanol absolute for analysis EMPARTA® ACS

Labelling
Hazard pictograms

Signal word
Danger

Hazard statements
H225 Highly flammable liquid and vapour.
H319 Causes serious eye irritation.

Precautionary statements
Prevention
P210 Keep away from heat/sparks/open flames/hot surfaces. No smoking.
P240 Ground/bond container and receiving equipment.
Response
P305 + P351 + P338 IF IN EYES: Rinse cautiously with water for several minutes. Remove contact lenses, if present and easy to do. Continue rinsing.
Storage
P403 + P233 Store in a well-ventilated place. Keep container tightly closed.

Key or legend to abbreviations and acronyms used in the safety data sheet
Used abbreviations and acronyms can be looked up at www.wikipedia.org.

Regional representation
This information is given on the authorised Safety Data Sheet for your country.

The information contained herein is based on the present state of our knowledge. It characterises the product with regard to the appropriate safety precautions. It does not represent a guarantee of any properties of the product.

SAFETY DATA SHEET
according to Regulation (EC) No. 1907/2006

Catalogue No.	107017
Product name	Ethanol absolute for analysis EMPARTA® ACS

EXPOSURE SCENARIO 1 (Industrial use)

1. Industrial use Reagent for analysis)

Sectors of end-use

SU 3	Industrial uses: Uses of substances as such or in preparations at industrial sites
SU9	Manufacture of fine chemicals
SU 10	Formulation [mixing] of preparations and/ or re-packaging (excluding alloys)

Chemical product category

PC21	Laboratory chemicals

Process categories

PROC1	Use in closed process, no likelihood of exposure
PROC2	Use in closed, continuous process with occasional controlled exposure
PROC3	Use in closed batch process (synthesis or formulation)
PROC4	Use in batch and other process (synthesis) where opportunity for exposure arises
PROC5	Mixing or blending in batch processes for formulation of preparations and articles (multistage and/ or significant contact)
PROC8a	Transfer of substance or preparation (charging/ discharging) from/ to vessels/ large containers at non-dedicated facilities
PROC8b	Transfer of substance or preparation (charging/ discharging) from/ to vessels/ large containers at dedicated facilities
PROC9	Transfer of substance or preparation into small containers (dedicated filling line, including weighing)
PROC10	Roller application or brushing
PROC14	Production of preparations or articles by tabletting, compression, extrusion, pelletisation
PROC15	Use as laboratory reagent

Environmental Release Categories

ERC1	Manufacture of substances
ERC2	Formulation of preparations
ERC4	Industrial use of processing aids in processes and products, not becoming part of articles
ERC6a	Industrial use resulting in manufacture of another substance (use of intermediates)

2. Contributing scenarios: Operational conditions and risk management measures
2.1 Contributing scenario controlling environmental exposure for: ERC1, ERC4, ERC6a

Amount used

Annual amount per site	400000 t

Environment factors not influenced by risk management

Flow rate	18.000 m3/d

Other given operational conditions affecting environmental exposure

Number of emission days per year	350
Emission or Release Factor: Air	70 %
Emission or Release Factor: Water	87 %

Conditions and measures related to municipal sewage treatment plant

Type of Sewage Treatment Plant	Municipal sewage treatment plant
Effectiveness (of a measure)	90 %

2.2 Contributing scenario controlling environmental exposure for: ERC2

Amount used

Annual amount per site	75000 t

Environment factors not influenced by risk management

Flow rate	18.000 m3/d

Other given operational conditions affecting environmental exposure

Number of emission days per year	300

Conditions and measures related to municipal sewage treatment plant

Type of Sewage Treatment Plant	Municipal sewage treatment plant
Effectiveness (of a measure)	90 %

2.3 Contributing scenario controlling worker exposure for: PROC1, PROC2, PROC3, PROC4, PROC5, PROC8a, PROC8b, PROC9, PROC10, PROC14, PROC15

Product characteristics

Concentration of the Substance in Mixture/Article	Covers the percentage of the substance in the product up to 100 % (unless stated differently).
Physical Form (at time of use)	High volatile liquid

Frequency and duration of use

Frequency of use	8 hours/day

Other operational conditions affecting workers exposure

Outdoor / Indoor	Indoor without local exhaust ventilation (LEV)

Additional good practice advice beyond the REACH Chemical Safety Assessment

Additional good practice advice	Wear suitable gloves (tested to EN374) and eye protection.

3. Exposure estimation and reference to its source

Environment

CS	Use descriptor	Msafe	Compartment	RCR	Exposure Assessment Method
2.1	ERC1		Fresh water	< 0,01	ECETOC TRA
			Marine water	< 0,01	ECETOC TRA
			Soil	< 0,01	ECETOC TRA
2.1	ERC4		Fresh water	< 0,01	ECETOC TRA
			Marine water	< 0,01	ECETOC TRA
			Soil	< 0,01	ECETOC TRA
2.1	ERC6a		Fresh water	< 0,01	ECETOC TRA
			Marine water	< 0,01	ECETOC TRA
			Soil	< 0,01	ECETOC TRA
2.2	ERC2		Fresh water	0,11	ECETOC TRA
			Marine water	0,01	ECETOC TRA
			Soil	< 0,01	ECETOC TRA

SAFETY DATA SHEET
according to Regulation (EC) No. 1907/2006

Catalogue No. 107017
Product name Ethanol absolute for analysis EMPARTA® ACS

Workers

CS	Use descriptor	Exposure duration, route, effect	RCR	Exposure Assessment Method
2.3	PROC1	longterm, inhalative, systemic	< 0,01	ECETOC TRA 3
		longterm, dermal, systemic	< 0,01	ECETOC TRA 3
		longterm, combined, systemic	< 0,01	
2.3	PROC2	longterm, inhalative, systemic	0,05	ECETOC TRA 3
		longterm, dermal, systemic	< 0,01	ECETOC TRA 3
		longterm, combined, systemic	0,05	
2.3	PROC3	longterm, inhalative, systemic	0,10	ECETOC TRA 3
		longterm, dermal, systemic	< 0,01	ECETOC TRA 3
		longterm, combined, systemic	0,10	
2.3	PROC4	longterm, inhalative, systemic	0,20	ECETOC TRA 3
		longterm, dermal, systemic	0,02	ECETOC TRA 3
		longterm, combined, systemic	0,22	
2.3	PROC5	longterm, inhalative, systemic	0,50	ECETOC TRA 3
		longterm, dermal, systemic	0,04	ECETOC TRA 3
		longterm, combined, systemic	0,54	
2.3	PROC8a	longterm, inhalative, systemic	0,50	ECETOC TRA 3
		longterm, dermal, systemic	0,04	ECETOC TRA 3
		longterm, combined, systemic	0,54	
2.3	PROC8b	longterm, inhalative, systemic	0,30	ECETOC TRA 3
		longterm, dermal, systemic	0,04	ECETOC TRA 3
		longterm, combined, systemic	0,34	
2.3	PROC9	longterm, inhalative, systemic	0,40	ECETOC TRA 3
		longterm, dermal, systemic	0,02	ECETOC TRA 3
		longterm, combined, systemic	0,42	
2.3	PROC10	longterm, inhalative, systemic	0,50	ECETOC TRA 3
		longterm, dermal, systemic	0,08	ECETOC TRA 3
		longterm, combined, systemic	0,58	
2.3	PROC14	longterm, inhalative, systemic	0,50	ECETOC TRA 3
		longterm, dermal, systemic	0,01	ECETOC TRA 3
		longterm, combined, systemic	0,51	
2.3	PROC15	longterm, inhalative, systemic	0,10	ECETOC TRA 3
		longterm, dermal, systemic	< 0,01	ECETOC TRA 3
		longterm, combined, systemic	0,10	

The default parameters and -efficiencies of the applied exposure assessment model were used for the calculation (unless stated differently).

SAFETY DATA SHEET
according to Regulation (EC) No. 1907/2006

Catalogue No.	107017
Product name	Ethanol absolute for analysis EMPARTA® ACS

4. Guidance to Downstream User to evaluate whether he works inside the boundaries set by the Exposure Scenario

Please refer to the following documents: ECHA Guidance on information requirements and chemical safety assessment Chapter R.12: Use descriptor system; ECHA Guidance for downstream users; ECHA Guidance on information requirements and chemical safety assessment Part D: Exposure Scenario Building, Part E: Risk Characterisation and Part G: Extending the SDS; VCI/Cefic REACH Practical Guides on Exposure Assessment and Communications in the Supply Chain; CEFIC Guidance Specific Environmental Release Categories (SPERCs).

For scaling of worker exposure assessments performed with ECETOC TRA, please consult the Merck tool ScIDeEx® at www.merckmillipore.com/scideex.

SAFETY DATA SHEET
according to Regulation (EC) No. 1907/2006

Catalogue No.	107017
Product name	Ethanol absolute for analysis EMPARTA® ACS

EXPOSURE SCENARIO 2 (Professional use)

1. Professional use Reagent for analysis)

Sectors of end-use
SU 22 Professional uses: Public domain (administration, education, entertainment, services, craftsmen)

Chemical product category
PC21 Laboratory chemicals

Process categories
PROC15 Use as laboratory reagent

Environmental Release Categories
ERC2 Formulation of preparations
ERC6a Industrial use resulting in manufacture of another substance (use of intermediates)

2. Contributing scenarios: Operational conditions and risk management measures
2.1 Contributing scenario controlling environmental exposure for: ERC2

Amount used

Annual amount per site	75000 t

Environment factors not influenced by risk management

Flow rate	18.000 m3/d

Other given operational conditions affecting environmental exposure

Number of emission days per year	300

Conditions and measures related to municipal sewage treatment plant

Type of Sewage Treatment Plant	Municipal sewage treatment plant
Effectiveness (of a measure)	90 %

2.2 Contributing scenario controlling environmental exposure for: ERC6a

Amount used

Annual amount per site	400000 t

Environment factors not influenced by risk management

Flow rate	18.000 m3/d

Other given operational conditions affecting environmental exposure

Number of emission days per year	350
Emission or Release Factor: Air	70 %

Emission or Release Factor: Water	87 %

Conditions and measures related to municipal sewage treatment plant

Type of Sewage Treatment Plant	Municipal sewage treatment plant
Effectiveness (of a measure)	90 %

2.3 Contributing scenario controlling worker exposure for: PROC15

Product characteristics

Concentration of the Substance in Mixture/Article	Covers the percentage of the substance in the product up to 100 % (unless stated differently).
Physical Form (at time of use)	High volatile liquid

Frequency and duration of use

Frequency of use	8 hours/day

Other operational conditions affecting workers exposure

Outdoor / Indoor	Indoor without local exhaust ventilation (LEV)

Additional good practice advice beyond the REACH Chemical Safety Assessment

Additional good practice advice	Wear suitable gloves (tested to EN374) and eye protection.

3. Exposure estimation and reference to its source

Environment

CS	Use descriptor	Msafe	Compartment	RCR	Exposure Assessment Method
2.1	ERC2		Fresh water	0,11	ECETOC TRA
			Marine water	0,01	ECETOC TRA
			Soil	< 0,01	ECETOC TRA
2.2	ERC6a		Fresh water	< 0,01	ECETOC TRA
			Marine water	< 0,01	ECETOC TRA
			Soil	< 0,01	ECETOC TRA

Workers

CS	Use descriptor	Exposure duration, route, effect	RCR	Exposure Assessment Method
2.3	PROC15	longterm, inhalative, systemic	0,10	ECETOC TRA 3
		longterm, dermal, systemic	< 0,01	ECETOC TRA 3
		longterm, combined, systemic	0,10	

The default parameters and -efficiencies of the applied exposure assessment model were used for the calculation (unless stated differently).

SAFETY DATA SHEET
according to Regulation (EC) No. 1907/2006

Catalogue No.	107017
Product name	Ethanol absolute for analysis EMPARTA® ACS

4. Guidance to Downstream User to evaluate whether he works inside the boundaries set by the Exposure Scenario

Please refer to the following documents: ECHA Guidance on information requirements and chemical safety assessment Chapter R.12: Use descriptor system; ECHA Guidance for downstream users; ECHA Guidance on information requirements and chemical safety assessment Part D: Exposure Scenario Building, Part E: Risk Characterisation and Part G: Extending the SDS; VCI/Cefic REACH Practical Guides on Exposure Assessment and Communications in the Supply Chain; CEFIC Guidance Specific Environmental Release Categories (SPERCs).

For scaling of worker exposure assessments performed with ECETOC TRA, please consult the Merck tool ScIDeEx® at www.merckmillipore.com/scideex.

The branding on the header and/or footer of this document may temporarily not visually match the product purchased as we transition our branding. However, all of the information in the document regarding the product remains unchanged and matches the product ordered. For further information please contact mlsbranding@sial.com.

C.5. High speed camera information sheet for specifications

In this section, the specification sheet provided by the supplied of the Photron mini AX200 high speed camera is given.

Outstanding Light Sensitivity in a Compact Package

The Photron FASTCAM Mini AX200 camera provides very high frame rates, extraordinary light sensitivity and superior image quality in a compact, lightweight and rugged camera design. Providing 1,024 x 1,024 pixel resolution at up to 6,400 frames per second (fps) and reduced resolutions to 900,000 fps, the Mini AX200 delivers the performance required for very demanding industrial, military and laboratory applications.

With light sensitivity of ISO 40,000 monochrome and ISO 16,000 color (using the ISO 12232 Ssat standard), the FASTCAM Mini AX200 has better sensitivity than most, if not all other high-end high-speed cameras. Higher light sensitivity means that less additional lighting is required to capture a high-speed event. It also means that faster frame rates, shorter shutter speeds and greater depths of field are provided under equivalent lighting conditions.

Contained within a 120mm x 120mm x 94mm camera body weighing just 1.5kg, the FASTCAM Mini AX200 is uniquely suited for use in a wide range of applications. The camera is designed for operation in high shock and vibration environments, allowing it to be utilized in automotive crash test facilities and on military test ranges.

Target applications include:

- Biomechanics
- Life sciences
- Material sciences
- Onboard and offboard automotive safety testing
- Defense and aerospace research
- Fluid dynamics / PIV

Benefits

- Performance examples:
  - 6,400 fps @ 1,024 x 1,024 pixels
  - 10,000 fps @ 896 x 768 pixels
  - 20,000 fps @ 512 x 512 pixels
  - 50,000 fps @ 384 x 256 pixels
  - 100,000 fps @ 256 x 160 pixels
  - 200,000 fps @ 128 x 96 pixels
  - 900,000 fps @ 128 x 16 pixels
- Self-contained, compact and lightweight camera 120mm (4.7") H × 120mm (4.7") W × 94mm (3.7") D excluding protrusions, and 1.5kg (3.3lbs)
- Sensitivity: ISO 12232 Ssat standard
  - ISO 40,000 monochrome
  - ISO 16,000 color
- Suitable for operation in High-G environments. Operation tested to 100G, 10ms, 6 axes
- 4GB, 8GB and 16GB memory options and high performance Gigabit Ethernet interface to PC

Photron
www.photron.com

FASTCAM Mini AX200

COMPACT HIGH-SPEED CAMERAS

Specifications: Partial Frame Rate / Recording Duration Table

FRAME RATE (fps)	MAXIMUM RESOLUTION		RECORDING TIME* (Sec.)		
	Horizontal	Vertical	4GB	8GB	16GB
6,400	1,024	1,024	0.43	0.85	1.71
10,000	896	768	0.42	0.83	1.66
15,000	768	512	0.48	0.97	1.94
20,000	512	512	0.55	1.09	2.18
30,000	512	284	0.65	1.31	2.62
50,000	384	256	0.58	1.16	2.33
100,000	256	160	0.70	1.40	2.80
200,000	128	96	1.16	2.32	4.65
360,000	128	32	1.93	3.88	7.76
900,000	128	16	1.55	3.10	6.21

*Multiply frame rate by time to determine approximate number of frames recorded.

Sensor 1,024 x 1,024 pixels, 20μm pixel size,12-bit ADC (Bayer system color, 36 bit-single sensor)

Sensitivity ISO 40,000 monochrome, ISO 16,000 color (ISO 12232 Ssat standard)

Shutter Global electronic shutter from 1ms to 260ns independent of frame rate

Extended Dynamic Range Selectable in twenty steps (0 to 99%, in 5% increments) to prevent over-exposure of pixels in brightly lit areas of the image

Lens Mount Interchangeable G-type F, C standard; M42 optional

Memory 4GB (2,726 frames @ maximum resolution) standard
8GB (5,457 frames @ maximum resolution) optional
16GB (10,918 frames @ maximum resolution) optional

Camera Control High-speed Gigabit Ethernet

Low Light Mode Low light mode drops the frame rate and shutter time to their maximum values, while maintaining other set parameters, to enable users to position and focus the camera

Triggering Selectable positive or negative TTL 5Vp-p or switch closure

Timing Internal clock or external source

I/O Input: Trigger (TTL/Switch), Sync, Ready, Event, IRIG
Output: Trigger, Sync, Ready, Rec, Expose

Phase Lock Enables cameras to precisely synchronize to a master camera or external source, such as IRIG time codes

Trigger Modes Start, Center, End, Manual, Random, Random Reset

Saved Image Formats JPEG, AVI, TIFF, BMP, RAW, RAWW, MRAW, PNG, MOV and FTIF. Images can be saved with or without embedded camera settings

Partition Up to 64 memory segments (includes option to record images to one segment while downloading images from another segment)

Data Display Frame Rate, Shutter Speed, Trigger Mode, Date or Time, Status (Playback /Record), Real Time, Frame Count and Resolution

Cooling Actively cooled

High-G Operation Tested to 100G, 10ms, 6 axes

Fan Control Allows fan to be temporarily disabled, eliminating vibration

Operating Temp/Humidity 0 - 40C (32 - 104°F) / 85% or less (no condensation)

Storage Temp/Humidity 0 - 60C (32 - 140°F) / 85% or less (no condensation)

Mounting 4 x1/4-20UNC, 4 x M5

Dimensions 120mm (4.7") H × 120mm (4.7") W × 94mm (3.7") D excluding protrusions

Weight 1.5kg (3.3lbs)

Power Requirement 100V-240V AC 55W , 50-60Hz DC operation 22-32 VDC, 55W

October 9, 2015 — Specifications subject to change without notice

PHOTRON USA, INC.
9520 Padgett Street, Suite 110
San Diego, CA 92126-4446
USA
Tel: 858.684.3555 or 800.585.2129
Fax: 858.684.3558
Email: image@photron.com
www.photron.com

PHOTRON (EUROPE) LIMITED
The Barn, Bottom Road
West Wycombe, Bucks, HP14 4BS
United Kingdom
Tel: +44 (0) 1494 481011
Fax: +44 (0) 1494 487011
Email: image@photron.com
www.photron.com

PHOTRON LIMITED
Kanda Jinbo-cho 1-105
Chiyoda-ku, Tokyo 101-0051
Japan
Tel: +81 (0) 3-3518-6271
Fax: +81 (0) 3-3518-6279
Email: image@photron.co.jp
www.photron.co.jp

PHOTRON (SHANGHAI) LIMITED
Room 20C Zhao-Feng World Trade Building
No. 369 Jiangsu Road, ChangNing District
Shanghai 200050 China
Tel: +86 (0) 21-5268-3700
Fax: +86 (0) 21-5268-3702
Email: info@photron.cn.com
www.photron.cn.com

D

Codes

In this chapter, the main codes relevant to the development of this thesis are presented. The codes are written in Python 2.7, unless otherwise stated. The make use of the most common modules, such as scipy, numpy and matplotlib. They include a code to find the density of H_2O_2 Appendix D.1, a code for translating the brix to the refractive index and the concentration of H_2O_2 Appendix D.2, a code for the adiabatic flame temperature of H_2O_2 decomposition in Appendix D.3, the LabView code used for thermocouple reading Appendix D.4 and the NASA CEA log outputs for the combustion of HTP with ethanol at different concentrations Appendix D.5

D.1. Density of H_2O_2 calculation

The following code includes the calculator for the density of hydrogen peroxide [47].

```
# -*- coding: utf-8 -*-
"""
Created on Mon Jul  8 15:03:52 2019

@author: Jaime Quesada
-------------------------------------------------------------------
        Density of HTP calculator
            based on the book info by Schumb
-------------------------------------------------------------------
"""

# ------------------------------------------------------------------------
#
#   Density of hydrogen peroxide calculator
#
#   Version:    1
#   Date:       08.07.2019
#   Author:     J. Quesada
#
# ------------------------------------------------------------------------
#   Description:
#   Density calcualtor given the temeprature and density of hydrogen peroxide
#   - Based on info from book by Schumb
#   -
#
# ------------------------------------------------------------------------
#  INPUT
#      0    :w              : weight concentraiton HTP      [%]
#      1    :T              : temperature of measurment     [C]
#      2    :K              : Boolean for kelvin(1=K, 0=C)  [bool]
```

```
# ------------------------------------------------------------------------
#  OUTPUT
#      0    :rho            : density                          [g/cm3]
# ------------------------------------------------------------------------

import numpy as np
from sys import exit


# ---------------------------------
# Water density calculator
# ---------------------------------
# IN
#    T [K]
# OUT
#    rho [g/cm^3]
def h2o_rho(T):

    # Constants
    A = 0.14395
    B = 0.0112
    C = 649.717
    D = 0.05107
    Tmin = 273.
    Tmax = 648.

    # Check it is wihtin bounds
    if T<Tmin or T>Tmax:
        print "Temperature is out of bounds for water density calculator"
        exit
    # If in bounds, find rho [kg/m3]
    else:
        rho_w = (A)/(B**(1.+((1.-(T/C))**D)))

        # Translate to right units
        rho_w = rho_w * (1./1000)

        return rho_w

# Other function for density of water calculation
def h2o_rho2(T):
    rho = (999.83952+16.945176*T-7.987041*T*T*10**(-3)-46.170461*10**(-6)*T*T*T
    +105.56302*10**(-9)*T*T*T*T-280.54253*10**(-12)*T*T*T*T*T)/(1+16.897850*10**(-3)*T)

    rho = rho/1000

    return rho

# Function for density of hydrogen peroxide

def rho(w, T, K=0):

    # Change w from % to qota
    w = np.float(w)/100.
```

```
    if K == 1:
        T = T-273.15

    # Define the functions that define the constants
    #   First the constants
    Jb = 0.39763
    Jc = 0.02206
    Jd = 0.05187

    Kb = -2.8732
    Kc = 3.5357
    Kd = -1.9414

    Lb = 3.2488
    Lc = -6.0947
    Ld = 3.9061

    Mb = -1.6363
    Mc = 3.6165
    Md = -2.55

    #   Function for constants
    b = Jb + Kb*T*(10**-3) + Lb*T*T*(10**-5) + Mb*T*T*T*(10**-7)
    c = Jc + Kc*T*(10**-3) + Lc*T*T*(10**-5) + Mc*T*T*T*(10**-7)
    d = Jd + Kd*T*(10**-3) + Ld*T*T*(10**-5) + Md*T*T*T*(10**-7)

    #   Functions for a
    a = h2o_rho2(T)

    # Now the rho
    #   Find the a constants
    rho = a + b*w + c*w*w + d*w*w*w

    return rho
```

D.2. Brix to refractive index to concentration of H_2O_2 for 20°Ccalculator

In this section the code presented is used for transformation from the brix sugar content index to the refractive index, which is later tranlated to the concentration of H_2O_2 always at 20°C. The data comes from [47]. Here the function nd2concen20 is used to return the concentration as a function of the refractive index.

```
# -*- coding: utf-8 -*-
"""
Created on Thu Jul 25 13:27:20 2019

@author: Jaime Quesada
"""

# ----------------------------------------------------------------------
#
#   Concentration of hydrogen peroxide calculator based on refractive index
#
#   Version:    1
#   Date:       25.07.2019
#   Author:     J. Quesada
#
# ----------------------------------------------------------------------
```

```
#    Description:
#    Returns the concentration of hydrogen peroxide based on the input of the
#                          Brix index from refractometer
#    - Brix to refractive index from polyfit of ICUMSA
#    - Refractive index to concentration from Schumb
#
# ------------------------------------------------------------------------
#  INPUT
#      0    :Bx            : Brix index                    [-]
#      1    :T             : temperature (20)              [C]
# ------------------------------------------------------------------------
#  OUTPUT
#      0    :conc          : concentration of HTP          [%]
# ------------------------------------------------------------------------

import numpy as np
import scipy.optimize as sp

# -------------
# Ask for input
# -------------
T = float(raw_input('Temperature (C) [20 if passed]:') or '20')
Bx_test = input('Brix index:')


# --------------------
# Brix to refractive
# --------------------
# Define the function as given by ICUMSA sodium D line (589.3 nm) at 20 Celsius
# http://mymathforum.com/physics/338099-brix-calculations.html

def nd2brix(nd, Bx_test):
    # IN:
    #   nd        : refractive index
    #   Bx_test   : value of brix to fit solver
    Bx = (((((11758.74*nd -88885.21)*nd +
     270177.93)*nd - 413145.80)*nd + 318417.95)*nd -99127.4536)
    return Bx - Bx_test


# Solve for refractive index

nD = sp.fsolve(nd2brix, 1.3, args=Bx_test, xtol=0.000001)
print nD

# ------------------------------------
# Refractive to concentration of HTP
# ------------------------------------

def nd2concen20(nD):
    # Concentration of HTP [%] from nD for 20C
    # From polyfit EXCEL
    # ------------------------------------------
    # IN:
    #   nD          : refractive index at 20C [-]
    # OUT
```

```
    #    conc         : concentration HTP [%]

    # Intercepts
    A = -3329.39189877
    B = 10452.30292012
    C = -8016.92732741

    conc = A*nD*nD + B*nD + C

    return conc


conc = nd2concen20(nD)


print 'The final concentration lays around: ', conc, ' %.'
```

D.3. Adiabatic flame temperature calculation for decomposition of H_2O_2

In this section, the adiabatic flame temperature calculation is presented, for which the cp are integrated over the range of temperatures.

```
# -*- coding: utf-8 -*-
"""
Created on Mon Dec  9 16:59:27 2019

@author: Jaime Quesada
"""

import pandas as pd
import numpy as np
import matplotlib.pyplot as plt
import matplotlib
import matplotlib.ticker as ticker
from sympy import *


valuefinal = []
# sym,bols
t, tabd, z = symbols("x y z", real=True)
# z = 0.365 gives boiling!!
z_ = np.linspace(0,0.355,50)
for z in z_:

    expr = 3.776*z/(1-z)

    cph = 30.092 + 6.832*t/1000. + 6.793*t*t/(1000.)**2 - 2.534*t*t*t/(1000.)**3 +
     (0.082*1000*1000/(t*t))
    cpol = 31.322 -20.235*t/(1000.) +57.866*t*t/(1000.)**2 -36.506*t*t*t/(1000.)**3
    -0.007*1000*1000/(t*t)
    cpoh = 30.032 +8.773*t/(1000.) -3.988*t*t/(1000.)**2 +0.788*t*t*t/(1000.)**3
    -0.741*1000*1000/(t*t)

    # Calculate for the case of T<500K for Cpo
    #intt = integrate(cpol + (2+expr)*cph, (t, 298.15, tabd)) # J

    intt = integrate(cpol + (2+expr)*cph, (t, 418.15, tabd)) # J
```

```
    #  Three options depending on the assumption
    #total = (108.28 ) *1000. # J  Assume that water is boiling out already
    #total = (108.28 +51) *1000. # J  Assume that water is boiling and h2o2 is fully gas
    total = (108.28 ) *1000 # J normal, all reactants in liquid

    outcome = solve([tabd>0, tabd<2000, intt-total], tabd, dict=True)

    tout = outcome.args[2].args[1].args[1]

    #  Correct if temperature is too high, a different one has to be used!
    if tout > 500: # Then use the right cp for o2
            #intt = integrate(cpol + (2+expr)*cph, (t, 298.15, 500))
             + integrate(cpoh + (2+expr)*cph, (t, 500, tabd))  # J
            intt = integrate(cpol + (2+expr)*cph, (t, 418.15, 500))
            + integrate(cpoh + (2+expr)*cph, (t, 500, tabd))  # J
            outcome = solve([tabd>0, tabd<2000, intt-total], tabd, dict=True)

            tout = outcome.args[2].args[1].args[1]

    valuefinal.append(tout)

    print tout


# Prepare the data for the area where only boiling of water is happening
# Temperature stays constant at 100C or 398.15K
x_ = [0.9, 0.355]
y_ = [398.15, 398.15]

# The increase in temperature is also linear before it reaches the boiling point
xl_ = [1, 0.9]
yl_ = [298.15, 398.15]

# Plot the resulting figure


# Tex font
matplotlib.rc('text', usetex=True)
matplotlib.rc('font', family='Arial')

fig = plt.figure(1)
ax1 = fig.add_subplot(111)
ax2 = ax1.twiny()

ax1.plot(z_, valuefinal, label='Analytical', c='b')
ax1.plot(x_, y_, c='b')
ax1.plot(xl_, yl_, c='b')
ax1.set_xlim(1, 0)
ax1.set_xticks(np.arange(1, -0.1, -0.1))
ax1.set_xlabel(r'Mass fraction H$_2$O [-]')
ax1.set_ylabel(r'Adiabatic flame temperature [K]')
ax1.legend(loc='top center', numpoints=1)
ax1.grid()
```

```
ax1.text(0.6, 1100,
         'H$_2$O (l) \n + \n H$_2$O (g) \n + \n O$_2$ (g)',
            horizontalalignment='center',
            verticalalignment='top',
            multialignment='center')

ax1.text(0.6, 1100,
         'H$_2$O (l) \n + \n H$_2$O (g) \n + \n O$_2$ (g)',
            horizontalalignment='center',
            verticalalignment='top',
            multialignment='center')

ax1.text(0.2, 1050,
         'H$_2$O (g) \n + \n O$_2$ (g)',
            horizontalalignment='center',
            verticalalignment='top',
            multialignment='center')
ax1.text(0.2, 1050,
         'H$_2$O (g) \n + \n O$_2$ (g)',
            horizontalalignment='center',
            verticalalignment='top',
            multialignment='center')
ax1.text(0.95, 1050,
         'H$_2$O (l) \n + \n O$_2$ (g)',
            horizontalalignment='center',
            verticalalignment='top',
            multialignment='center')
ax1.text(0.95, 1050,
         'H$_2$O (l) \n + \n O$_2$ (g)',
            horizontalalignment='center',
            verticalalignment='top',
            multialignment='center')


ax1.axvline(x=0.355, linestyle='-.', c='red')
ax1.axvline(x=0.9, linestyle='-.',c='red')
ax1.axhline(y=638.15, linestyle='-.', c='green')

ax2.set_xlim([0,100])
ax2.set_xticks(np.arange(0,101,5))
ax2.set_xlabel(r'Concentration of H$_2$O$_2$[\%]')

plt.show()
```

D.4. Labview code for thermocouple readings

This code is run and prepared in LabView 2017 for Windows and run on a parallel machine.

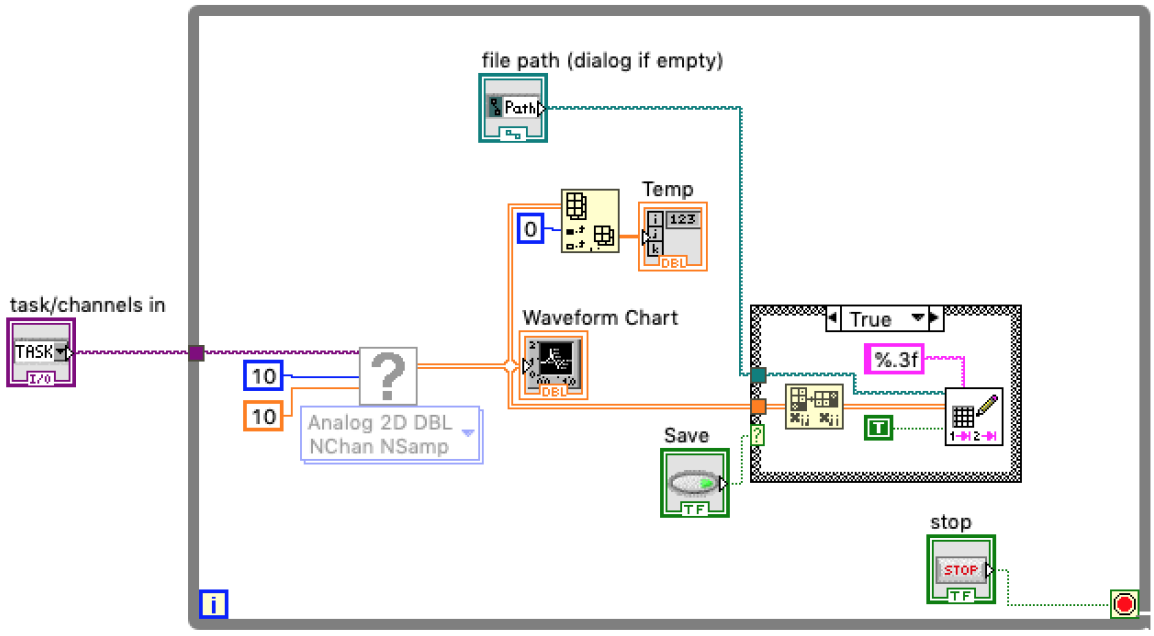

Figure D.1: LabView code for thermocouple reading,. the number of thermocouples can be altered in the Task Manager of the program, as well as the reading rate hereby set to 55 Hz.

D.5. NASA CEA combustion results for various concentration of HTP

In this section the results from running the NASA CEA are presented. The results are from the combustion of H_2O_2 at concentrations of 80, 85 , 90 and 95% with ethanol. The combustion is fixed at 1 atm and the reactants in liquid form are fixed to be at room temperature, except H_2O_2 which could only be set to maximum of 282K.

D.5.1. Combustion for 80% HTP

```
        NASA-GLENN CHEMICAL EQUILIBRIUM PROGRAM CEA2, FEBRUARY 5, 2004
                  BY  BONNIE MCBRIDE AND SANFORD GORDON
     REFS: NASA RP-1311, PART I, 1994 AND NASA RP-1311, PART II, 1996

*******************************************************************************


### CEA analysis performed on Thu 19-Dec-2019 07:11:42

# Problem Type: "Assigned Enthalpy and Pressure"

prob case=trial__________7912 hp

# Pressure (1 value):
p,atm= 1

# Oxidizer/Fuel Wt. ratio (1 value):
o/f= 3.684

# You selected the following fuels and oxidizers:
reac
fuel C2H5OH(L)          wt%=100.0000  t,k= 298.150
oxid H2O(L)             wt%= 20.0000  t,k= 298.150
oxid H2O2(L)            wt%= 80.0000  t,k= 282.000

# Consider ONLY these selected species. (4 selected)
only C2H5OH CO2 H2O O2


# You selected these options for output:
# long version of output
# Proportions of any products will be expressed as Mass Fractions.
output massf
# Heat will be expressed as siunits
output siunits

# Input prepared by this script:prepareInputFile.cgi

### IMPORTANT:  The following line is the end of your CEA input file!
end

OPTIONS: TP=F  HP=T  SP=F  TV=F  UV=F  SV=F  DETN=F  SHOCK=F  REFL=F  INCD=F
RKT=F  FROZ=F  EQL=F  IONS=F  SIUNIT=T  DEBUGF=F  SHKDBG=F  DETDBG=F  TRNSPT=F

TRACE= 0.00E+00  S/R= 0.000000E+00  H/R= 0.000000E+00  U/R= 0.000000E+00

P,BAR =     1.013250

NOTE! REACTANT H2O2(L)        HAS BEEN DEFINED FOR TEMPERATURE  272.74K ONLY.
YOUR TEMPERATURE ASSIGNMENT  282.00 IS NOT = BUT <10 K FROM THIS VALUE. (REACT)

   REACTANT          WT.FRAC   (ENERGY/R),K   TEMP,K  DENSITY
       EXPLODED FORMULA
F: C2H5OH(L)        1.000000  -0.333766E+05   298.15  0.0000
         C  2.00000  H  6.00000  O  1.00000
O: H2O(L)           0.200000  -0.343773E+05   298.15  0.0000
         H  2.00000  O  1.00000
O: H2O2(L)          0.800000  -0.225846E+05   272.74  0.0000
         H  2.00000  O  2.00000

 SPECIES BEING CONSIDERED IN THIS SYSTEM
```

D.5.2. Combustion for 80% HTP

```
(CONDENSED PHASE MAY HAVE NAME LISTED SEVERAL TIMES)
 LAST thermo.inp UPDATE:    9/09/04

 g 9/99  *CO2             g 8/88  C2H5OH           g 8/89  H2O
 tpis89  *O2

O/F =   3.684000

                       EFFECTIVE FUEL     EFFECTIVE OXIDANT        MIXTURE
ENTHALPY                    h(2)/R             h(1)/R               h0/R
(KG-MOL)(K)/KG       -0.72450014E+03    -0.91281895E+03     -0.87261425E+03

KG-FORM.WT./KG             bi(2)              bi(1)               b0i
 C                     0.43413669E-01     0.00000000E+00      0.92685032E-02
 H                     0.13024101E+00     0.69241888E-01      0.82264757E-01
 O                     0.21706834E-01     0.58140201E-01      0.50361942E-01

POINT ITN      T            C           H           O

        THERMODYNAMIC EQUILIBRIUM COMBUSTION PROPERTIES AT ASSIGNED

                                  PRESSURES

CASE = trial__________

            REACTANT                    WT FRACTION      ENERGY      TEMP
                                         (SEE NOTE)     KJ/KG-MOL      K
FUEL        C2H5OH(L)                    1.0000000   -277510.001    298.150
OXIDANT     H2O(L)                       0.2000000   -285830.088    298.150
OXIDANT     H2O2(L)                      0.8000000   -187780.000    272.740

O/F=    3.68400  %FUEL= 21.349274  R,EQ.RATIO= 1.184811  PHI,EQ.RATIO= 1.503158

THERMODYNAMIC PROPERTIES

P, BAR            1.0132
T, K             2292.37
RHO, KG/CU M    1.2029-1
H, KJ/KG        -7255.36
U, KJ/KG        -8097.73
G, KJ/KG        -36877.5
S, KJ/(KG)(K)    12.9221

M, (1/n)          22.627
(dLV/dLP)t      -1.00000
(dLV/dLT)p        1.0000
Cp, KJ/(KG)(K)    2.6173
GAMMAs            1.1633
SON VEL,M/SEC      989.9

MASS FRACTIONS

*CO2             0.27136
C2H5OH           0.07146
H2O              0.65717

 * THERMODYNAMIC PROPERTIES FITTED TO 20000.K

   PRODUCTS WHICH WERE CONSIDERED BUT WHOSE MASS FRACTIONS
   WERE LESS THAN 5.000000E-06 FOR ALL ASSIGNED CONDITIONS

*O2

NOTE. WEIGHT FRACTION OF FUEL IN TOTAL FUELS AND OF OXIDANT IN TOTAL OXIDANTS
```

D.5.3. Combustion for 85% HTP

```
        NASA-GLENN CHEMICAL EQUILIBRIUM PROGRAM CEA2, FEBRUARY 5, 2004
                  BY  BONNIE MCBRIDE AND SANFORD GORDON
     REFS: NASA RP-1311, PART I, 1994 AND NASA RP-1311, PART II, 1996

*******************************************************************************


### CEA analysis performed on Thu 19-Dec-2019 07:13:17

# Problem Type: "Assigned Enthalpy and Pressure"

prob case=trial__________7912 hp

# Pressure (1 value):
p,atm= 1

# Oxidizer/Fuel Wt. ratio (1 value):
o/f= 3.756

# You selected the following fuels and oxidizers:
reac
fuel C2H5OH(L)          wt%=100.0000  t,k= 298.150
oxid H2O(L)             wt%= 15.0000  t,k= 298.150
oxid H2O2(L)            wt%= 85.0000  t,k= 282.000

# Consider ONLY these selected species. (4 selected)
only C2H5OH CO2 H2O O2


# You selected these options for output:
# long version of output
# Proportions of any products will be expressed as Mass Fractions.
output massf
# Heat will be expressed as siunits
output siunits

# Input prepared by this script:prepareInputFile.cgi

### IMPORTANT:  The following line is the end of your CEA input file!
end

OPTIONS: TP=F  HP=T  SP=F  TV=F  UV=F  SV=F  DETN=F  SHOCK=F  REFL=F  INCD=F
RKT=F  FROZ=F  EQL=F  IONS=F  SIUNIT=T  DEBUGF=F  SHKDBG=F  DETDBG=F  TRNSPT=F

TRACE= 0.00E+00  S/R= 0.000000E+00  H/R= 0.000000E+00  U/R= 0.000000E+00

P,BAR =     1.013250

NOTE! REACTANT H2O2(L)        HAS BEEN DEFINED FOR TEMPERATURE  272.74K ONLY.
YOUR TEMPERATURE ASSIGNMENT  282.00 IS NOT = BUT <10 K FROM THIS VALUE. (REACT)

   REACTANT          WT.FRAC   (ENERGY/R),K   TEMP,K  DENSITY
       EXPLODED FORMULA
F: C2H5OH(L)        1.000000  -0.333766E+05   298.15  0.0000
         C  2.00000  H  6.00000  O  1.00000
O: H2O(L)           0.150000  -0.343773E+05   298.15  0.0000
         H  2.00000  O  1.00000
O: H2O2(L)          0.850000  -0.225846E+05   272.74  0.0000
         H  2.00000  O  2.00000

 SPECIES BEING CONSIDERED IN THIS SYSTEM
```

D.5.4. Combustion for 85% HTP

```
(CONDENSED PHASE MAY HAVE NAME LISTED SEVERAL TIMES)
 LAST thermo.inp UPDATE:    9/09/04

 g 9/99  *CO2             g 8/88  C2H5OH           g 8/89  H2O
 tpis89  *O2

O/F =   3.756000

                       EFFECTIVE FUEL     EFFECTIVE OXIDANT        MIXTURE
ENTHALPY                   h(2)/R             h(1)/R               h0/R
(KG-MOL)(K)/KG       -0.72450014E+03    -0.85060588E+03     -0.82409079E+03

KG-FORM.WT./KG             bi(2)              bi(1)               b0i
 C                     0.43413669E-01     0.00000000E+00      0.91281894E-02
 H                     0.13024101E+00     0.66630952E-01      0.80005648E-01
 O                     0.21706834E-01     0.58304686E-01      0.50609596E-01

POINT ITN      T            C           H           O

        THERMODYNAMIC EQUILIBRIUM COMBUSTION PROPERTIES AT ASSIGNED

                                  PRESSURES

CASE = trial__________

            REACTANT                     WT FRACTION      ENERGY      TEMP
                                          (SEE NOTE)     KJ/KG-MOL      K
FUEL        C2H5OH(L)                     1.0000000   -277510.001    298.150
OXIDANT     H2O(L)                        0.1500000   -285830.088    298.150
OXIDANT     H2O2(L)                       0.8500000   -187780.000    272.740

O/F=    3.75600  %FUEL= 21.026072  R,EQ.RATIO= 1.151149  PHI,EQ.RATIO= 1.387617

THERMODYNAMIC PROPERTIES

P, BAR            1.0132
T, K             2481.39
RHO, KG/CU M    1.1154-1
H, KJ/KG        -6851.91
U, KJ/KG        -7760.35
G, KJ/KG        -39173.6
S, KJ/(KG)(K)    13.0256

M, (1/n)          22.711
(dLV/dLP)t      -1.00000
(dLV/dLT)p        1.0000
Cp, KJ/(KG)(K)    2.6180
GAMMAs            1.1626
SON VEL,M/SEC     1027.7

MASS FRACTIONS

*CO2             0.28951
C2H5OH           0.05873
H2O              0.65176

 * THERMODYNAMIC PROPERTIES FITTED TO 20000.K

   PRODUCTS WHICH WERE CONSIDERED BUT WHOSE MASS FRACTIONS
   WERE LESS THAN 5.000000E-06 FOR ALL ASSIGNED CONDITIONS

*O2

NOTE. WEIGHT FRACTION OF FUEL IN TOTAL FUELS AND OF OXIDANT IN TOTAL OXIDANTS
```

D.5.5. Combustion for 90% HTP

```
        NASA-GLENN CHEMICAL EQUILIBRIUM PROGRAM CEA2, FEBRUARY 5, 2004
                  BY  BONNIE MCBRIDE AND SANFORD GORDON
     REFS: NASA RP-1311, PART I, 1994 AND NASA RP-1311, PART II, 1996

*******************************************************************************


### CEA analysis performed on Thu 19-Dec-2019 07:14:42

# Problem Type: "Assigned Enthalpy and Pressure"

prob case=trial__________7912 hp

# Pressure (1 value):
p,atm= 1

# Oxidizer/Fuel Wt. ratio (1 value):
o/f= 3.83

# You selected the following fuels and oxidizers:
reac
fuel C2H5OH(L)          wt%=100.0000  t,k= 298.150
oxid H2O(L)             wt%= 10.0000  t,k= 298.150
oxid H2O2(L)            wt%= 90.0000  t,k= 282.000

# Consider ONLY these selected species. (4 selected)
only C2H5OH CO2 H2O O2


# You selected these options for output:
# long version of output
# Proportions of any products will be expressed as Mass Fractions.
output massf
# Heat will be expressed as siunits
output siunits

# Input prepared by this script:prepareInputFile.cgi

### IMPORTANT:  The following line is the end of your CEA input file!
end

OPTIONS: TP=F  HP=T  SP=F  TV=F  UV=F  SV=F  DETN=F  SHOCK=F  REFL=F  INCD=F
RKT=F  FROZ=F  EQL=F  IONS=F  SIUNIT=T  DEBUGF=F  SHKDBG=F  DETDBG=F  TRNSPT=F

TRACE= 0.00E+00  S/R= 0.000000E+00  H/R= 0.000000E+00  U/R= 0.000000E+00

P,BAR =     1.013250

NOTE! REACTANT H2O2(L)        HAS BEEN DEFINED FOR TEMPERATURE  272.74K ONLY.
YOUR TEMPERATURE ASSIGNMENT  282.00 IS NOT = BUT <10 K FROM THIS VALUE. (REACT)

   REACTANT          WT.FRAC   (ENERGY/R),K   TEMP,K  DENSITY
       EXPLODED FORMULA
F: C2H5OH(L)        1.000000  -0.333766E+05   298.15  0.0000
         C  2.00000  H  6.00000  O  1.00000
O: H2O(L)           0.100000  -0.343773E+05   298.15  0.0000
         H  2.00000  O  1.00000
O: H2O2(L)          0.900000  -0.225846E+05   272.74  0.0000
         H  2.00000  O  2.00000

 SPECIES BEING CONSIDERED IN THIS SYSTEM
```

D.5.6. Combustion for 90% HTP

```
(CONDENSED PHASE MAY HAVE NAME LISTED SEVERAL TIMES)
 LAST thermo.inp UPDATE:    9/09/04

 g 9/99  *CO2             g 8/88  C2H5OH           g 8/89  H2O
 tpis89  *O2

O/F =   3.830000

                       EFFECTIVE FUEL     EFFECTIVE OXIDANT        MIXTURE
ENTHALPY                    h(2)/R             h(1)/R               h0/R
(KG-MOL)(K)/KG       -0.72450014E+03    -0.78839281E+03    -0.77516452E+03

KG-FORM.WT./KG             bi(2)              bi(1)              b0i
 C                     0.43413669E-01     0.00000000E+00     0.89883372E-02
 H                     0.13024101E+00     0.64020015E-01     0.77730365E-01
 O                     0.21706834E-01     0.58469172E-01     0.50857922E-01

POINT ITN      T            C           H           O

        THERMODYNAMIC EQUILIBRIUM COMBUSTION PROPERTIES AT ASSIGNED

                                  PRESSURES

CASE = trial__________

            REACTANT                     WT FRACTION      ENERGY      TEMP
                                          (SEE NOTE)     KJ/KG-MOL      K
FUEL        C2H5OH(L)                     1.0000000   -277510.001    298.150
OXIDANT     H2O(L)                        0.1000000   -285830.088    298.150
OXIDANT     H2O2(L)                       0.9000000   -187780.000    272.740

O/F=    3.83000  %FUEL= 20.703934  R,EQ.RATIO= 1.117660  PHI,EQ.RATIO= 1.285206

THERMODYNAMIC PROPERTIES

P, BAR            1.0132
T, K             2675.14
RHO, KG/CU M    1.0385-1
H, KJ/KG        -6445.11
U, KJ/KG        -7420.76
G, KJ/KG        -41525.5
S, KJ/(KG)(K)    13.1135

M, (1/n)          22.798
(dLV/dLP)t      -1.00000
(dLV/dLT)p        1.0000
Cp, KJ/(KG)(K)    2.6118
GAMMAs            1.1623
SON VEL,M/SEC     1064.9

MASS FRACTIONS

*CO2             0.30779
C2H5OH           0.04595
H2O              0.64627

 * THERMODYNAMIC PROPERTIES FITTED TO 20000.K

   PRODUCTS WHICH WERE CONSIDERED BUT WHOSE MASS FRACTIONS
   WERE LESS THAN 5.000000E-06 FOR ALL ASSIGNED CONDITIONS

*O2

NOTE. WEIGHT FRACTION OF FUEL IN TOTAL FUELS AND OF OXIDANT IN TOTAL OXIDANTS
```

D.5.7. Combustion for 95% HTP

```
        NASA-GLENN CHEMICAL EQUILIBRIUM PROGRAM CEA2, FEBRUARY 5, 2004
                  BY  BONNIE MCBRIDE AND SANFORD GORDON
     REFS: NASA RP-1311, PART I, 1994 AND NASA RP-1311, PART II, 1996

*******************************************************************************


### CEA analysis performed on Thu 19-Dec-2019 07:15:41

# Problem Type: "Assigned Enthalpy and Pressure"

prob case=trial__________7912 hp

# Pressure (1 value):
p,atm= 1

# Oxidizer/Fuel Wt. ratio (1 value):
o/f= 3.9

# You selected the following fuels and oxidizers:
reac
fuel C2H5OH(L)          wt%=100.0000  t,k= 298.150
oxid H2O(L)             wt%=  5.0000  t,k= 298.150
oxid H2O2(L)            wt%= 95.0000  t,k= 282.000

# Consider ONLY these selected species. (4 selected)
only C2H5OH CO2 H2O O2


# You selected these options for output:
# long version of output
# Proportions of any products will be expressed as Mass Fractions.
output massf
# Heat will be expressed as siunits
output siunits

# Input prepared by this script:prepareInputFile.cgi

### IMPORTANT:  The following line is the end of your CEA input file!
end

OPTIONS: TP=F  HP=T  SP=F  TV=F  UV=F  SV=F  DETN=F  SHOCK=F  REFL=F  INCD=F
RKT=F  FROZ=F  EQL=F  IONS=F  SIUNIT=T  DEBUGF=F  SHKDBG=F  DETDBG=F  TRNSPT=F

TRACE= 0.00E+00  S/R= 0.000000E+00  H/R= 0.000000E+00  U/R= 0.000000E+00

P,BAR =     1.013250

NOTE! REACTANT H2O2(L)        HAS BEEN DEFINED FOR TEMPERATURE  272.74K ONLY.
YOUR TEMPERATURE ASSIGNMENT  282.00 IS NOT = BUT <10 K FROM THIS VALUE. (REACT)

   REACTANT          WT.FRAC   (ENERGY/R),K   TEMP,K  DENSITY
       EXPLODED FORMULA
F: C2H5OH(L)        1.000000  -0.333766E+05   298.15  0.0000
         C  2.00000  H  6.00000  O  1.00000
O: H2O(L)           0.050000  -0.343773E+05   298.15  0.0000
         H  2.00000  O  1.00000
O: H2O2(L)          0.950000  -0.225846E+05   272.74  0.0000
         H  2.00000  O  2.00000

 SPECIES BEING CONSIDERED IN THIS SYSTEM
```

D.5.8. Combustion for 95% HTP

```
(CONDENSED PHASE MAY HAVE NAME LISTED SEVERAL TIMES)
 LAST thermo.inp UPDATE:    9/09/04

 g 9/99  *CO2             g 8/88  C2H5OH           g 8/89  H2O
 tpis89  *O2

O/F =   3.900000

                       EFFECTIVE FUEL     EFFECTIVE OXIDANT        MIXTURE
ENTHALPY                   h(2)/R             h(1)/R               h0/R
(KG-MOL)(K)/KG       -0.72450014E+03    -0.72617975E+03     -0.72583697E+03

KG-FORM.WT./KG             bi(2)              bi(1)               b0i
 C                     0.43413669E-01     0.00000000E+00      0.88599324E-02
 H                     0.13024101E+00     0.61409079E-01      0.75456411E-01
 O                     0.21706834E-01     0.58633657E-01      0.51097571E-01

POINT ITN      T            C           H           O

        THERMODYNAMIC EQUILIBRIUM COMBUSTION PROPERTIES AT ASSIGNED

                                  PRESSURES

CASE = trial__________

            REACTANT                    WT FRACTION      ENERGY      TEMP
                                         (SEE NOTE)     KJ/KG-MOL      K
FUEL        C2H5OH(L)                    1.0000000   -277510.001    298.150
OXIDANT     H2O(L)                       0.0500000   -285830.088    298.150
OXIDANT     H2O2(L)                      0.9500000   -187780.000    272.740

O/F=    3.90000  %FUEL= 20.408163  R,EQ.RATIO= 1.085141  PHI,EQ.RATIO= 1.195710

THERMODYNAMIC PROPERTIES

P, BAR            1.0132
T, K             2873.09
RHO, KG/CU M    9.7089-2
H, KJ/KG        -6034.98
U, KJ/KG        -7078.61
G, KJ/KG        -43919.0
S, KJ/(KG)(K)    13.1858

M, (1/n)          22.890
(dLV/dLP)t      -1.00000
(dLV/dLT)p        1.0000
Cp, KJ/(KG)(K)    2.6002
GAMMAs            1.1624
SON VEL,M/SEC     1101.4

MASS FRACTIONS

*CO2             0.32610
C2H5OH           0.03340
H2O              0.64050

 * THERMODYNAMIC PROPERTIES FITTED TO 20000.K

   PRODUCTS WHICH WERE CONSIDERED BUT WHOSE MASS FRACTIONS
   WERE LESS THAN 5.000000E-06 FOR ALL ASSIGNED CONDITIONS

*O2

NOTE. WEIGHT FRACTION OF FUEL IN TOTAL FUELS AND OF OXIDANT IN TOTAL OXIDANTS
```

E

Thermocouple calibration

In this chapter the thermocouple calibration is presented for the boiling point, Figure E.1 and Figure E.2. This temperature is more relevant to the regime the thermocouples will be working in. Nonetheless, for the freezing method, they also proved to be at 0°C±3°C.

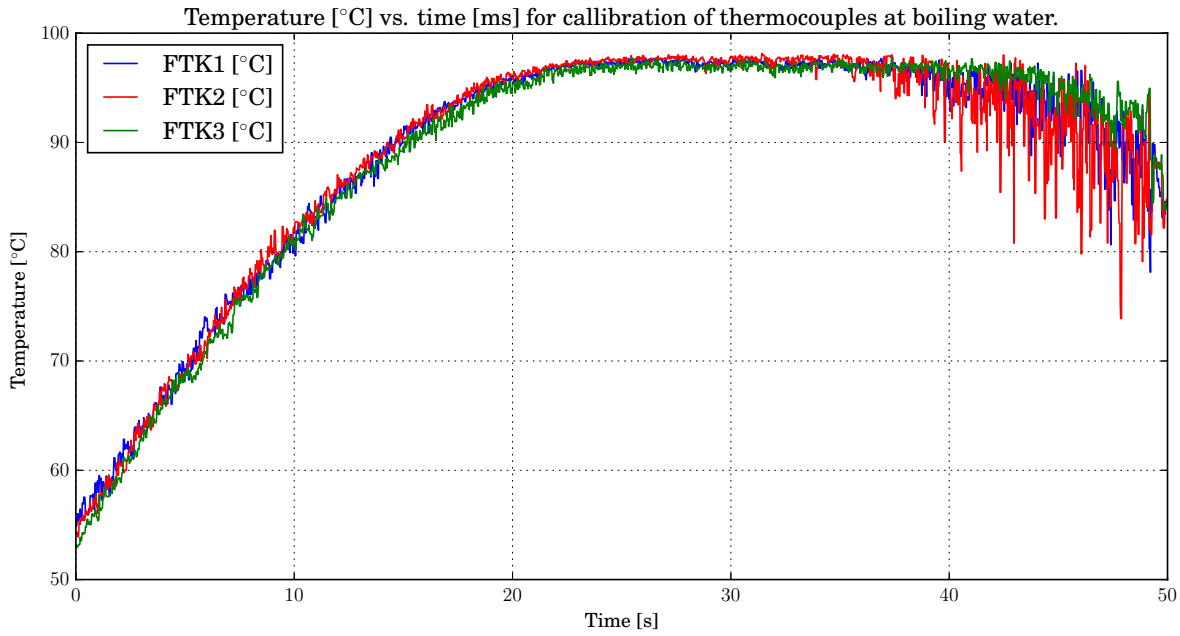

Figure E.1: Calibration of thermocouples to boiling temperature of water around 100°C. The temperature in °Cis plotted against the time [s]. FTK1 achieved around 97.5, FTK2 around 98 and FTK3 around 97 °C. The accuracy is set at 3°Cfor conservative approach.

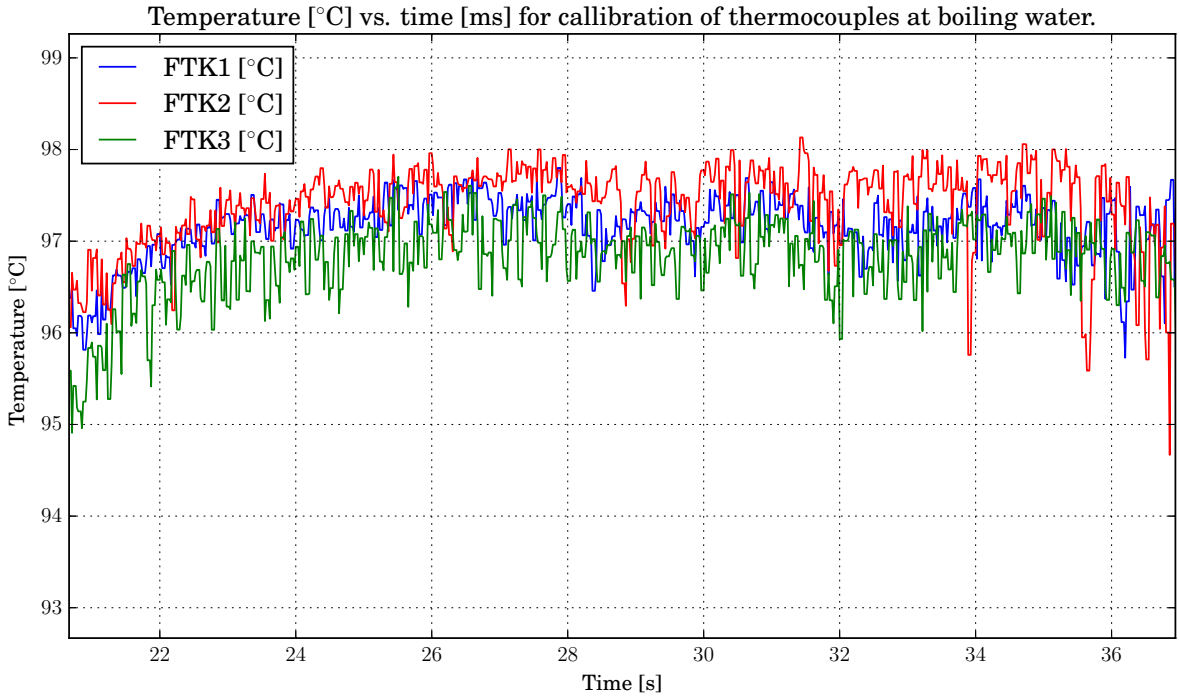

Figure E.2: Calibration of thermocouples to boiling temperature of water around 100°C zoomed in. The temperature in °Cis plotted against the time [s]. FTK1 achieved around 97.5, FTK2 around 98 and FTK3 around 97 °C. The accuracy is set at 3°Cfor conservative approach.